*Exxon Valdez* Oil Spill
Restoration Project Annual Report

# SEA: Observational Oceanography in Prince William Sound

Restoration Project 96320-M
Annual Report

This annual report has been prepared for peer review as part of the *Exxon Valdez* Oil Spill Trustee Council restoration program for the purpose of assessing project progress. Peer review comments have not been addressed in this annual report.

Shari L. Vaughan
Shelton M. Gay III
Loren B. Tuttle
Kenric E. Osgood

Prince William Sound Science Center
P. O. Box 705
Cordova, Alaska 99574

April 1998

SEA: Observational Oceanography in Prince William Sound

Restoration Project 96320-M
Annual Report

**Study History:** Unexpectedly small Prince William Sound pink salmon runs in 1992 and 1993, and the almost complete collapse of the herring fishery in 1993, prompted the EVOS Trustee Council to initiate ecosystem-level studies of the region to investigate possible environmental reasons for these disasters. A collaborative effort involving the University of Alaska Fairbanks, the Prince William Sound Science Center, the Prince William Sound Aquaculture Corporation, and Alaska Department of Fish and Game resulted in the development of a coordinated plan in the fall of 1993. After substantial review, Sound Ecosystem Assessment (SEA) was approved for funding April 11, 1994. A scope of work for SEA was projected over 5-8 years at that time. Annual reports were issued in 1995 by D. K. Salmon entitled Descriptive Physical Oceanography (project number 94320-M), in 1996 by S. L. Vaughan entitled Observational Physical Oceanography in Prince William Sound and the Gulf of Alaska (project number 95320-M), and in 1997 by S. L. Vaughan entitled Water Mass Variability and Circulation of PWS (project number 96320-M), all as chapter contributions to the single compiled report of all SEA FY94, FY95 and FY96 projects. Project results were presented in 1996-1998 at several professional meetings. A journal article was submitted for publication in 1996 (Gay, S.M., 1996: Seasonal Changes in Hydrography of Embayments and Fjords of Prince William Sound, Alaska during Spring and Summer 1994, Fall 1995, and Late Winter 1996. In IAPSO Conference Proceedings).

**Abstract:** Hydrographic surveys and current velocity measurements in 1994 through 1997 show significant seasonal and interannual variability in water mass properties and circulation patterns in central Prince William Sound (PWS), and in the PWS nearshore areas. Intrusion of Gulf of Alaska (GOA) water into PWS was indicated in June 1996, but not in June 1994 or 1995. In September, the Sound seems to be sealed off from the GOA entirely. The dominant circulation feature in September is the cyclonic gyre in the central Sound. A mooring deployed at Hinchinbrook Entrance showed that the summer months were characterized by outflow above 150m and inflow below. The fall and early winter months were characterized by inflow above 150m and weak outflow below. Late winter and early spring months were characterized by more barotropic flows. Spring of 1996 was the most productive year for zooplankton in the Sound. Warming and stratification started earlier in 1996 than in 1995. Stratification was greater in May 1996 than in May of either 1995 or 1997. In May 1996, there were greater numbers of zooplankton and less fluorescence than in May 1997. In the nearshore regions of PWS, fjords generally exhibited greater vertical stratification from both heat and freshwater input, while bays became only partially stratified. Tidal currents within bays and fjords appear to be influenced by the relative strength of tidal flows within passes outside the respective basins. Locations with strong surface inflows from these sources may exhibit frontal zones caused by convergence with outflows from within the bay.

**Key Words:** physical oceanography, temperature, salinity, circulation, Prince William Sound.

**Citation:** Vaughan, S.L., S.M. Gay, L.B. Tuttle, and K.E. Osgood, 1998: SEA: Observational Oceanography in Prince William Sound. *Exxon Valdez* Oil Spill Restoration Project Annual Report (Restoration Project 96320-M), Prince William Sound Science Center, Cordova, Alaska, 99574.

# Circulation in Prince William Sound from Satellite Tracked Drifting Buoys

by

Shari L. Vaughan

Presented at the AAAS 48th Arctic Division Science Conference
September 24-27, 1997 in Valdez, Alaska

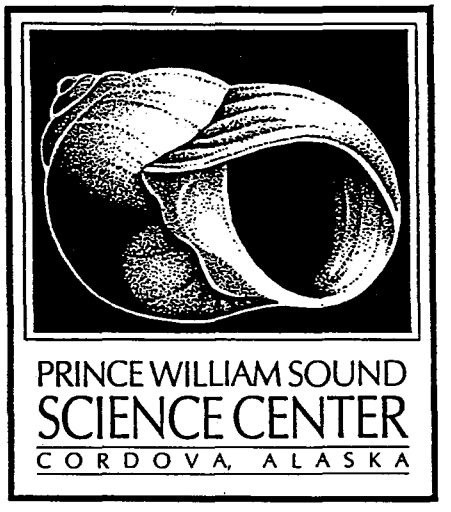


Prince William Sound Science Center
P. O. Box 705
Cordova, Alaska 99574

February 1998

**Technical Report No. 9801**

## Introduction

ARGOS satellite tracked drogued drifting buoys provide near real time visualization of ocean current velocity structure. Other advantages include autonomous data collection (no vessel requirements), and unambiguous interpretation of results. Five ARGOS drifters were deployed in Prince William Sound (PWS), Alaska, as part of the Sound Ecosystem Assessment program sponcered by the Exxon-Valdez Oil Spill (EVOS) Trustee Council. Two were released near Hinchinbrook Entrance (Figure 1) in 1996, and three were released in the central Sound in 1997. While many more than 5 trajectories are required to make statistically sound conclusions about probable flow patters, these drifter paths document some interesting features of the circulation, which are presented here.

The drifters are ClearSat-GPS WOCE drifters manufactured by Clearwater Instrumentation, Inc. They consist of a roughly 20 inch diameter surface float with a radio antenna mounted on top, and a canvas drogue connected to the bottom (Figure 2). The buoy houses the electronics and provides floatation. The antenna communicates the buoy's position to a satellite (operated by the French company ARGOS), which relays the information to an ARGOS service and data distribution center. Roughly hourly position updates are delivered by the service center to the user via email. A roughly 7 meter long, 1 meter diameter hollow cylindrical drogue is connected to the underside of the surface buoy by a roughly 9 meter long coated wire cable and a 2.5 meter long tether. A smaller shock absorbing buoy is connected in between. This design allows the drifter to follow currents at depths of roughly 9 to 16 meters (about 30 to 50 feet) without contamination by near surface wind induced flow.

In this report, 4 of the 5 drifter paths are presented. One of the two 1996 releases (25651) stopped transmitting a few days after deployment, probably due to damage from a collision with a vessel. For clarity in the trajectory figures, positions are plotted approximately every 12 hours (about 1200 and 2400 GMT), although many more positions are available. This means the spacing between positions is roughly proportional to the speed of the drifter (farther spacing means faster flow). The initial release position is shown as a larger, lighter colored dot. Release dates, the date of the last transmission, and the approximate record length are shown in the table below.

| Drifter | Released | End of Record | Length of Record |
|---|---|---|---|
| 25651 | August 2, 1996 | August 5, 1996 | 3 days |
| 25652 | August 2, 1996 | September 12, 1996 | 6 weeks |
| 25653 | May 8, 1997 | November 24, 1997 | 6.5 months |
| 25654 | May 8, 1997 | September 30, 1997 | 4.7 months |
| 25655 | July 15, 1997 | October 23, 1997 | 3.2 months |

## Results

Drifter 25652 deployed in Hinchinbrook Entrance (Figure 3) in August 1996 exited PWS about 3 days after deployment. It moved southwestward then westward past southern Montague Island. It continued moving southwestward past the Kenai Peninsula, making a large anticyclonic loop south of Aialik Bay. It entered Cook Inlet at Stevenson Entrance, and continued moving southwestward. It stopped transmitting in Shelikof Strait near the southern end of Kodiak Island.

Drifter 25653 was released in central PWS in May 1997. The entire path is shown in Figure 4a. Due to the complexity of the trajectory, positions before and after September 17 are shown in Figure 4b and 4c. Drifter 25653 moved north initially and spent roughly 10 days in Valdez Arm (Figure 4b). It then returned to the central Sound and remained motionless for several days before curving in an anticyclonic path to the west. It moved slowly through the western Sound, being retained for several days in the nearshore regions of Perry Island, Dangerous Passage, Icy Bay, Whale Bay, and northern Latouche Passage. The drifter transited to southern Montague Strait east of Latouche Island, where it reversed direction and traveled north through Montague Strait (8/25 - 9/4). It crossed Hinchinbrook Entrance and moved north past Hinchinbrook Island to Orca Bay. After about 2 weeks in Orca Bay, the drifter moved northward again to Valdez Arm, stopping at Knowles Head, Bligh Island, and Rocky Point. From there it moved southwestward and quickly southward through Knight Island Passage. It entered Bainbridge Passage from the north and moved through to Port Bainbridge. It remain near the head of Port Bainbridge until it stopped transmitting on November 24, 1997.

Drifter 25654 was released in central PWS in May 1997 roughly 4 miles west of drifter 25653. The entire path is shown in Figure 5a, with paths before and after July 29 shown in Figures 5b and 5c for clarity. Drifter 25654 moved west initially passing south of Naked Island (Figure 5a). It made 2 cyclonic circulations over the deep basin known as the 'Black Hole'. From there it proceeded south through Knight Island Passage to southern Montague Strait where it, like drifter 25653, reversed direction and moved north through Montague Strait (6/21 - 6/26). Drifter 25654 exited the Sound on 6/27 and moved eastward south of the Copper River Flats, making two cyclonic revolutions before almost reaching Kayak Island. Just west of Kayak Island, it made 3 cyclonic revolutions, and a fourth revolution farther to the west. It started moving rapidly westward on about August 12. It passed southern Montague Island and then curved northward entering Montague Strait. It again traveled north through Montague Strait (8/23 - 9/4) and exited PWS at Hinchinbrook Entrance, but this time moved southwestward past Montague Island. It proceeded westward south of the Kenai Peninsula, similar to drifter 25652, and entered Cook Inlet at Kennedy Entrance (not shown). It stopped transmitting near Augustine Island in Cook Inlet on September 30, 1997.

Drifter 25655, released July 15, 1997 in the central Sound, moved westward and spent several days south of Naked Island (Figure 6). It then returned to the central Sound and made two cyclonic circulations. Afterward, it moved toward Smith Island and then south to Montague Point. It entered Zaikof Bay on September 9 and remained there until it was retrieved on October 23, 1997.

## Discussion

Drifters 25651, 25652 and 25654 indicated that in the summer and early fall 1996 and 1997, southward flow is present in the upper (9 - 16 meter) layers at Hinchinbrook Entrane. Drifters 25653 and 25654 showed northward flow through Montague Strait in late August and early September 1997. Drifter 25654 also showed northward flow through Montague Strait in June 1997. Using data from 1977 to 1979, Niebauer et al (1994) found that in all months the vertically integrated mean monthly transports were into the Sound at Hinchinbrook Entrance and out of the Sound at Montague Strait. Closer inspection of their moored current meter velocities reveals periods of southward flow at Hinchinbrook Entrance

and northward flow at Montague Strait.

Drifters 25653 and 25655 suggest that cyclonic circulation was present in the central sound in the summer of 1997. Drifter 25654 showed cyclonic circulation over the 'Black Hole' in late spring and summer 1997. Retention in several nearshore areas (most strongly in Zaikof Bay) was suggested by drifters 25653 and 25655.

Although this experiment was designed to capture the circulation patterns of PWS, 2 drifters escaped and provided some information on the circulation outside the Sound. Westward flow past the Kenai Peninsula was documented by drifters 25652 and 25654. Drifter 25654 first showed eastward flow with some large eddies south of the Copper River Flats, and then flow to the west. This drifter also documented the existance of one or more cyclonic eddies west of Kayak Island. An eddy at this location has been documented previously using drifters and hydrography (e.g. Royer, Hansen, and Pashinski, 1979), but with anticyclonic rotation. Closer inspection of the drifter tracks in Royer, Hanson, and Pashinski does reveal cyclonic circulation in one case (their drifter 1142). Multiple dipole eddies shed from Kayak Island have also been observed in satellite images (Ahlnas, Royer, and George, 1987).

## References


Ahlnas, K., T.C. Royer, and T.H. George, 1987: Multiple Dipole Eddies in the Alaska Coastal Current Detected With Landsat Thematic Mapper Data. *J. Geophys. Res.*, **92**, C12, pp 13,041-13,047.

Niebauer, H.J., T.C. Royer, and T.J. Weingartner, 1994: Circulation of Prince William Sound, Alaska. *J. Geophys. Res.*, **99**, C7, pp 14,113-14,126.

Royer, T.C., D.V. Hansen, and D.J. Pashinski, 1979: Coastal Flow in the Northern Gulf of Alaska as Observed by Dynamic Topography and Satellite Tracked Drogued Drift Buoys. *J. Phys. Oceanog.*, **9**, 4, pp 785-801.

Figure 1: Map of Prince William Sound.

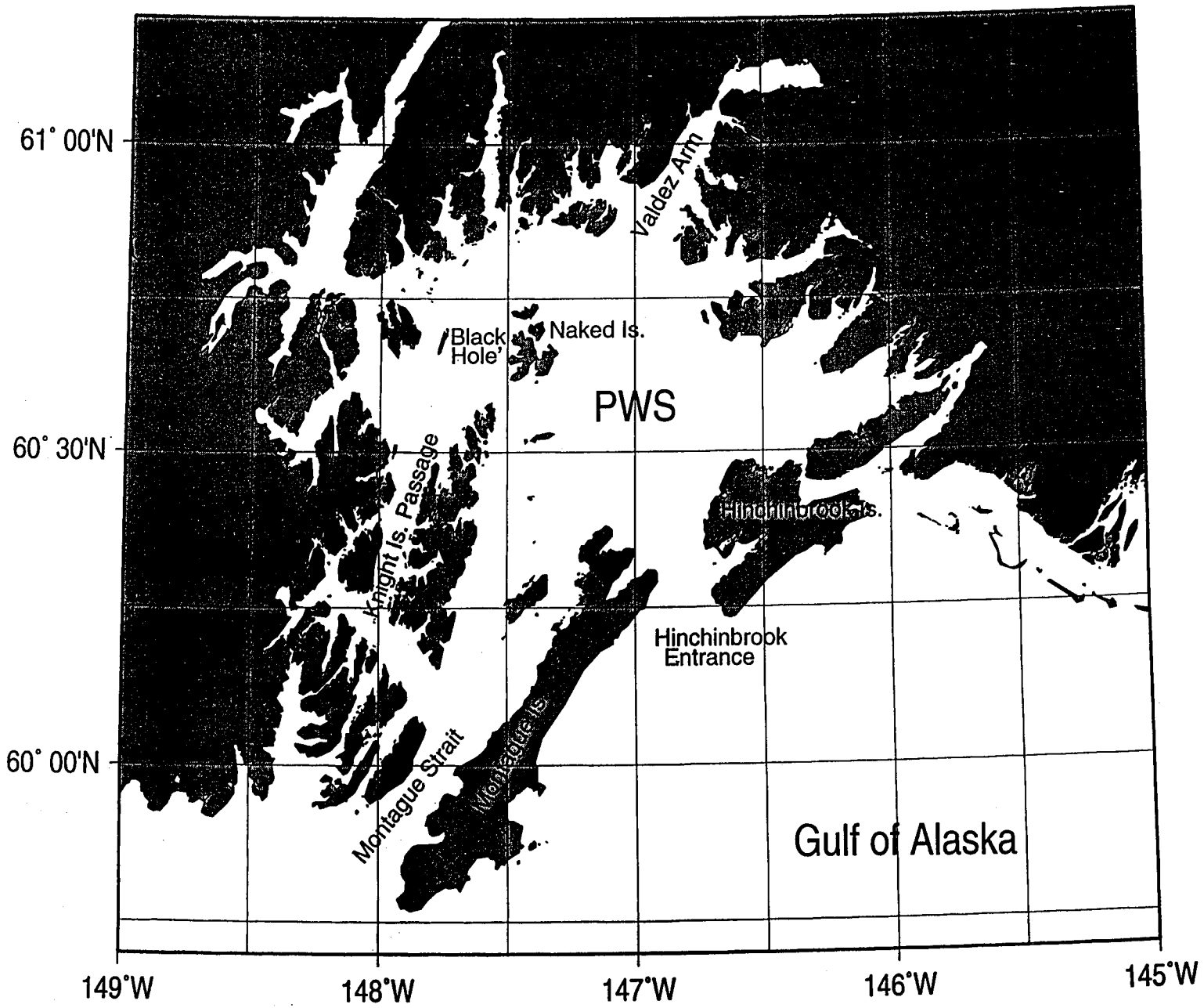

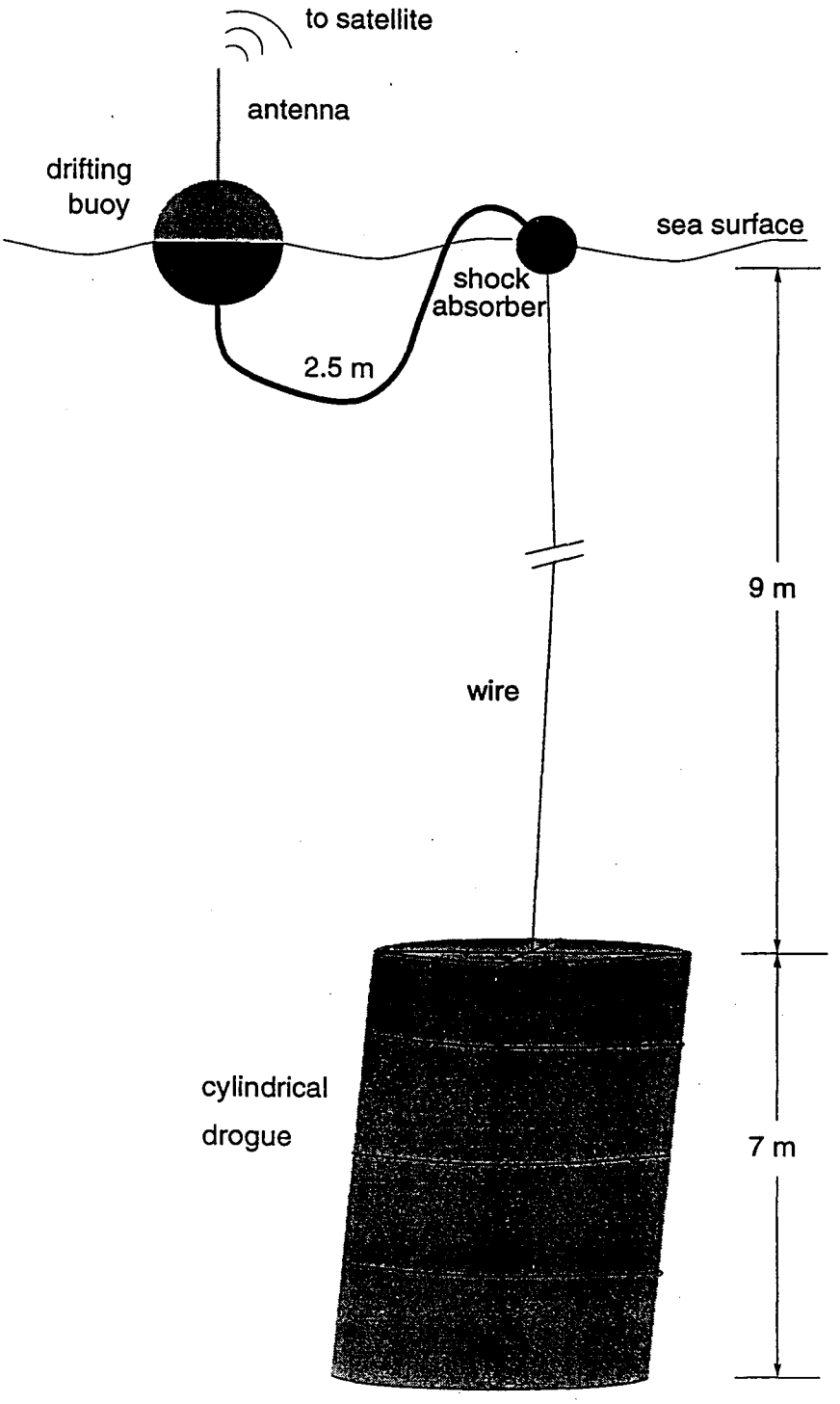


Figure 2: Schematic diagram of satellite tracked drifting buoy.

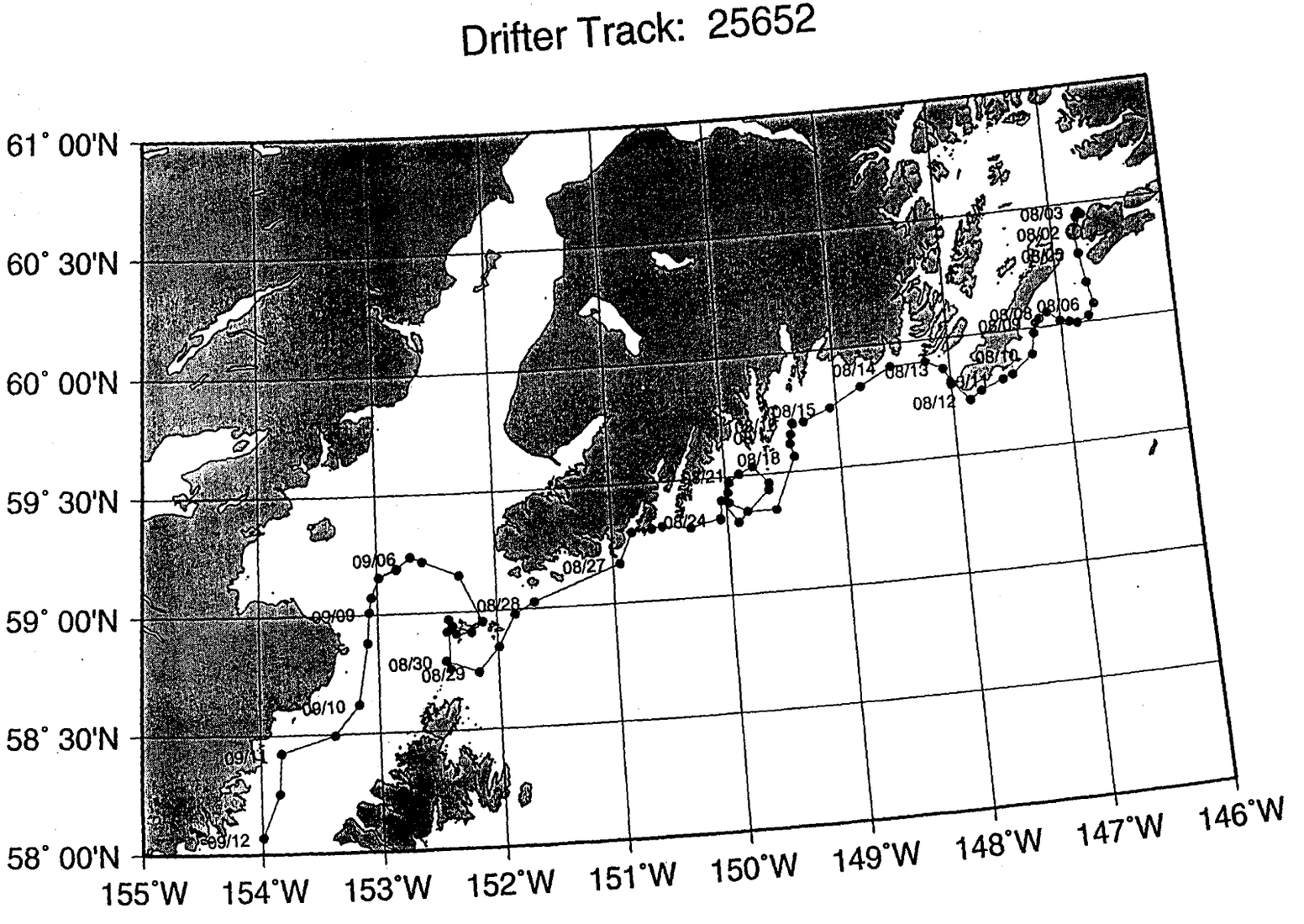


Figure 3: Entire track of drifting buoy 25652, drogued at 9 to 16 meters. Positions are plotted approximately every 12 hours.

# Drifter Track: 25653

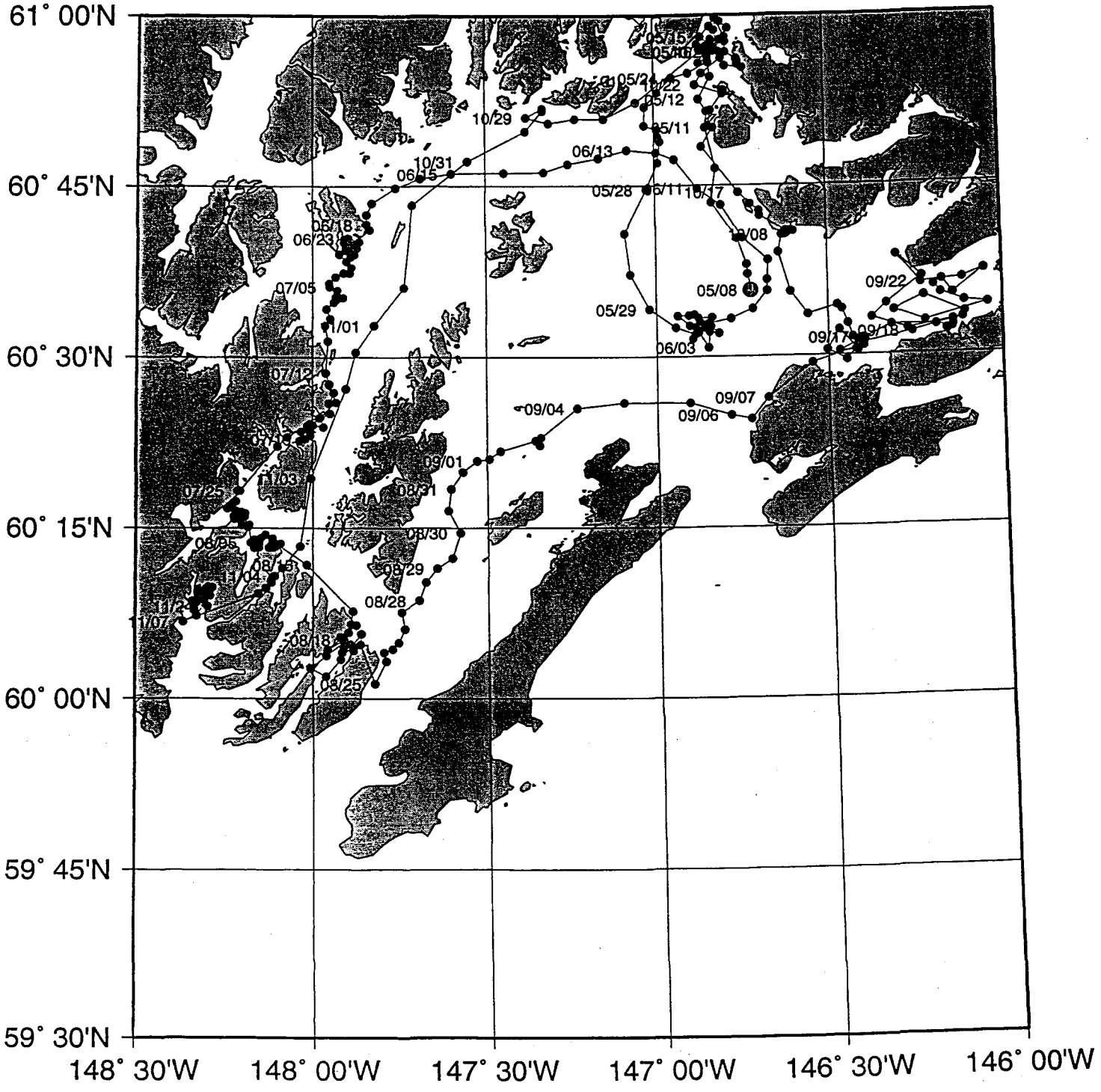


Figure 4a: Entire track of buoy 25653, drogued at 9 to 16 meters. Positions are plotted approximately every 12 hours.

# Drifter Track: 25653

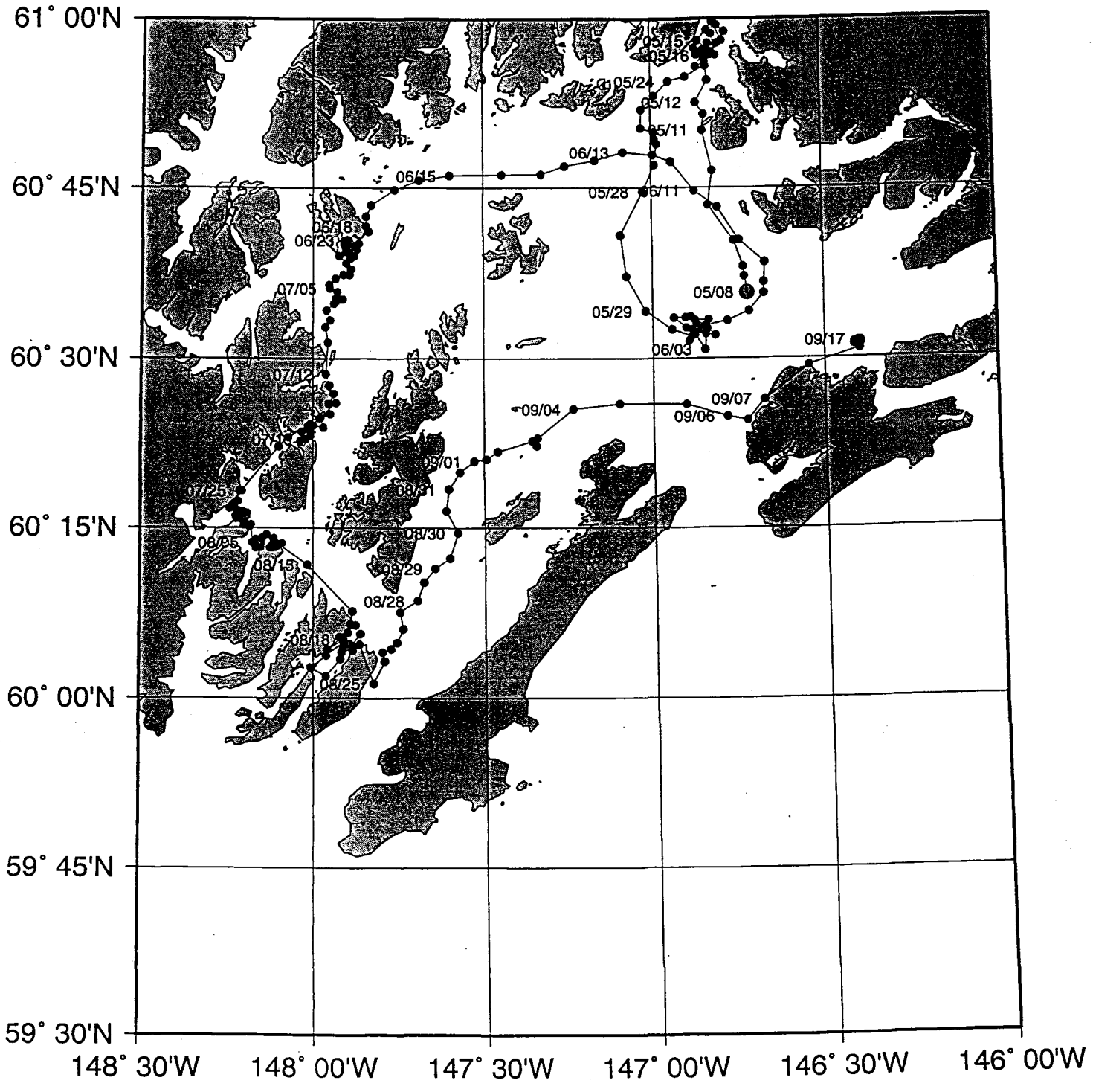


Figure 4b: Track of buoy 25653 from May 8 to September 17, 1997. Positions are plotted approximately every 12 hours.

# Drifter Track: 25653

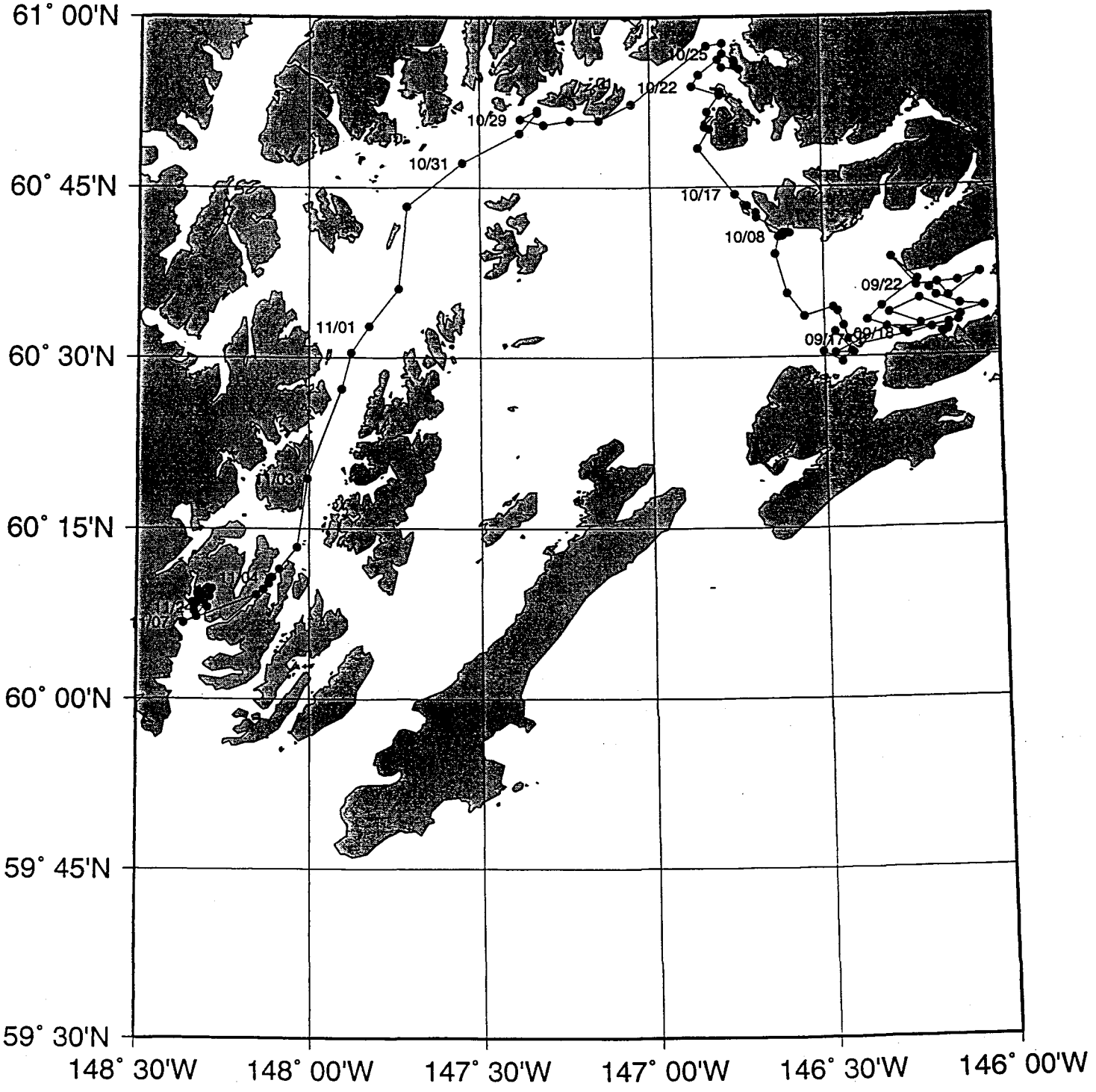


Figure 4c: Track of buoy 25653 from September 17 to November 24, 1997. Positions are plotted approximately every 12 hours.

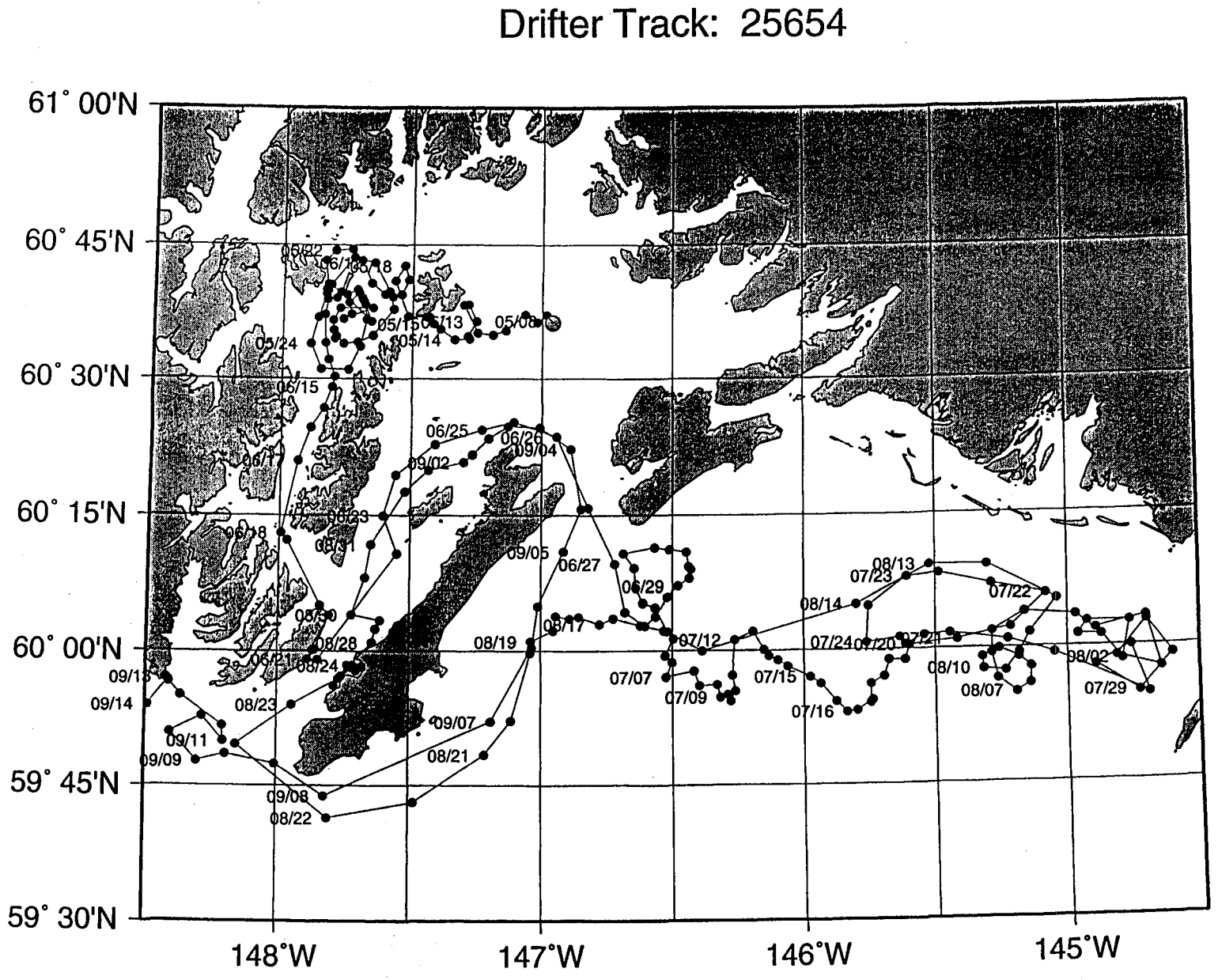


Figure 5a: Entire track of buoy 25654, drogued at 9 to 16 meters.
Positions are plotted approximately every 12 hours.

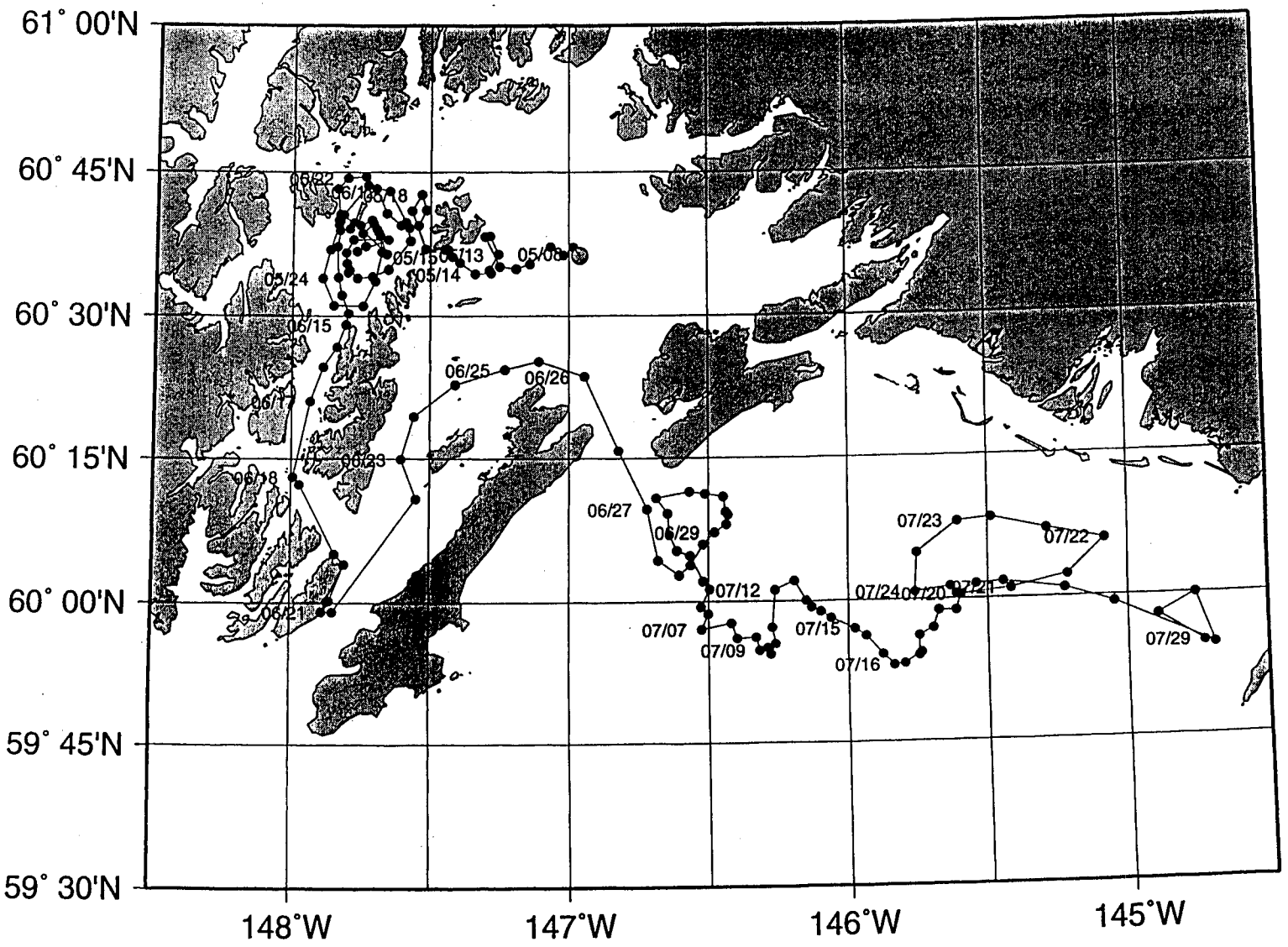


Figure 5b: Track of buoy 25654 from May 8 to July 29, 1997.
Positions are plotted approximately every 12 hours.

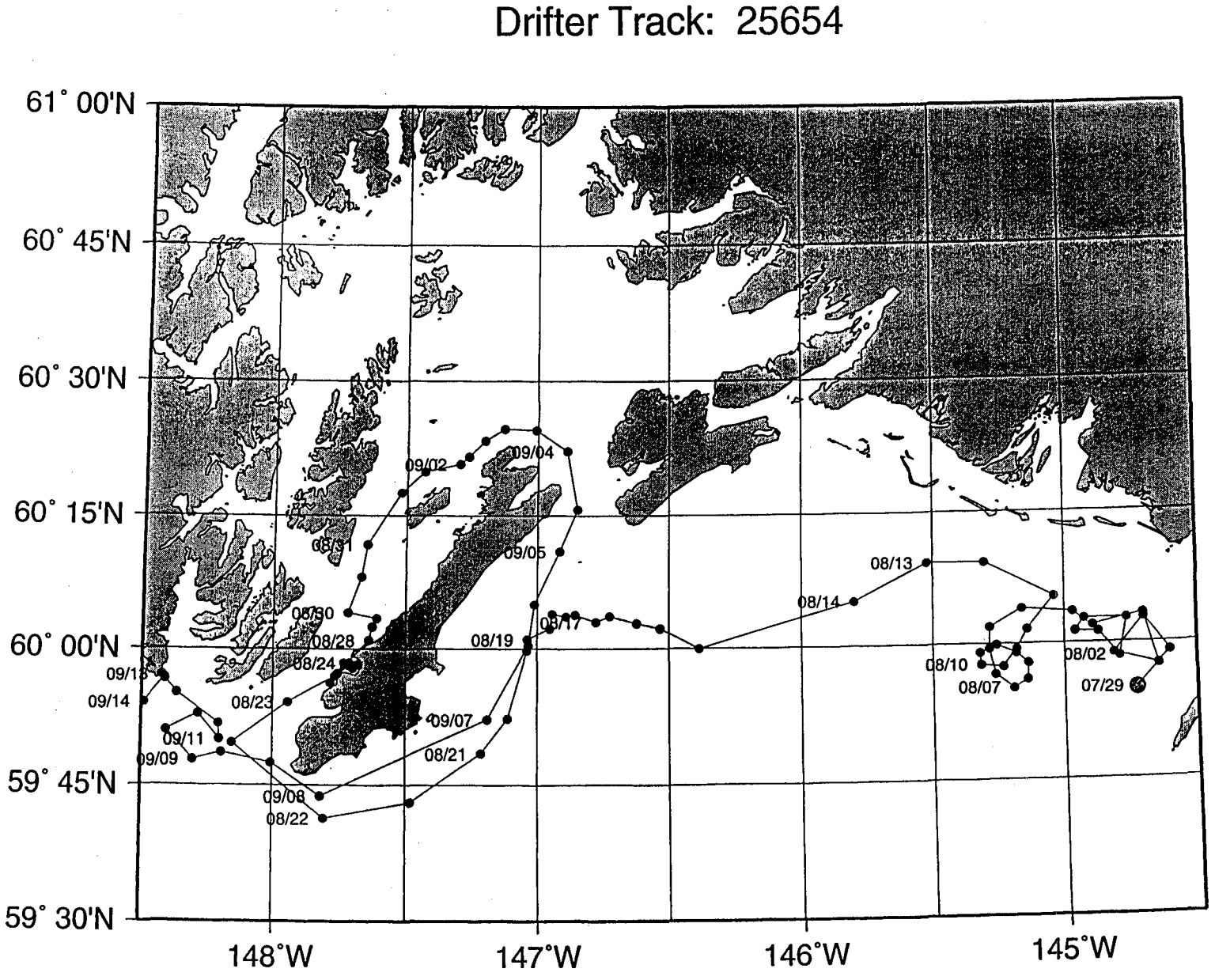


Figure 5c: Track of buoy 25654 from July 29 to September 14, 1997. Positions are plotted approximately every 12 hours.

# Drifter Track: 25655

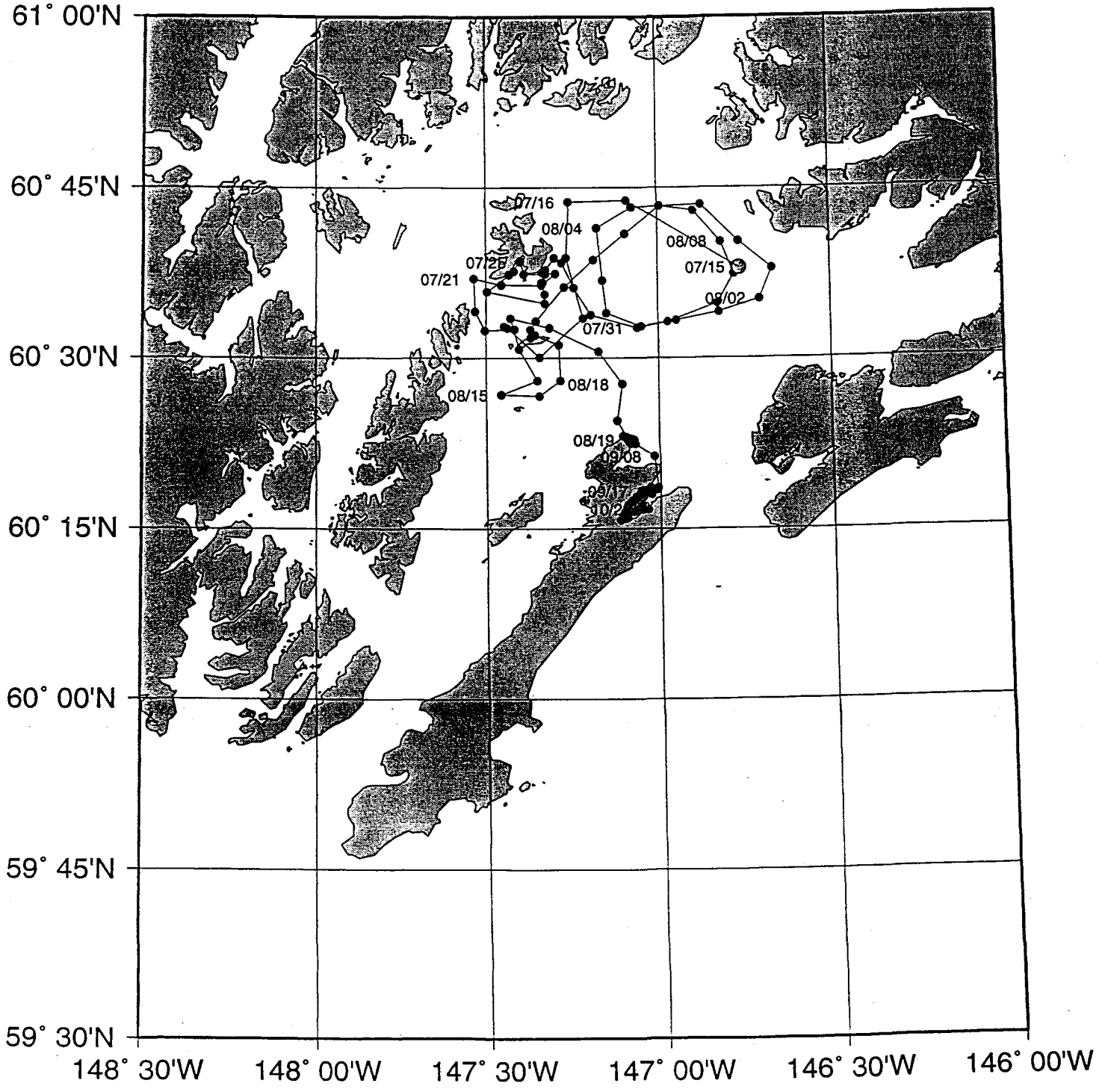


Figure 6: Entire track of buoy 25655, drogued at 9 to 16 meters. Positions are plotted approximately every 12 hours.

DRAFT

# Upper Layer Circulation and Water Mass Variability in Prince William Sound, Alaska

S.L. Vaughan, L.B. Tuttle, K.E. Osgood, and S.M. Gay
Prince William Sound Science Center

## Introduction

Prince William Sound (PWS), Alaska is a shallow (mostly $\leq$ 350 m) estuarine, subarctic sea, surrounded by mountains, numerous fjords, and coastal rivers (e.g. Muench and Schmidt, 1975). The circulation within the Sound is generally cyclonic, with water entering from the Gulf of Alaska (GOA) through Hinchinbrook Entrance, and exiting through Montague Straight (Niebauer, Royer and Weingartner, 1994; Royer, Hansen and Pashinski, 1979). Seasonal changes in wind forcing and precipitation produce departures from this general pattern. Light westerly winds in the summer are replaced by strong easterlies in the winter. This reversal modulates the volume of Gulf of Alaska water entering Prince William Sound. Fresh water input, a combination of precipitation and snow melt/river runoff, reaches a maximum in fall and a minimum in spring (e.g. Royer, Hansen, and Pashinski, 1979). The upper layer density structure of the Sound responds to both types of variability.

PWS is also a region of high biological production, and supports a large Alaskan salmon fishery. Oil tankers transverse this region regularly and pose a finite risk in the event of a spill, yet little is know about the seasonal and interannual changes in the physical and biological conditions. The devastation caused by the 1989 Exxon-Valdez oil spill demonstrated the need for a comprehensive description of the seasonal variability of the circulation and water mass properties of PWS, in relation to plankton and nekton distributions.

In 1993, the Exxon-Valdez Oil Spill (EVOS) Trust Council funded a comprehensive ecosystem study called the Sound Ecosystem Assessment (SEA). A main goal of the physical oceanographic part of the SEA program was to identify the physical processes that influence the production of two commercially harvested species, pink salmon and Pacific herring. It was hypothesized that food (zooplankton) was the dominant limiting factor to growth and survival. Since phytoplankton and zooplankton biomass fields are closely coupled to the water mass properties of the surface layer, a specific goal was to document the monthly and seasonal upper layer water mass variability in Prince William Sound.

This paper examines the relation of the upper layer water mass properties and circulation to the fluorescence and zooplankton distributions in the spring and early summer of 1995 through 1997. Differences in the timing and intensity of vertical stratification formation appear to be the primary link.

## Data

Large scale hydrographic cruises were conducted in PWS in spring and summer months of 1995, 1996 and 1997. Cruise dates are shown below.

| 1995 | 1996 | 1997 |
|---|---|---|
| April 10-17 | April 15-21 | |
| May 4-11 | May 2-11 | May 7-13 |
| June 15-20 | June 15-21 | |

Station locations and transects for each cruise are shown in Figure 1. Measurements of temperature (T), salinity (S), oxygen, and current velocities were made with simultaneous measurements of fluourescence and zooplankton abundance. The hydrographic data was collected using a SeaBird 911 CTD. Conductivity, temperature, and oxygen as a function of pressure were recorded at 1 dbar intervals. Salinity was calculated from conductivity using standard SeaBird software. The CTD sensors were calibrated annually by SeaBird Electronics. The CTD salinities and oxygens were not calibrated with bottle samples because of minimal annual sensor drift rate. In December 1996 and May 1997, expendable CTDs (XCTDs) were used when conditions were too rough to use the CTD.

To relate temperature and salinity to zooplankton distributions and fluorescence (a proxy for phytoplankton), a combined instrument designed by Chelsea Instruments called an Aquashuttle was towed from the ship. The Aquashuttle consists of a Focal Technologies optical plankton counter (OPC), to count and size particles in the water, and a Chelsea Instruments Aquapack, which measures temperature, salinity, and fluorescence. The Aquashuttle is raised and lowered vertically from the surface to about 50 meters as it is towed, sampling continuously.

Instantaneous current velocity transects were collected using an RDI 150 kHz broadband acoustic Doppler current profiler (ADCP) deployed from the stern of the ship in a towed body. Most transects were in water less than 400 m depth so that bottom tracking was available. The bin length was 8 m for most of the data. The ADCP generally measured flows from about 20 m depth to the bottom.

The echo intensity data collected with the ADCP can be used to infer relative zooplankton abundance along the current velocity transects (e.g. Heywood et al, 1991; Roe and Griffiths, 1993). The ADCP measures the acoustic backscatter from particles in the water column. These particles are primarily zooplankton and micronekton. Due to the frequency of the ADCP, 150 kHz, the acoustic return is weighted towards larger zooplankton, including micronekton, euphausiids, amphipods and possibly large copepods. The range-corrected, relative backscatter intensity (Flagg and Smith, 1989) was calculated by averaging the echo intensity data for the ADCP's 4 beams and converting to relative backscatter intensity (dB) using the conversion factor supplied by RDI (San Diego, CA). The range correction was then applied, as described by Flagg and Smith (1989).

From an ADCP moored in Hinchinbrook Entrance it was observed that at times diel vertical migration contributed a large signal to the variability of the relative backscatter data. To segregate the effects of diel vertical migration from the relative backscatter data obtained with the towed ADCP, the data were categorized as day or night. Day was taken to be the period from 30 min after sunrise to 30 min before sunset. Night was considered

to be 30 min after sunset to 30 min before sunrise.

Meteorological data from C-MAN stations in PWS is available from the National Data Buoy Center (NDBC), and from a station at Middleton Island. The C-MAN stations are located at Bligh Reef, Potato Point, Seal Rocks, and Mid-Sound (in the central Sound). Wind speed, wind direction, wave height, barometric pressure, air temperature, water temperature, dew point temperature, and visibility are measured every 30 minutes. The C-MAN stations became operational in May 1995, but May and June records are incomplete. The Middleton Island data will be used for 1995, and the Mid-Sound data will be used for 1996 and 1997.

## Physical Properties

*April 1995 and 1996*

South to north sections of temperature (T), salinity (S), potential density ($\sigma$), and Brunt-Vaisala frequency ($N^2$) are shown for April 1995 (Figure 2(a) and (b)) and April 1996 (Figure 3(a) and (b)). Upper layer stratification is present by April 1996 in the central and northern Sound, but 1995 still is well mixed down to 20m. The temperature minimum layer volume (3.8 isotherm) is larger in 1995 than in 1996. A density front is present between CS12 and NS4 in April 1996.

Contours of temperature and salinity averaged over the upper 20m layer are shown for April 1995 (Figure 4(a) and (b)) and April 1996 (Figure 5(a) and (b)). Since potential density is mainly determined by salinity at these latitutes, only salinity is shown here. Temperature is more uniform in April 1995, and no contours less than 4.0 degrees are present. In April 1996, the 3.8 isotherm outcrops in the northern Sound, west of the vertical section in Figure 3. Variability in salinity exists in 1995 (Figure 4b), but does not appear in the vertical section (Figure 2(a)) because of the narrow range of station locations. Freshening as shown by the 31.4 isohaline, extends much farther south in 1995 than in 1996. A weak density front at around 60°30′N separates the cold, fresh northern waters from the warmer saltier southern waters (not shown). A dome of dense, high salinity water (31.8) is present north of Hinchinbrook Entrance in April 1996.

Wind speed and direction from April 1995 and April 1996 are shown in Figures 6(a) and (b). The cruise dates are highlighted. The April 1995 cruise had 2 wind bursts up to 15 m/s, while the April 1996 cruise was relatively calm. Wind forcing was at least partly responsible for the well mixed April 1995 structure.

*May 1995, 1996, and 1997*

South to north sections of temperature (T), salinity (S), potential density ($\sigma$), and Brunt-Vaisala frequency ($N^2$) are shown for May 1995, 1996, and 1997 in Figures 7, 8, and 9. May 1996 exhibits the warmest surface temperatures and the greatest stratification. The stratification is weaker in the south at CS12 (Figure 8(b)). Compared to 1995, the 25.2 isopycnal is much higher in the water column. The volume of the temperature minimum layer as indicated by the 4.0 isotherm, is the smallest of the 3 years in 1996.

A slight doming in the near surface (< 20m) isohalines and isopycnals appears in May

1995, centered around CFOS13 (Figure 7(a)). The stratification is weakest in the central Sound, with weak fronts to the south and north. The temperature minimum layer (4.0 isotherm) extends deeper than 100m.

In May 1997, a deep (30m) mixed layer exists in the central Sound (Figure 9(a)). Strong density fronts are present to the north and south. Maximum stratification is from 30-40m depth. This density structure is due to both temperature and salinity. The temperature minimum layer is warmer (T$\sim$ 4.2) and is located between roughly 60 and 100m (not shown).

Contours of temperature and salinity averaged over the upper 20m layer are shown for May 1995, 1996 and 1997 in Figures 10, 11, and 12. Warm ($T \geq 6.0$), fresh ($S \leq 31.0$) surface water has intruded at Hinchinbrook Entrance in May 1995 and 1997. Density fronts are associated with these inflows. Salinity is fairly uniform in 1996. Temperatures in 1996 are warmest in the north, probably due to sensible heating. In May 1997, the densest water (coldest and saltiest) is north of northern Montague Island. Temperatures of 5.0 or less are not present in either 1995 or 1996. Salinities greater than 31.6 are not present in the Sound in 1995, and are only present at Hinchinbrook Entrance and southern Montague Strait in 1996. Whether this is Gulf of Alaska inflow or upwelled deep water is uncertain.

Wind speed and direction from May 1995, 1996, and 1997 are shown in Figures 13(a)-(c). The cruise dates are highlighted. Wind bursts in excess of 15m/s occurred during the 1995 and 1997 cruises. Conditions in 1996 were calm. Reduced wind forcing in May 1996 was undoubtedly responsible for the large thermal surface stratification.

*June 1995 and 1996*

South to north sections of temperature (T), salinity (S), and potential density ($\sigma$) are shown for June 1995 and June 1996 in Figures 14 and 15. The water column is well stratified in both years, but more in the northern Sound in 1996. A density front is present near NS4 in 1996. The 25.0 isopycnal is higher in the water column in 1996 than in 1995. The temperature minimum layer (4.5 isotherm) is still present in June 1995.

Contours of temperature and salinity averaged over the upper 20m layer are shown for June 1995 in Figure 16 and June 1996 in Figure 17. Warm, fresh water has intruded from the Gulf of Alaska at Hinchinbrook Entrance in both years. Another source of fresh water is in the northwest Sound. June 1995 is fresher and colder than June 1996. The coldest and saltiest water in both years occured north of Montague Island, similar to what was seen in May 1997. It could be that conditions in 1997 were accelerated, with May 1997 resembling June months in other years.

Wind speed and direction from June 1995 and 1996 are shown in Figures 18(a) and (b). The cruise dates are highlighted. Conditions during both June cruises were calm.

## Biological Properties

Contours of the relative backscatter from 20 m for April 1995 (Figure 19(a)) indicate generally higher relative backscatter, and hence inferred zooplankton biomass, in the northern and western parts of PWS. This corresponds to the regions of colder, fresher water (Figures 4(a) and (b)). In April 1996 there was a region of lower relative backscatter roughly

coinciding with the dome of high salinity water just north of Hinchinbrook Entrance (Figures 19(a) and 5(b)). There was also generally higher backscatter from 20 m in central PWS in April 1996 than in April 1995. This may have been due to the earlier onset of the phytoplankton bloom and the subsequent earlier zooplankton biomass increase in 1996 compared with 1995. Stratification formation started earlier (Figures 2(b) and 3(b)), and the wind forcing was less (Figures 6(a) and (b)) in April 1996 than April 1995.

During May 1995 levels of relative backscatter were reduced in the central portion of the sound at 20 m (Figure 19(b)). This region coincides with the region of uplifted isohalines and isopycnals (weakened stratification) in the central sound (Figure 7(a)). There were also generally higher levels of backscatter in May 1995 than in April 1995 (indicative of the increase of the zooplankton biomass with the progression of the zooplankton bloom). During May 1997, the relative backscatter levels were reduced over most of PWS compared to May 1995 (Figure 19(b)). This may have been due to conditions in 1997 being accelerated, and the peak of the zooplankton bloom having already passed. There was no indication in the backscatter data of the intrusion of water at Hinchinbrook Entrance that was apparent in the May 1995 and 1997 temperature and salinity data.

The relative backscatter data from June 1995 indicate generally lower levels of zooplankton at 20 m in the northern portion of central PWS compared with the southern portion of the central sound (Figure 19(c)). The higher backscatter levels correspond to the slightly less stratified region of the sound (Figure 14(a)). In June 1996 there were also generally higher backscatter values from the southern, less stratified portion of PWS (Figures 19(c) and 15(a)). Less stratifcation may have lead to higher primary production, and hence more zooplankton. There is a slight indication that the warm, fresh water intruded from the Gulf of Alaska at Hinchinbrook Entrance is also water of elevated relative backscatter. Whether in increased backscatter in the southern portion of the Sound was primarily due to weakened stratification, or GOA inflow is unclear.

Panels of temperature, salinity, and fluorescence derived from the Aquapack, and particle distribution derived from the OPC, for May 1996 and May 1997 are shown in Figures 20(a) and (b). The tow track in May 1996 (Figure 20(a)) runs from south to north (left to right), roughly from station NS4 to CFOS13. The temperatures and salinities agree with those in Figures 8(a) and 9(a). Maximum values of fluorescence are found at a depth of 20 to 25m along or just below the pycnocline, with largest values (0.89) closer to CFOS13. A greater number of Neocalanus sized (1-4mm) particles (maximum 6.87) were associated with regions of lower fluorescence, possibly due to grazing by the zooplankton on the phytoplankton.

The tow track in May 1997 (Figure 20(b)) runs from north to south (left to right), roughly from station CFOS13 to NS4. The surface temperatures were cooler than in May 1996. Fluorescense was greater (2.15) over all depths than in May 1996, with the maximum near CFOS13. Zooplankton were fewer in number (maximum 2.5) and were scattered through more of the water column in May 1997 compared to May 1996.

## Conclusions

Warming and stratification started earlier in 1996 than in 1995. Stratification was greater in May 1996 than in May of either 1995 or 1997. In May 1996, there were greater numbers of zooplankton and less fluorescence than in May 1997. In May 1996, the low

numbers of phytoplankton in the stratified layer may have resulted from nutrients being depleted and not renewed. The deep mixed layer in May 1997 may have allowed phytoplankton growth and zooplankton dispersal.

The relative backscatter calculations also suggested that zooplankton abundance was reduced in May 1997, and that April 1996 values were increased. Backscatter was lower in the central Sound in May 1997 than in May 1995, and higher in April 1996 than in April 1995. Backscatter was also higher in May 1995 than in April 1995. Backscatter was high over the 'black hole' in the northwest Sound in June 1995. This maximum was not present in June 1996.

The spatial distribution of the zooplankton, as inferred from relative backscatter, changed seasonally. In April and especially May of both 1995 and 1997, more zooplankton were in the northern Sound, in regions of increased surface stratification. By June, more zooplankton were found in the southern Sound, in regions of reduced stratification. The movement of zooplankton from regions of high stratification to low stratification as the seasons progress is in agreement with theoretical primary productivity curve dynamics.

Spring of 1996 was the most productive year for zooplankton. May 1996 was unusually calm and warm. A strongly stratified surface layer formed. It is unclear whether the large number of zooplankton observed resulted from this mixed layer formation, or from favorable conditions in a prior season, like increased zooplankton abundance over the 'black hole' diapausing region in the previous June (1995).

## References


Flagg, C.N. and S.L. Smith, 1989: On the use of the acoustic Doppler current profiler to measure zooplankton abundance. *Deep-Sea Res.*, **36**, 3, pp 455-474.

Heyward, K.J., S. Scrope-Howe, and E.D. Barton, 1991: Estimation of zooplankton abundance from shipboard ADCP backscatter. *Deep-Sea Res.*, **38**, 6, pp 677-691.

Muench, R. D. and G. M. Schmidt, 1975: Variations in the Hydrographic Structure of Prince William Sound. IMS Report R75-1, 135pp.

Niebauer, H.J., T.C. Royer, and T.J. Weingartner, 1994: Circulation of Prince William Sound, Alaska. *J. Geophys. Res.*, **99**, C7, pp 14,113-14,126.

Roe, H.S.J. and G. Griffiths, 1993: Biological information from an Acoustic Doppler Current Profiler. *Mar. Biol*, **115**, 339-346.

Royer, T.C., D.V. Hansen, and D.J. Pashinski, 1979: Coastal Flow in the Northern Gulf of Alaska as Observed by Dynamic Topography and Satellite Tracked Drogued Drift Buoys. *J. Phys. Oceanog.*, **9**, 4, pp 785-801.

List of Figures

**Figure 16** : Mean (a) temperature and (b) salinity averaged over the upper 20m from June 1995.

**Figure 17** : Mean (a) temperature and (b) salinity averaged over the upper 20m from June 1996.

**Figure 18** : Wind speed and direction from (a) June 1995, and (b) June 1996.

**Figure 19** : Relative backscatter from 20m for (a) April 1995 and April 1996, (b) May 1995 and May 1997, and (c) June 1995 and June 1996.

**Figure 20** : Aquashuttle temperature, salinity, fluorescence, and particle size for (a) May 1996 and (b) May 1997.

# SEA Oceanography Cruise - June 1996

FIG. 1

9609

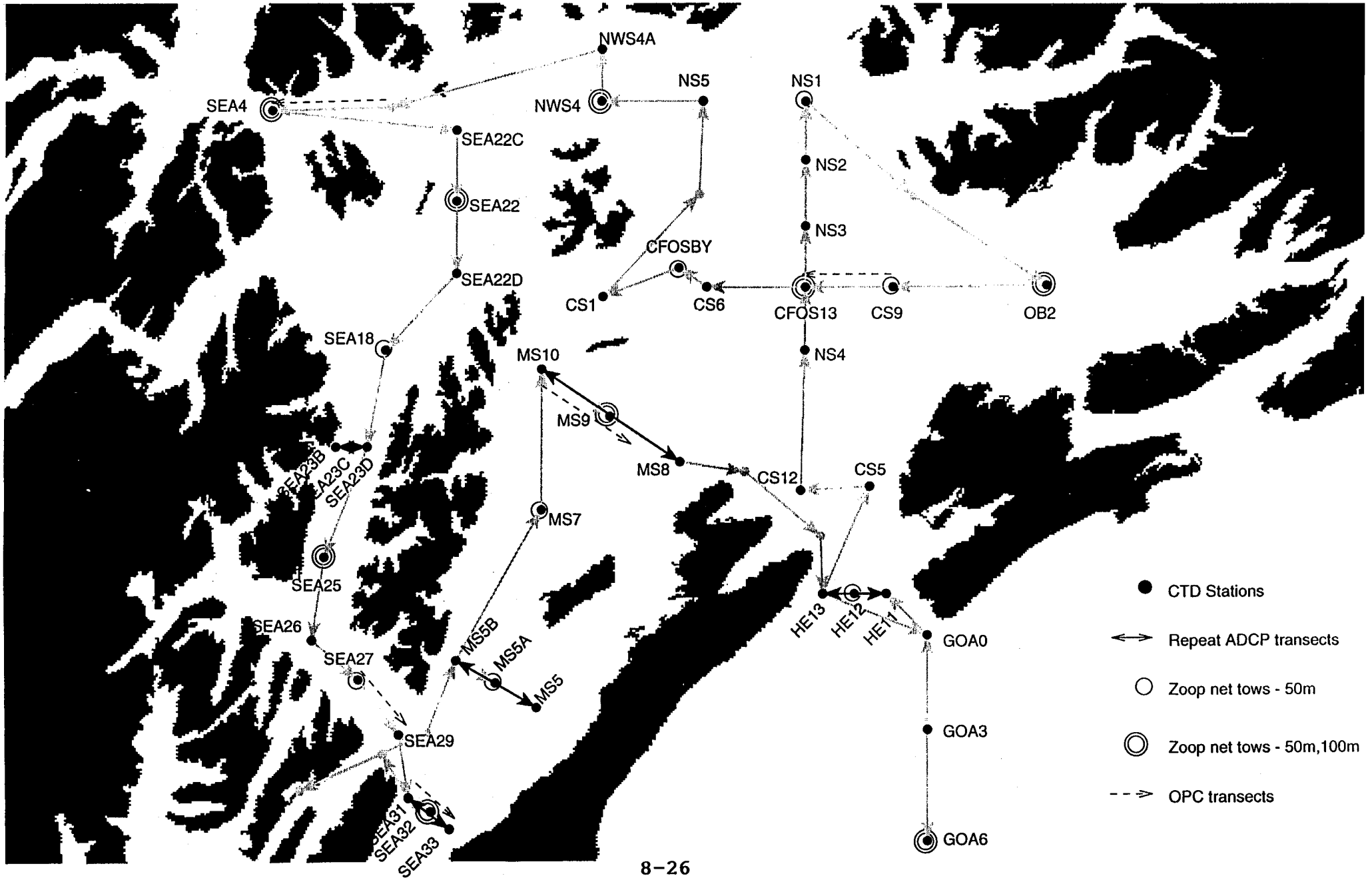

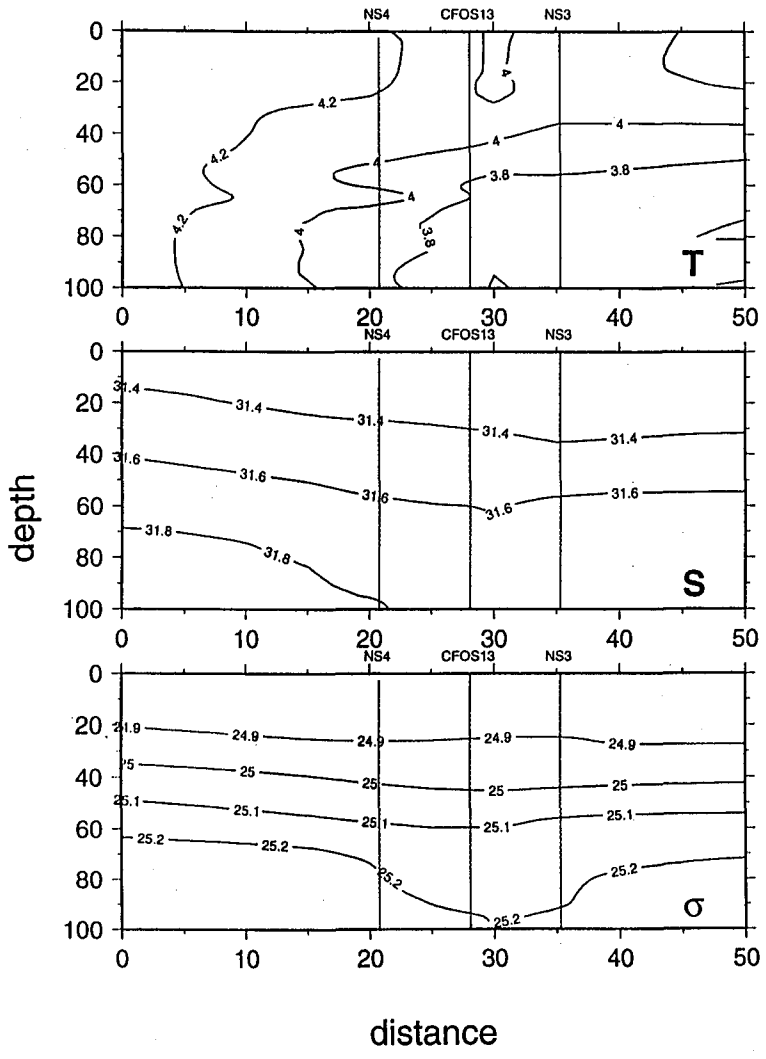
SNCS - be504
NS4
CFOS13
NS3
T
S
σ
depth
distance

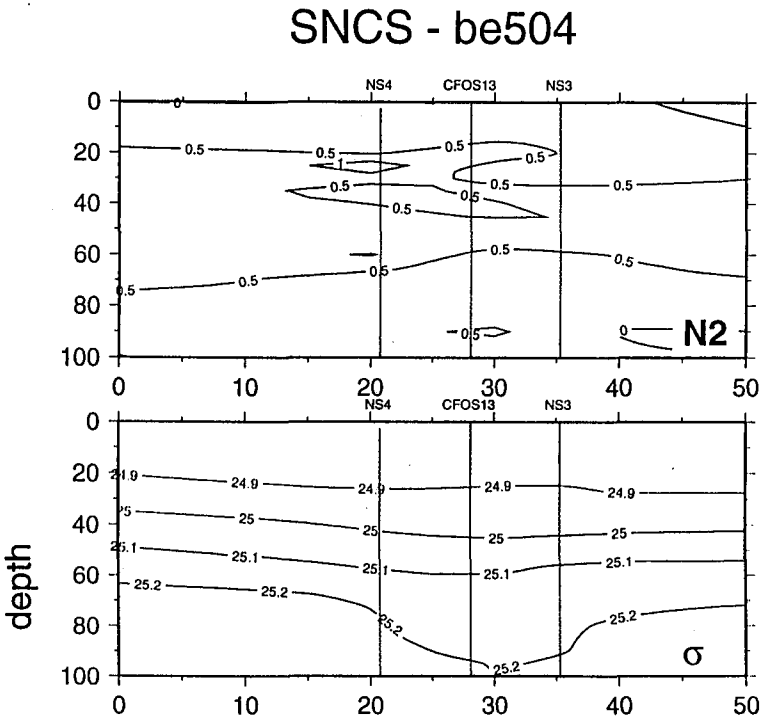
SNCS - be504
NS4
CFOS13
NS3
N2
σ
depth

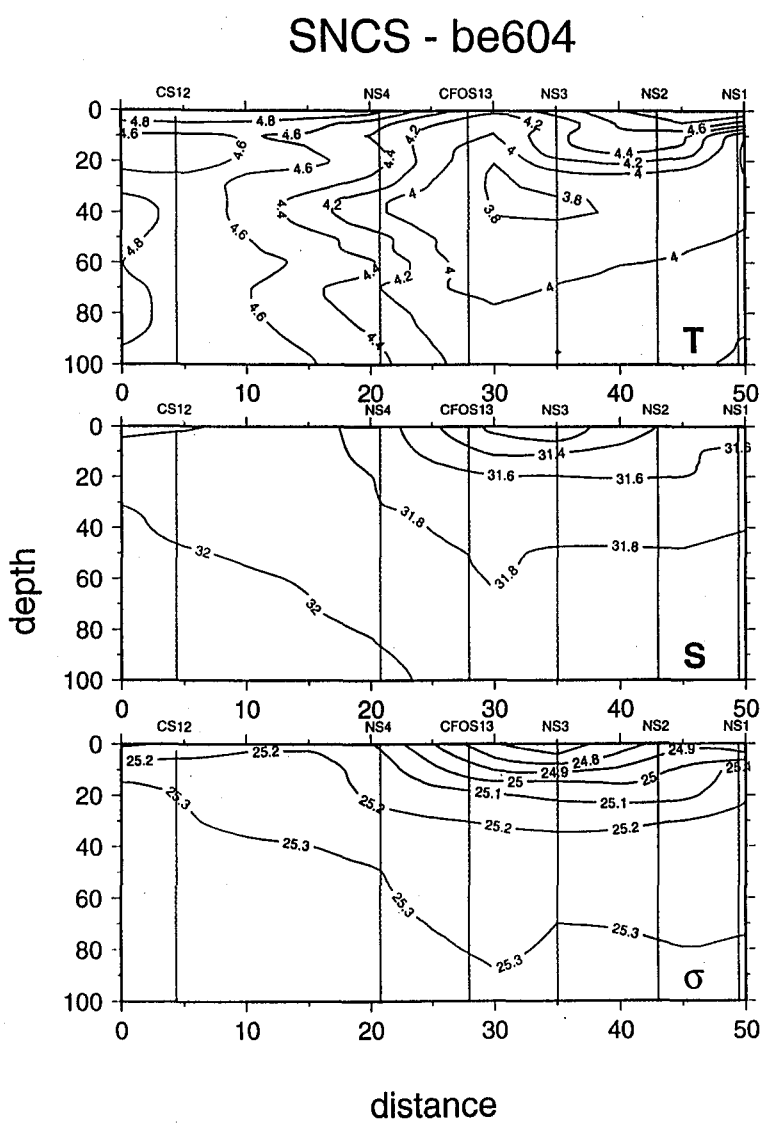
SNCS - be604
CS12
NS4
CFOS13
NS3
NS2
NS1
T
S
σ
depth
distance

Fig 3(L)

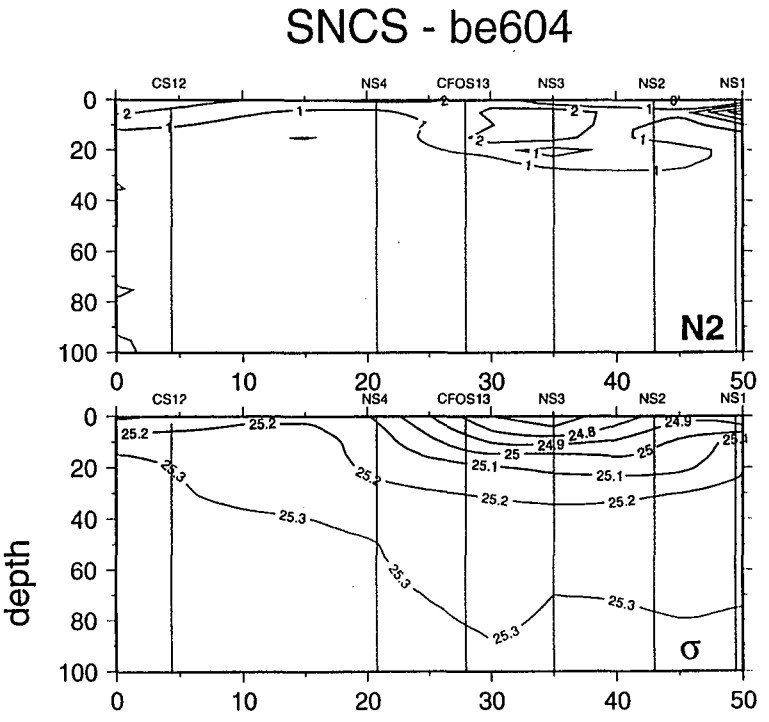
SNCS - be604
CS12
NS4
CFOS13
NS3
NS2
NS1
N2
σ
depth

Mean Temperature (001to020m) - be504

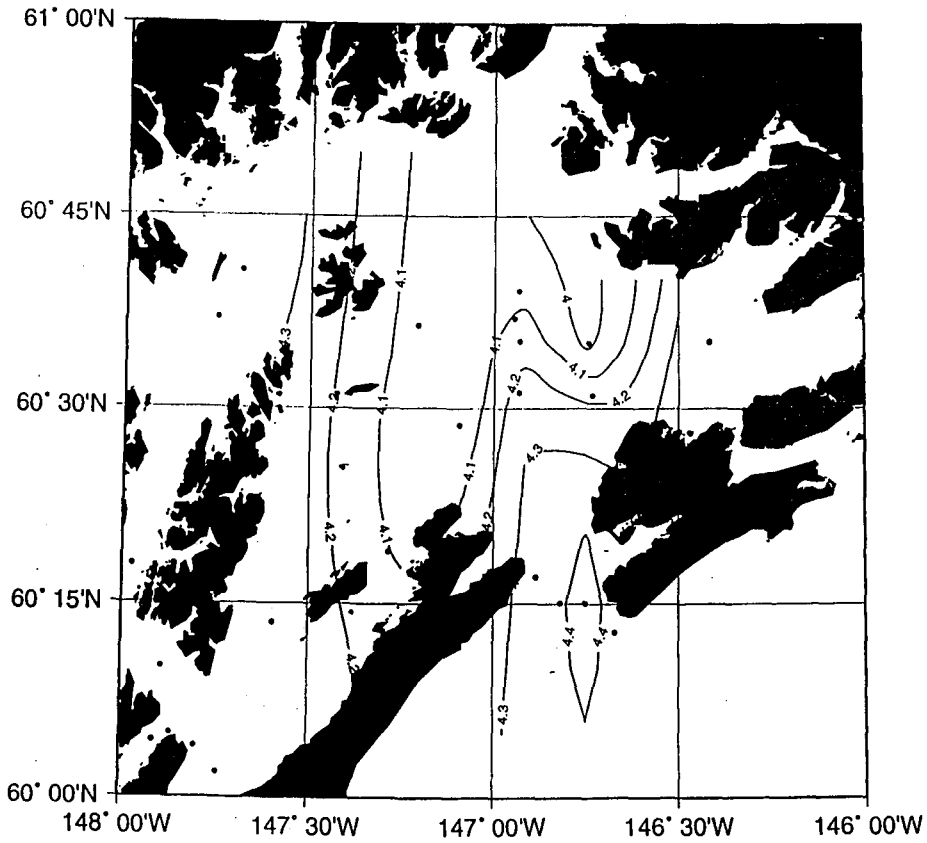


Mean Salinity (001to020m) - be504

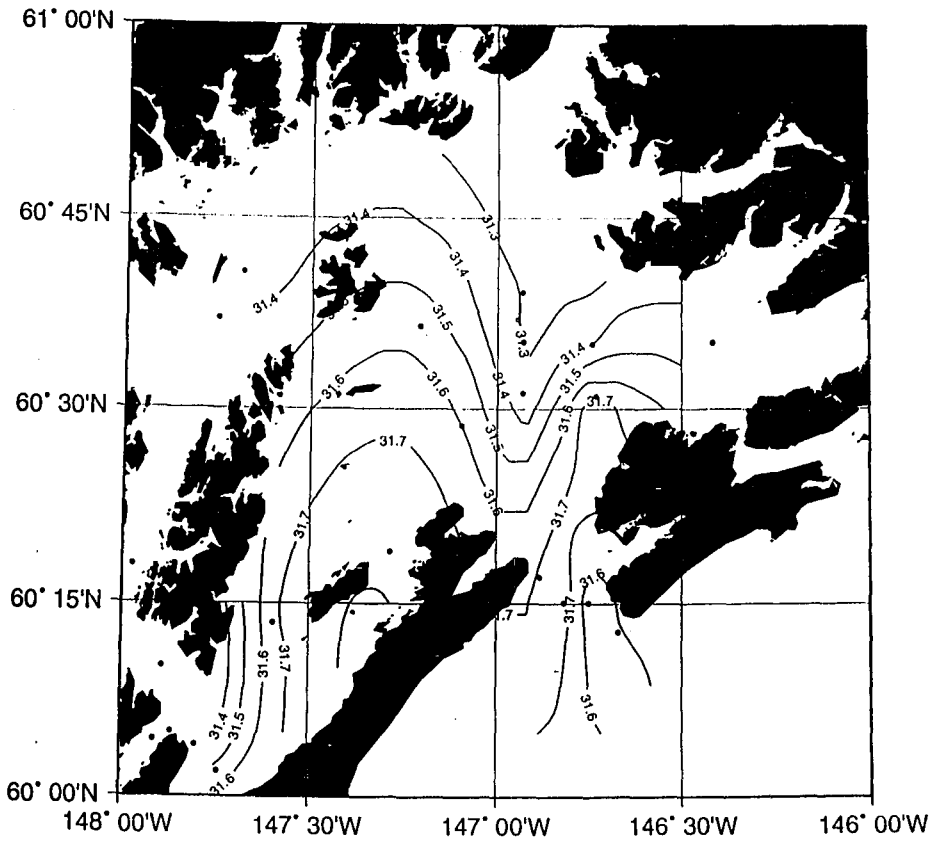

Mean Temperature (001to020m) - be604

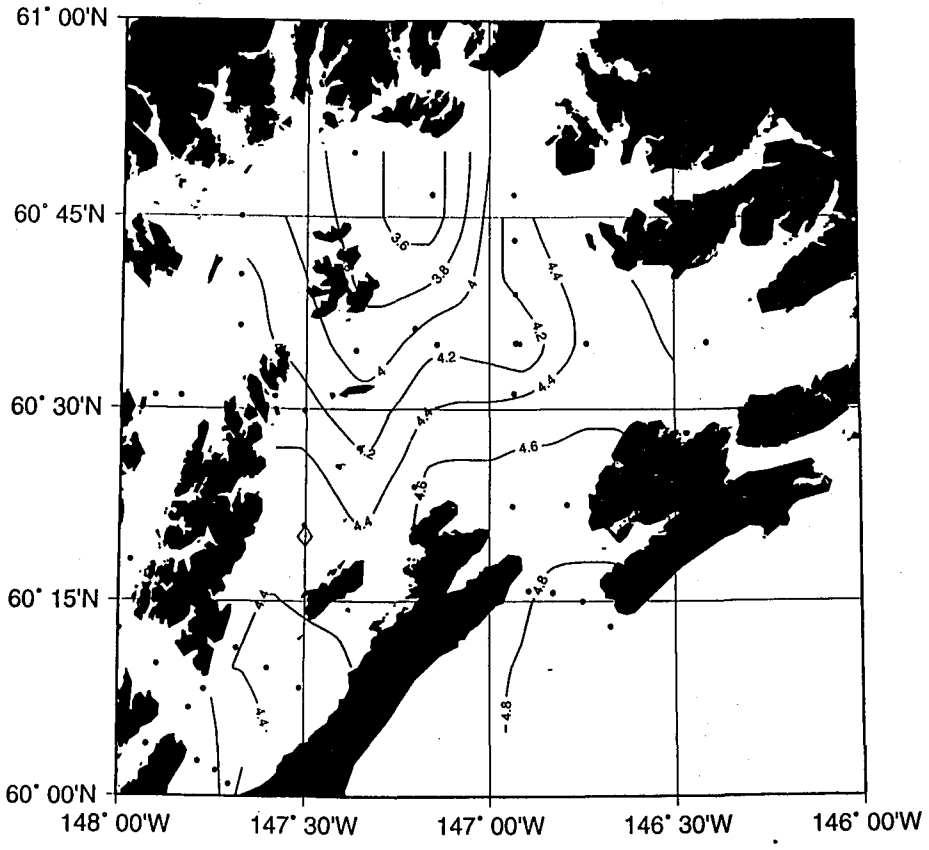


Mean Salinity (001to020m) - be604

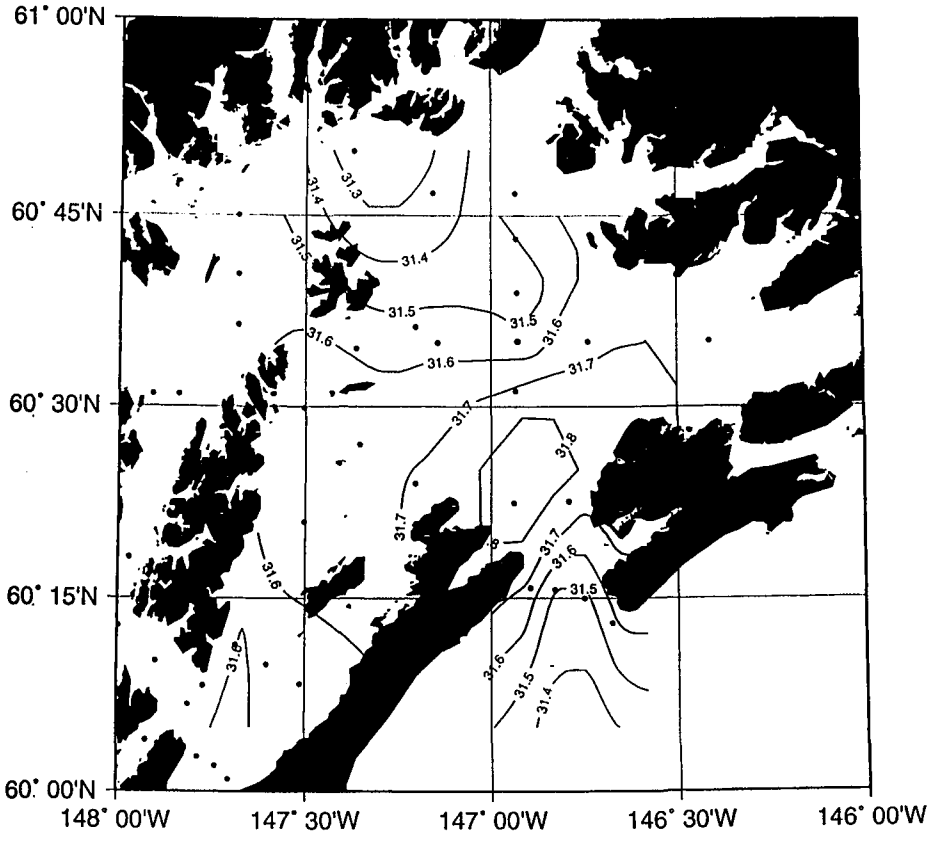

Fig 6(a)

## Middleton Island Wind - April - 1995

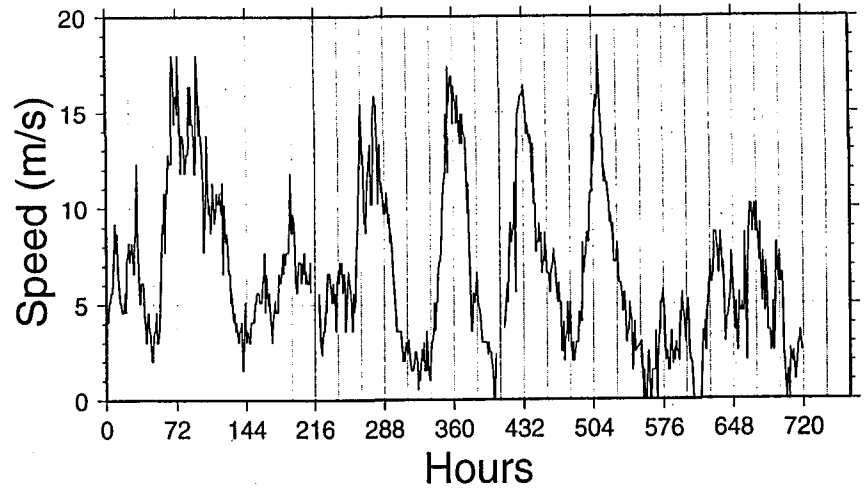


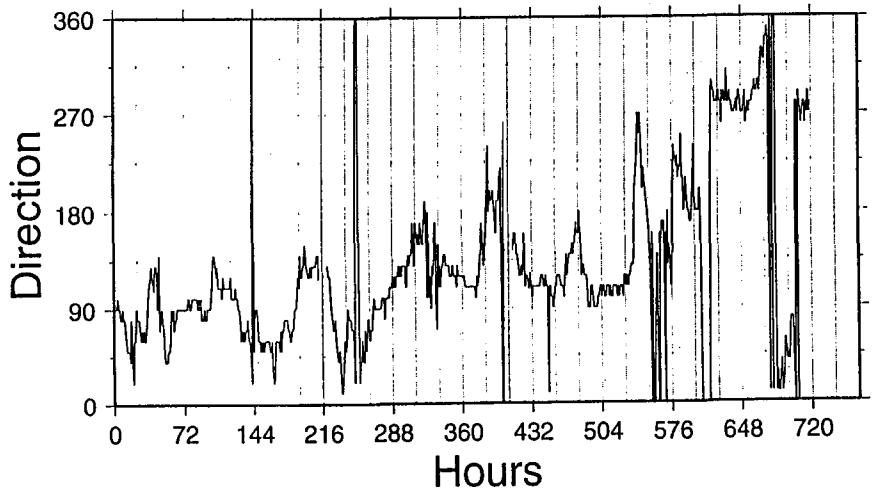


Fig 6(b)

## Mid-Sound Wind - April - 1996

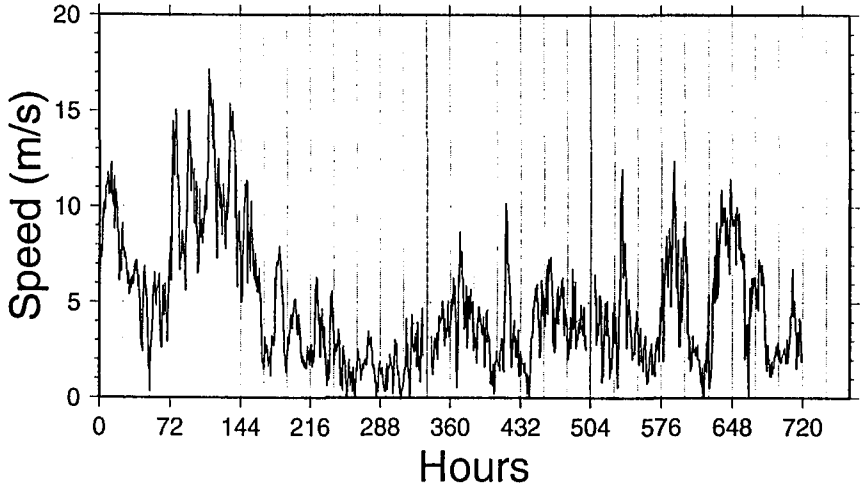


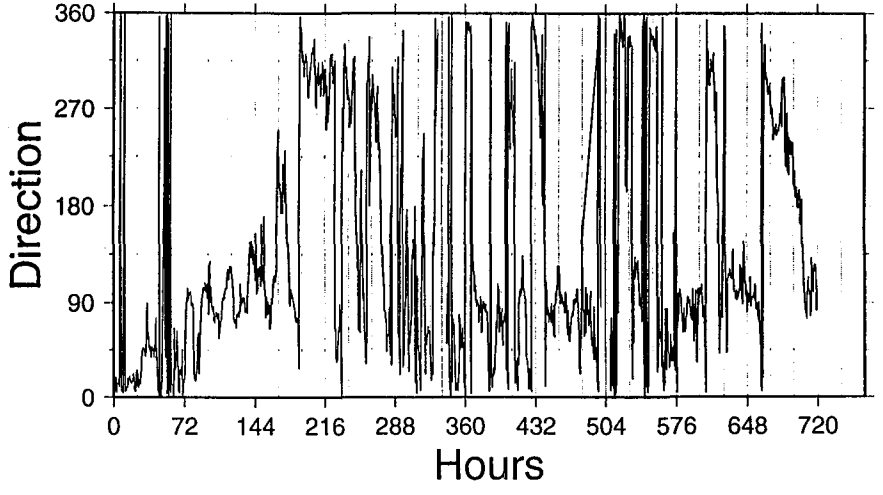

Fig. 7(b)

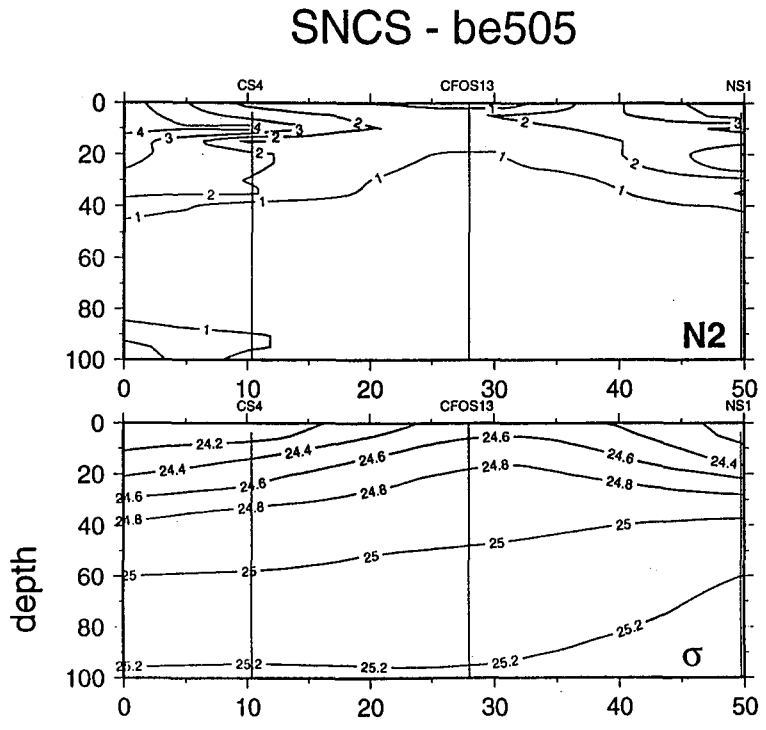
SNCS - be505
CS4
CFOS13
NS1
N2
σ
depth

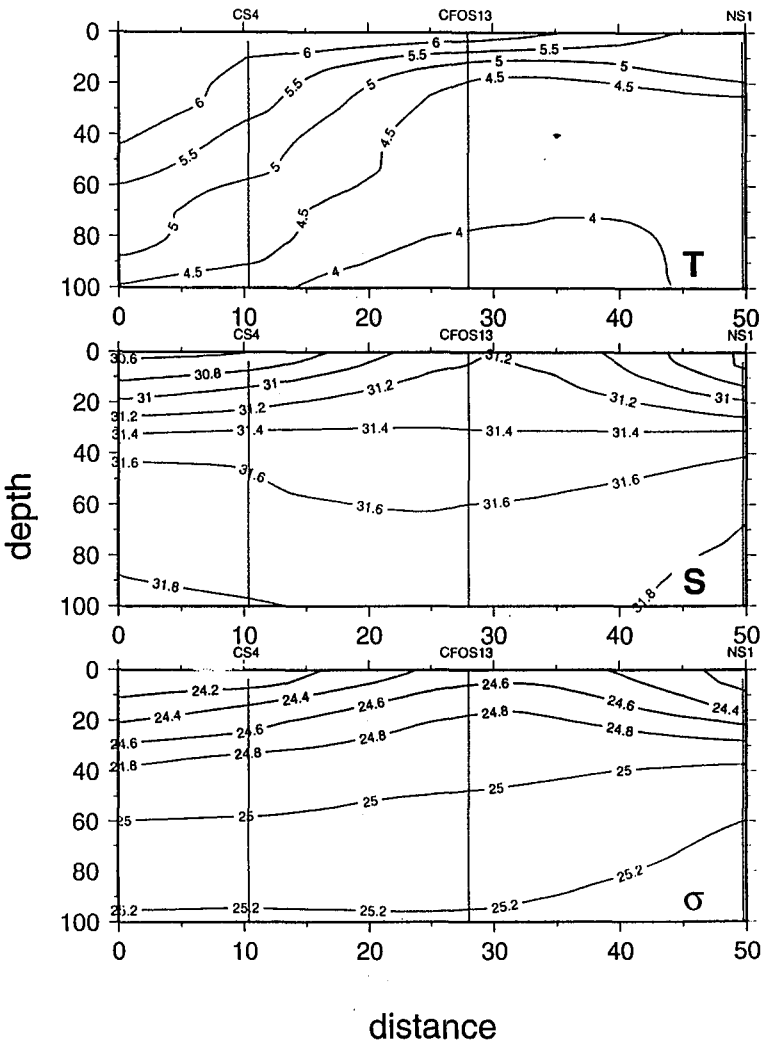
SNCS - be505
CS4
CFOS13
NS1
T
S
σ
depth
distance

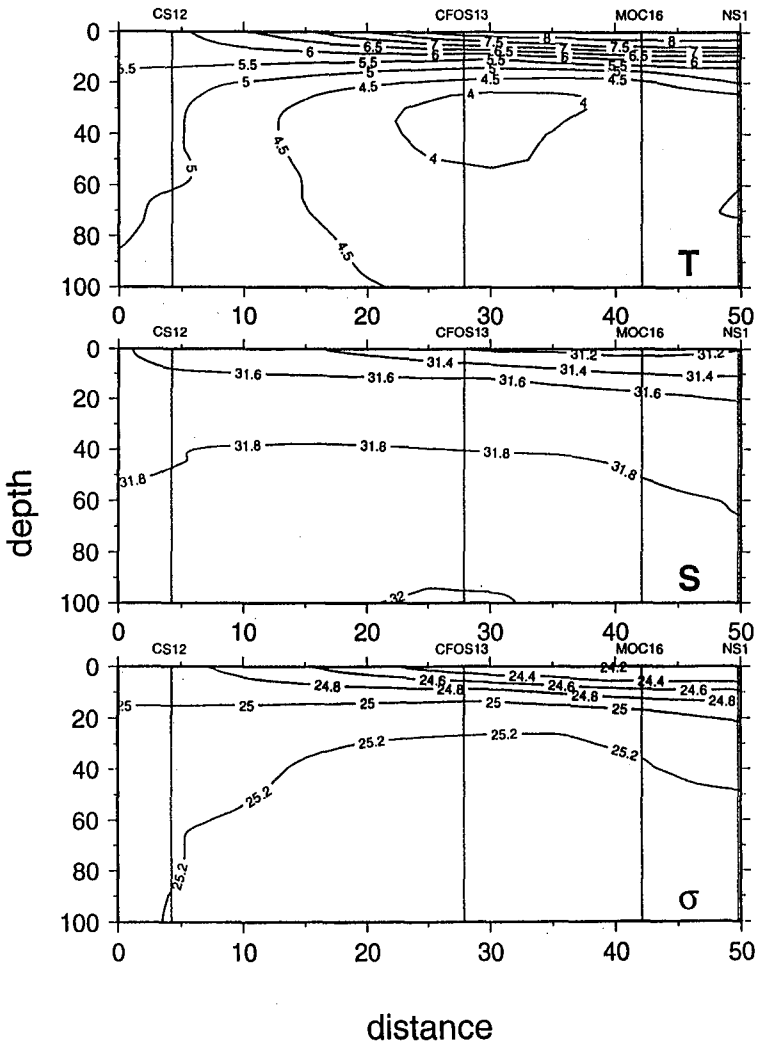
SNCS - hx605
CS12
CFOS13
MOC16
NS1
T
S
σ
depth
distance

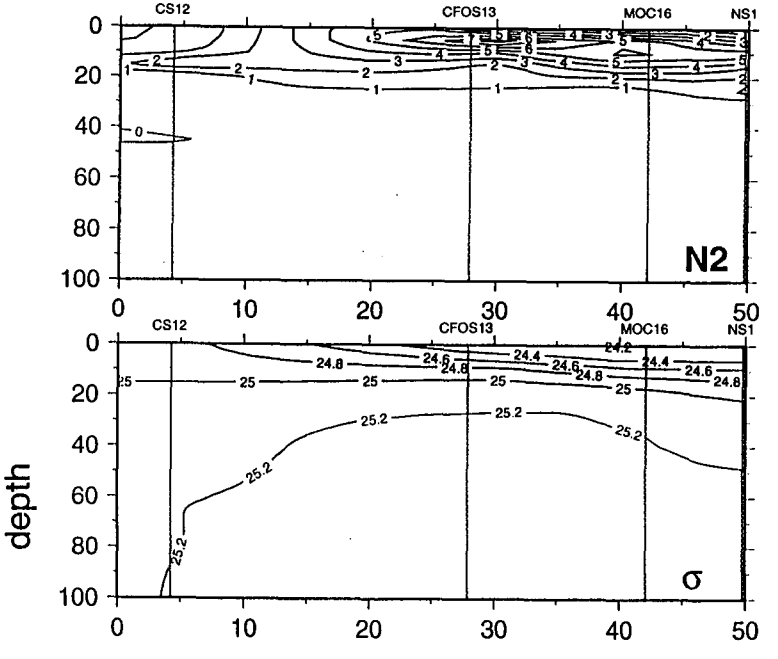
SNCS - hx605
CS12
CFOS13
MOC16
NS1
N2
σ
depth

SNCS - be705

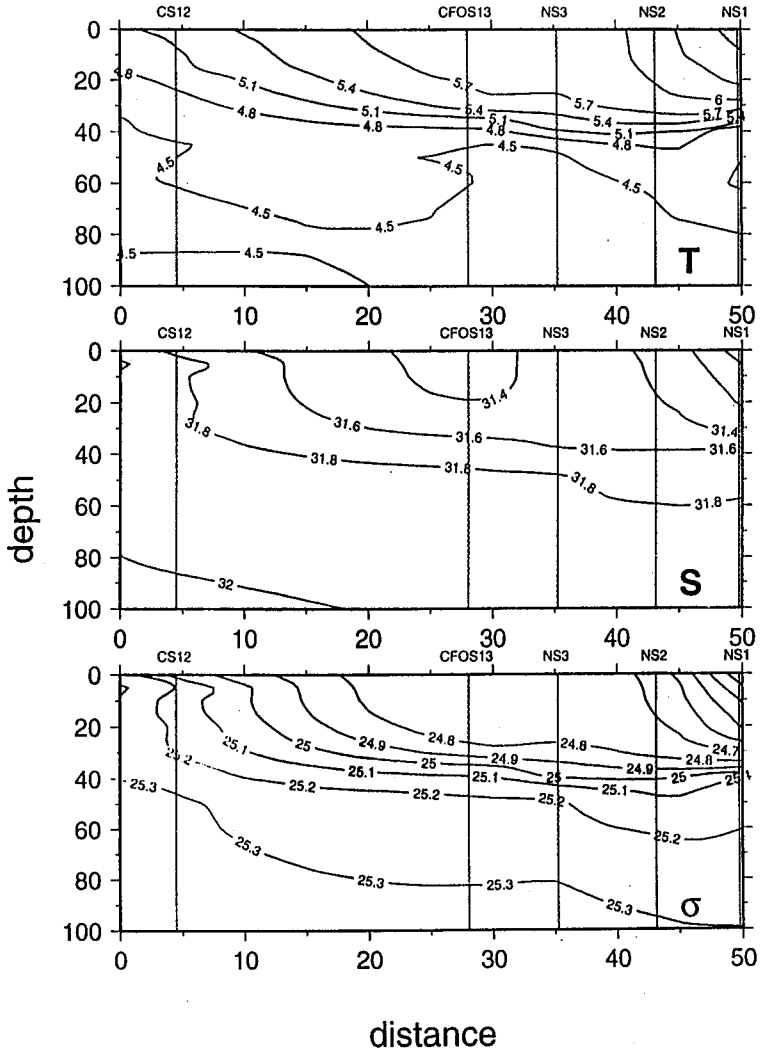


SNCS - be705

Fig. 9(b)

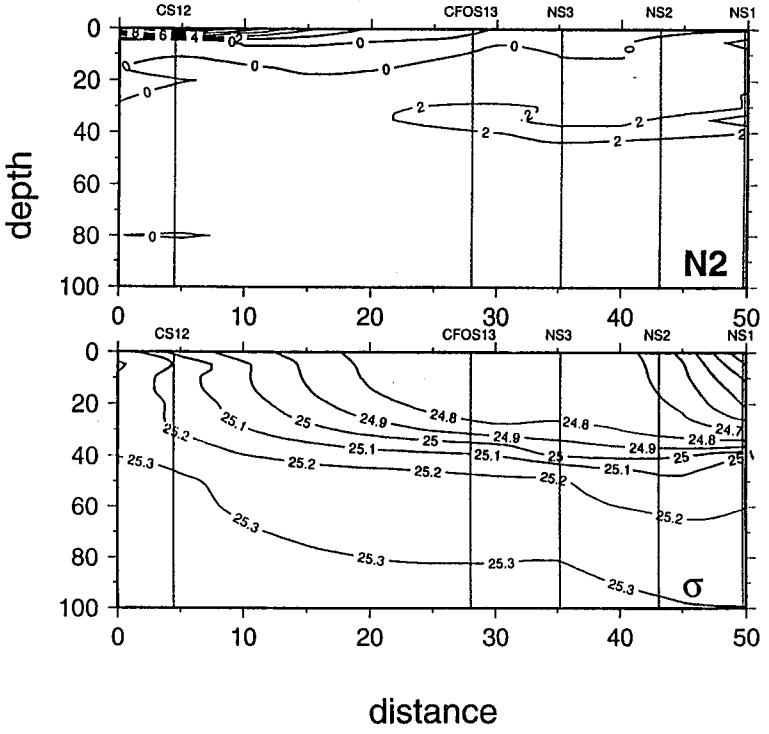

Mean Temperature (001to020m) - be505

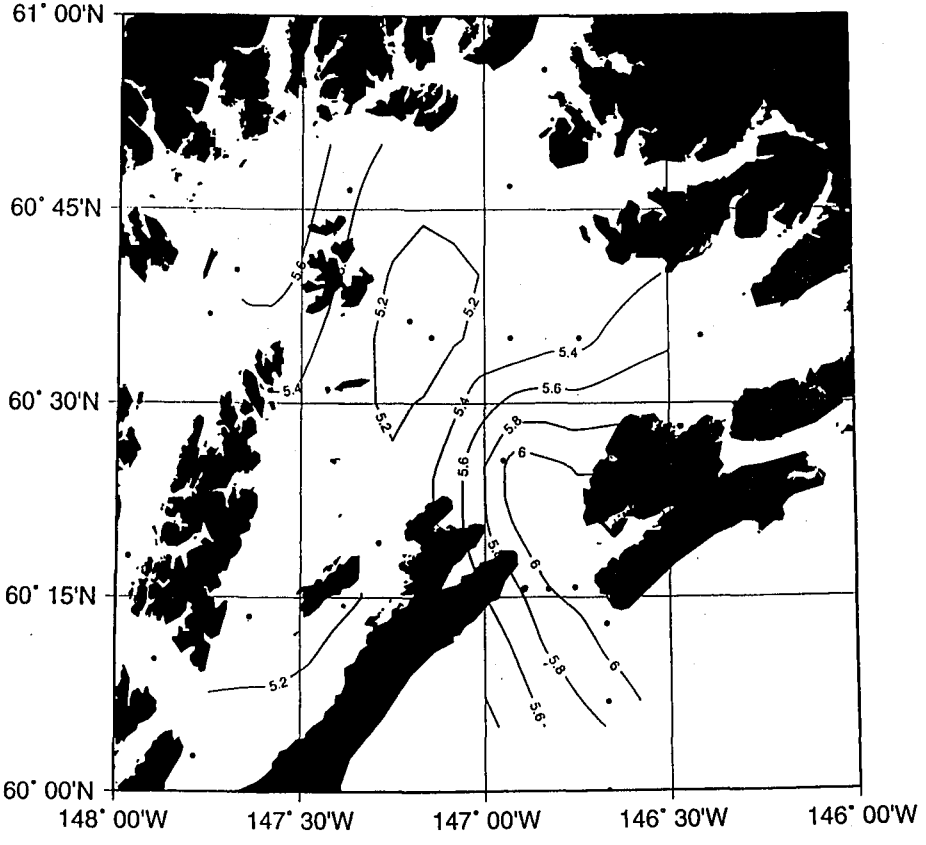


Mean Salinity (001to020m) - be505

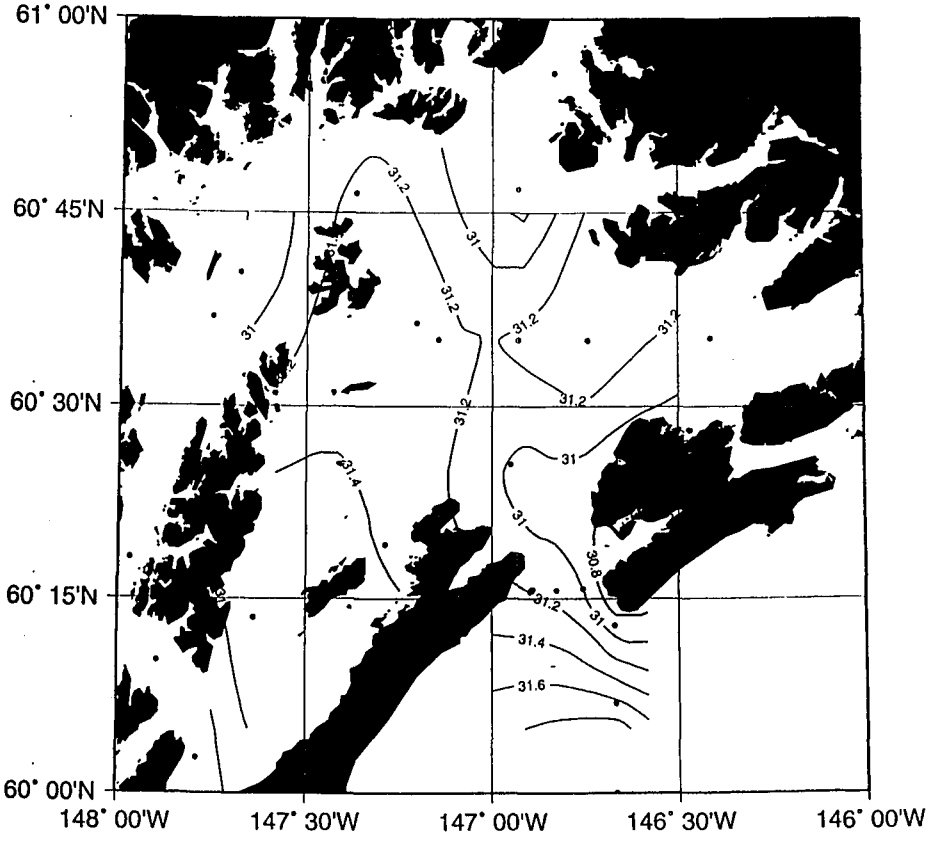

Mean Temperature (001to020m) - hx605

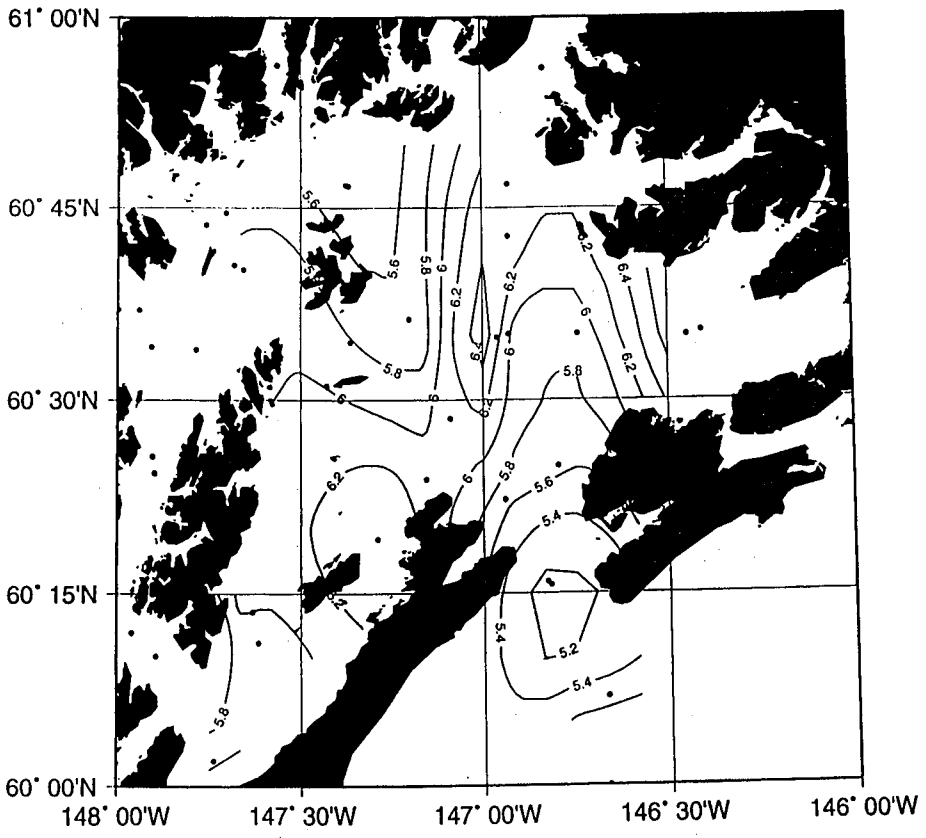


Mean Salinity (001to020m) - hx605

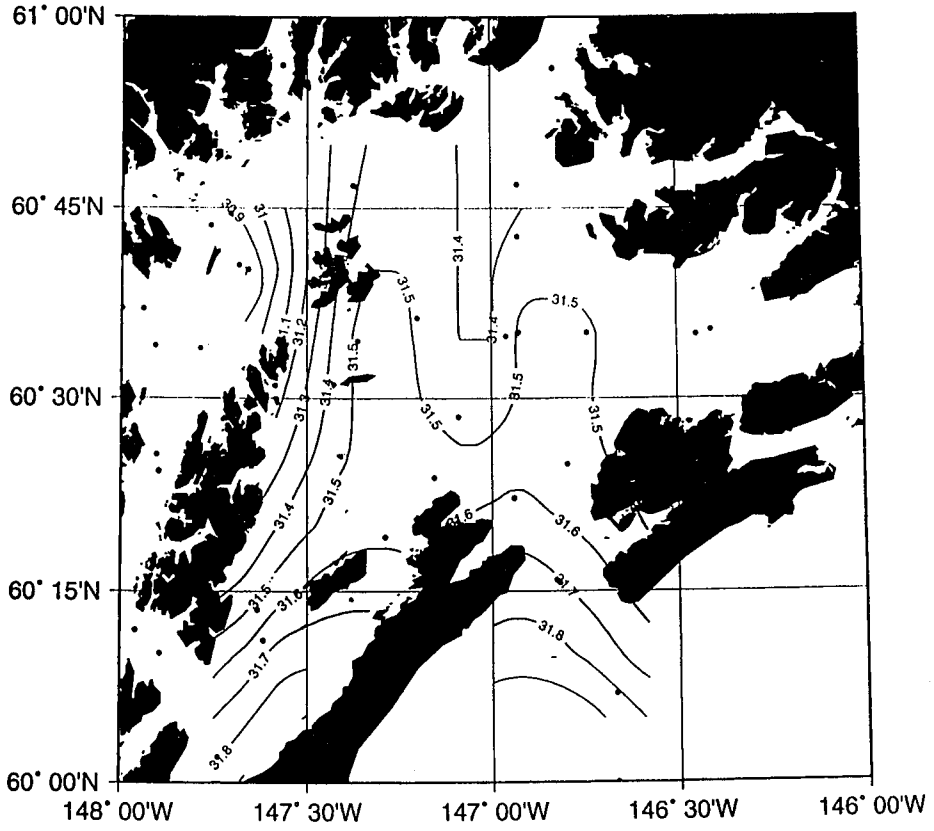

Fig 12(a)

Mean Temperature (001to020m) - be705

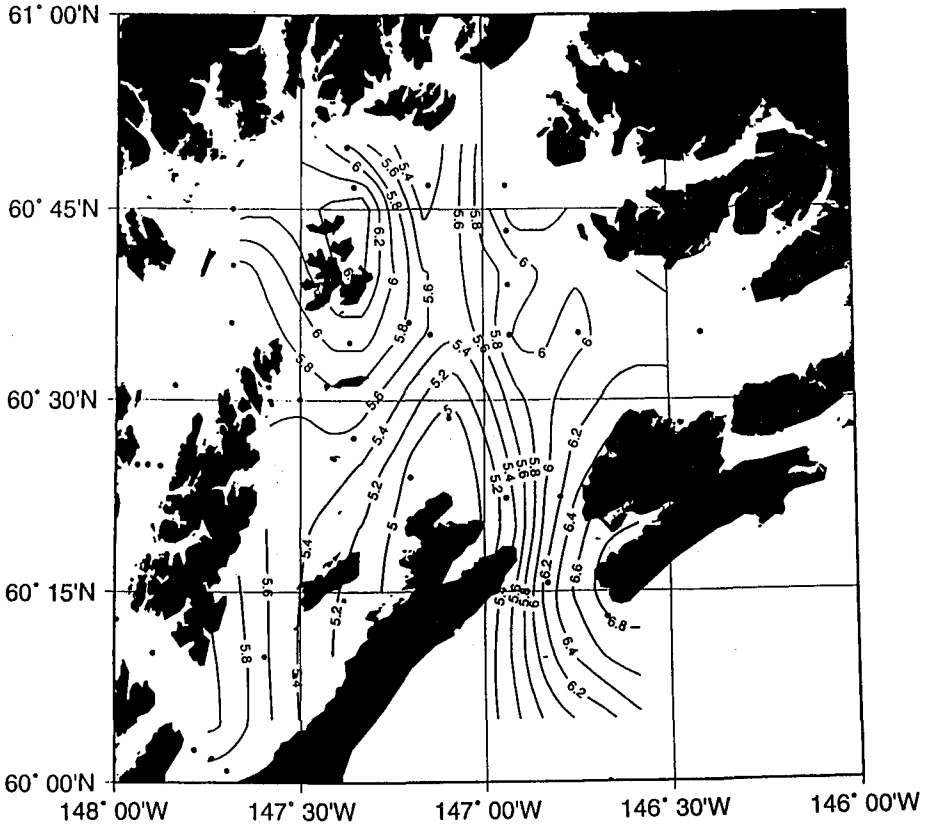


Mean Salinity (001to020m) - be705

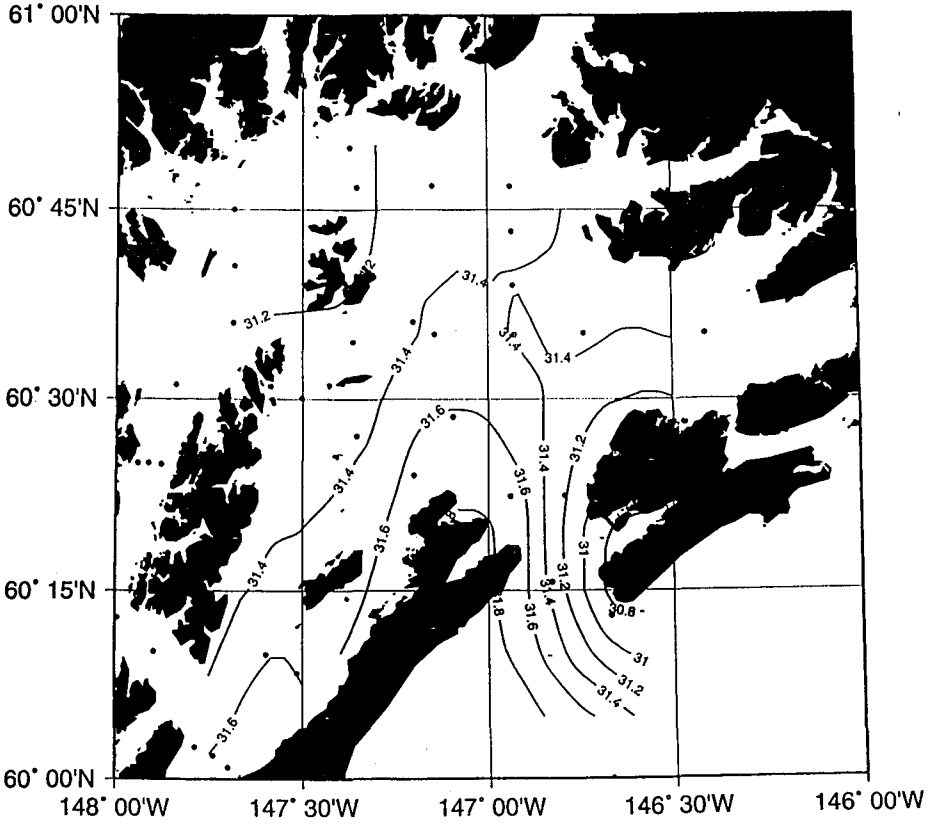

## Middleton Island Wind - May - 1995

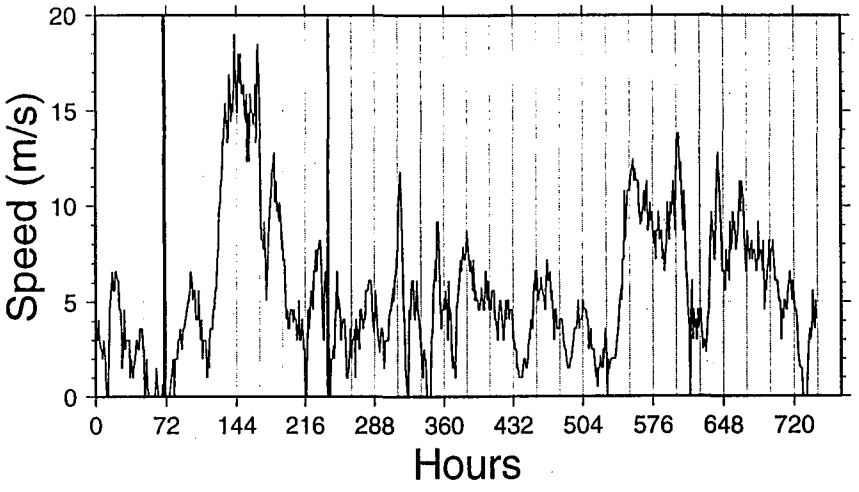


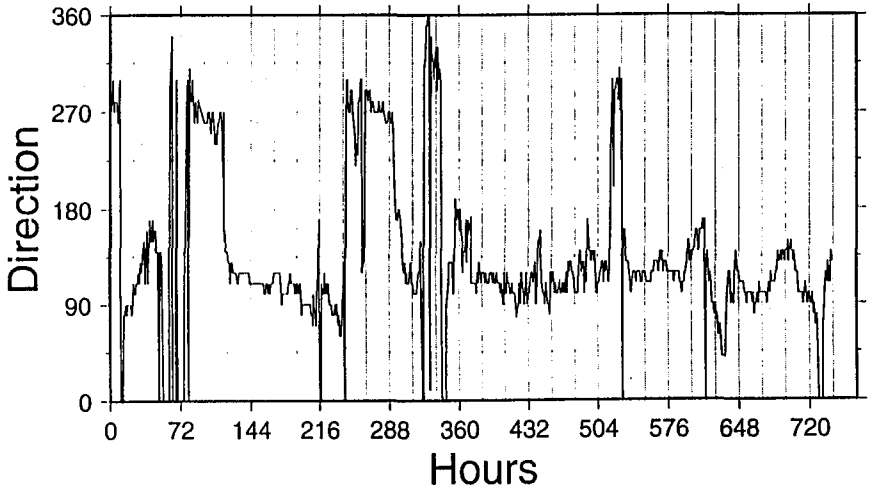


## Mid-Sound Wind - May - 1996

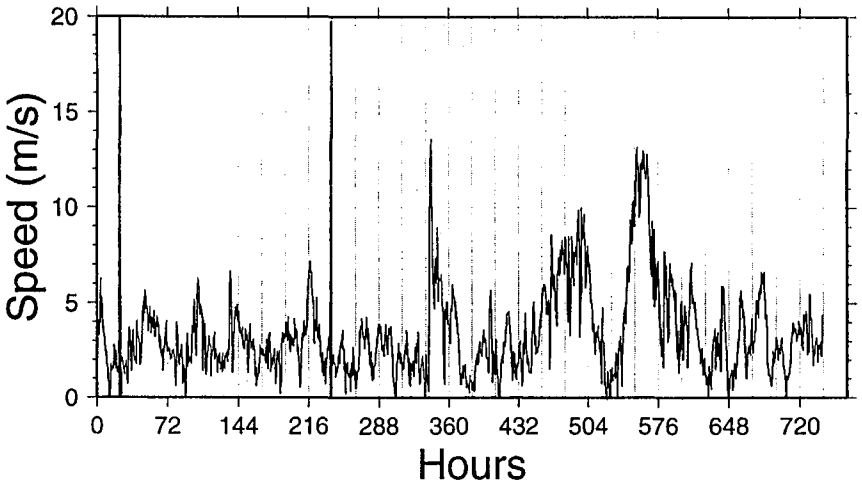


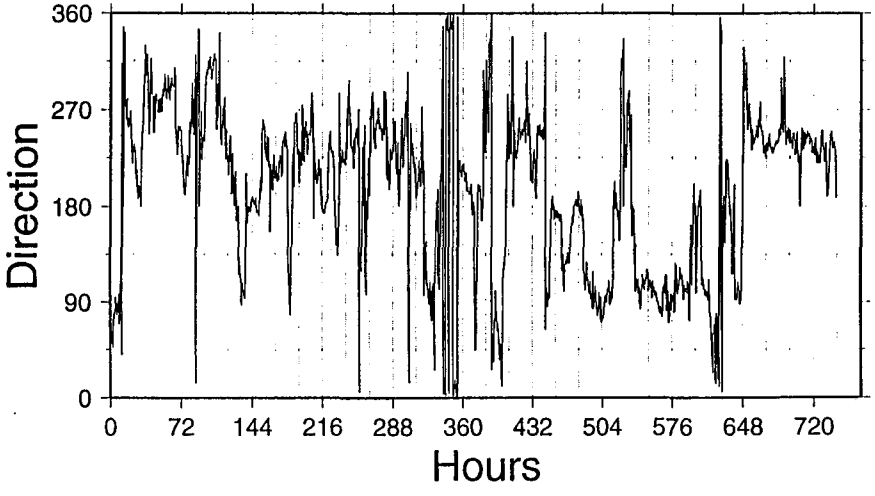

# Mid-Sound Wind - May - 1997

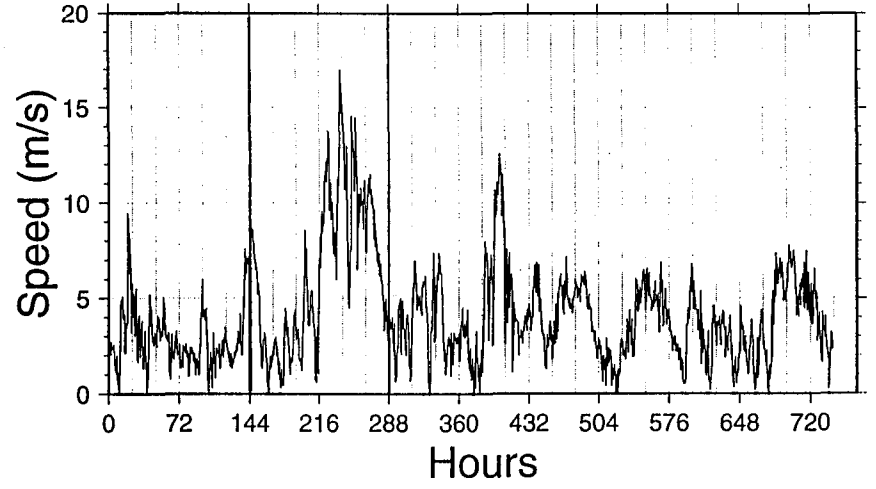


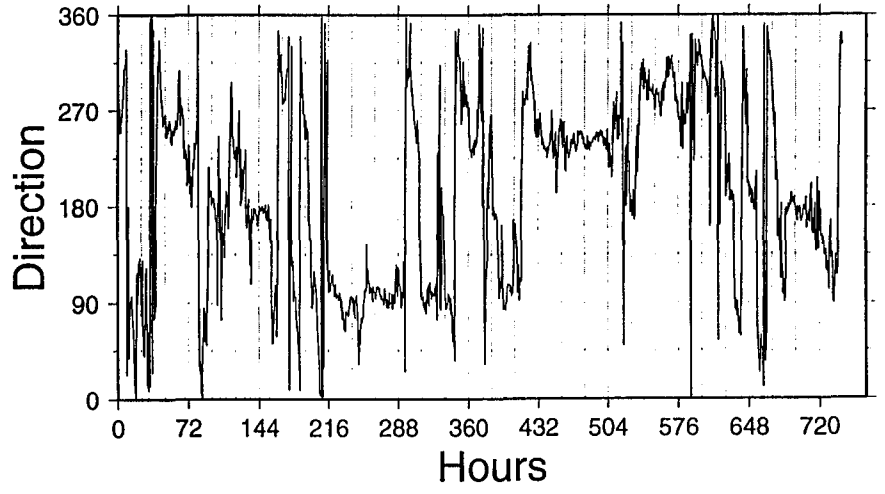

Fig. 14 (a)

# SNCS - be506

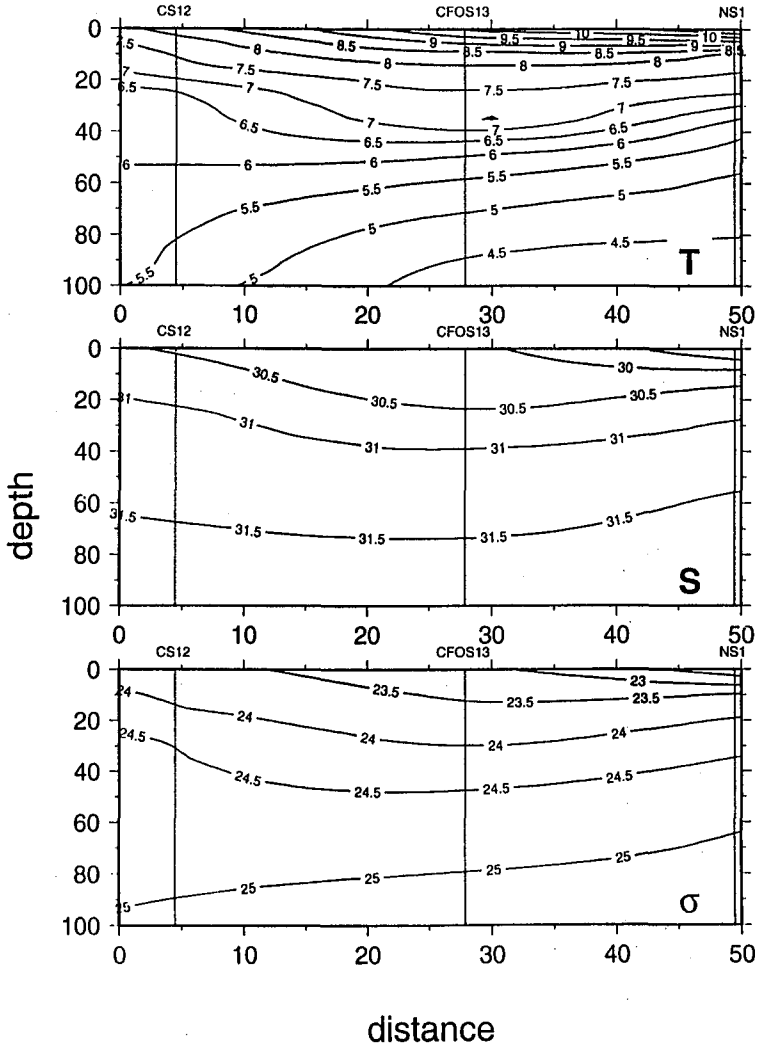


Fig. 14 (b)

# SNCS - be506

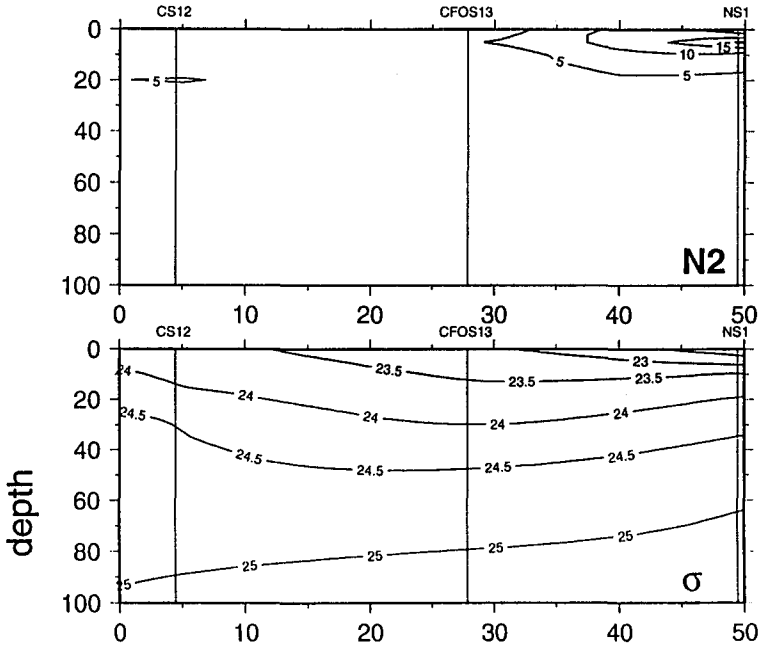

FIG. 13(a)

# SNCS - be606

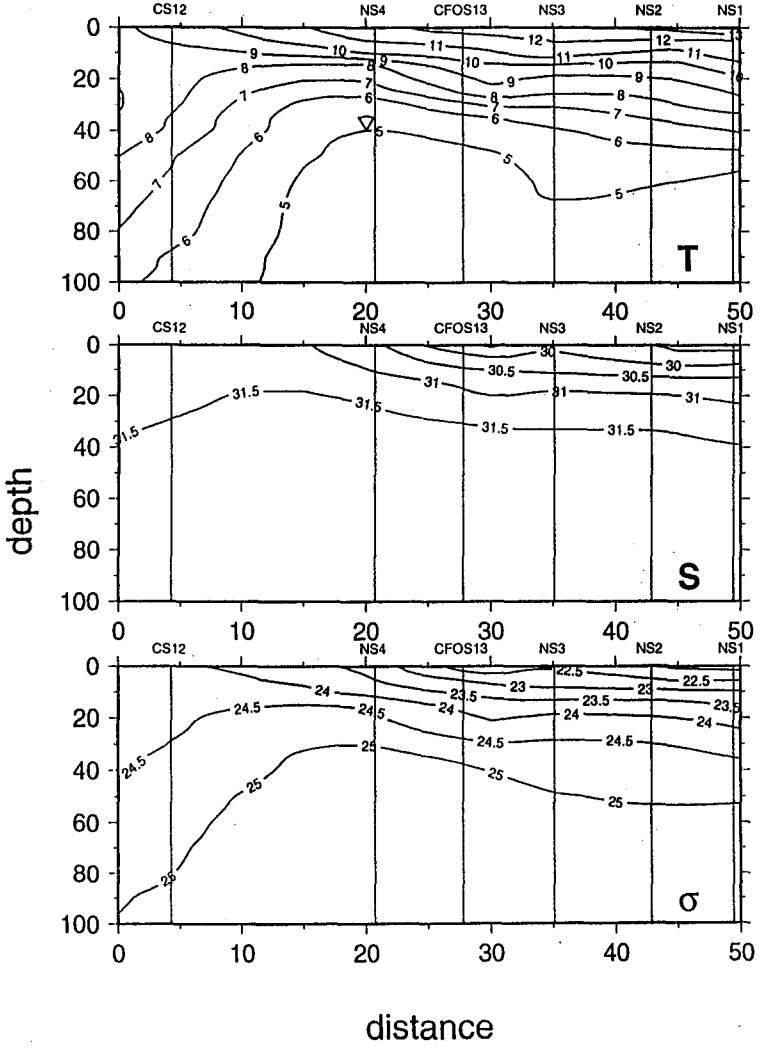


FIG. 13(b)

# SNCS - be606

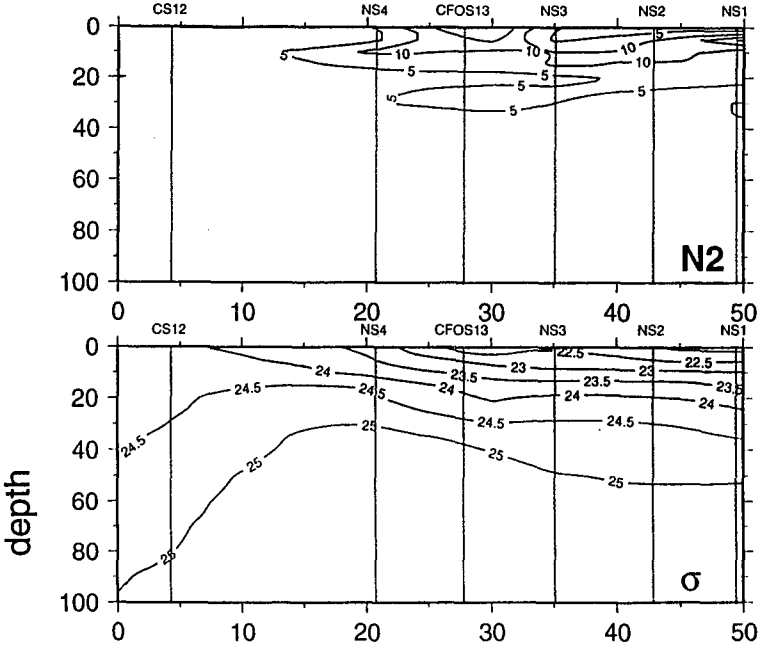

FIG. 16(a)

Mean Temperature (001to020m) - be506

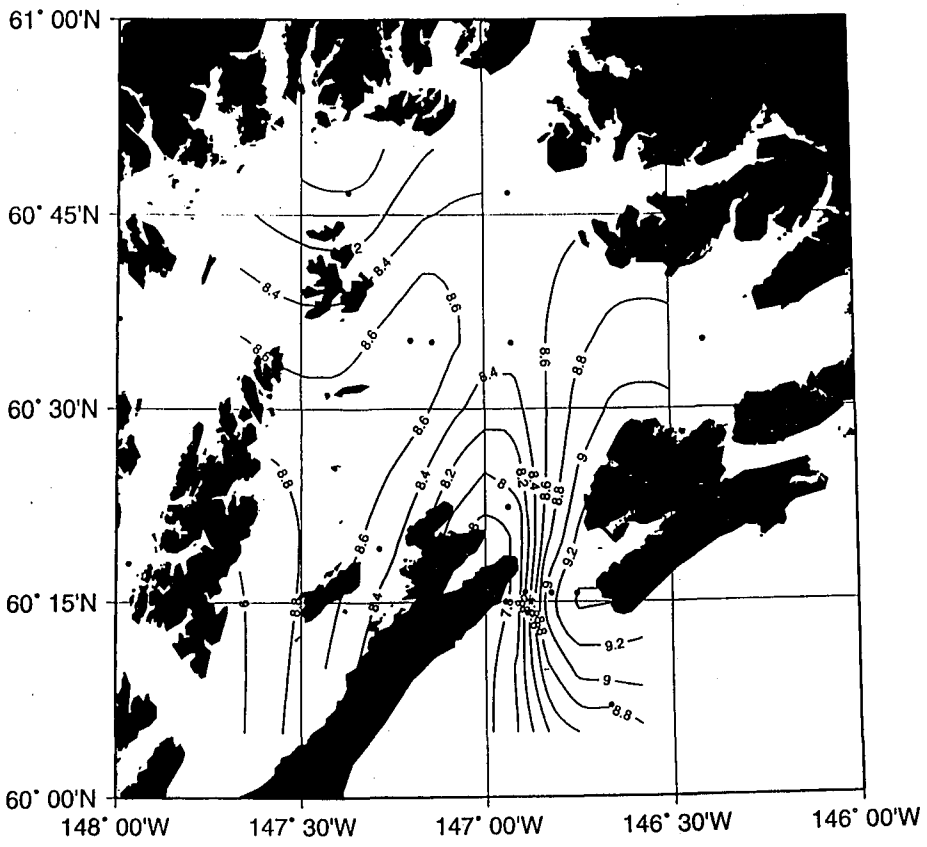


Mean Salinity (001to020m) - be506

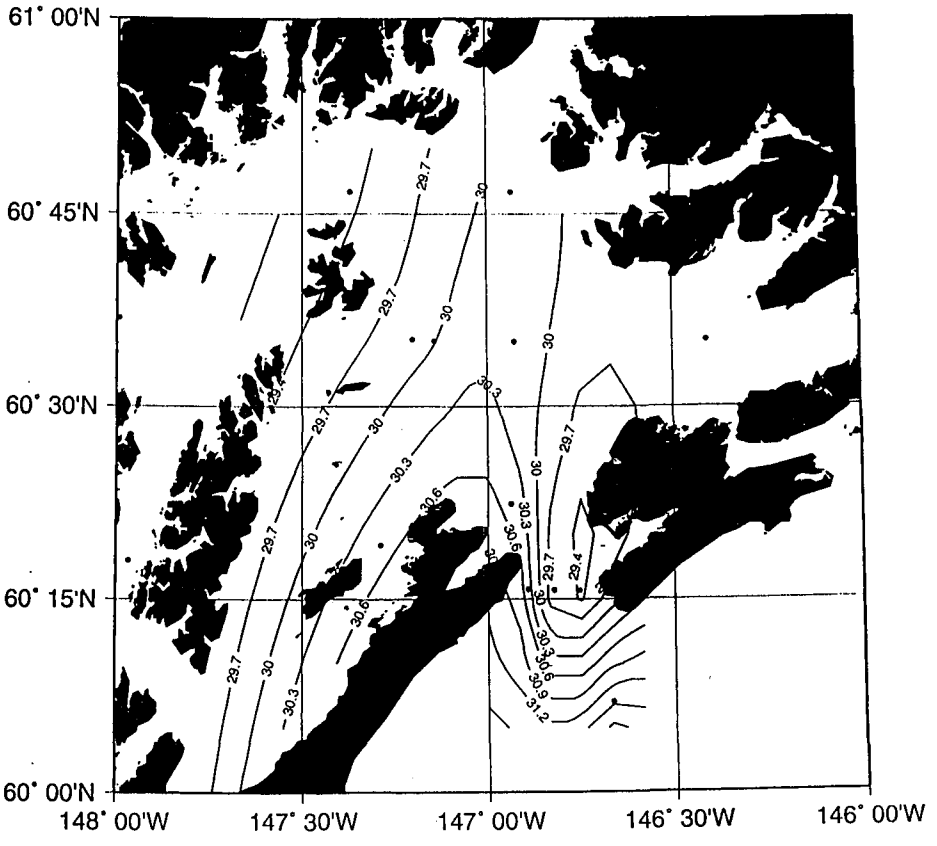

Mean Temperature (001to020m) - be606

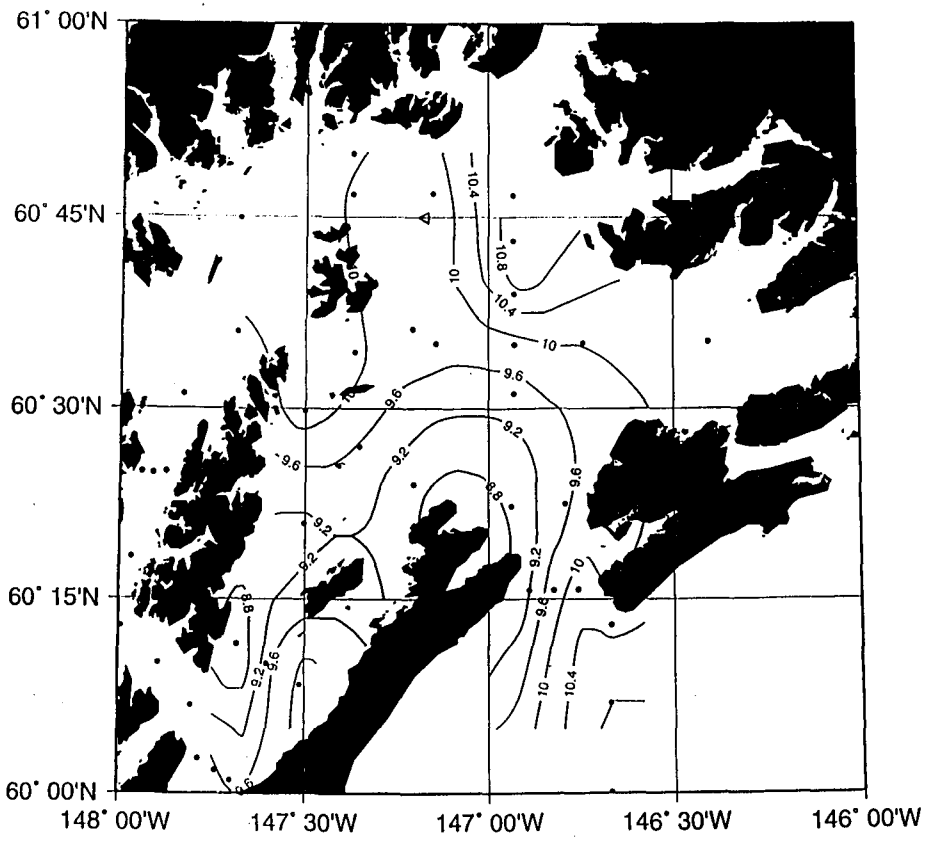


Mean Salinity (001to020m) - be606

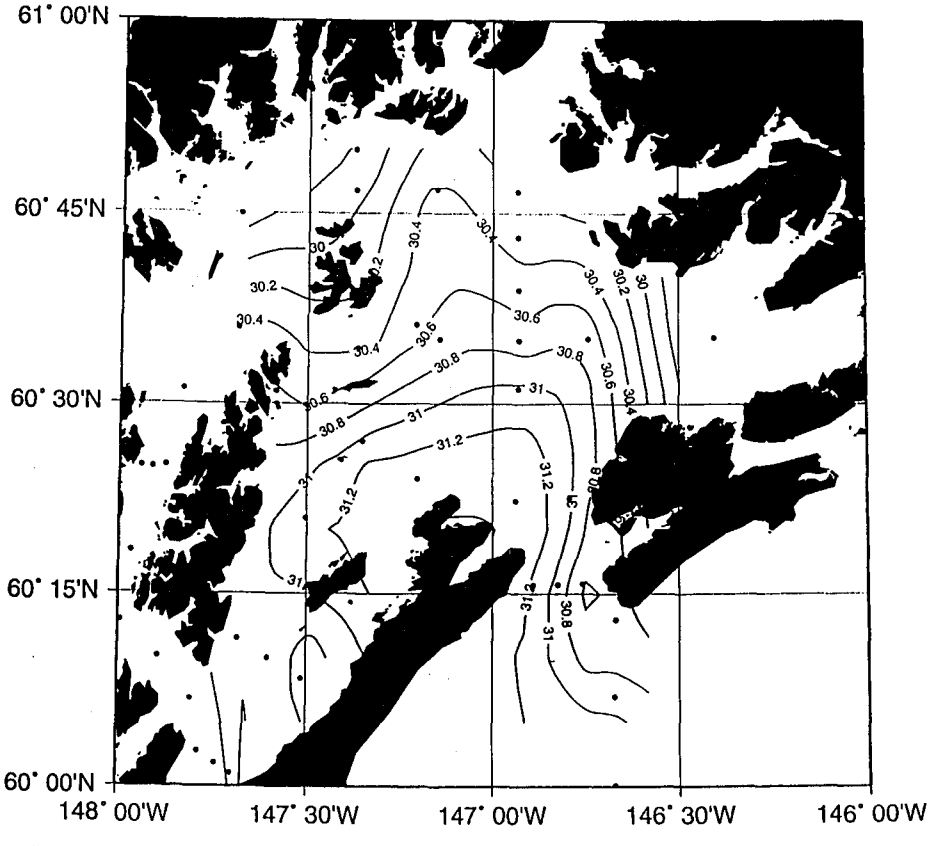

Fig. 18(a)

## Middleton Island Wind - June - 1995

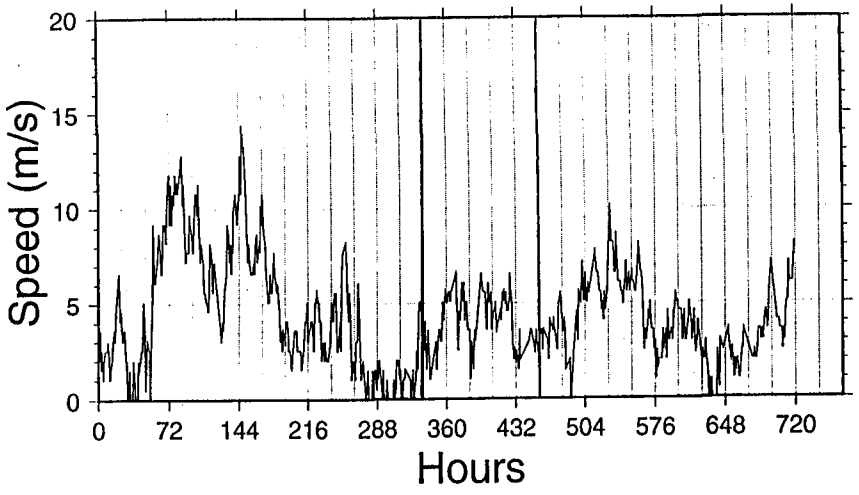


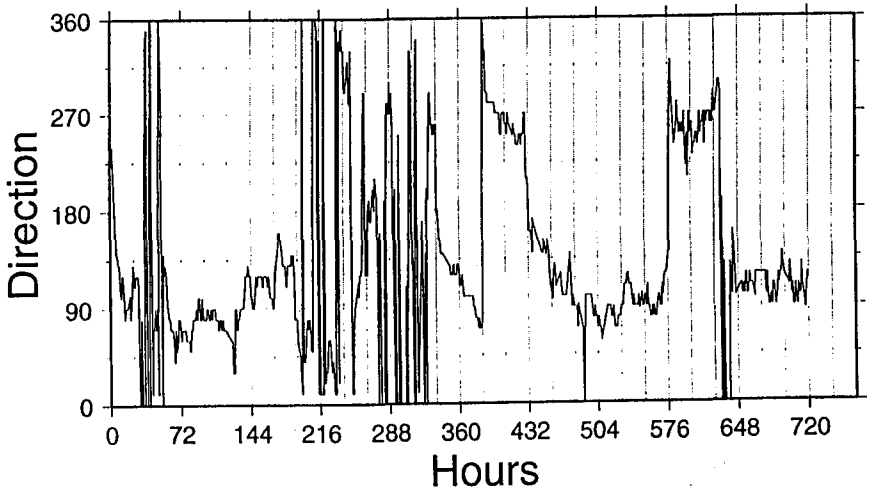


## Mid-Sound Wind - June - 1996

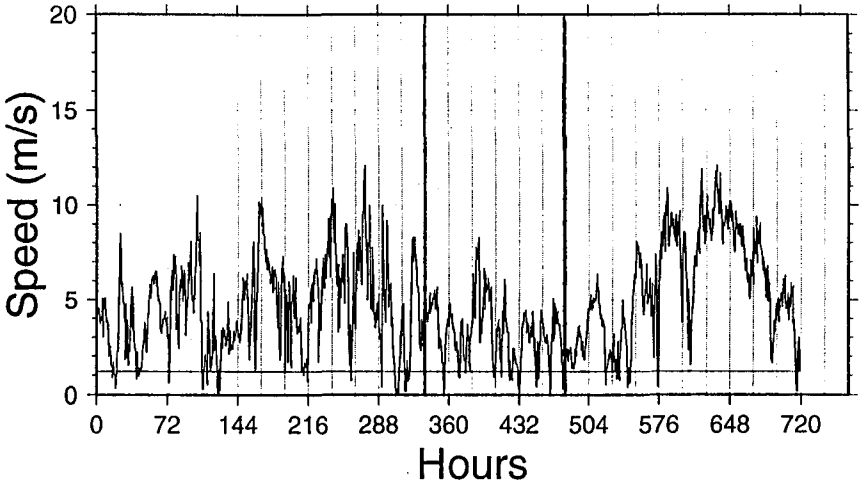


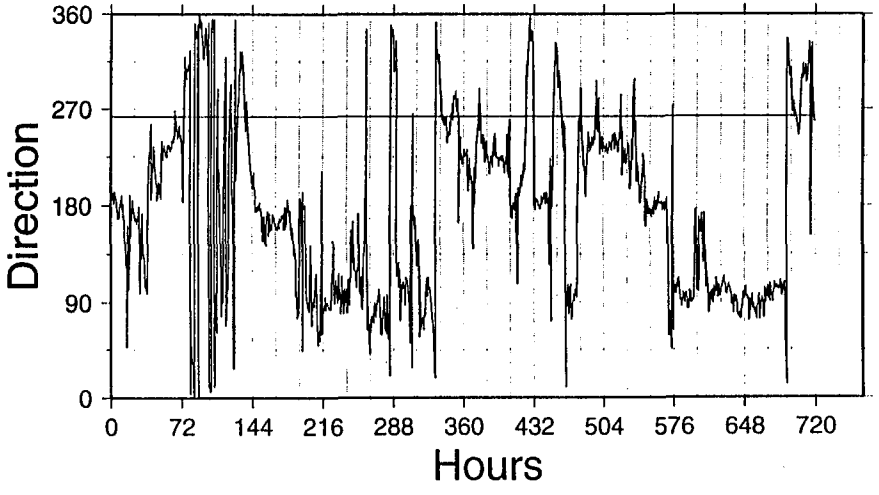

FIG. 17(a)

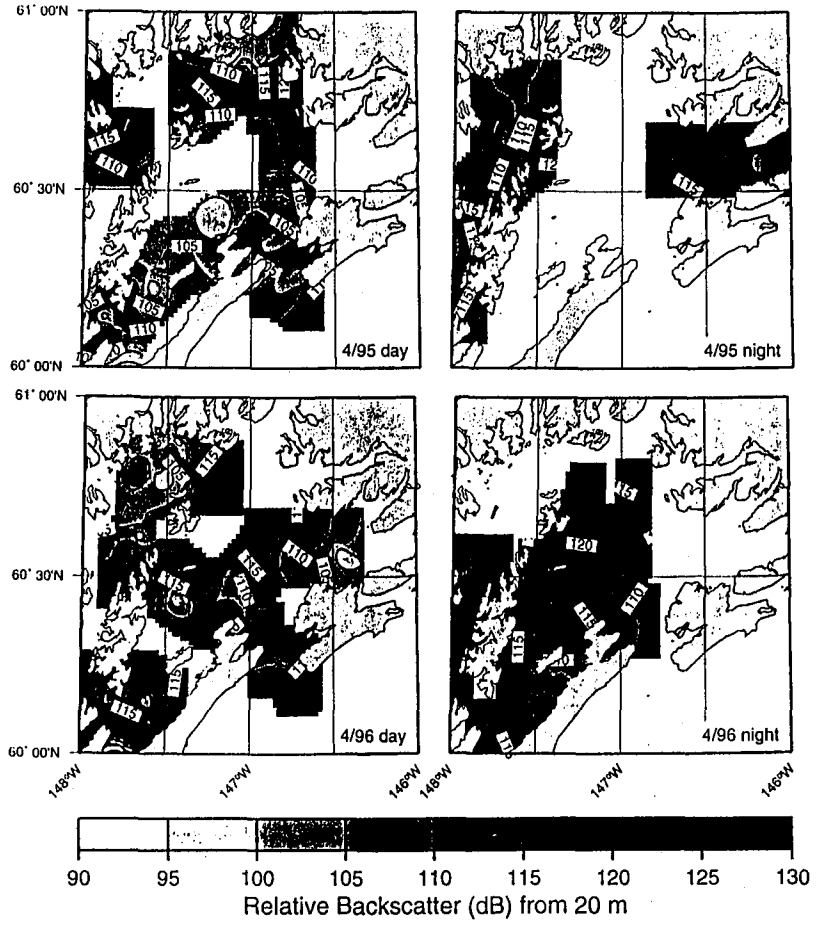


FIG. 17(b)

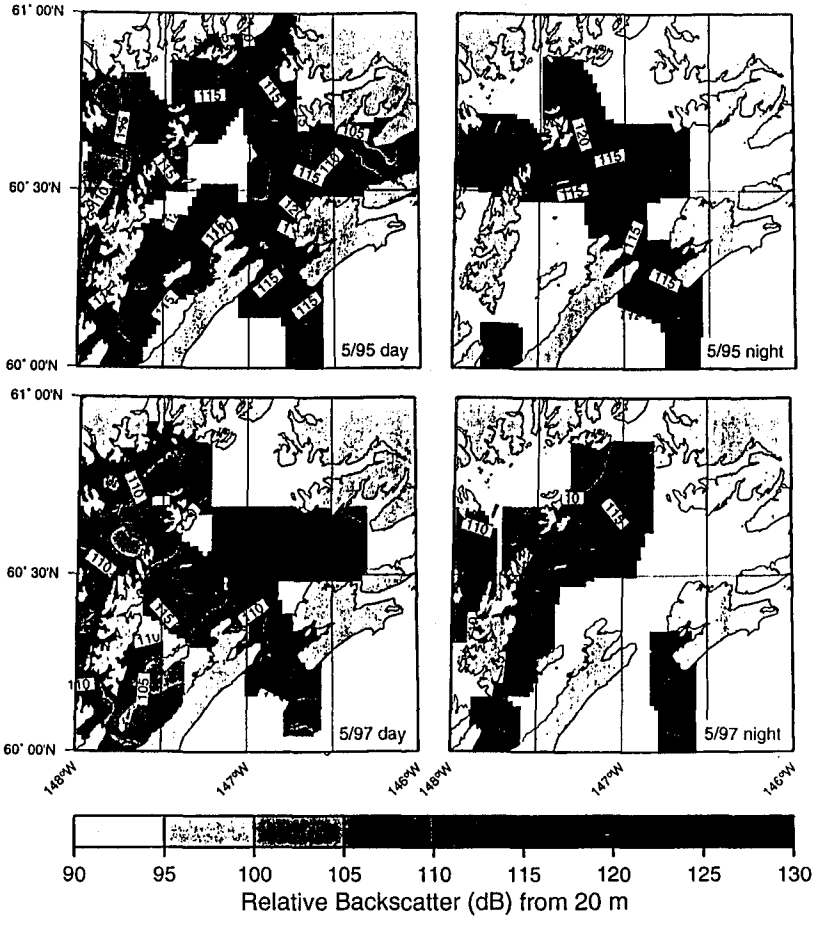

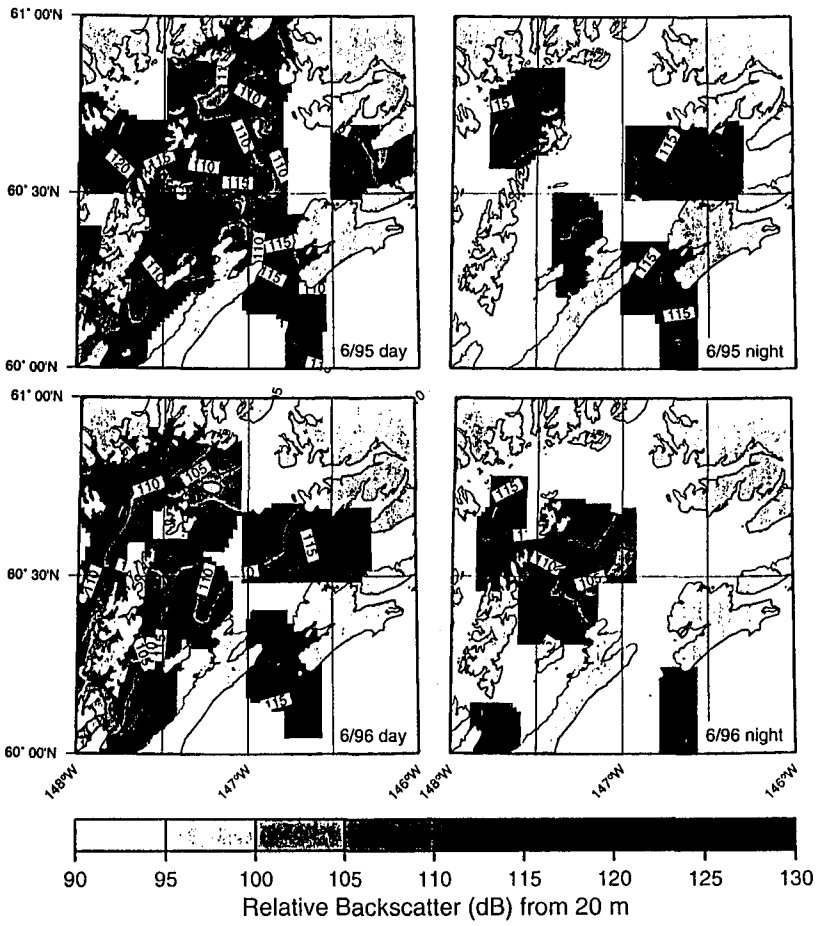
61° 00'N
60° 30'N
60° 00'N
6/95 day
6/95 night
6/96 day
6/96 night
148°W
147°W
146°W
90
95
100
105
110
115
120
125
130
Relative Backscatter (dB) from 20 m

FIG. 20(a)

May 1996

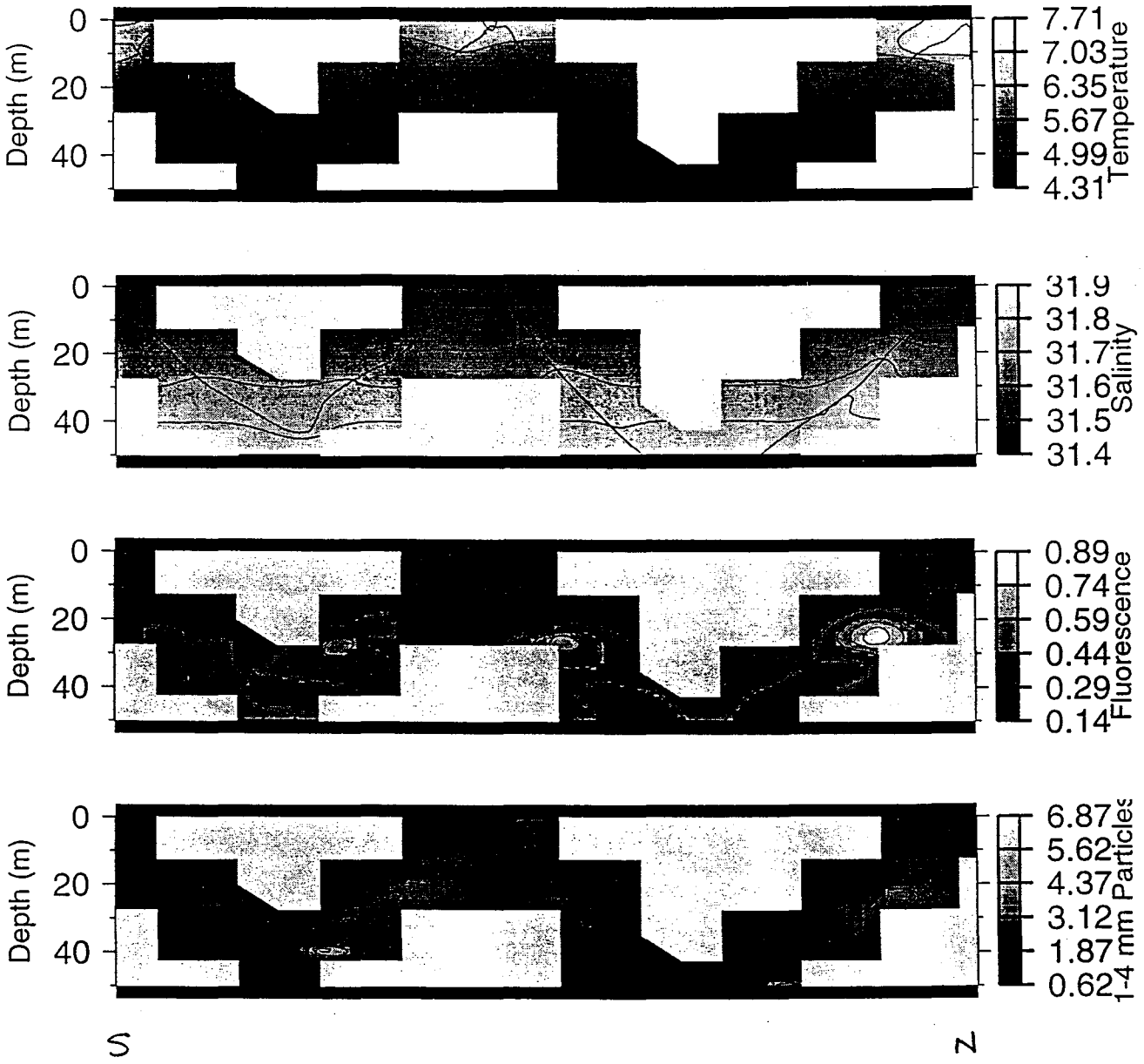

FIG. 20(b)

May 1997

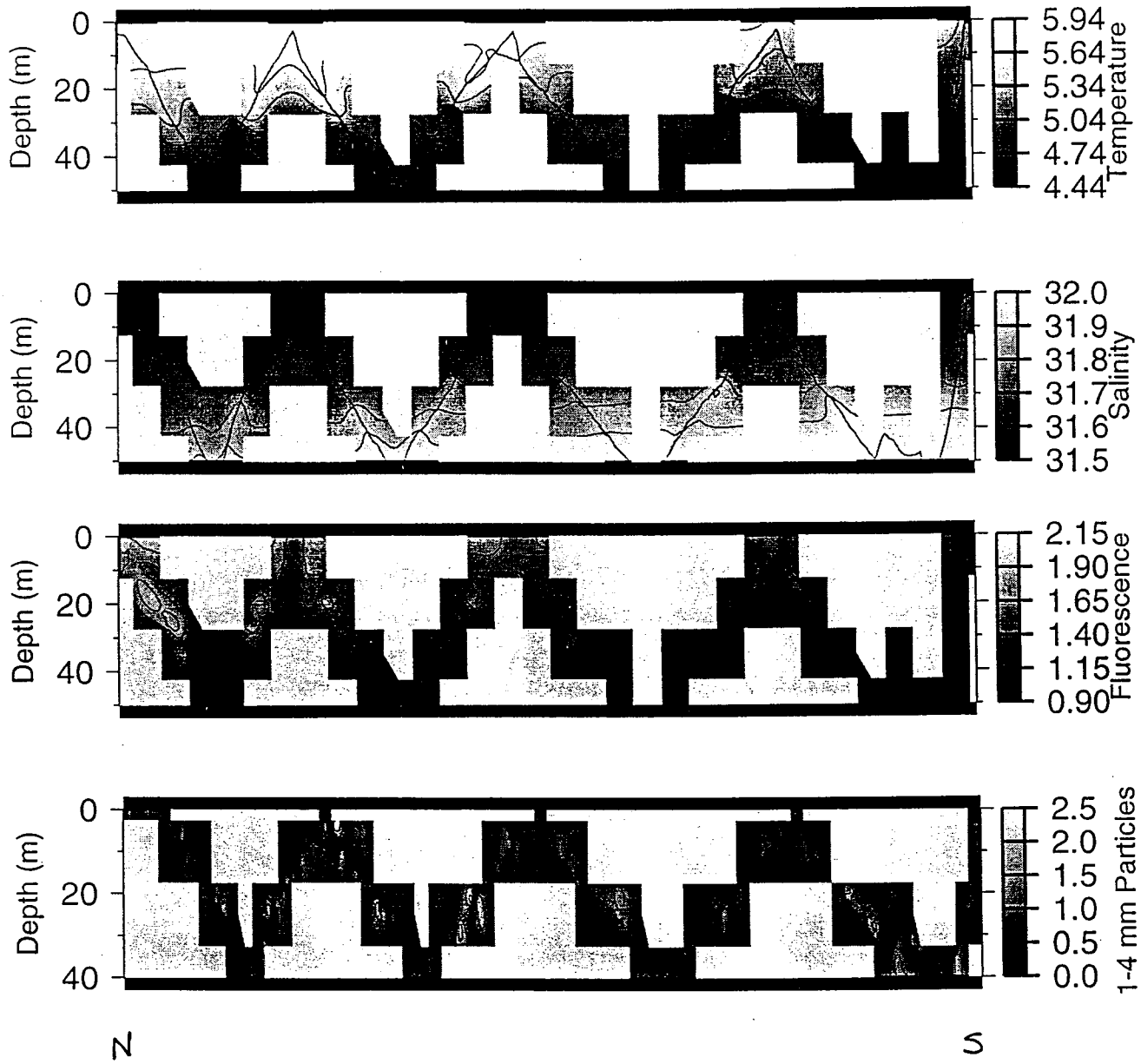

DRAFT

# Seasonal Variability of the Large Scale Circulation and Water Mass Variability in Prince William Sound, Alaska

S.L. Vaughan, K.E. Osgood, S.M. Gay, and L.B. Tuttle
Prince William Sound Science Center

## Introduction

Prince William Sound (PWS), Alaska is a shallow, estuarine, subarctic sea, surrounded by mountains, numerous fjords, and coastal rivers (e.g. Muench and Schmidt, 1975). The central basin is roughly 350 m deep. A deep basin in the northwest Sound (the 'black hole') reaches depths of 730m. The main connections between the Sound and the northern Gulf of Alaska (GOA) are Hinchinbrook Entrance and Montague Strait. The flow is generally thought to be inward at Hinchinbrook Entrance and outward at Montague Strait (Niebauer, Royer and Weingartner, 1994; Royer, Hansen and Pashinski, 1979), but seasonal changes in wind forcing and precipitation produce departures from this general pattern. Instanteous current velocities are dominated by tides.

Meteorological conditions in PWS are dominated by the strength and location of the Aleutian Low and the Siberian High (Wilson and Overland, 1986). Light westerly winds in the summer are replaced by strong easterlies in the winter, which produces downwelling along the north Gulf coast and inflow into PWS. Fresh water input, a combination of precipitation and snow melt/river runoff, reaches a maximum in fall and a minimum in spring (e.g. Royer, Hansen, and Pashinski, 1979).

Mid-depth temperature minima and maxima occur as a result of seasonal surface warming and cooling (Muench and Schmidt, 1975). Density is primarily determined by salinity. The coldest, saltiest, and most homogeneous water occurs in March. The warmest, freshest, and most stratified water occurs in September (e.g. Muench and Schmidt, 1975).

Niebauer et al (1994) presented hydrographic and current velocity data from the late 1970s and 1989. They calculated transports into and out of the Sound from current meter moorings deployed in Hinchinbrook Entrance and Montague Strait from November 1977 to February 1979. The total vertically integrated transport was inward at Hinchinbrook Entrance, and outward at Montague Strait in all months, with most of the transport occuring in winter. Based on these transport calculations, they estimated that roughly 40% of PWS was flushed during the summer months. From October to April, they estimated that the Sound was flushed at least twice.

PWS is a region of high biological production, and supports a large Alaskan salmon fishery. Oil tankers transverse this region regularly and pose a finite risk in the event of a spill, yet little is know about the seasonal and interannual changes in the circulation. In 1993, the Exxon-Valdez Oil Spill (EVOS) Trust Council funded a comprehensive, multidisciplinary ecosystem study called the Sound Ecosystem Assessment (SEA). A main goal of the physical oceanographic part of the SEA program was to identify the physical processes that influence the production of two commercially harvested species, pink salmon and Pa-

cific herring. The initial task was to document the seasonal dominant circulations patterns and water mass properties in PWS.

## Data

Large scale hydrographic cruises were conducted in PWS in 1994 - 1997. Cruise dates are shown below.

| 1994 | 1995 | 1996 | 1997 |
|---|---|---|---|
| | March 15-23 | | |
| | April 10-17 | April 15-21 | |
| | May 4-11 | May 2-11 | May 7-13 |
| June 1-7, 10-18, 23-30 | June 15-20 | June 15-21 | |
| July 6-12, 15-20 | | | |
| September 20-29 | Sept. 29-Oct. 3 | Sept. 10-16 | |
| | | Dec.5-11 | |

Station locations and transects for each cruise are shown in Figure 1. Measurements of temperature (T), salinity (S), oxygen, and current velocities were made with simultaneous measurements of fluourescence and zooplankton abundance. The hydrographic data was collected using a SeaBird 911 CTD. Conductivity, temperature, and oxygen as a function of pressure were recorded at 1 dbar intervals. Salinity was calculated from conductivity using standard SeaBird software. The CTD sensors were calibrated annually by SeaBird Electronics. The CTD salinities and oxygens were not calibrated with bottle samples because of minimal annual sensor drift rate. In December 1996 and May 1997, expendable CTDs (XCTDs) were used when conditions were too rough to use the CTD.

Instantaneous current velocity transects were collected using an RDI 150 kHz broadband acoustic Doppler current profiler (ADCP) deployed from the stern of the ship in a towed body. Most transects were in water less than 400 m depth so that bottom tracking was available. The bin length was 8 m for most of the data. The ADCP generally measured flows from about 20 m depth to the bottom.

To calculate a coarse approximation of the mean flow without the tidal component, repeat ADCP transects were made during periods of maximum flood and maximum ebb tide at critical transport regions in Hinchinbrook Entrance, Montague Straight, and Knight Island Passage in April, June, September, and December 1996 (see Figure 1). The tidal component was assumed to be barotropic and approximately equal during flood and ebb tides. Mean velocities were calculated by averaging over both tide stages. Vertical sections of along-channel and cross channel velocities were created for each cruise.

In addition to the large scale hydrographic cruises, an an upward looking ADCP moorring (RDI 150 kHz broadband) was deployed in Hinchinbrook Entrance from June 1995 to October 1995, and from September 1996 to May 1997 (Figure 1). Velocities were recorded from a depth of about 300m to within roughly 50m of the surface using an 8 m bin length. The sampling interval was 30 minutes in 1995, and 2 hours in 1996-97.

Meteorological data from C-MAN stations in PWS is available from the National Data Buoy Center (NDBC). The stations are located at Bligh Reef, Potato Point, Seal Rocks,

and Mid-Sound buoy (in the central Sound). Wind speed, wind direction, wave height, barometric pressure, air temperature, water temperature, dew point temperature, and visibility are measured every 30 minutes. The buoys became operational in May 1995, and have collected mostly uninteruped data since then. Meteorological data prior to 1995 is available from a station on Middleton Island, south of PWS. Upwelling indices were obtained from the NOAA Pacific Fisheries Environmental Group (PFEG) web page.

## Oceanographic Cruises

*March 1995*

A T/S diagram with 4 stations in PWS and the GOA is shown in Figure 2. Station SEA32 is in southern Montague Strait, SEA22 is in the 'black hole' in the northwest Sound, CFOS13 is in the central Sound, and GOA3 (and other GOA stations) is located south of PWS on the GOA shelf. The surface temperatures are colder and fresher than those at depth. The densest water is in the central Sound (CFOS13) and in the 'black hole' (SEA22), with a density of 26.1. The deep water at CFOS13 and SEA22 has similar properties. The Montague Strait water (SEA32) is intermediate T/S properties, which may indicate it resulted from mixing of central and northwest Sound water. The GOA water is more homogeneous than the PWS water, and is slighly colder and fresher along isopycnals. Freshening of the very upper layers is apparent at SEA32. The GOA water is unlike any of the other types. The temperature minimum layer has not yet formed, but it is the surface water around $\sigma_\theta = 25.0$ that will become the temperature minimum.

Dynamic heights calculated from 0 to 100 m is shown in Figure 3. The station locations are shown as dots. Very weak geostrophic flow is indicated.

*April 1994, 1995, and 1996*

By April in all 3 years, the temperature minimum layer has started to form as a result of warming and freshening of the surface waters. An example is shown from April 1996 is Figure 4. The density of the coldest water is between 25.0 and 25.2. In all 3 years the water deeper than the temperature minimum is the same at SEA22 and CFOS13. In 1995 and 1996, the water mass properties in southern Montague Strait (SEA32) is the same as well. Figure 4 shows the shelf GOA water mass proporties (GOA0) are warmer and slightly saltier along the same isopycnal (warmer and fresher at the surface) except at the very bottom. In April 1995, the deep GOA water coincides with the mid-depth Sound water.

Dynamic heights (0/100m) for April 1995 and 1996 are shown in Figures 5(a) and (b). Weak anticyclonic curvature in indicated in the central Sound in April 1995. Baroclinic (20-100m) velocity vectors from April 1995 (Figure 6) also indicate a weak anticyclonic circulation. In April 1996, the dynamic heights suggest a weak anticyclonic circulation at Hinchinbrook Entrance (Figure 5(b)). The vertical section of along-channel velocity, calculated from the repeat ADCP transects, from Hinchinbrook Entrance in April 1996 also indicate an anticyclonic circulation above about 150m (Figure 7(a) along channel). The flow pattern is also spatially variable at Montague Strait during April 1996 (Figure 7(b), with mostly inflow except for a small region of surface outflow in the west.

Neither the dynamic heights or the repeat ADCP sections show strong inflow at Hinchinbrook Entrance in April. The T/S plots show that the Sound has fairly uniform water mass properties thoughout, even in the most remote northwest region. It is likely that the surface warming and freshening observed in April is due to sensible heating and precipitation rather than GOA intrusions.

*May 1994-1997*

Surface warming and freshening continues at all stations in all years (Figures 8(a)-(d). The deepest water at SEA22 remained at a density of roughly 26.1 (the cast in May 1997) may not have reached the bottom). At CFOS13 in the central Sound, the density of the deepest water decreased primarily due to freshening. In all years except 1994 (no data available), the upper layer water mass properties at SEA32 resemble those at GOA0 more closely than those in PWS (CFOS13 and SEA22). Water mass properties in May 1997 are shown more clearly in Figures 9(a) and (b). Stations HE12 and SEA32 resemble GOA water at the surface and PWS water at depth (Figure 9(a)). Stations in the southern Sound (CS12) and in Montague Strait (MS8 and MS5A) exhibit PWS (CFOS13) properties at all depths (Figure 9(b).

Repeat ADCP velocity transects in May 1997 at Hinchinbrook Entrance show northward velocities above about 50m and southward velocities below (Figure 10(a)). Meteorological data from Seal Rocks buoy shows a strong easterly wind burst (in excess of 15m/s occurred on May 10-13, 1997, which probably forced an inflow in the surface Ekman layer. The theoretical Ekman depth for latitude 60° and a wind speed of 15m/s is 69m. Repeat transects from Montague Strait (Figure 10(b)) do not show a surface inflow, but these transects were perform at the beginning of the wind burst. Repeat ADCP velocity transects from May 1995 are shown in Figure 10(c). A subsurface anticyclonic structure, similar to that in April 1996, was present.

Dynamic height contours for May 1995, 1996, and 1997 are shown in Figures 11(a)-(c). A weak anticyclonic circulation is suggested in the central Sound in 1995 and a weak cyclonic circulation is suggested in 1996. A strong inflow at Hinchinbrook Entrance is suggested in 1997 (Figure 11(c)), with cyclonic curvature around Montague Island and outflow in Montague Strait. None of these features are verified by the baroclinic velocity vectors (not shown). It may be that geostrophic balance is not a good assumption in May, or that the density gradients are too weak or too recently formed to set up a geostrophic flow.

*June and July 1994, June 1995 and 1996*

T/S diagrams from June 1994, July 1994, June 1995, and June 1996 are shown in Figures 12(a)-(d). By June, the temperature minimum layer is well defined at all PWS station. The isopycnal where the minimum occurs varies from 25.0 in 1994 (Figures 12(a) and (b), to 25.2 in 1995 and 1996. The density of the bottom water in the 'black hole' (SEA22) is still about 26.1, with the CFOS13 bottom water density slightly less (26.0). The difference between PWS and GOA water mass properties is more pronounced than in previous months. In 1994 and 1995, the GOA water is both warmer and saltier along isopycnals, except at the very near surface. Properties at SEA32 more closely resemble PWS properties than GOA. In June 1996, the water mass properties at SEA32 and GOA0

are similar to each other, and to the other PWS stations.

Comparison of Figures 12(a), (c) and (d) show that in June 1996 it was the PWS water above the temperature minimum layer that became warmer and saltier, rather than a change in the GOA water mass that resulted in the similarity. In June 1996. the temperature minimum layer T/S signature is sharper. and the overlying PWS water mass properties are between the 1995 PWS properties and the 1996 GOA. Intrusion and mixing of GOA water into PWS probably occured in June 1996.

Dynamic height contours from June 1996 also show evidence of inflow from the GOA at Hinchinbrook Entrance. and a basin scale cyclonic circulation (Figure 13(a)). Some agreement between the dynamic heights and the baroclinic velocity vectors (Figure 13(b)) can be seen in the central and northwest Sound. and at Hinchinbrook Entrance. Dynamic heights in June 1995 indicate very weak flow (Figure 13 (c)), which is not verified by observed baroclinic velocities.

*September 1994, 1995 and 1996*

T/S diagrams for September 1994, 1995 and 1996 are shown in Figures 14(a)-(c). By September of all years, the temperature minimum layer, while still detectable, has become much less pronounced. The surface waters are the warmest and freshest in September. The density of the deepest water at CFOS13 and SEA22 is still roughly 26.0-26.1. In 1995 and 1996, the PWS stations (CFOS13, SEA22, and SEA32) have similar water mass properties, which differ from the shelf GOA. In 1994, stations CFOS13 and SEA22 are similar and differ from the GOA, but the water mass propoerties of station SEA32 are inbetween.

Dynamic height contours from September of each year show cyclonic circulation in the central Sound (Figures 15(a)-(c)). Outflow at Montague Strait is indicated in September 1994 and 1995. Baroclinic velocity vectors from 1994, 1995 and 1996 (Figures 16(a)-(c)) also indicate cyclonic circulation in the central Sound. The baroclinic velocities show some outflow at Montague Strait in 1994 (Figure 16(a)), and inflow in 1996 (Figure 16(c)). Repeat ADCP velocity sections also show inflow at Montague Strait at the surface (Figure 17). The transects coincided with an easterly wind burst on September 15-16, 1996, which may have pushed water in the surface Ekman layer into the Sound.

*December 1996*

The T/S diagram for December 1996 shows a temperature maximum layer at a density of roughly 24.8 (Figure 18). The density of the bottom water is slightly less than in March 1995, and throughout the entire observation period. Stations SEA22 and CFOS13 no long closely resemble each other as they did in September. CFOS13 is warmer and fresher along isopycnals, and SEA22 is fresher at the surface by $\sim$ 0.5. The water mass properties at SEA32 more closely resemble CFOS13.

Dynamic height contours from December 1996 show a cyclonic curvature around the central Sound basin, and outflow Montague Striat (Figure 19(a)). The baroclinic velocity vectors confirm this general circulation (Figure 19(b)). Repeat ADCP velocity sections show inflow at Hinchinbrook Entrance above about 150m, and outflow below ((Figure 20).

## ADCP Mooring Velocity Time Series

Time series of north-south (v-component) velocities at Hinchinbrook Entrance, 40 hour low-pass filtered, for the summer 1995 deployment are shown in Figure 21(a). The flow was generally out of the Sound (southward) above about 150m. and inward (northward) below. This pattern was interupted by high velocity bursts of inflow at the surface. Inspection of wind speed and direction time series show that these inflow bursts are correlated with easterly wind speed bursts, as indicated by the arrows at the top of the figure. An example from September (the last 2 bursts) is shown in Figure 21(b). For a wind speed of 20m/s (the second event in Figure 21(b)), the theoretical Ekman depth is 90m, in agreement with the observed inflow depth. Associated with the upper layer inflow bursts are periods of outflow in the deeper layers. The upper bin depth is about 44m, and even when the inward surface burst is not visible, the deeper outflow is (arrows in July).

The 40 hour low-pass filtered velocity time series from the 1996-1997 deployment are shown in Figures 22(a) and (b). From September 1996 to the end of December the summer inflow/outflow pattern was reversed with inflow generally above 150m and outflow below. The transition depth increased as the season progressed. The bursts of inflow at the surface, corresponding to strong easterly wind events, is apparent until January. From roughly January to May 1997 the velocity was nearly barotropic. After mid-February, the flow was mostly inward except for periods in early April and in early May.

Volume transports were calculated using mean monthly velocities, for the portion of the water column above and below 150m. The channel width, measured at its greatest constriction between the 50 fathom depth contours, was approximately 10 km. The mooring was actually located about 5km north of this point. The width at the actual mooring location was not used because of the broad shelf regions on either side. The total depth at the mooring location was 280m. The area above 150m used in the calculation was then $1.5 \times 10^6 m^2$, and the area below 150m used was $1.3 \times 10^6 m^2$.

It was assumed that (1) there was no horizontal varibility, (2) that the ADCP mooring velocities were representative of velocities farther south, and (3) the the velocities from 50m depth to the surface (in the ADCP shadow zone) did not change the mean significantly. The assumption of no horizontal varibility was shown by the repeat ADCP sections to be valid in most seasons, but invalid in April for example. Comparison of the repeat ADCP velocities from the cruises with the moored velocities showed that the second assumption is fairly good. Some repeat ADCP sections show increased velocities near the surface, which were not captured by the mooring. The velocities from the upper 50m layer were assumed to be equal to the mean.

Transports during the 1995 and 1996-1997 deployments are shown in Figures 23(a) and (b). In summer 1995, the upper and lower layer transports roughly balanced each other. The net flow was close to zero. In fall and early winter 1996, the upper layer transport reached a maximum of 0.2 Sv (Figure 23(b)). Niebauer et al (1994) found maximums in excess of 0.3 Sv in 1978. The standard deviations of these averages was often close to 0.1 Sv, so this difference may not be significant. From January 1997 on, transports were either positive or close to zero.

To compare the 1996-1997 transports to those calculated by Niebauer et al, the 1978-1979 tranports were summed into layers above and below 150m, and plotted along with the 1995-1997 values in Figures 24(a)-(d). The maximum upper layer transport at Hinchinbrook

Entrance peaked in October and December of both 1978 and 1996, although the magnitudes in 1996 were less. The seasonal trends in transports both above and below 150m were similar.

Monthly mean upwelling indices from 60°N, 146°W for the periods 1975 - 1979 and 1993 - 1997 are shown in Figure 25. Except for 1979, mean meteorological conditions were approximately the same during both time periods. Unfortunately, the Niebauer et al mooring was retreived before the intense downwelling event in February 1979.

## Summary

Densest water is constant at $\sigma_\theta = 26.0 - 26.1$ for all seasons of all years. The density of the temperature minimum layer varies interannually from 25 to 25.2. In T/S space, the dip of the temperature minimum layer becomes more shallow as the seasons progress, from maximum in June to a minimum in December, and is non-existant in March. During most of the year, the water properties of the central Sound (CFOS13) and the northwestern Sound (SEA22) deeper than the temperature minimum layer are similar.

The water mass properties in March are the coldest and saltiest of all the seasons observed, and the most spatially uniform. In April, the surface waters start to warm and freshen, probably due to heating and precipitation rather than GOA inflow, so that a temperature minimum layer is formed. An anticyclonic baroclinic eddy present in the central Sound in April 1995 is not present in April 1996. Inflow and outflow at Hinchinbrook Entrance and Montague Strait have both horizontal and vertical shears.

By May the deepest water in the central Sound has freshened compared to April. The deepest water in the 'black hole' remains unchanged. In May 1997, the water at both Montague Strait and Hinchinbrook Entrance resembled the GOA water at the surface and PWS water at depth. T/S plots for stations throughout Montague Strait show that the exchange took place at southern Montague Strait and Hinchinbrook Entrance, rather than in through Hinchinbrook, around Montague Island, and out through Montague Strait. An easterly wind burst occurred during this time that may have pushed water in the surface Ekman layer into the Sound.

Some intrusion from the GOA into PWS through both Montague Strait and Hinchinbrook Entrance is indicated in June 1996. Water mass properties between the shelf GOA water and PWS are separate in summer 1994 and 1995, and in September of all years. A closed basin scale cyclonic circulation was present in the central Sound in September 1994, 1995, and 1996. Dynamic heights from Niebauer et al (1994) also indicated a cyclonic circulation was present in September 1978. September of all years exhibited the warmest and freshest surface waters.

In December, in addition to the temperature maximum layer formation, warming and freshening penetrated down to the bottom water at both CFOS13 and SEA22. The central Sound and northwestern Sound deep water mass properties were much less similar in December. Whether this was due to vertical exchange or GOA influence is unclear. A basin scale cyclonic circulation was observed, with outflow at Montague Strait.

Geostrophic balance may be a good assumption during seasons when the density gradients are strongest. The Rossby number $\epsilon = U/fL$ for velocity $U \sim 25cm/s$, Coriolis parameter $f = 1.26 \times 10^{-4}s^{-1}$, and length scale $L \sim 20km$ is $O(0.1)$. While other process

certainly effect the circulation, the influence from the geostrophic component should be fairly large.

## Conclusions

No indication of intrusion of GOA water into the central Sound was found in April or May. Intrusion was indicated in June 1996, but not in June 1994 or 1995. In September, the Sound seems to be sealed off from the GOA entirely. The dominant circulation feature in September is the cyclonic gyre in the central Sound. In December, several processes seem to be acting simultaneously. Indentifying these processes will require further investigation.

The T/S plots indicate 4 water masses are present in PWS. The bottom water with $\sigma_\theta \sim 26.0 - 26.1$, is present most of the year (except maybe December) throughout the Sound with constant T $\sim 5.9°C$ and S $\sim$ 33.0. Deep water, defined from the density of the temperature minimum to the bottom, or $25.2 \leq \sigma_\theta \leq 26.0$, is present from March to at least September. The temperature minimum in April and May is defined by roughly T$\sim$ 4.0, S$\sim$ 31.8, and $\sigma_\theta \sim 25.2$. Warming and salinification along isopycnals occurs from March to December, where the layer becomes less well defined. In September, the temperature minimum is defined by T$\sim$ 5.0, S$\sim$ 32.0, and $\sigma_\theta \sim 25.2$. Intermediate water, resulting from upper layer warming, at roughly $24.8 \leq \sigma_\theta \leq 25.2$, starts to form in April. The upper limit of this layer (24.8) corresponds roughly to the density of the temperature maximum observed in December. The stratified upper layer water with $\sigma_\theta \leq 24.8$ changes T/S properties seasonally.

Comparisons between the transports calculated by Niebauer et al (1994) and those presented here, and the upwelling indices for both periods, suggest that conditions during the late 1970s and mid-1990s were similar. At Hinchinbrook Entrance the summer months were characterized by outflow above 150m and inflow below. The fall and early winter months were characterized by inflow above 150m and weak outflow below. Late winter and early spring months were characterized by more barotropic flows. Finally, strong easterly wind events in 1996 and 1997 caused upper layer inflow velocity bursts down to the Ekman depth. Associated with the Ekman layer inflow, were periods of outflow a deeper depths. It is not clear if the surface inflow penetrated far into the central or northern Sound, or if it was limited to just north of Hinchinbrook Entrance. Without this information, accurate flushing rates and residence times can not be calculated.

In some seasons, some aspects of the circulation and water mass properties of PWS are fairly predictable and geostrophic. Especially in the fall and winter (September through March), the dynamics of the Sound seem fairly stable. More variability exists in April, May and June. These transition months correspond to the period of highest biological activity, and even small changes may effect phytoplankton and zooplankton growth rates and distributions. The next step is to examine the effect of the seasonal and interannual variability on the biological components of the Sound.

## References


Muench, R. D. and G. M. Schmidt, 1975: Variations in the Hydrographic Structure of Prince William Sound. IMS Report R75-1, 135pp.

Niebauer, H.J., T.C. Royer, and T.J. Weingartner, 1994: Circulation of Prince William Sound, Alaska. *J. Geophys. Res.*, **99**, C7, pp 14,113-14,126.

Royer, T.C., D.V. Hansen, and D.J. Pashinski, 1979: Coastal Flow in the Northern Gulf of Alaska as Observed by Dynamic Topography and Satellite Tracked Drogued Drift Buoys. *J. Phys. Oceanog.*, **9**, 4, pp 785-801.

Wilson, J.G. and J.E. Overland, 1986: Meteorology, in The Gulf of Alaska. Physical and Biological Resources. Hood, D.W. and S. T. Zimmerman, eds. Alaska Office, Ocean Assessments Div., NOAA, 655pp.

## List of Figures

**Figure 19** : Dynamic heights (0/100m) from (a) December 1996 and (b) baroclinic (20-100m) velocities from December 1996.

**Figure 20** : Along channel and cross channel velocities with tides removed from Hinchinbrook Entrance in December 1996.

**Figure 21** : (a) ADCP mooring velocities (v-component, 40 hour low-passed filter) from June to September 1995 and (b) wind speed and direction from Mid-Sound buoy in September 1995.

**Figure 22** : ADCP mooring velocities (v-component, 40 hour low-passed filter) from (a) September 1996 to January 1997 and (b) January to May 1997.

**Figure 23** : Upper and lower layer transports in Sv from (a) 1995 deployment and (b) 1996-1997 deployment.

**Figure 24** : Comparison of transports to 1978-1979 mooring deployment from (a) 1995 above 150m, (b) 1996-97 above 150m, (c) 1995 below 150m, and (d) 1996-97 below 150m.

**Figure 25** : Upwelling Index from 1975 to 1979 and from 1993 to 1997.

# Oceanography Cruise - May 1997

FIG. 1

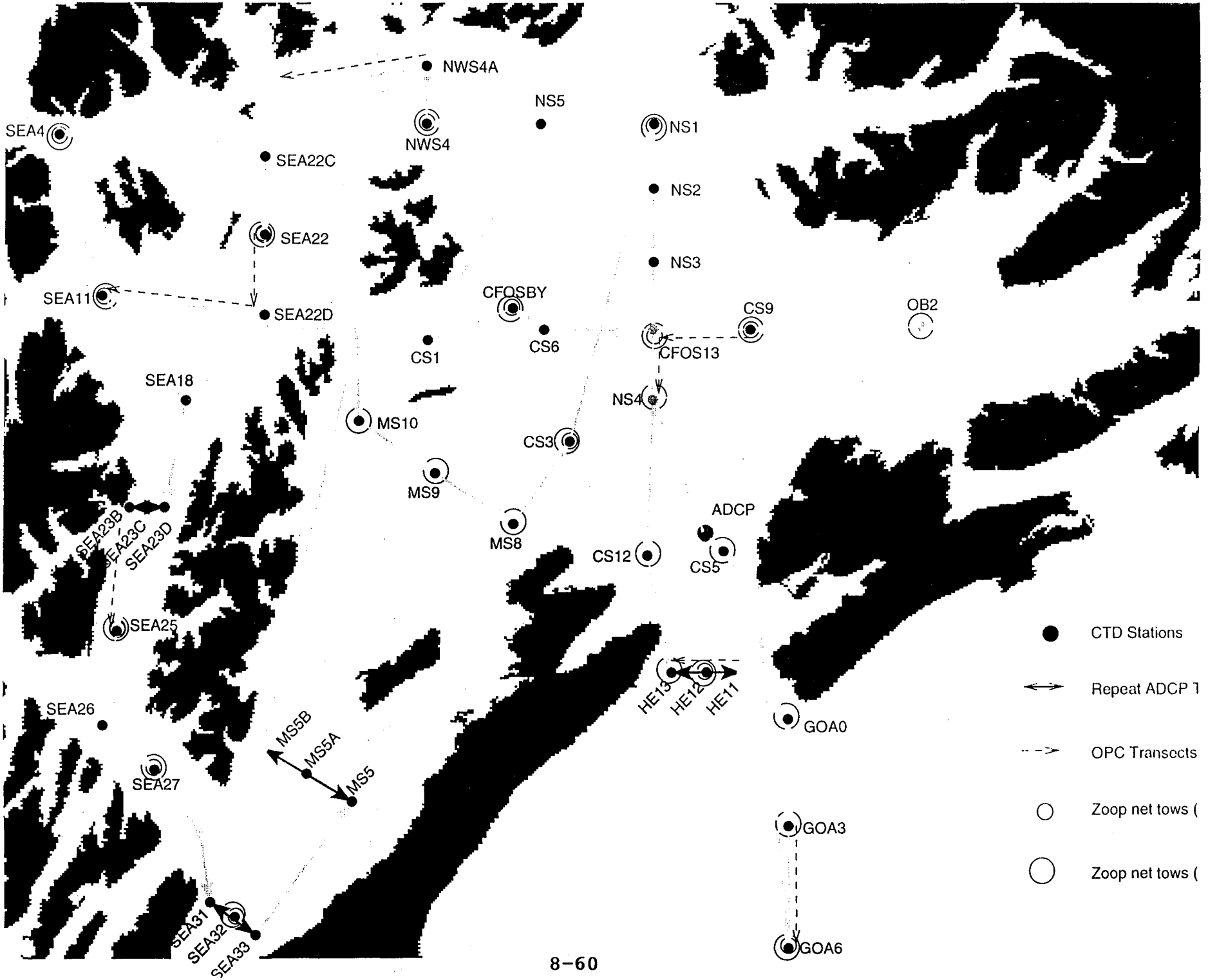

FIG 2

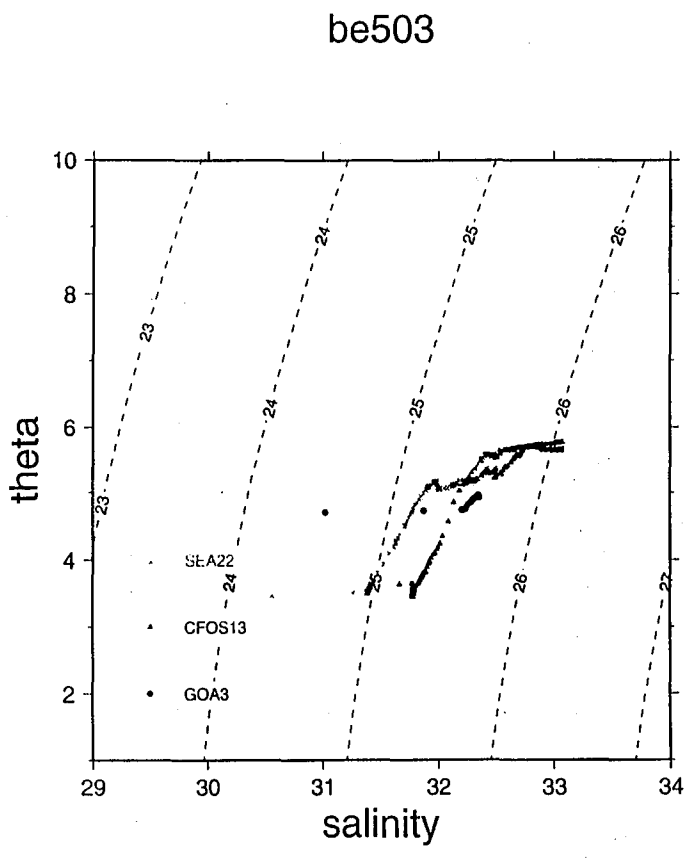
be503
theta
salinity
10
8
6
4
2
29
30
31
32
33
34
SEA22
CFOS13
GOA3
23
24
25
26
27

FIG 3

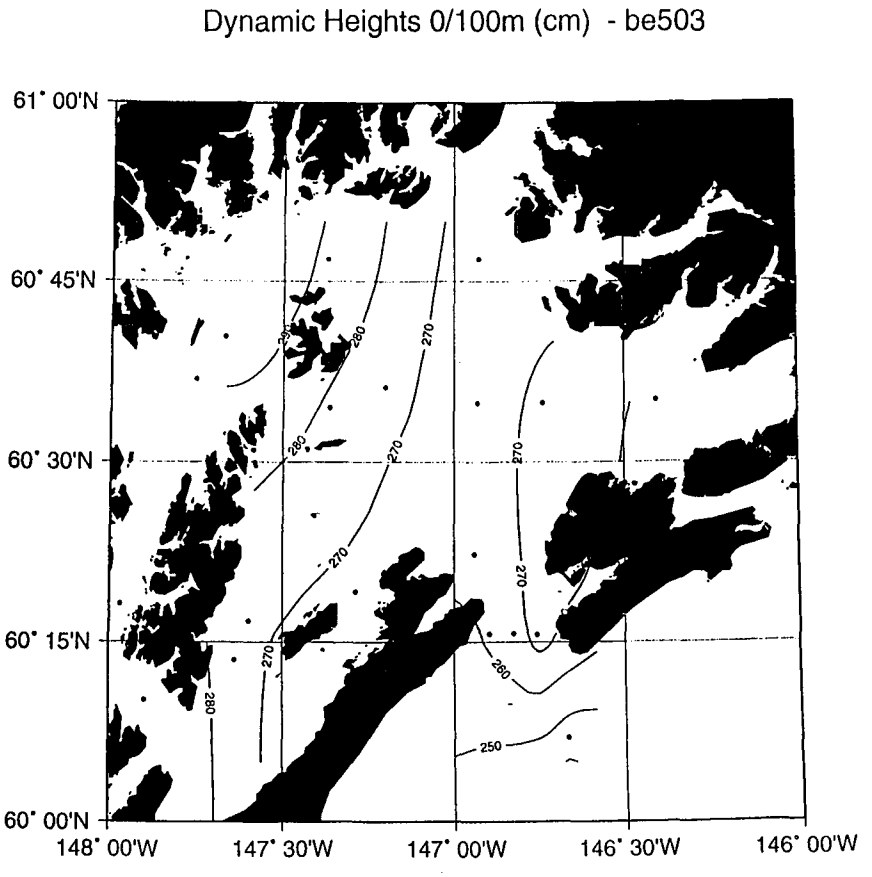
Dynamic Heights 0/100m (cm) - be503
61° 00'N
60° 45'N
60° 30'N
60° 15'N
60° 00'N
148° 00'W
147° 30'W
147° 00'W
146° 30'W
146° 00'W
250
260
270
280

FIG 4

be604

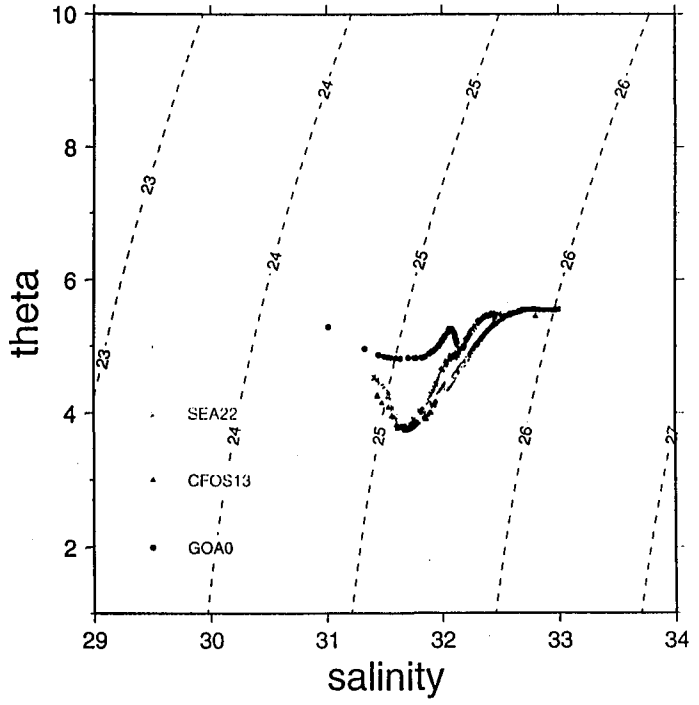
10
8
6
4
2
theta
29
30
31
32
33
34
salinity
23
24
25
26
27
SEA22
CFOS13
GOA0

FIG 5(a)

Dynamic Heights 0/100m (cm) - be504

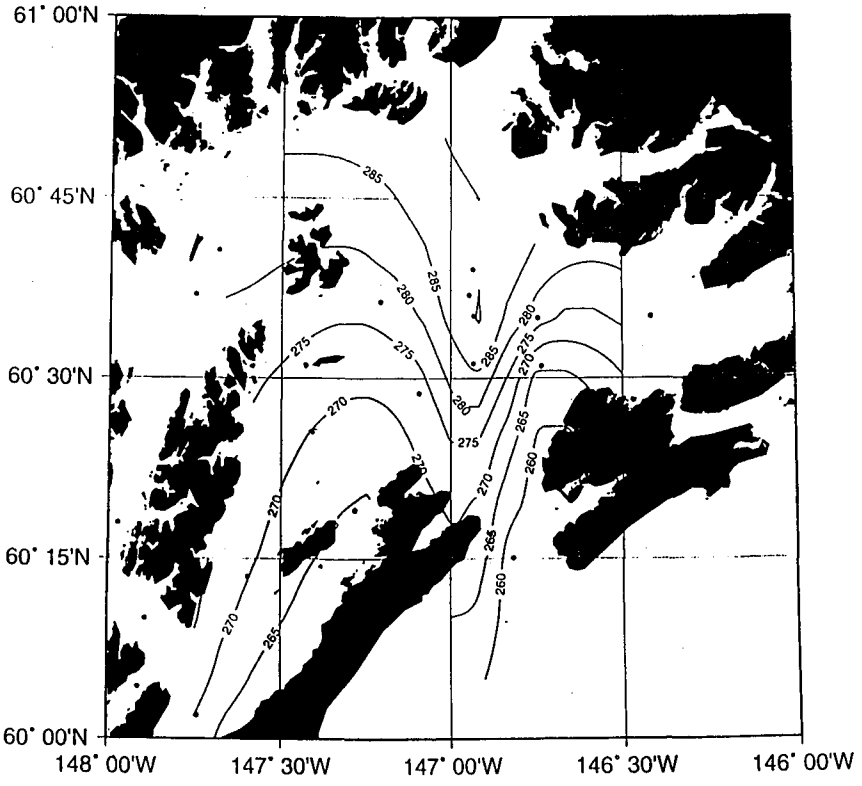


FIG 5(b)

Dynamic Heights 0/100m (cm) - be604

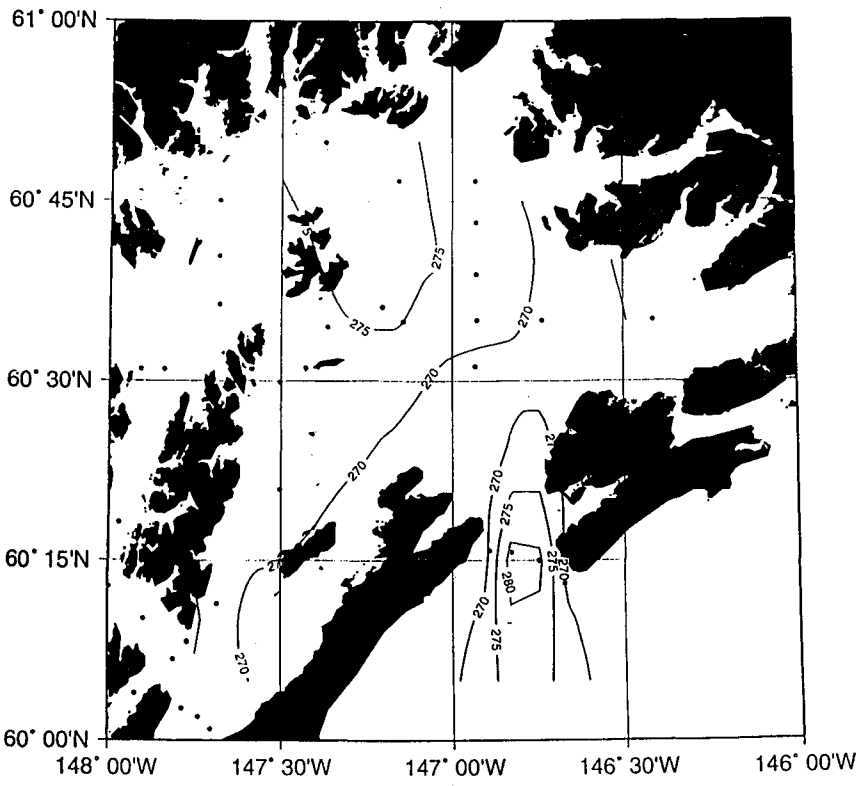

FIG 6

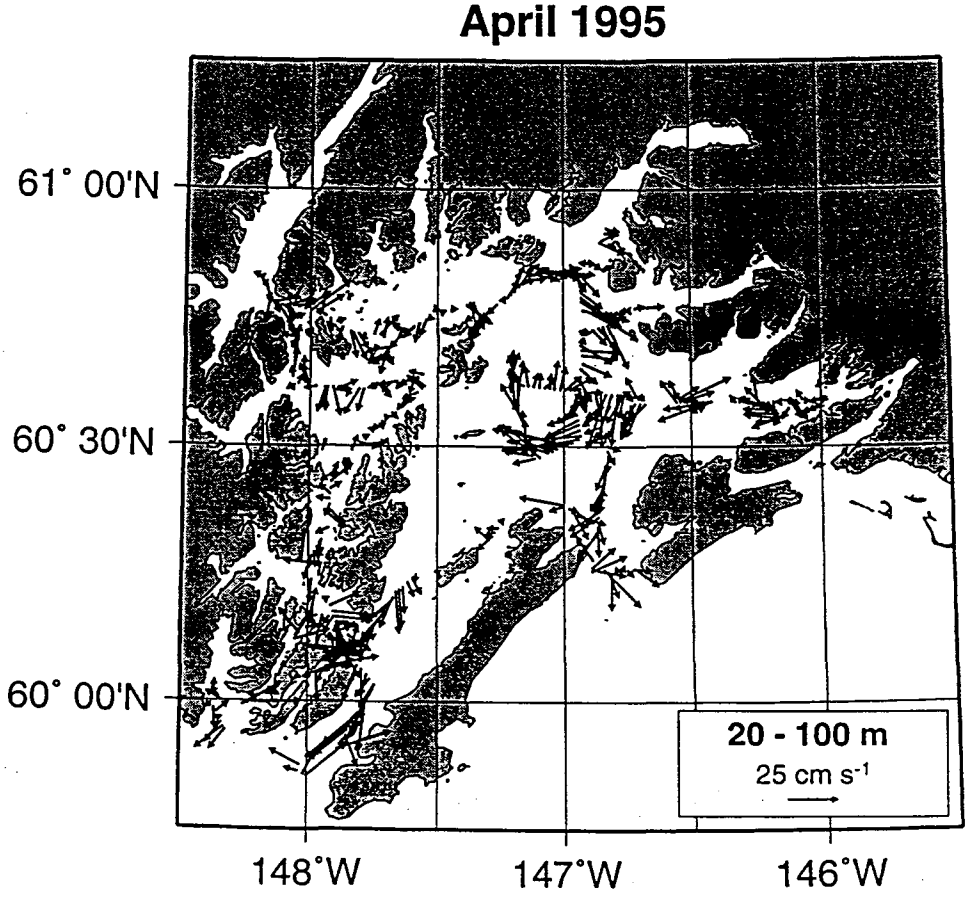

FIG 7(a)

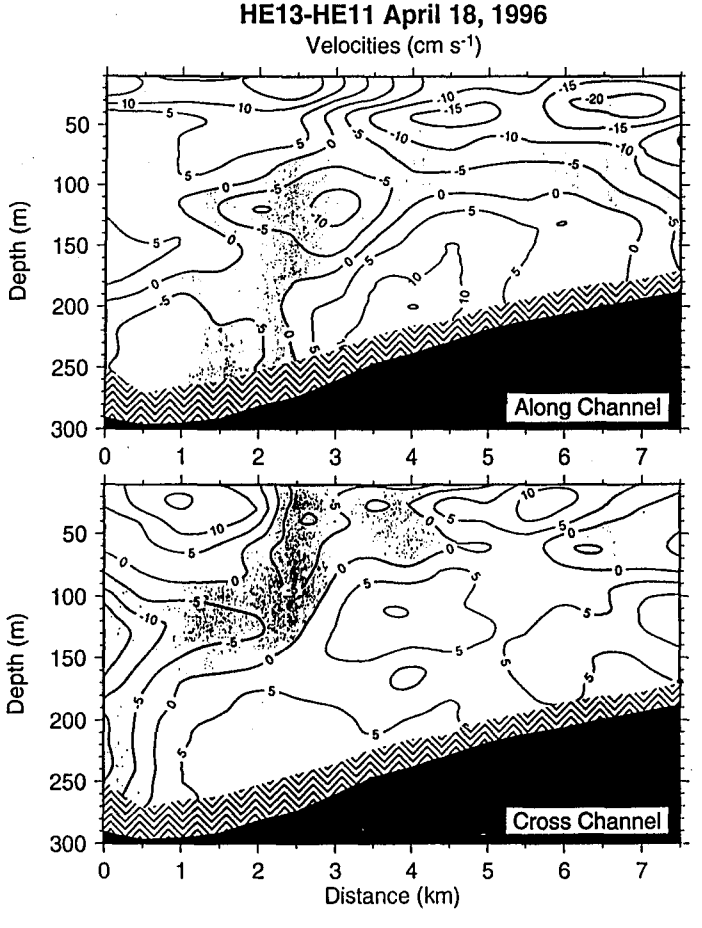


be46044, 46, 49
(avg flood + ebb)/2

FIG 7(b)

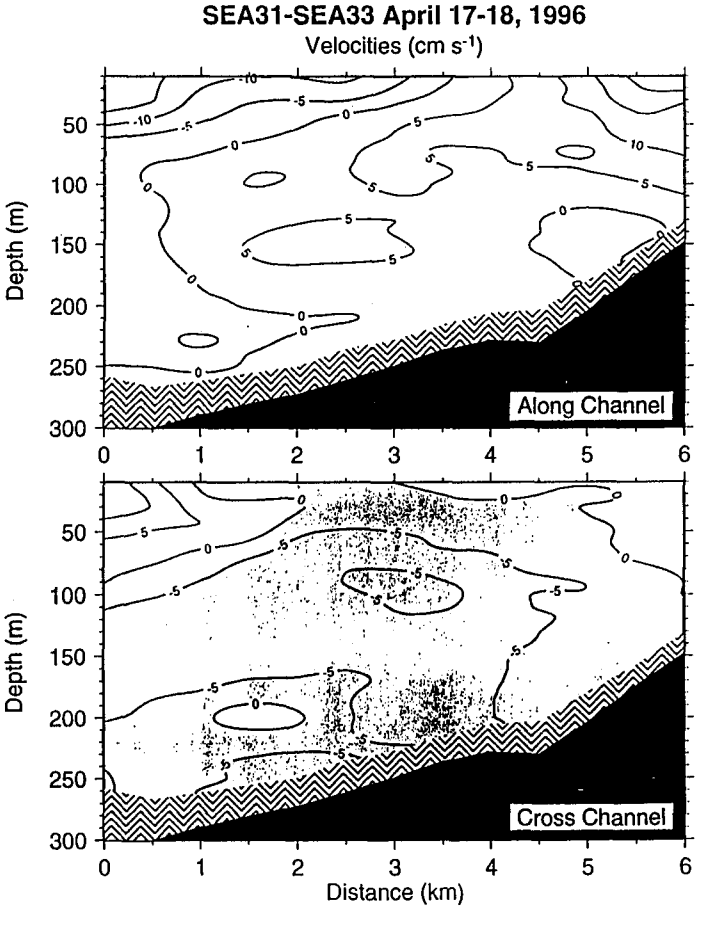


be46037, 38, 40, 41
avg of 2 flood and 2 ebb tides

FIG 8(a)

ab405

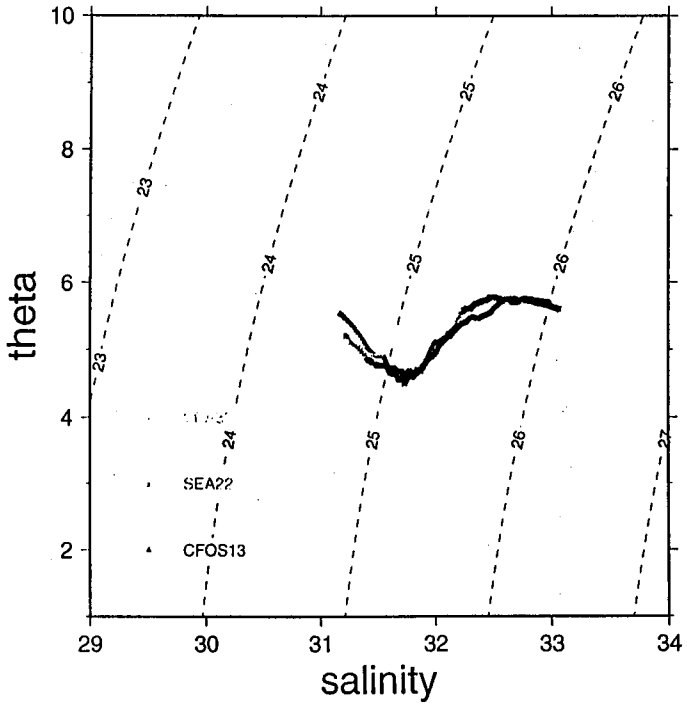


FIG 8(b)

be505

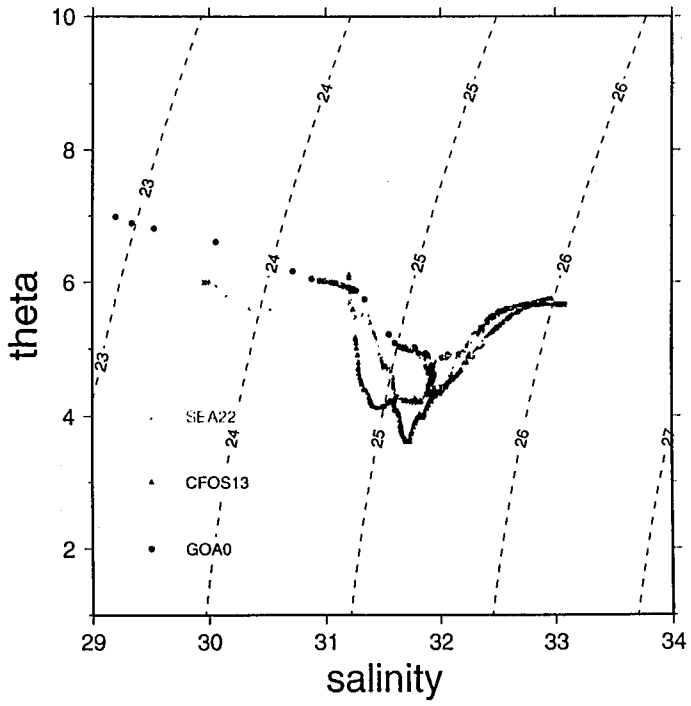

Fig 8(c)

hx605

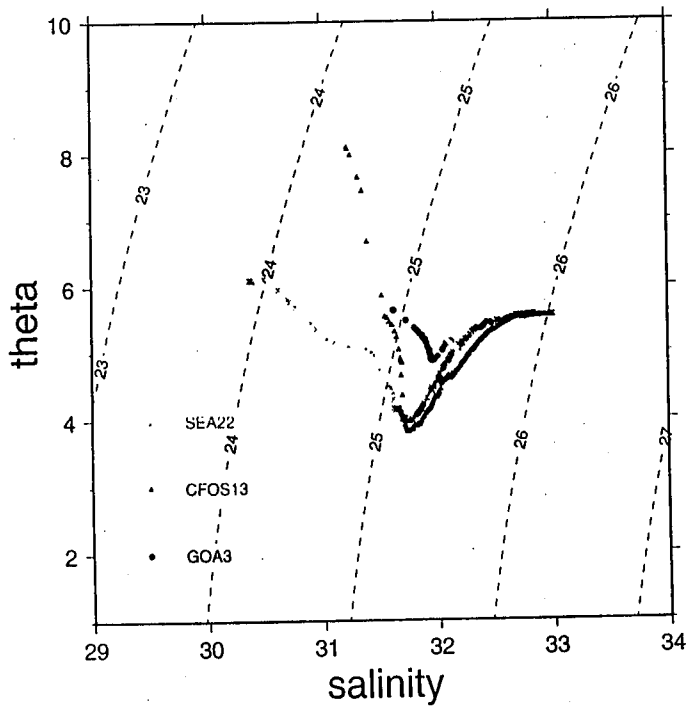


Fig 8(d)

be705

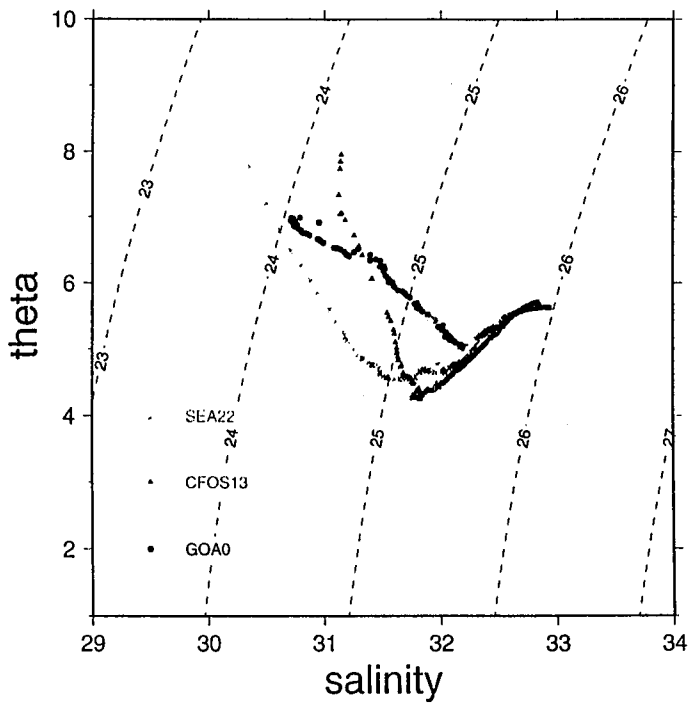

Fig9(a)

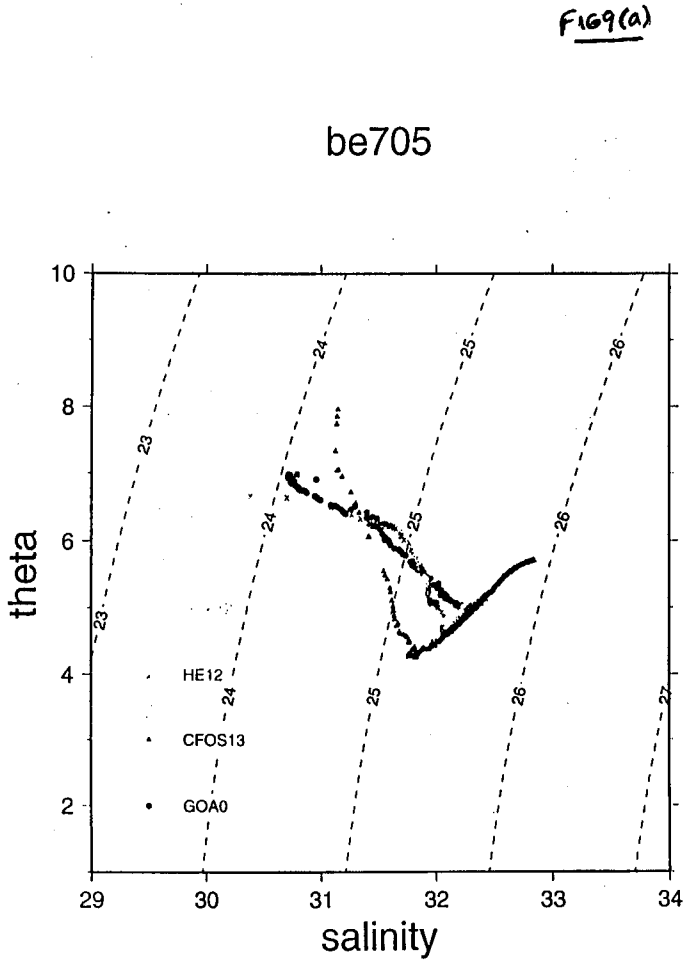
be705
theta
salinity
HE12
CFOS13
GOA0
23
24
25
26
27
10
8
6
4
2
29
30
31
32
33
34

Fig9(b)

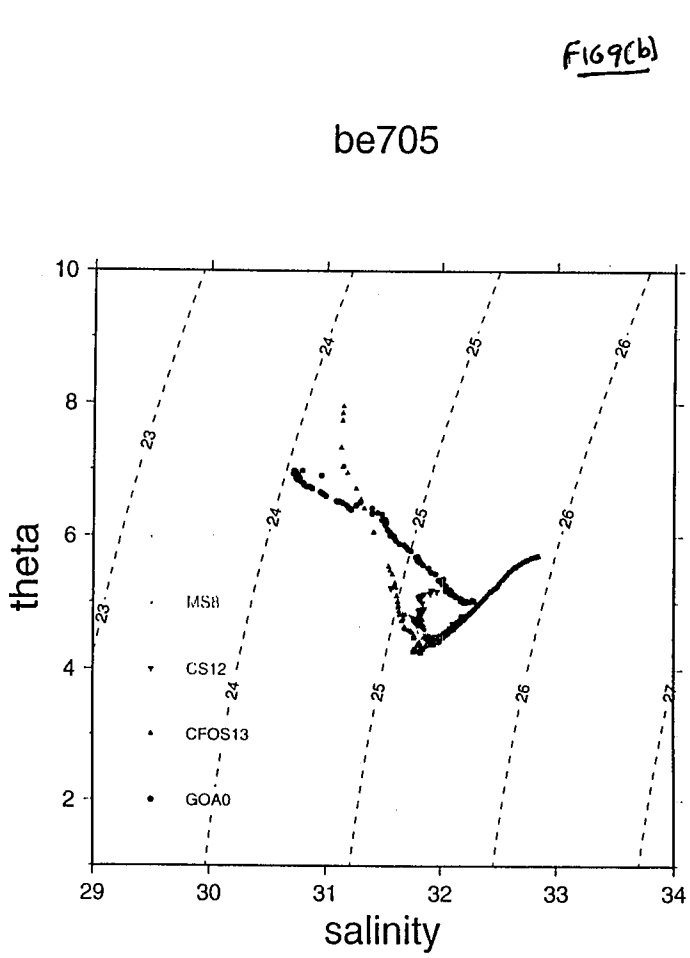
be705
theta
salinity
MSB
CS12
CFOS13
GOA0
23
24
25
26
27
10
8
6
4
2
29
30
31
32
33
34

FIG 10(a)

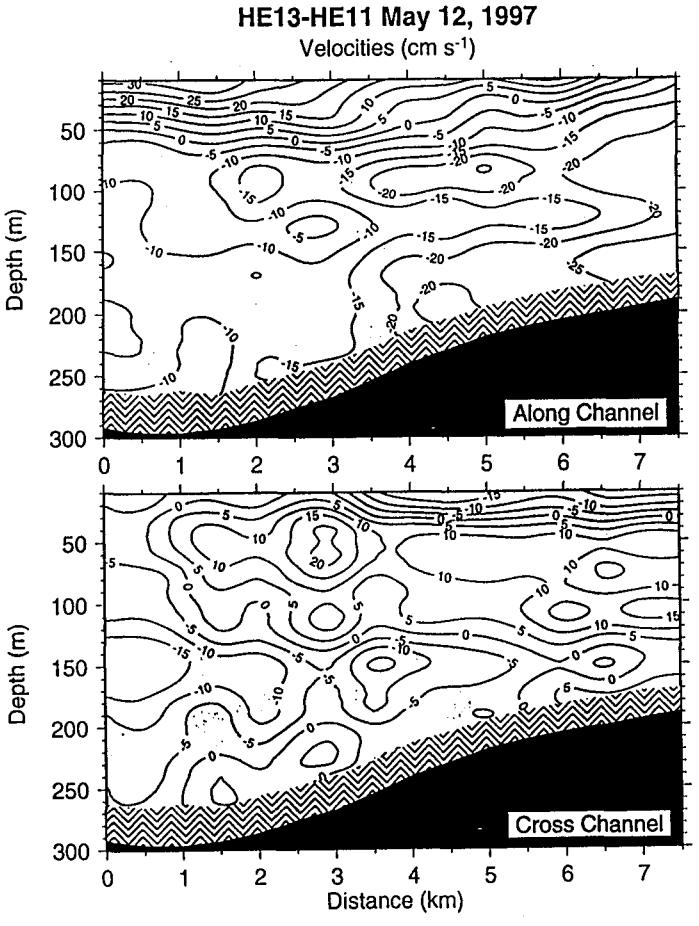


be57046, 47, 49, 50
avg of 2 flood and 2 ebb tides

FIG 10(b)

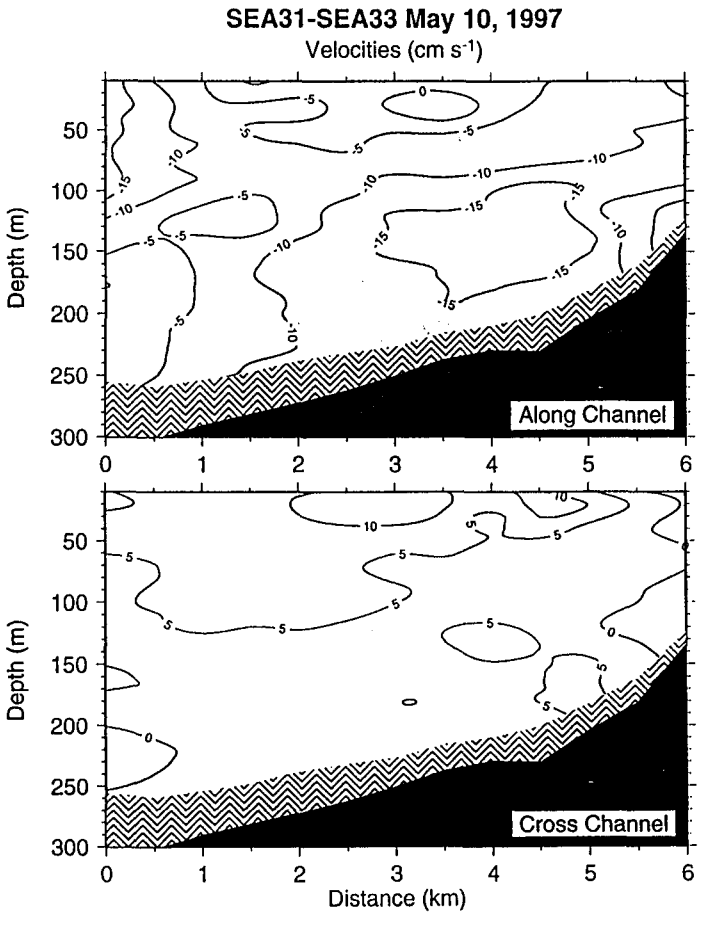


be57022, 23, 24, 25
avg of 2 flood and 2 ebb tides

FIG 10(c)

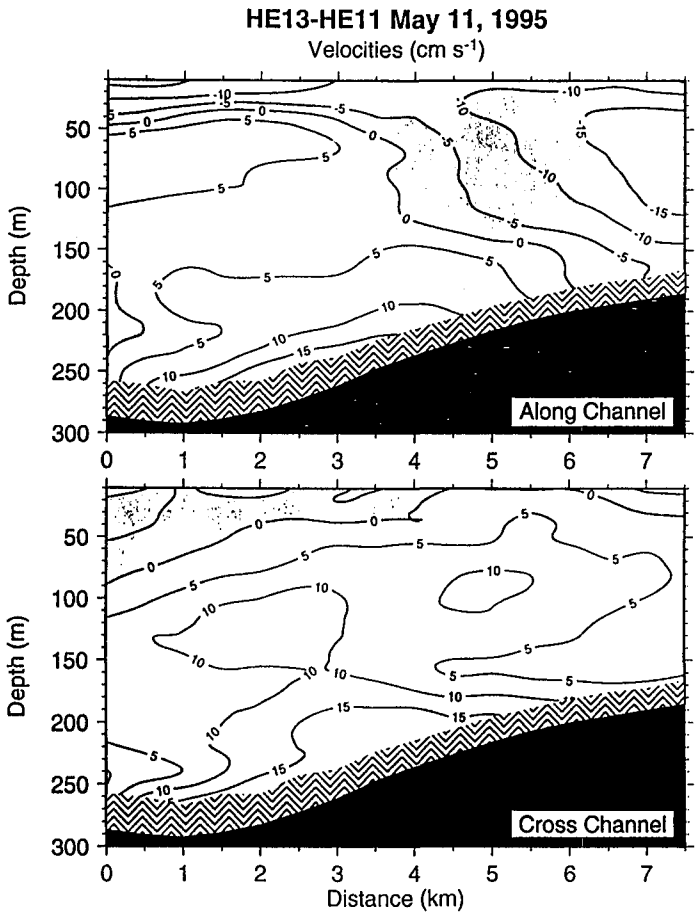


be95073a, c, d, e, g, h
avg of 3 flood and 3 ebb tides

FIG 11(a)

Dynamic Heights 0/100m (cm) - be505

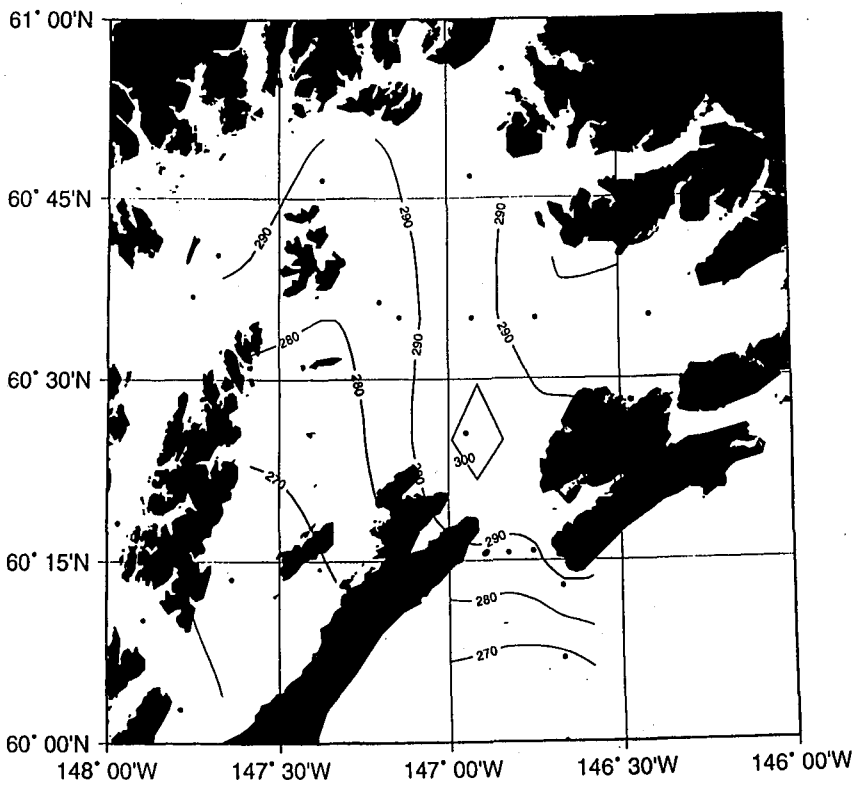


FIG 11(b)

Dynamic Heights 0/100m (cm) - hx605

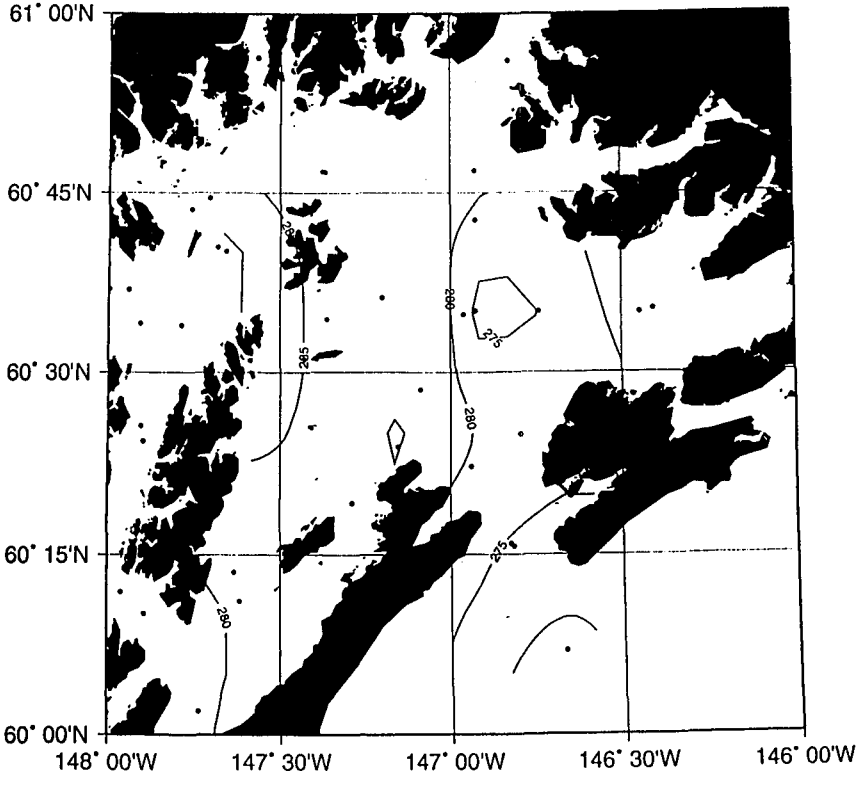

FIG. 11 (c)

Dynamic Heights 0/100m (cm) - be705

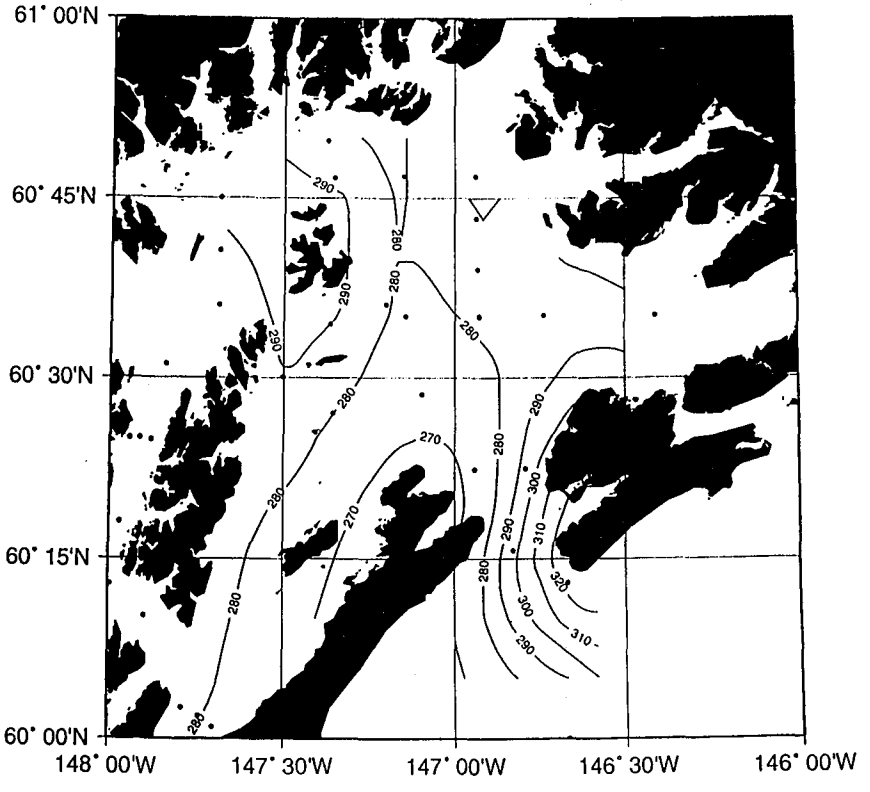

FIG 12(a)

ab406

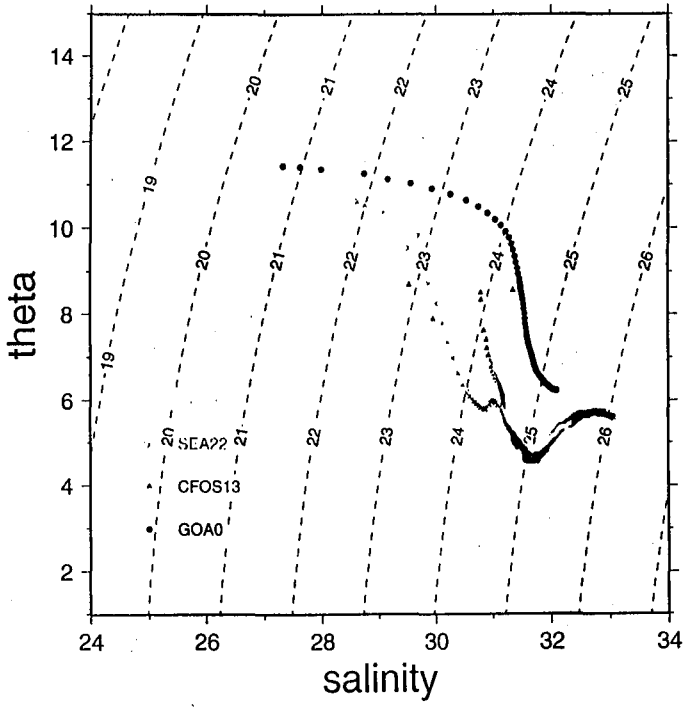


FIG 12(b)

ab407

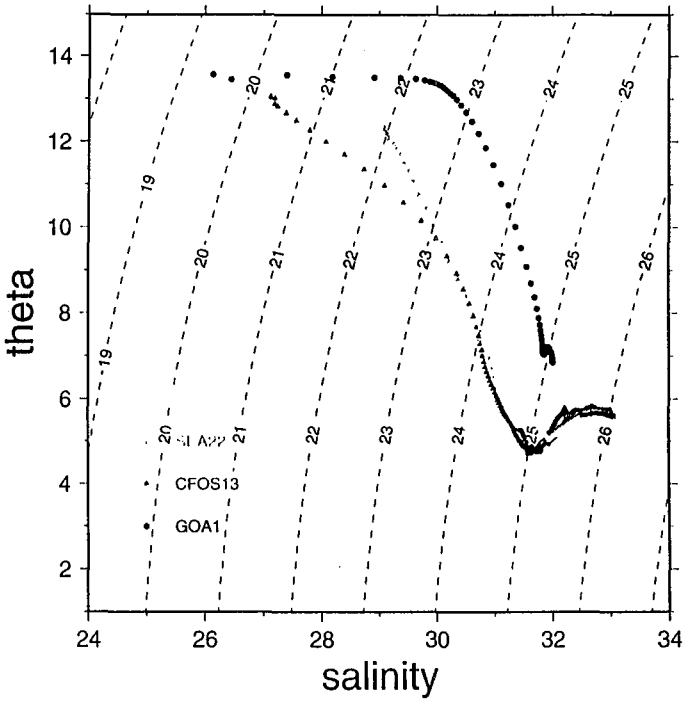

FIG 12 (c)

be506

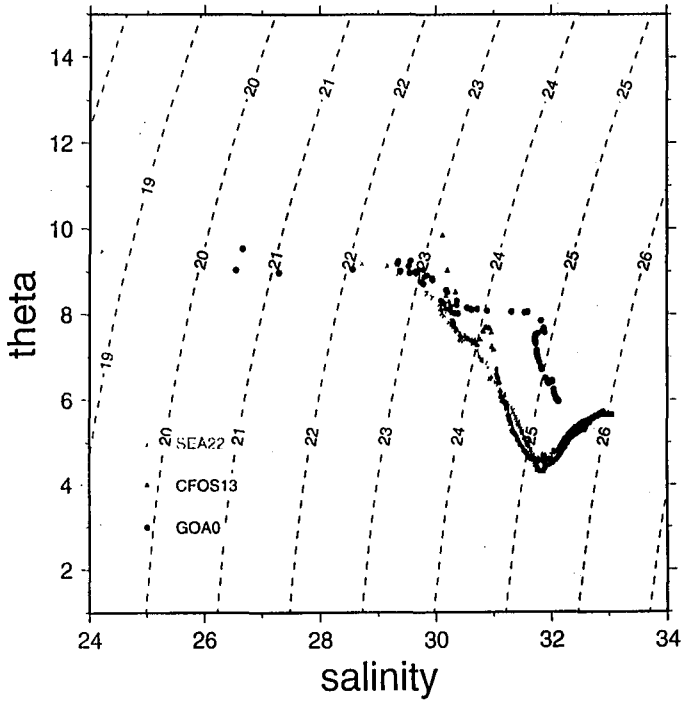


FIG 12 (d)

be606

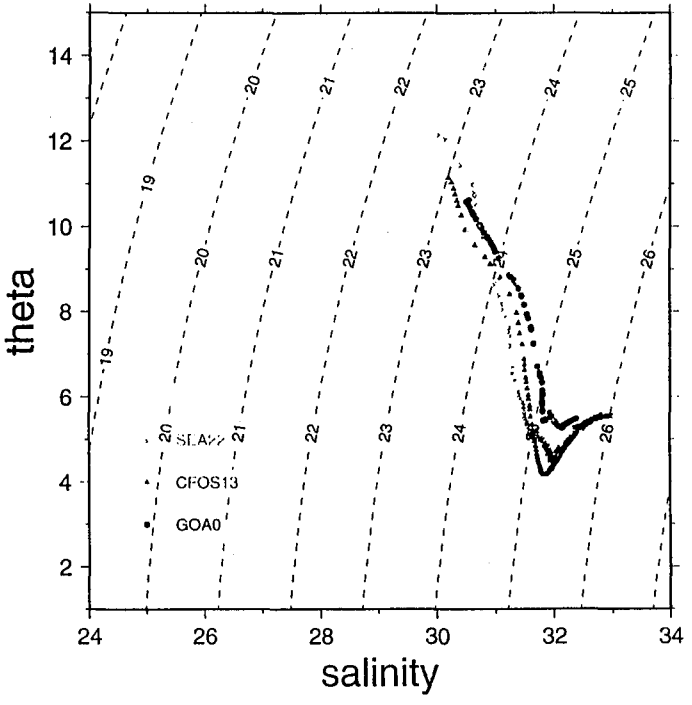

FIG. 13 (a)

Dynamic Heights 0/100m (cm) - be606

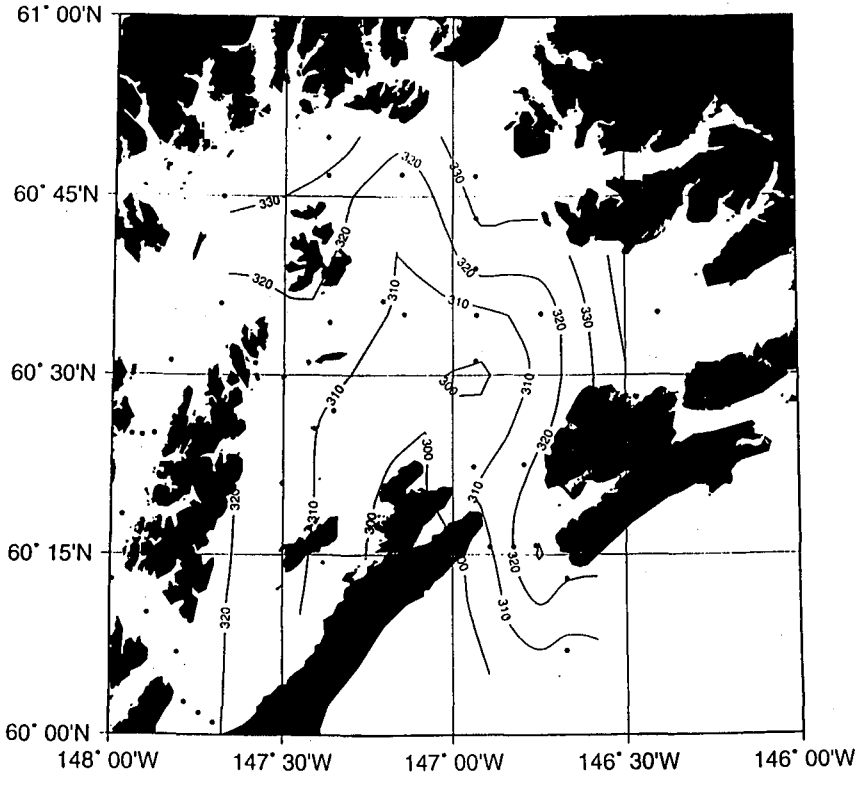


FIG 13(c)

Dynamic Heights 0/100m (cm) - be506

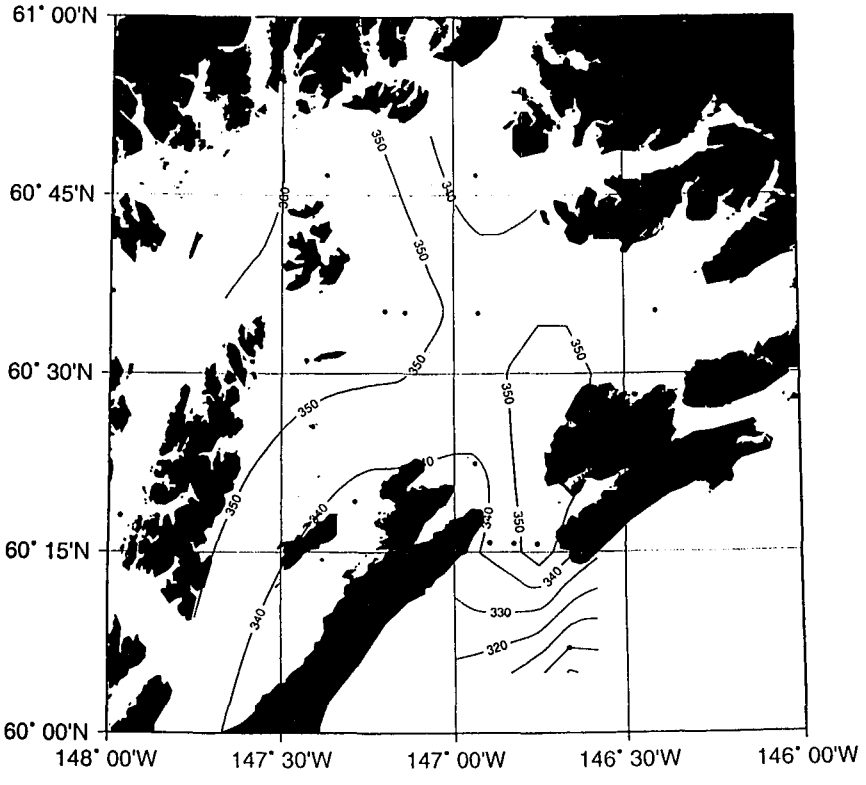

FIG. 13(b)

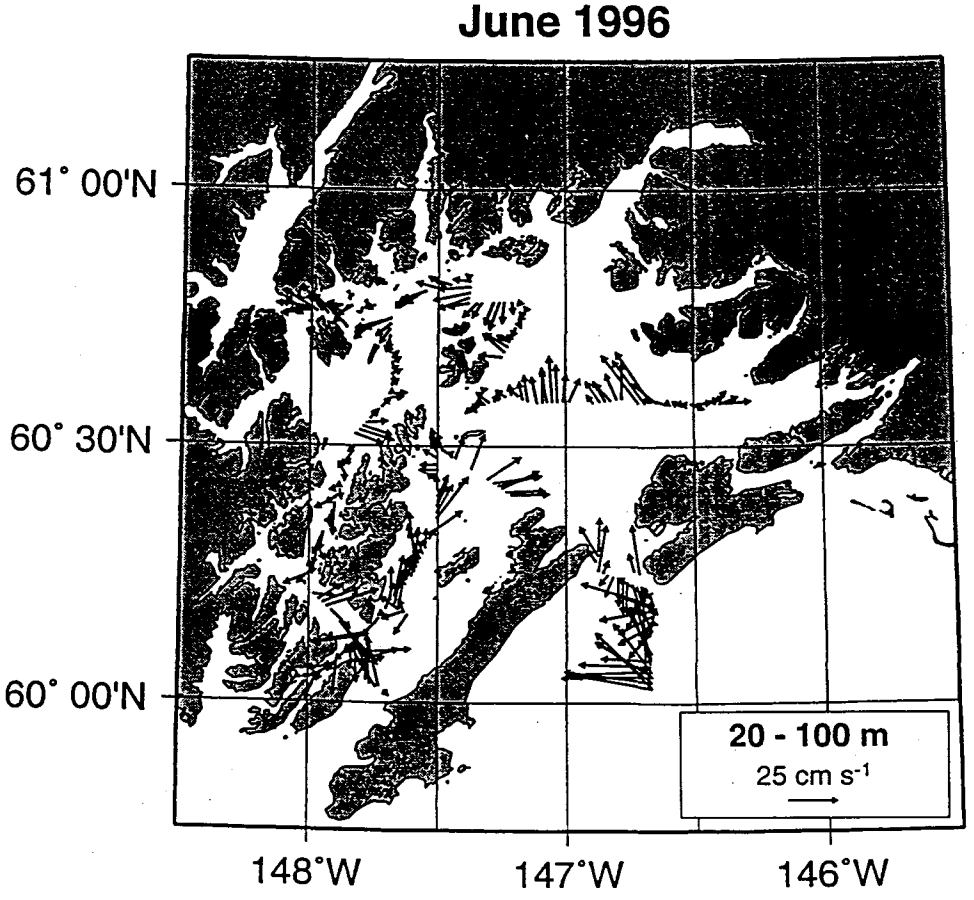

FIG. 14(a)

be409

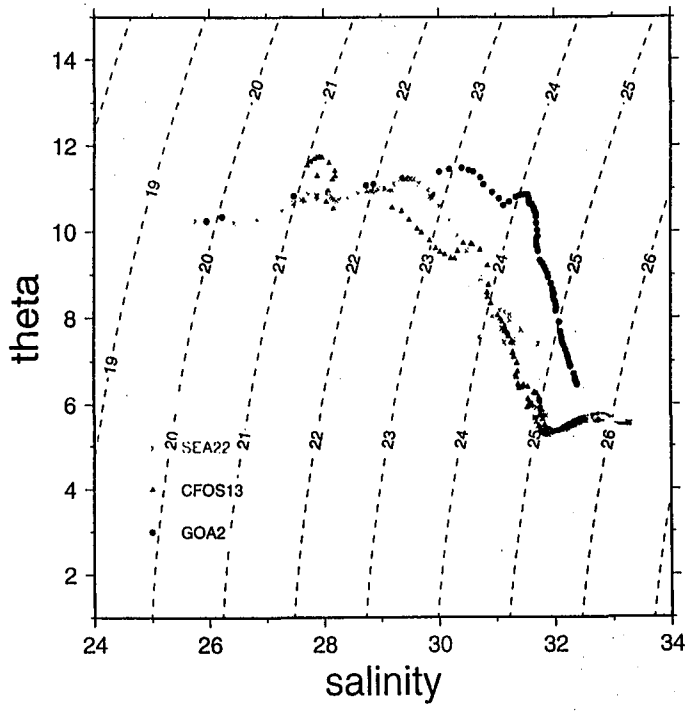


FIG. 14(b)

be509

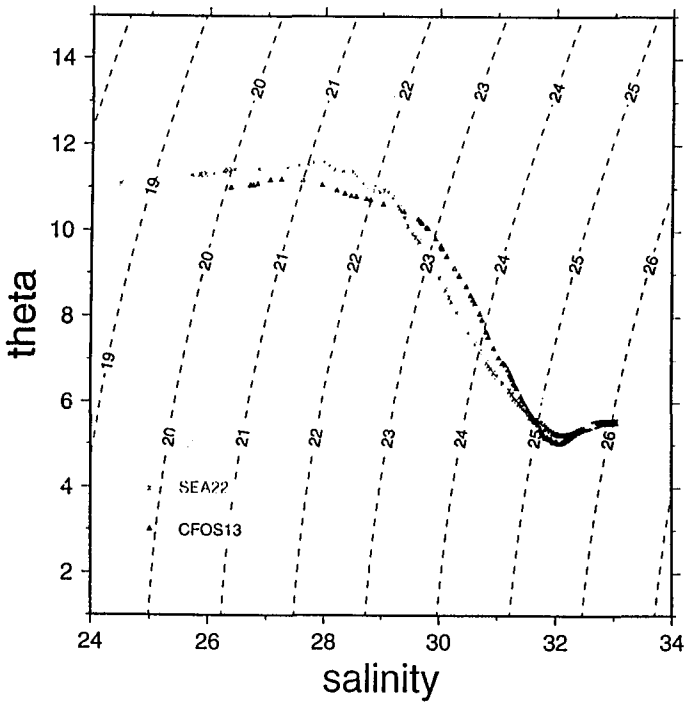

FIG. 14(c)

be609

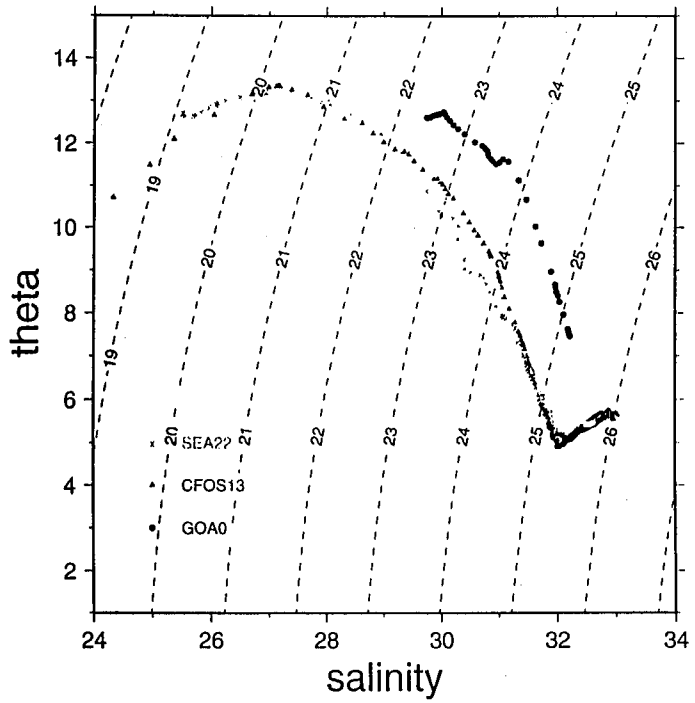

FIG. 15(a)

Dynamic Heights 0/100m (cm) - be409

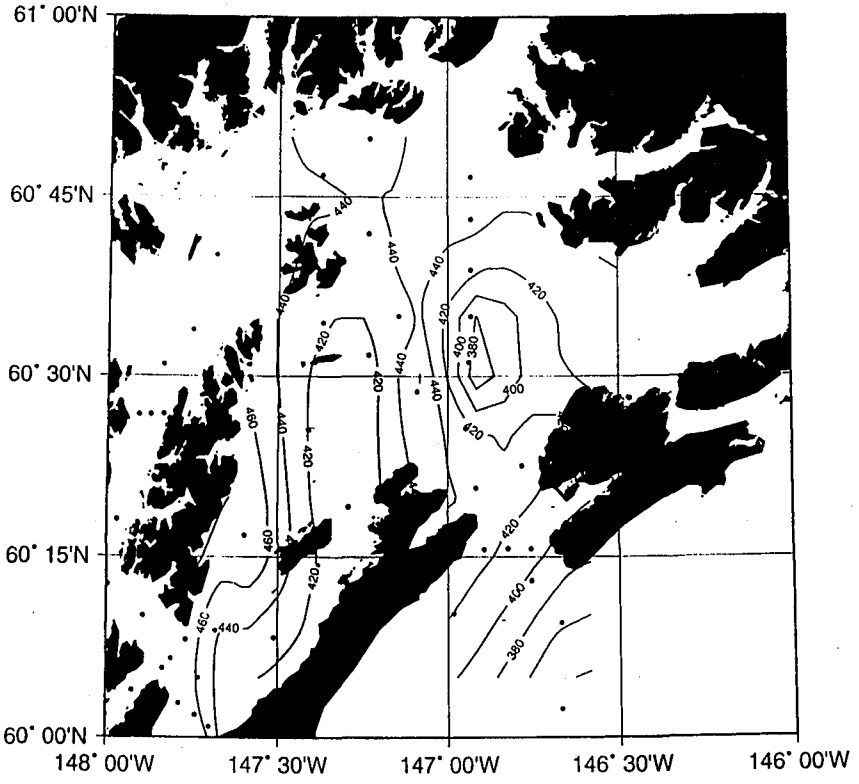


FIG 15(b)

Dynamic Heights 0/100m (cm) - be509

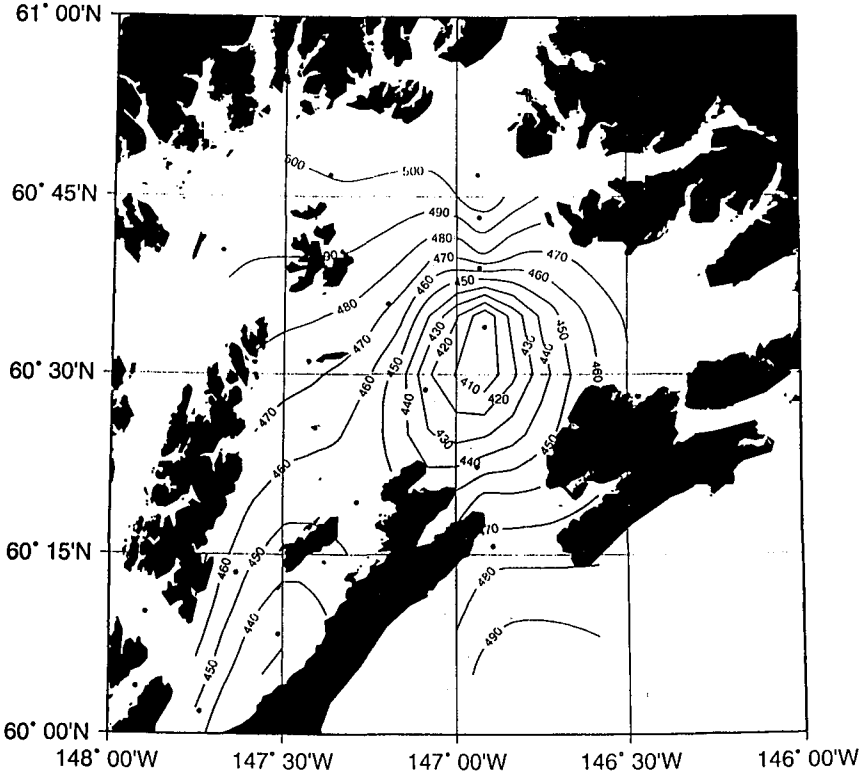

FIG 15(c)

Dynamic Heights 0/100m (cm) - be609

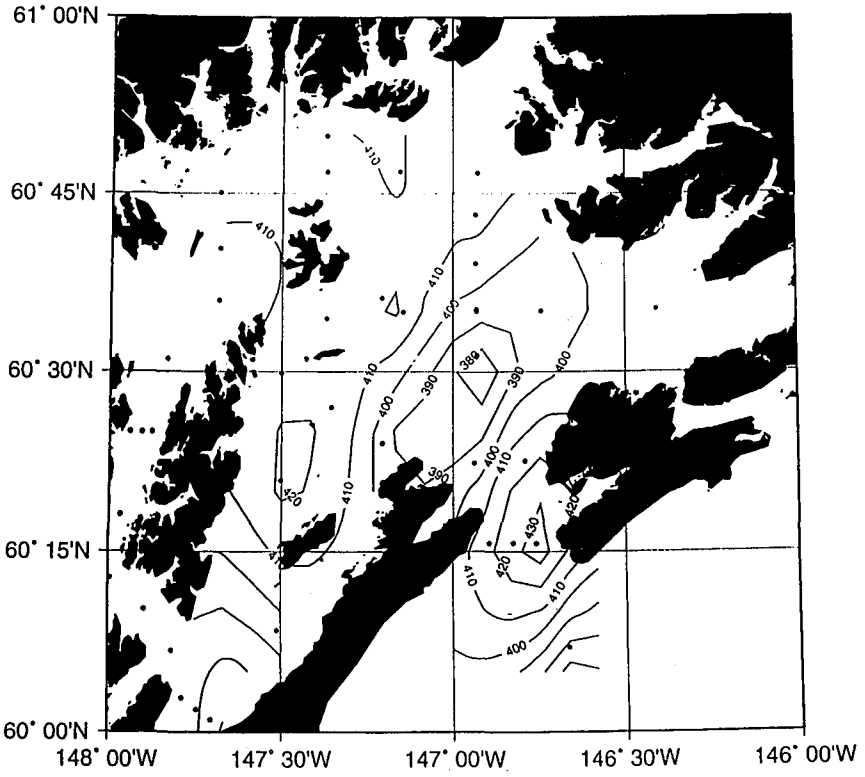

FIG. 16(a)

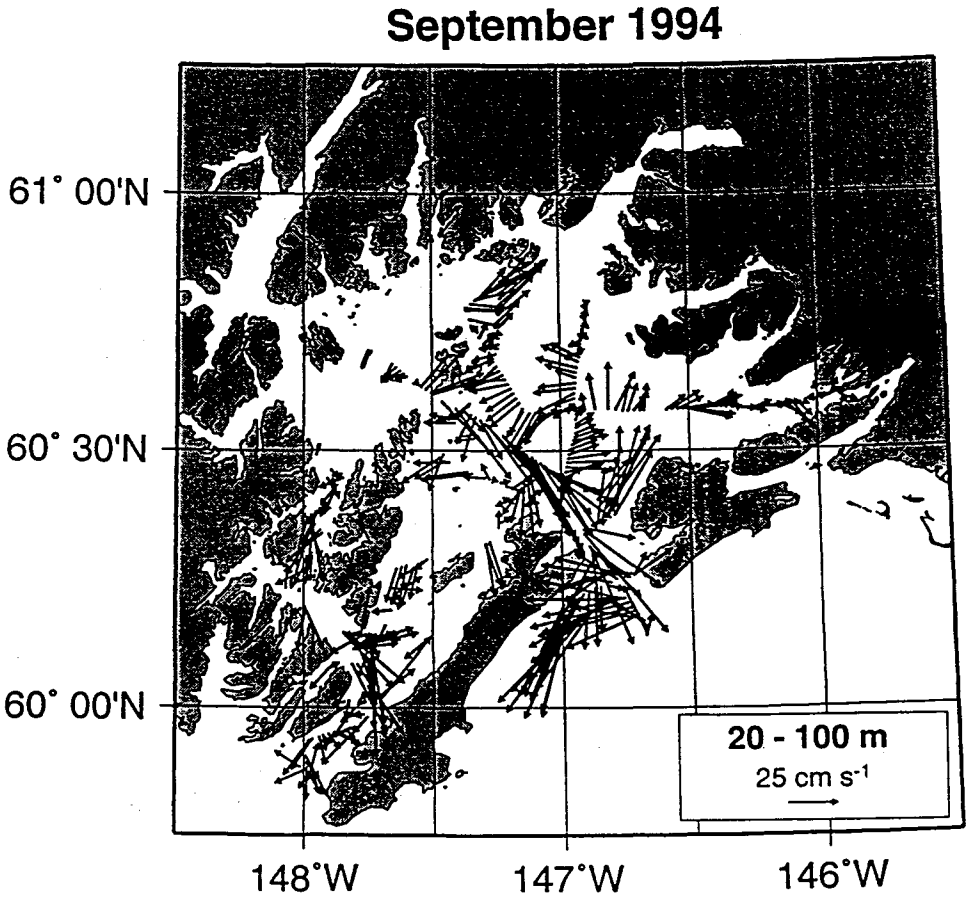
September 1994
61° 00'N
60° 30'N
60° 00'N
148°W
147°W
146°W
20 - 100 m
25 cm s-1

FIG. 16(b)

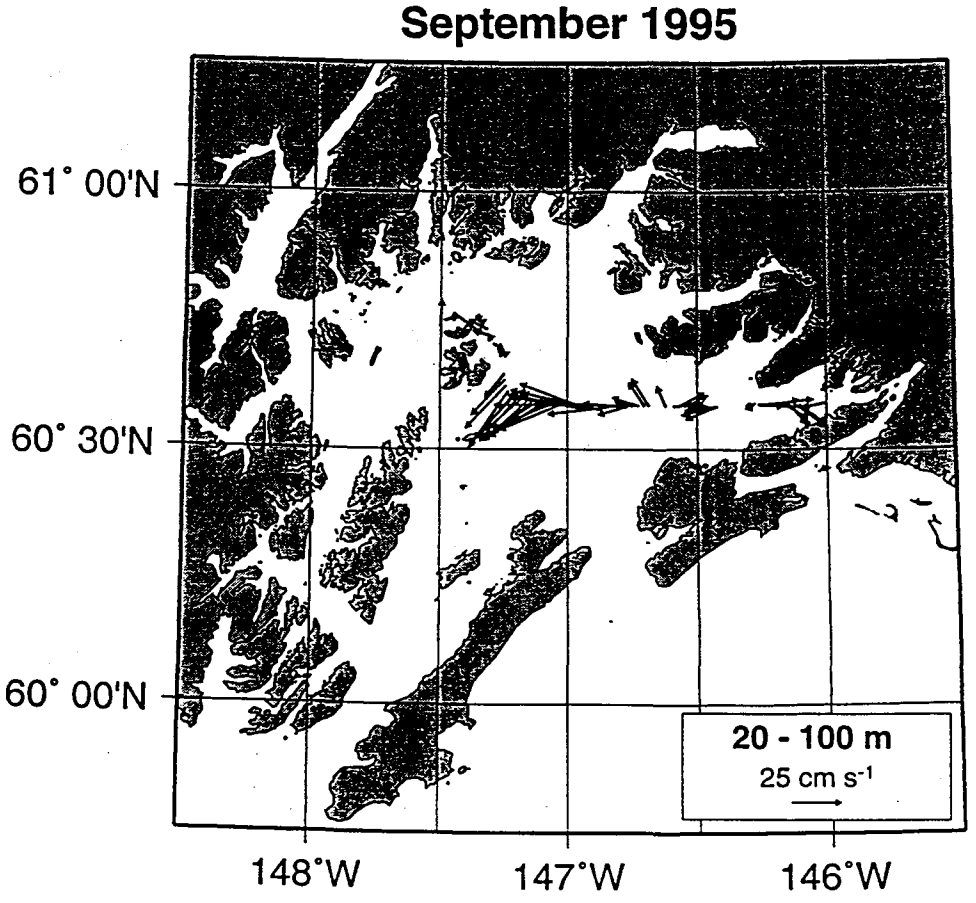
September 1995
61° 00'N
60° 30'N
60° 00'N
148°W
147°W
146°W
20 - 100 m
25 cm s-1

FIG. 16(c)

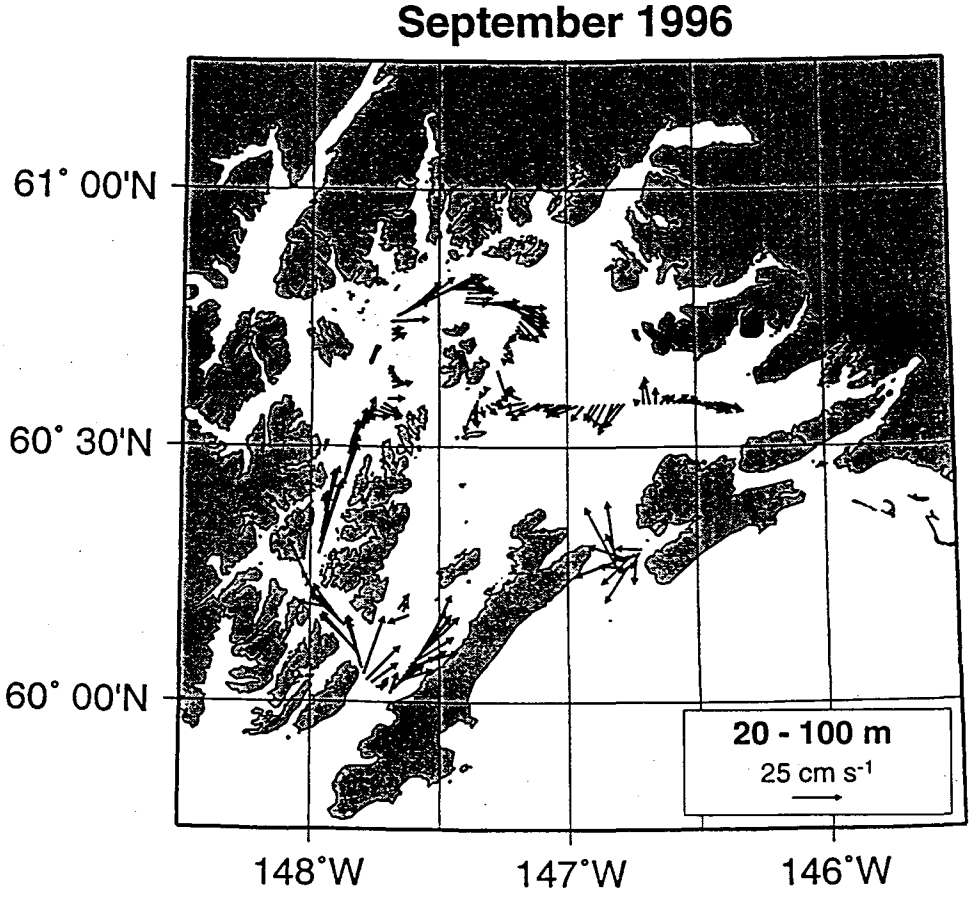
September 1996
61° 00'N
60° 30'N
60° 00'N
148°W
147°W
146°W
20 - 100 m
25 cm s-1

FIG. 17

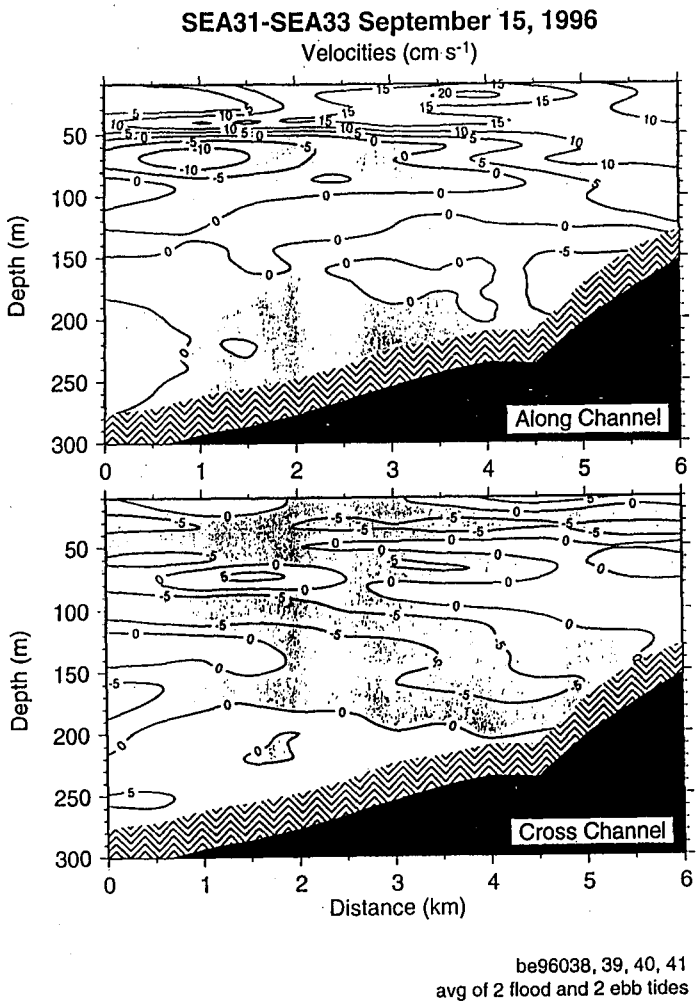


be96038, 39, 40, 41
avg of 2 flood and 2 ebb tides

FIG. 18

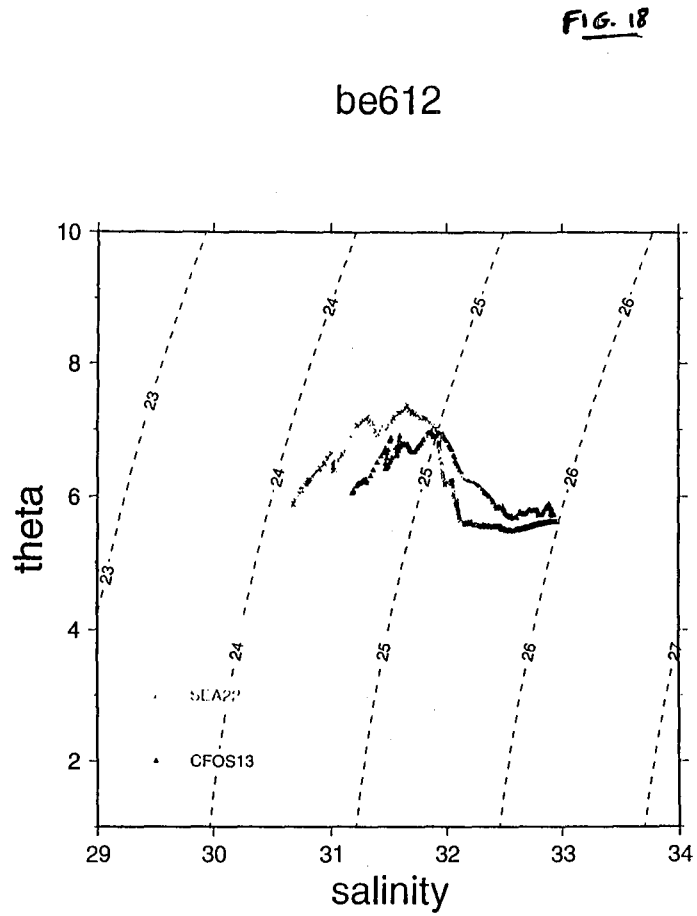

FIG. 19(a)

Dynamic Heights 0/100m (cm) - be612

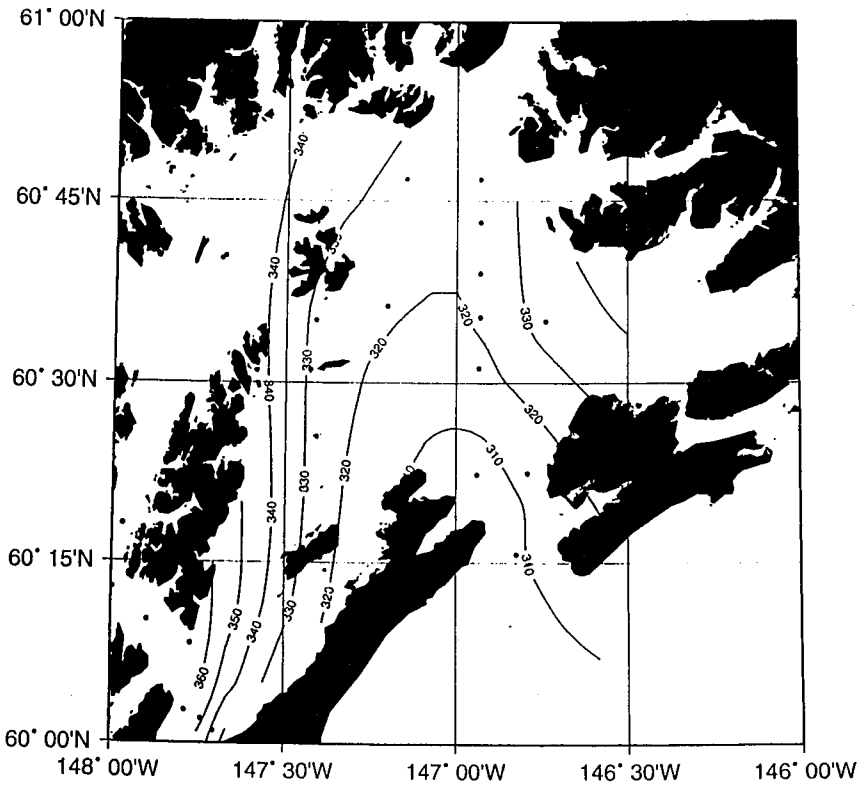

FIG. 19(b)

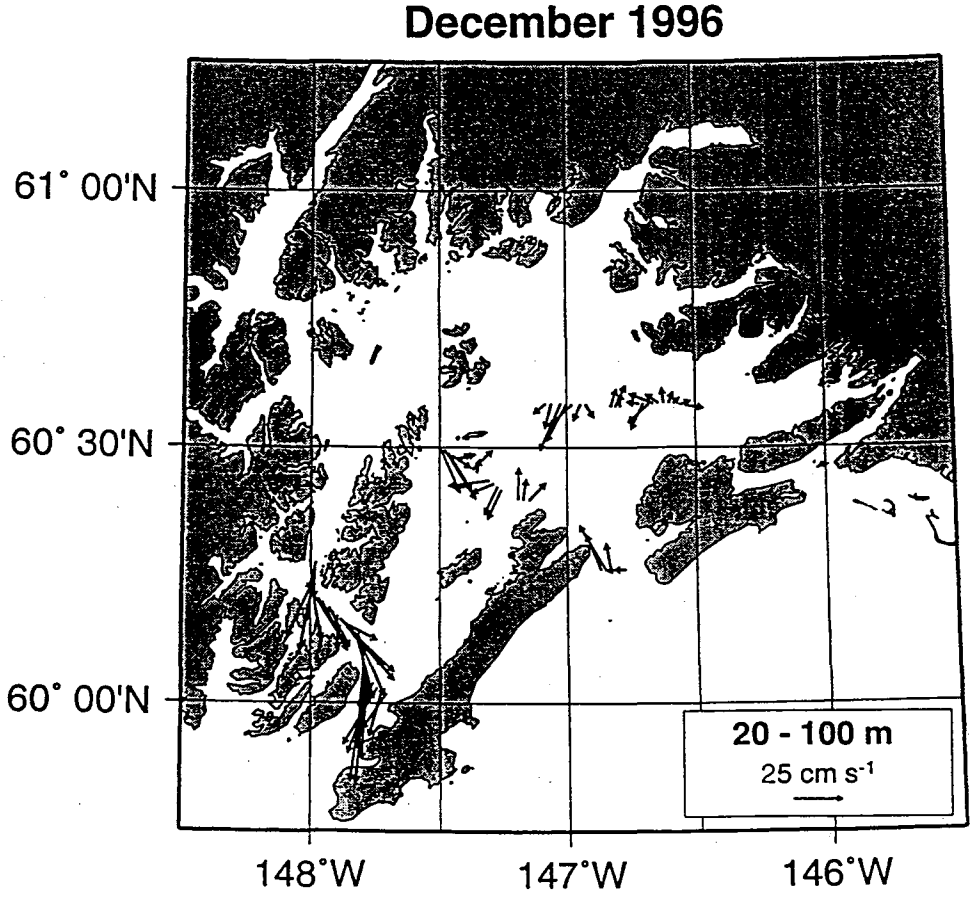
December 1996
61° 00'N
60° 30'N
60° 00'N
148°W
147°W
146°W
20 - 100 m
25 cm s-1

FIG. 20

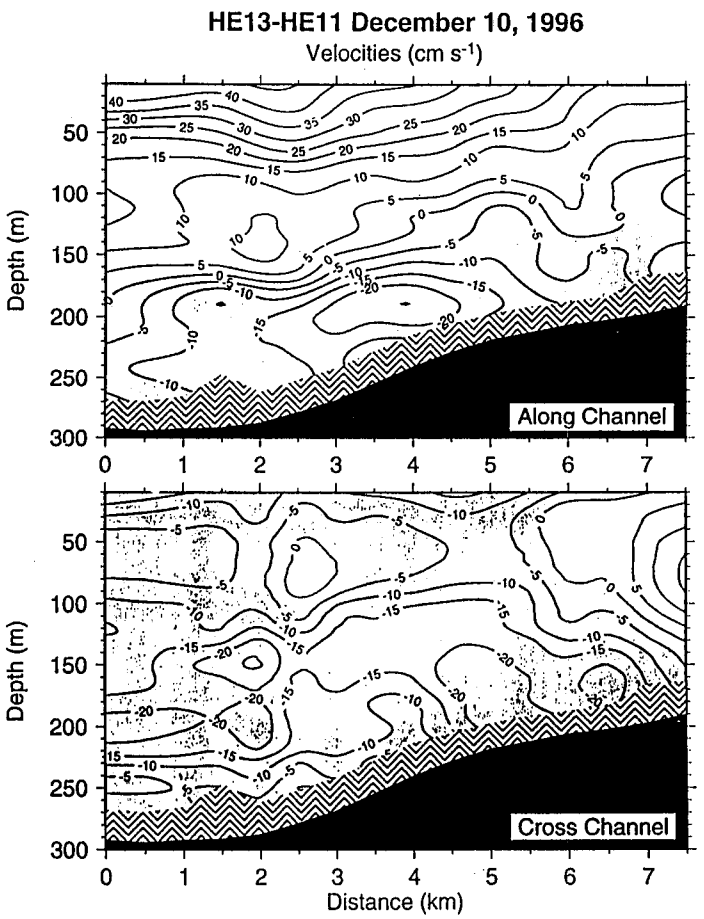


be12026, 27
avg of 1 flood and 1 ebb tide

FIG. 21(b)

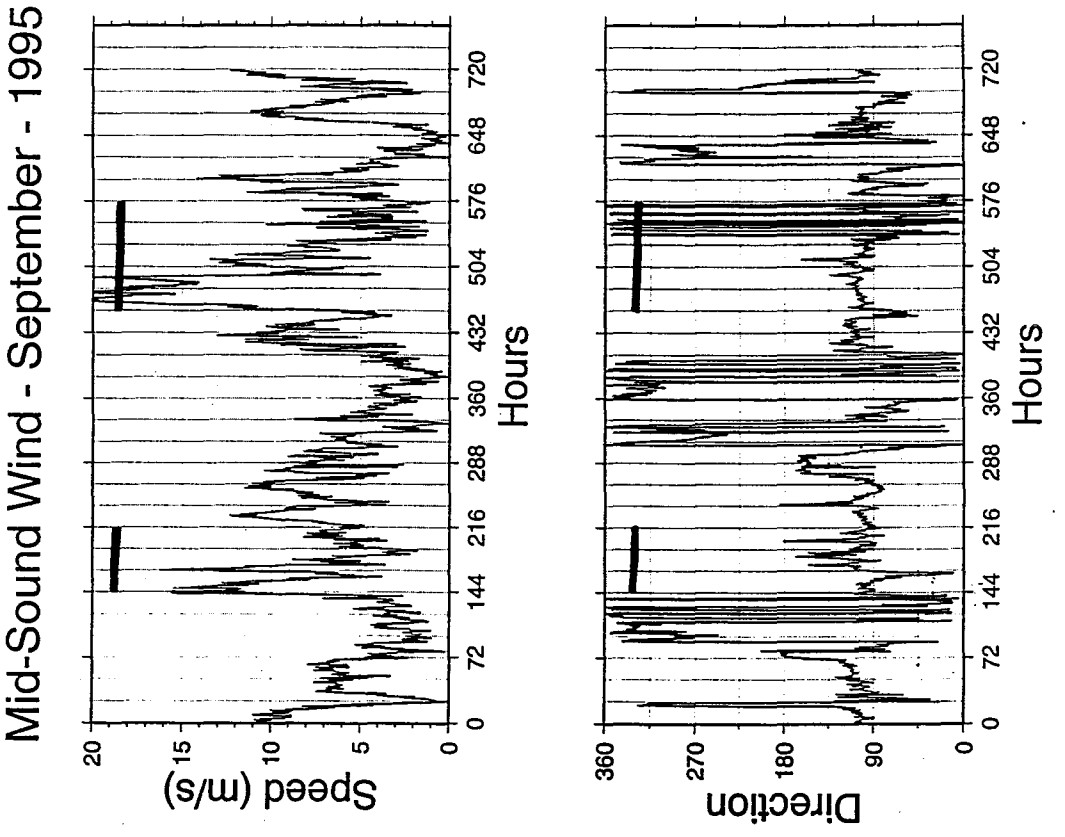


FIG. 21(a)

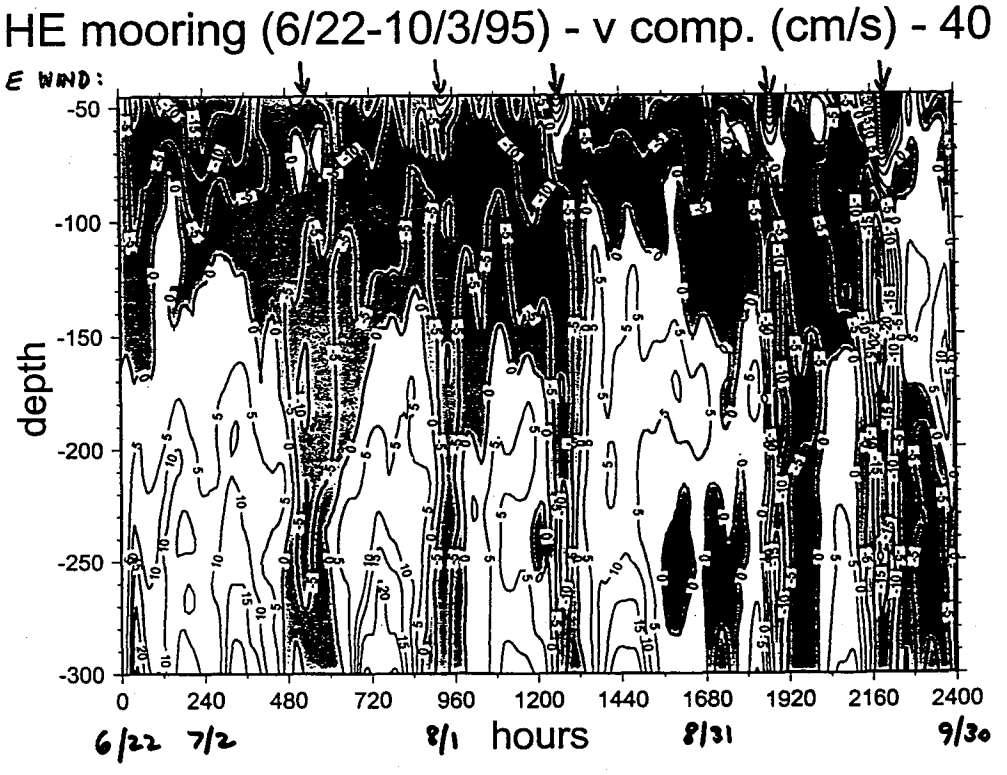

FIG. 22(a)

## HE mooring (9/15-5/13/97) - v comp. (cm/s) - 40 hlp

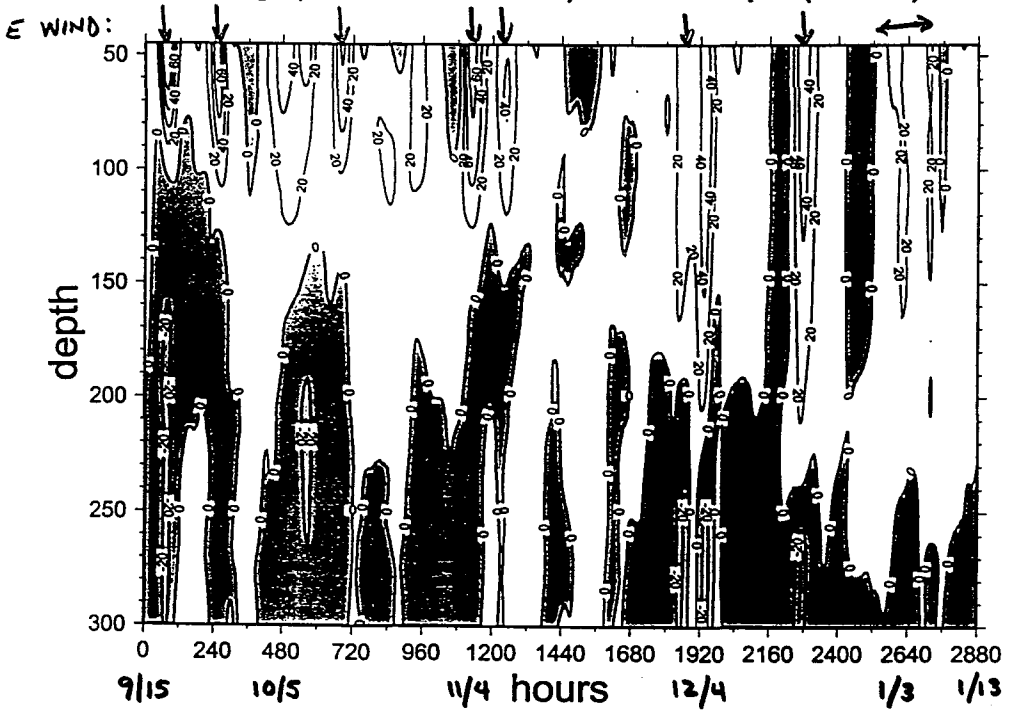


FIG. 22(b)

## HE mooring (9/15-5/13/97) - v comp. (cm/s) - 40 hlp

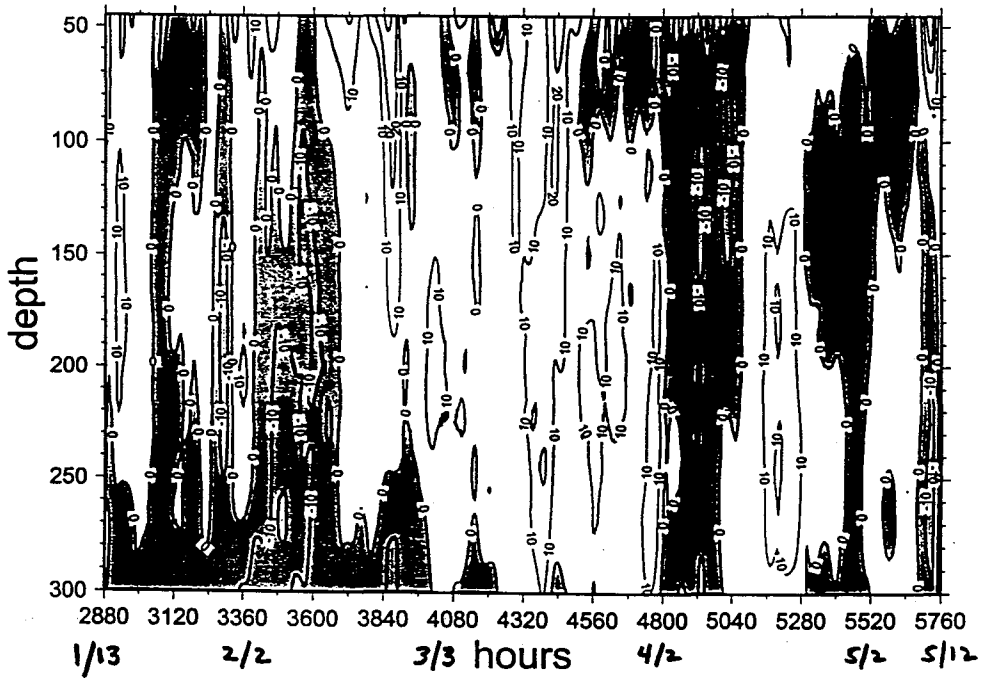

FIG. 23(a)

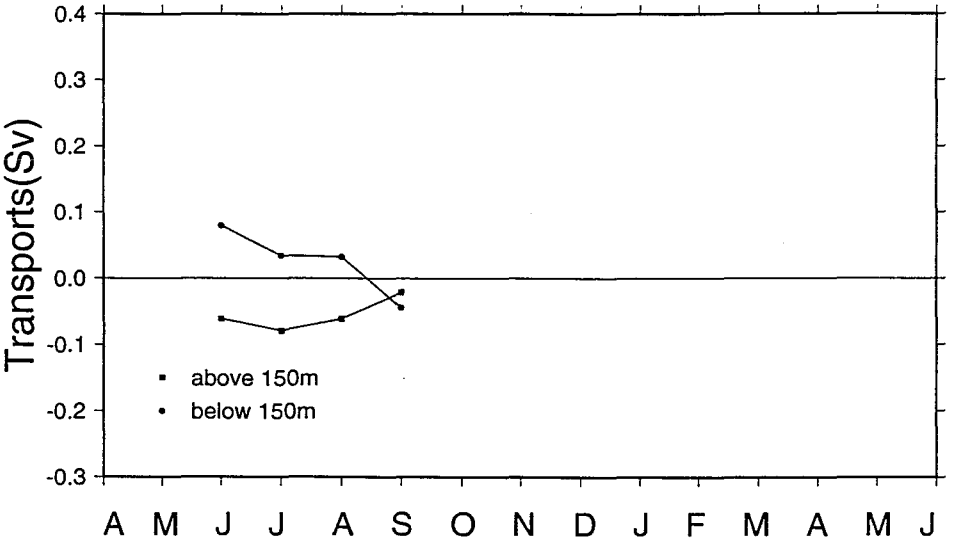


FIG. 23(b)

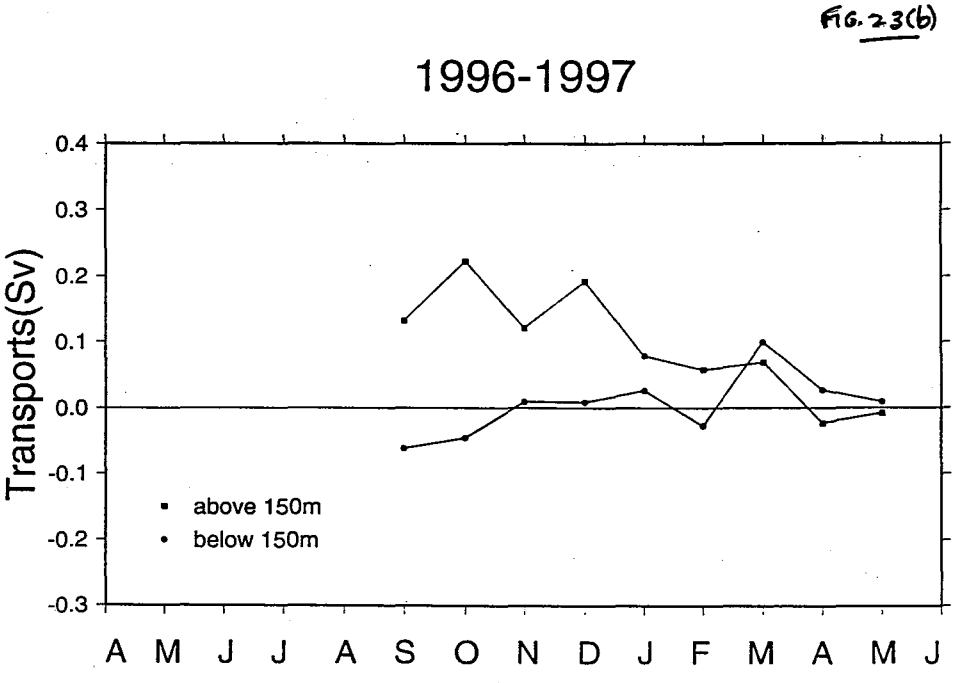

FIG. 24(a)

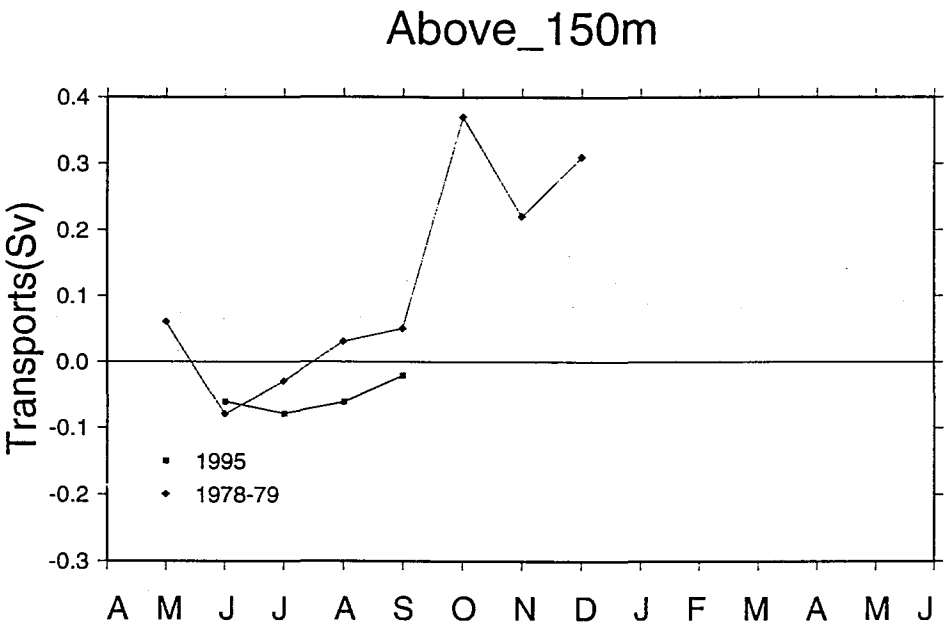


FIG. 24(b)

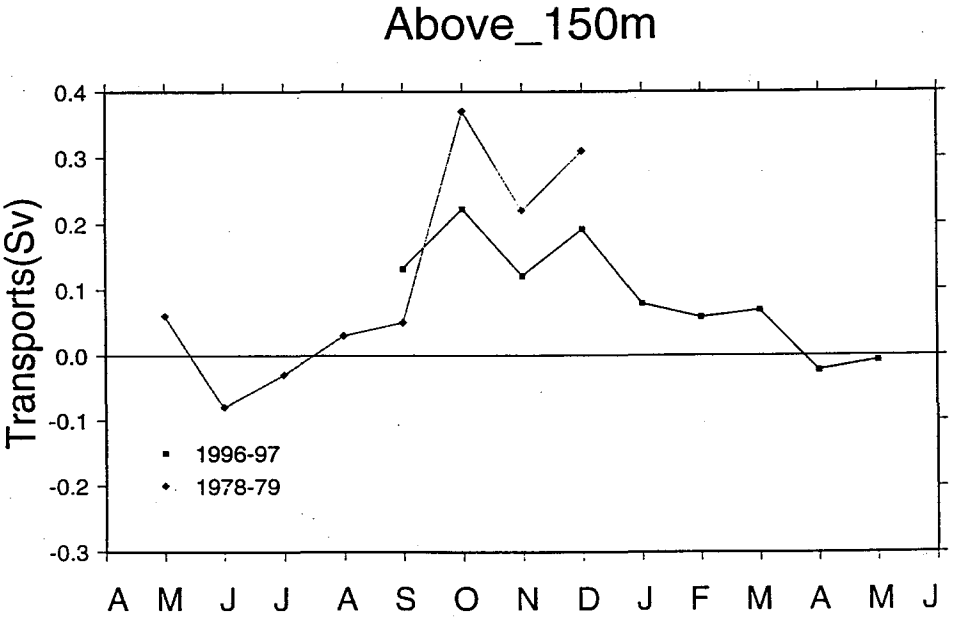

FIG 24(c)

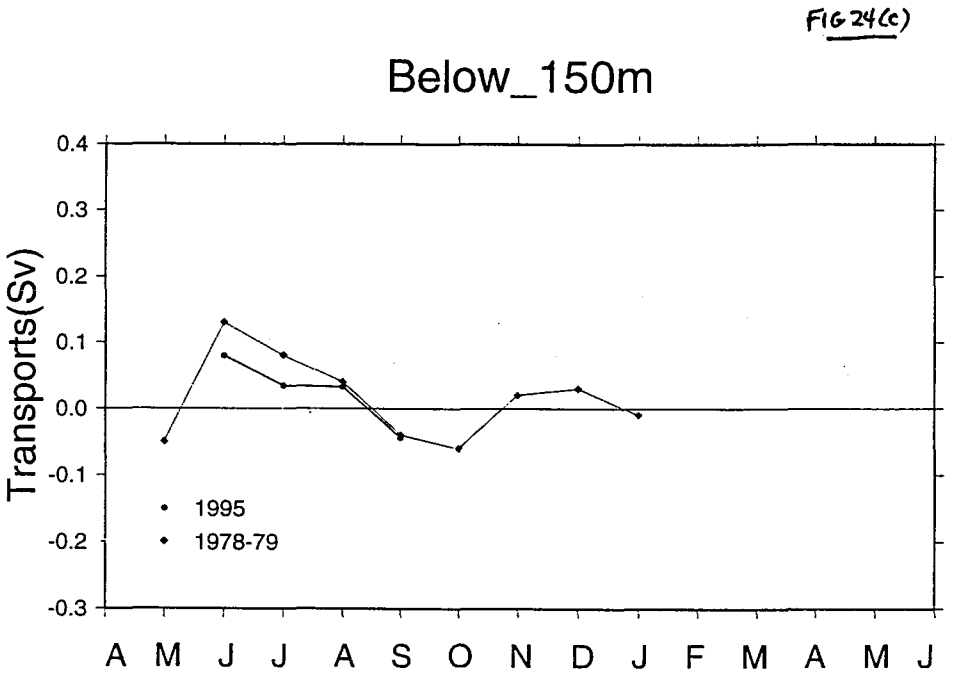


FIG. 24(d)

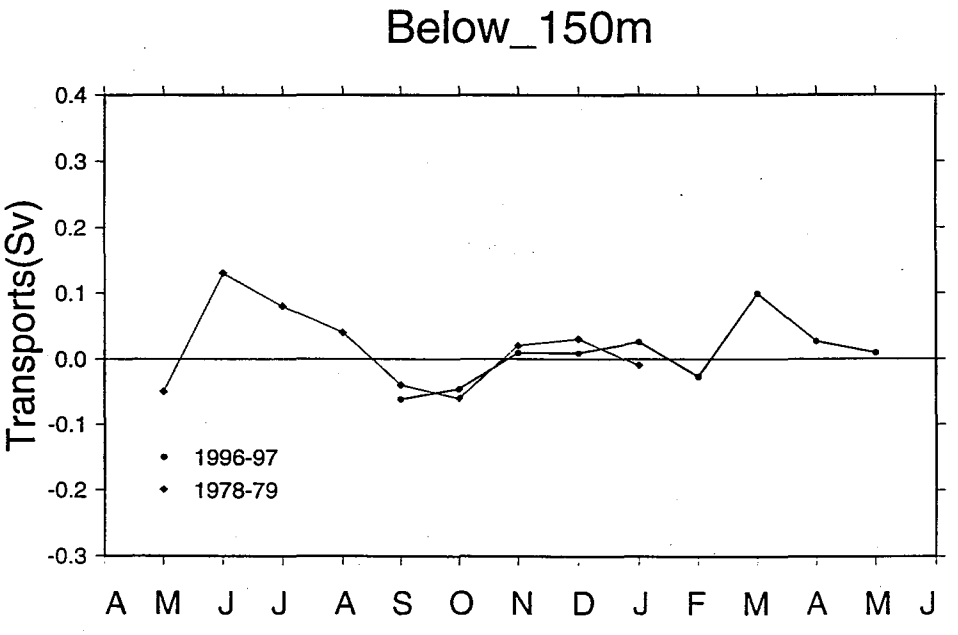

FIG. 25

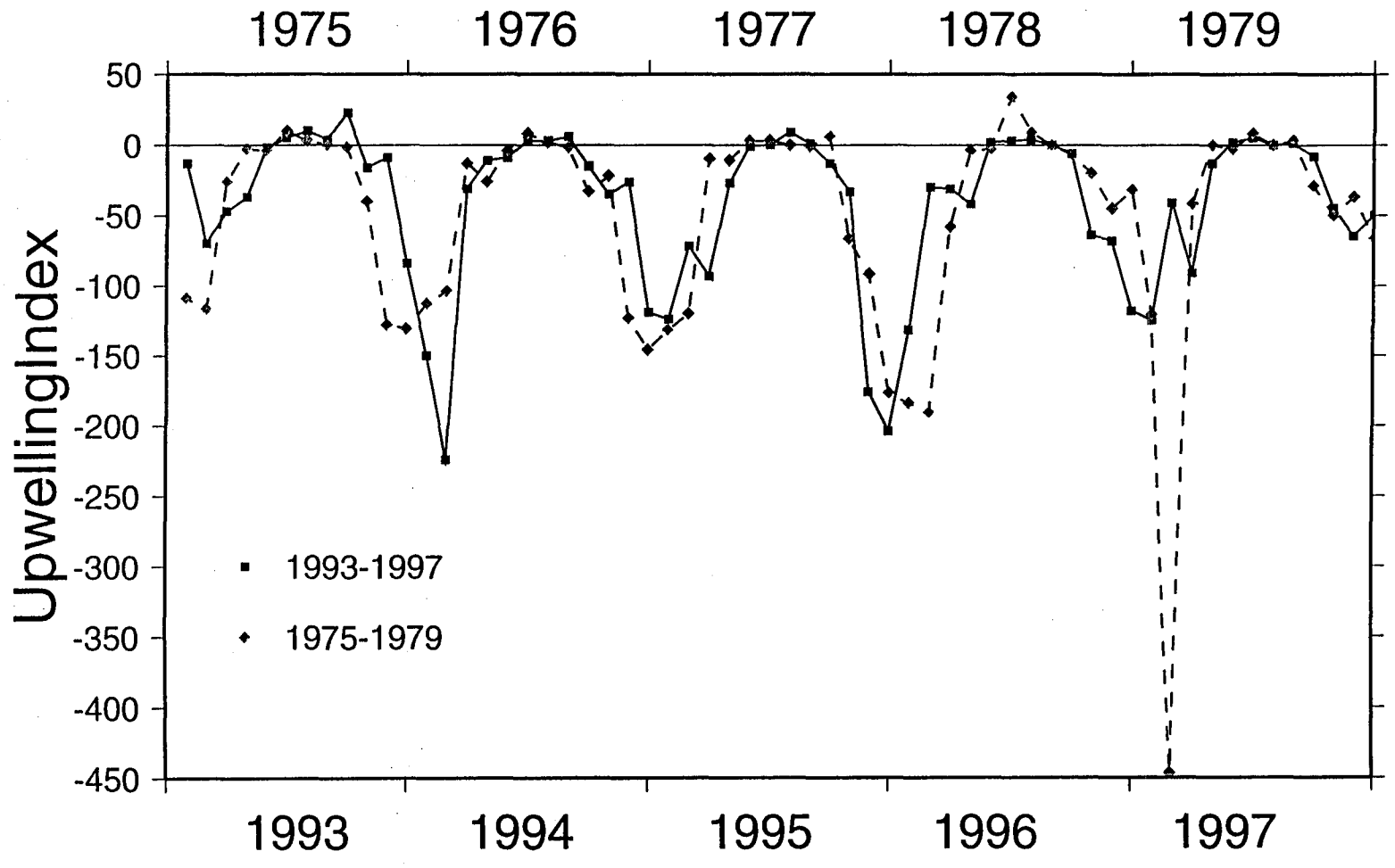
1975
1976
1977
1978
1979
50
0
-50
-100
-150
-200
-250
-300
-350
-400
-450
UpwellingIndex
1993-1997
1975-1979
1993
1994
1995
1996
1997

*Exxon Valdez* Oil Spill
Restoration Project Annual Report

# DESCRIPTIVE PHYSICAL OCEANOGRAPHY OF BAYS AND FJORDS IN PRINCE WILLIAM SOUND, ALASKA USED AS NURSERY HABITAT BY JUVENILE PACIFIC HERRING (*Clupea pallasi*)

Shelton M. Gay III and Shari L. Vaughan

Prince William Sound Science Center
P.O. Box 705
Cordova, Alaska

April 1998

8-94

Descriptive Oceanography of Bays and Fjords in Prince William Sound, Alaska used as Nursery Habititat by Juvenile Pacific Herring (*Clupea pallasi*)

Abstract: Hydrographic surveys performed between spring, 1994 and late winter, 1998 revealed regional variability in the profiles of thermal and haline stratification both seasonally and annually for various bays, fjords and shallow passes within Prince William Sound (PWS), Alaska. Observations in 1994 revealed regional patterns in surface estuarine conditions during spring and summer that were associated directly with the relative sizes (i.e. surface area ratios) of the basins and their respective watersheds. The general hydrographic conditions in the spring showed substantial thermal and haline stratification in comparison to more uniform T/S profiles of late winter. These were a result of both rapid initial surface heating as air temperatures increased during April and May, 1994 and substantial increases in surface freshwater content resulting from higher precipitation rates and melting of lower elevation snow-pack. Precipitation rates appeared to decline during the summer of 1994, and climatic conditions were relatively mild from June through August. However, certain fjords showed disproportionate increases in estuarine conditions in relation to their watershed:basin size ratios. This additional runoff was presumably caused by discharge from higher elevation snow fields. At this time most locations also exhibited maximal summer vertical temperature and salinity gradients within the upper 10 to 20 m. The degree of vertical stratification varied between bays and fjords during the summer, with bays tending to be only partially stratified in comparison with fjords which exhibited prominent vertical T/S gradients in the surface layers. During the summer of 1994, the degree of vertical stratification among bays varied sub-regionally within the southwestern portion of PWS, and during later years certain bays exhibited brief periods during summer in which the T/S conditions were more like fjords. These conditions were short-lived within shallow bays, however, and by the fall these basins typically exhibited partially mixed T/S profiles. Observations within fjords during the fall revealed a general cooling of the upper 20 to 30 m as air temperatures rapidly diminished from October to November, and certain basins exhibited maximum seasonal haloclines at this time. T/S conditions tended to be the most variable at this transitional time of year, and apparently reflected differences in mixing and heat loss due to variable affects of winds geographically. However, this situation was probably further complicated within certain fjords by additional inputs of freshwater from late seasonal snow melt, and mixing. Tidal currents also exhibited varied patterns seasonally and between successive ebb-flood cycles for certain locations. Currents tended to be highest in general at the mouth of bays, with evidence of considerable horizontal shear during both ebb and flood tides at Zaikof Bay, and during ebb tides at Whale Bay. Simpson and Eaglek Bays had much more variable patterns in the currents, which were generally lower in magnitude. Frontal regions associated with the tidal flows were observed in the spacial distribution of the horizontal gradients in temperature, salinity and density. These occurred consistently within Zaikof Bay and Whale Bay, and to a varying extent within Simpson Bay and Eaglek Bay.

## *Introduction*

The following report describes the results of physical oceanographic surveys of bays and fjords which comprise nursery habitats of juvenile fish species in Prince William Sound (PWS). This research is a part of Sound Ecosystem Assessment (SEA), an ecosystem study of Pacific herring (*Clupea pallasi*) and pink salmon (*Oncorhynchus gorbuscha*) in PWS sponsored by SEA project no.320-M in support of SEA Herring project no. 320-T. The objectives of this portion of SEA included determining the seasonal distribution of young herring within PWS, and measuring characteristics of their nursery habitats that might influence recruitment of juvenile fish into the adult populations. In this regard, the main purpose of the physical oceanographic surveys was to quantify the changes in temperature, salinity and density within bays on both annual and seasonal time scales to provide part of the habitat descriptions. A secondary objective involved measuring tidal currents synoptically with high resolution profiles of temperature (T) and salinity (S) in an attempt to identify eddies and frontal zones within bays. Such zones may form where surface currents converge, and tend to be ephemeral in nature, shifting in location within bays during the course of the tidal cycle. The role of tidal currents in the mixing of water masses and drift or retention of larval fish within bays of PWS is unknown and thus identifying such features of circulation would be of value in describing the physical aspects of the habitats.

### *Background*

Past research of oceanographic characteristics within PWS has focused mainly on the influence of the Northern Gulf of Alaska (GOA) on the circulation and seasonal variation of the physical properties of water masses within the main basins of the sound. This work is summarized within the preceding chapter on broadscale physical oceanography. Studies within the bays and fjords, however, are very limited and much of the past work focused on the hydrography and circulation within Port Valdez, due to the location of the oil pipeline terminal within this fjord (Meunch and Niebert, 1973; Colonell, 1981). The circulation within Port Valdez was found to vary seasonally between 2 and 3 layered flow, modified by factors such as local winds, barometric pressure gradients and estuarine surface flows. Additional work was done between 1968 and 1972 by the Institute of Marine Science, UAF in which the characteristics of deep water exchange in relation to sill depths were described for fjords located along the northern gulf coast (Meunch and Heggie, 1978). These included two fjords within PWS: Unakwik Inlet and Port Valdez. Results of this work revealed that sill depth in relation to the level of minimum annual density variation within the water column is important in influencing the timing and extent of advection of dense marine source water into fjord basins. This process is crucial in preventing anoxic conditions from developing within the deep water layer, particularly within fjords with very shallow sills (< 20 m).

Study of the recently formed fjord in Columbia Bay was conducted in 1982 by Walters et. al. (1988) in which a form of estuarine circulation that is unique to fjords with tidewater glaciers is described. This circulation occurs during the summer when glacial runoff is at a maximum, and is governed principally by the massive inflow of fresh water entering from the bottom of the glacier. This subglacial river rises vertically upon entering the estuary and mixes with the higher salinity basin water to form a subsurface buoyant layer, that moves seaward in a manner believed to be similar to entrainment type estuarine flow. The latter form of circulation has been well documented for fjords of British Columbia and Southeast Alaska that have very large inflows of

runoff from fluvial sources at the head of the basins (Pickard 1961 and 1967). The motion of the subsurface estuarine layer across the sill at Columbia Bay was evident from both increased current velocities and a temperature minimum occurring between 3 and 10 m. depth. Its presence in water below the sill was detected in the form of a prominent temperature minimum and maximum occurring respectively at about 10 and 20 m. depth.

Hydrographic surveys measuring T/S profiles within bays, fjords, and nearshore zones, were conducted by the Prince William Sound Science Center (PWSSC) during joint cruises with the Alaska Dept. of Fish and Game in the spring and summer of 1994. This research was expanded to include measurements of tidal currents and high resolution T/S profiles within the upper 50 m. of the water column during joint cruises with the University of Alaska at Fairbanks (UAF), from the fall of 1995 to early spring of 1998. At this time acoustic surveys of fish density and biomass were also conducted by PWSSC while samples of fish for age, length, weight and stomach contents were collected by UAF. Samples of zooplankton and larval fish were also collected by UAF, and additional T/S profiles were collected at selected stations to augment the data from the physical oceanographic surveys.

The results from the initial oceanographic surveys from spring, 1994 to late winter, 1996 were described in a paper submitted for publication to the Journal of Marine Systems (Elsevier Publ.) (Gay - in review). This work revealed regional variability in the T/S conditions within bays and fjords during all seasons that was related to local topography, hydrology and climatic conditions. A summary of this work is included in the present report along with the results of work conducted through FY96.

## *Methods*

Hydrography data were collected using a SeaBird Electronics 19.03 CTD while occupying oceanographic stations established in bays, fjords and passes during the various surveys (Fig. 1). In addition to individual casts, high resolution CTD samples were also collected using either a Chelsea Instruents Aquack CTDF or a SBE 19.03 profiler mounted to a Chelsea Instruments Aquashuttle.. The Aquapack data (which included fluorometry) were collected in real time via a conductive tow cable, whereas data collected with the SBE instrument were saved to a buffer and uploaded following the deployments.

During all cruises in which the Aquashuttle was deployed, particles within the water column were also enumerated using an Optical Plankton Counter (OPC). In August and October, 1996, however, the Aquapack was mounted to a Biosonics sled, modified for towing with the conductive cable used with the Aquashuttle; OPC data were not collected on these occasions. In all deployments, the tow-body (or sled) was lowered and raised manually via a deck winch (housing the conductive cable) while the vessel was underway.

Measurements of the tidal currents were made using an RDInstruments 150 khz Acoustic Doppler Current Profiler (ADCP) which was mounted to the hull of the survey vessel. These data were collected in March, August and October 1996, October 1997, and March 1998. The high resolution CTD data were collected synoptically over the ADCP transects, and all data were georeferenced from Global Positioning System (GPS) data collected by a Magellan 5000 .

## Study Area Description

The shoreline of PWS is quite rugged and complex due to its past glacial and tectonic history (Fig 1a). The bays and inlets of this region reflect this diversity, ranging from small, shallow basins with average depths of less than 50 m. to deep fjords, some exceeding 400 m. in depth. The Chugach mountains form a massif bordering the northern and western portions of PWS, and elevations rise abruptly to almost 1000 m at the coast to heights of up to 4000 m within 60 km of the shore. The orographic effect of this barrier has created extensive ice fields within the region, and numerous alpine and tidewater glaciers frequently extend into fjords located along the mainland from Port Valdez to Port Bainbridge. Glacial streams also enter into various bays located along the northern and western regions of the mainland.

The general physiography of the bays and fjords sampled during this study is shown in Table 1. Most locations were surveyed in 1994 and during the three broadscale cruises conducted in the fall, 1995, late winter, 1996 and summer, 1996. From these surveys four bays representing habitats within four regions of PWS were selected to be sampled regularly: Simpson Bay (Eastern PWS), Zaikof Bay (South Central PWS), Whale Bay (Southwest PWS), and Eaglek Bay (North Central PWS).

The majority of the bays sampled as juvenile herring habitats conformed to the standard definition of fjords (Pickard 1961, Pritchard 1967; Rattray 1967), in that they have steep-sided basins and are typically highly stratified during periods of freshwater runoff. However, cross-sections of the basins vary significantly in shape, and some locations can have considerable vertical structure in the form of ridges and pinnacles. Sills of varying depth may be present as well (Table 1), and these local bathymetric characteristics within each basin undoubtedly affected the patterns of hydrography and tidal currents that were observed during the surveys.

As a rule, the locations in Table 1 may be classified as either a bay or a fjord depending on the average basin depths: maximum depths of 100 m. or less would be associated with bays (e.g. Simpson, Zaikof, Paddy and Ewan Bays) and depths over 100 m. tend to occur in fjords (e.g. Herring, Lower Herring, Drier and Whale Bays) The fjords with tidewater glaciers included Unakwik Inlet, Icy Bay, and Nassau Fjord, which are classified separately due to their unique hydrography. Note that all the glacial fjords have sills ranging in depth from moderately shallow (20 - 30 m.) to extremely shallow (4 m.).

**Tides**. Tides within PWS are semidiurnal ($M_2$) with velocities ranging from 30 to 50 cm $sec^{-1}$ (Niebauer et. al. 1994). Tidal prisms in Cordova and Valdez range from less than 3 m. during neap tides to over 5 m. during spring tides, however, maximum tidal amplitudes have been reported for Unakik Inlet ranging from 6 to 8 m. (Meunch and Heggie 1978). The monthly pattern in tidal amplitudes for PWS tends to cycle between periods of neap or "hold-up" tides to periods of high tidal prisms or spring tides; the latter reaching a maximum of almost 6 m. in early spring. Pickard (1961) describes semidiurnal tides within fjords of British Columbia as being declinational, in that tidal prisms vary considerably between each successive cycle of flood and ebb tides. This pattern also occurs within PWS and influenced the timing of oceanographic surveys in order to sample the largest volume changes during the tidal period.

**Climatic and Oceanographic Conditions.** The climatic conditions of the Northern Gulf of Alaska Coast have been well documented by Royer (1979, 1982) in which he reported a substantial variability in average air temperatures and total precipitation both annually and regionally. Meteorological conditions within PWS during 1994 to early 1996 were described from data provided by hatcheries located at Main Bay, Lake Bay, Unakwik Inlet, and data from the CFOS buoy located in central PWS (Gay, 1996). The data from this paper are included in Figure 2 which shows annual differences in total precipitation and mean monthly air temperatures. Wind speed and direction measured at the CFOS buoy are shown for the same time period in Figure 3. Marked annual differences in air temperatures can be seen between years during winter, and most locations exhibited cooler mean temperatures during the summer of 1995 in comparison to 1994. There is also a greater degree of sub-regional variation in mean air temperatures in 1995. Although precipitation records at Main Bay and Lake Bay exhibited substantial monthly differences in 1995, the annual totals at the two locations were comparable (5.2 vs. 5.4 m.). Winds during the fall through the spring tend to cycle between southeasterly directions to northerly directions, reflecting the passage of low pressure systems from Gulf of Alaska, followed by a predominance of high pressure from the interior of Alaska (Fig. 3). Summer climatic conditions can sometimes be dominated by prolonged periods winds from the southwest.

The general oceanographic conditions within PWS tend to be influenced greatly by climatic conditions from the Gulf of Alaska. However, this effect within bays and fjords may vary depending upon the geographical location. Topographic channeling of winds along the Chugach Mountain Range and geographical gradients in air temperature across PWS create differential physical conditions within various bays, particularly during the winter months. For example, basins located within the northern and western regions along the Chugach Mountains tend to be affected more by cold winter temperatures than are bays located in the eastern side of PWS and along the main islands, such as Montague or Knight Island. Observations of sea-ice formation exclusively within the northern and western regions directly reflects the effects of this temperature gradient. Katabatic winds during periods of high pressure during winter have a differential effect across the northern regions of PWS, and have been observed to be predominate in locations such as Valdez Arm and Wells Pass (entrance to College Fjord) during fall and late winter cruises. These conditions create a complex pattern of winds and climate within PWS, and conditions within a given bay or fjord are governed by both the local topography and the geographical location within PWS.

To summarize, PWS's climate is influenced primarily by the location of the Aleutian Low during the fall through the spring, and the formation of high barometric pressure over the Northern Pacific during summer. Variability in this pattern directly affects the pattern of winds and air temperatures seasonally, and can thus result in substantial interannual variation in oceanographic conditions generally throughout PWS. Anomalous weather patterns caused by ENSO[2] events may also influence local climate, causing unusually warm years whenever a strong El Nino persists into the winter months, however, this effect needs to be more fully documented.

2 ENSO - El Nino and the Southern Oscillation

## *Results and Discussion*

The results of the oceanographic surveys will be divided into three main sections: 1) a comparison of physical conditions sound-wide among the various bays sampled during the broad scale surveys, 2) seasonal and annual variations in physical conditions among the four bays selected for long term measurements; and 3) the patterns of tidal currents within the four bays, and the fine scale T/S conditions observed during flood and ebb tides.

## Broadscale Surveys

. The locations within the western and southwestern portions of PWS, sampled during the spring and summer of 1994 were grouped into five primary subregions according to geography and similarities in hydrography (Fig. 1b). These regions are defined as follows: region 1- the west side of Knight Island; region 2- Perry Island, Culross Island and Ester Island; region 3- the mainland south of Port Nelly Juan to Dangerous Passage; region 4- the mainland from Whale Bay to Bainbridge Pass, and the northern locations of Prince of Wales Pass to Shelter Bay; and region 5- the extreme southwest portions of PWS, including the lower portions of Prince of Wales, and Elrington Passes.

During the fall survey of 1995 Hogg Bay and lower Bainbridge Pass were added to region 5, and in March, 1996 Icy Bay, Ewan Bay and Paddy Bay were added to region 3. The remaining basins were grouped according to their general locations within PWS (Table 1). The locations designated as glacial refer to fjords that are directly affected by tidewater glaciers.

*Spring and Summer, 1994*

Seasonal changes in temperature and salinity over the spring and summer of 1994 are presented for regions 1 to 5 to show the differences between these areas in terms of timing and magnitude of physical property changes (Figs. 4 to 7). Plots of T/S data are means calculated for all casts at each basin for the following standard depths: 1,3,5,10,15,20,30,40,50,....,100,120,140, 160,....300 m.

The relationship between estuarine conditions within embayments and the sizes of the respective watersheds was examined to determine if differences in surface freshwater between locations during given months could be attributed to relative concentrations of runoff. Higher ratios of watershed to bay surface area would theoretically predict greater concentrations of runoff and vice versa. These results are summarized in Table 2 and from here on the surface area ratios will be referred to as watershed ratios.

In spring of 1994 many locations exhibited marked inputs of both heat and freshwater relative to late winter conditions (indicated by data shown below for March 1996 and winter 1997. This was due to warming air temperatures in April and early May and initial runoff from both snow melt at lower elevations and direct precipitation (Fig. 2). However, the average surface temperature and salinity at Main Bay (region 3) and Culross Bay (region 2) was much lower in comparison to all other locations. These cold, fresh surface layers indicated that high initial runoff from snow melt was being concentrated in these bays (Fig. 4c). This would be expected for these bays on the basis that the watershed ratios were generally higher than in other regions

(Table 2). Eshamy Bay was exceptional, however, in that it did not exhibit the same surface freshening as either Culross Bay or Main Bay despite its high watershed ratio. Other notable differences occurred between bays in region 2 and the various nearshore locations (Fig. 4). The two locations in the northern portion of region 2 (Fig. 4f) appeared to still exhibit effects of surface cooling with minimal increases in runoff, whereas the locations along the south side of Perry Island had warmed, but remained fairly high in salinity. One exceptional nearshore location was West Crafton Island, which exhibited conditions similar to the hydrography of Main Bay.

In June all locations continued to rapidly gain heat within the surface layers in response to the prominent rise in average air temperatures (Fig. 2), and seasonal vertical temperature gradients were well developed (Fig. 5). The freshwater input evident in the surface salinities showed a disparity between bays in region 3 and all other regions, and the locations around the south side of Perry Island exhibited prominent increases in estuarine conditions relative to May with salinity decreases of -4.0 psu on average. The most notable changes, however, occurred in Eshamy Bay and West Crafton Island which decreased by almost -6.3 and -6.5 psu respectively (Fig. 5c and f). The lower surface salinities within region 3 would be expected on the basis of the higher watershed ratios relative to other regions, however, the prominent surface freshening exhibited behind Crafton Island in both May and June indicated that nearshore zones on the west side of Knight Island Pass were influenced by the marked estaurine conditions that affected the fjords of this region.

The two locations sampled in June from region 4, Whale Bay and Bainbridge Pass, exhibited relatively low surface salinities at this time, but Whale Bay appeared to have an exceptionally low value relative to its watershed ratio indicating that this fjord either had relatively greater amounts of runoff from within its watershed or was affected by advection of low salinity water from outside the bay. Measurements of tidal currents and high resolution upper layer hydrography in 1996 and 1997 indicated that the latter process occurs within Whale Bay and that glacial water from Icy Bay affects the upper layer temperatures. This glacial water apparently disperses southwestward towards Knight Island Pass and can be seen in the unique T/S signatures both within this fjord and the outer basin of Bainbridge Pass (Fig. 5d). In both locations the temperature drops rapidly within the upper 20 m, forming a temperature minimum at about 15 m depth. This signature is very similar to the hydrography of subsurface glacial water described by Walters et.al.(1988) flowing across the sill from Columbia Bay. Vertical sections (Fig. 6) also show that subtle variations in the temperature persist below the thermocline to depths of 50 m, within the outer portion of Bainbridge Pass, near the mouth, and across the main basin of Whale Bay. This is discussed further in the sections below regarding tidal currents and upper layer hydrography.

The nearshore locations and passes all exhibited more limited ranges of temperature and salinity relative to the bays and fjords. This may reflect a greater amount of mixing due to higher tidal flows observed within the passes from adcp transects.

Hydrographic conditions in July 1994 (Fig. 7) showed additional heating of the surface layers for bays within regions 1 and 4 as average air temperatures continued to increase in July (Fig. 2). However, salinity changes tended to vary within all regions. For example, within region 1, Drier Bay exhibited the largest decrease in salinity (-1.21 psu) and was significantly warmer and fresher than either Herring Bay or Lower Herring Bay (Fig. 7a). The additional freshwater inputs into these bays that occurred during July were likely from melting of higher elevation snow fields. This was consistent with both the warm, sunny weather conditions observed during the

cruise in July and weather conditions measured at Main Bay in July 1994 (Fig. 2). The pass in Long Channel and the two shallow bays along the southwest portion of Knight Island, however, all exhibited lower ranges of temperature than the fjords along the west side of the island, and one location, Mummy Bay, had a much lower range in salinity as well.

Whale Bay and Bainbridge Pass both had very minor increases in heat at the surface (< 0.2° C), however, the average surface salinities also increased by 0.72 psu and 0.08 psu respectively and indicated a drop in freshwater input in July (Fig. 8c). The shallow temperature minimum was still present in Whale Bay, but did not appear in the TS plot for Bainbridge Pass. The stations located in the outer mouth of Bainbridge (stns. 11 - 14 in Fig. 11) were not resampled in July due to time constraints and this may be the reason that the minimum was not observed. The two other locations in region 4, upper Prince of Wales Pass and Flemming Island both exhibited increases in heat and freshwater content in the upper layers (Fig. 7d).

Four additional locations were sampled within the extreme southwestern portion of PWS (region 5) which included Elrington Pass, Sawmill Bay, lower Prince of Wales Pass, and Twin Bays. This region exhibited much different conditions of hydrography than the other regions, apparently due to the effects of higher tidal currents within the narrow passes on mixing within the water column (Fig. 7e and f). The extremely small ranges in T/S conditions exhibited in lower Prince of Wales Pass and N. and S. Twin bays, located at the mouth of Port Bainbridge, were possibly influenced by mixing from both winds or tides and may also exhibit properties derived from exchange with Gulf of Alaska waters. However, this region of PWS will require further study to identify the actual proccesses affecting the hydrography.

*Fall, 1995 and Late Winter, 1996*

The hydrography of bays and fjords in mid October to early November, 1995 (Fig. 8) reflected a wide range of conditions that occurred at that time of year, following the period of maximum precipitation and fresh water input in September and October (Fig. 2). Although the amounts of fresh water and heat within the upper 40 m. layer appeared to vary significantly among locations, the T/S profiles tended to reflect the relative degree of surface cooling and mixing that had occurred among the various basins; deeper fjords tending to remain stratified and shallow bays and passes exhibiting more mixed profiles. Differences within these groups was most likely due to the variable effect of winds within bays, depending upon their geographical location and local topography.

Examples of locations that were apparently sheltered included Herring Bay and Whale Bay. In these cases stratification persisted well into the fall and surface cooling had resulted in the formation of a prominent temperature maximum located at about 20 m. in both fjords (Fig. 8a). Eaglek Bay and Jack Bay, both fjords, exhibited varying effects of wind mixing within their basins (Fig. 8d). Although the temperature maximum within Eaglek Bay was located at about 40 m. depth its T/S profiles indicated that it still remained stratified. Jack Bay, however, exhibited an erosion of both the seasonal thermocline and halocline. (This fjord was observed later to be highly stratified in July, 1996.) During the sampling within Jack Bay in early November, strong katabatic winds from the mainland were observed to blow down this fjord and also down Port Valdez for days. These wind events were episodic during the fall months of 1995, and were the most likely cause of the unusual T/S signature within this bay (Fig. 8d).

The varied conditions of hydrography within bays and fjords in late fall probably reflected both a subregional variability in precipitation and wind effects due to differences in geographical location, orientation (aspect) to the prevailing wind directions, and topographic effects on channeling winds into their basins. The combination of protection from prevailing winds and the stabilizing effect of large amounts of fresh water at Herring Bay and Whale Bay may prevent mixing of the upper water column of these fjords until later in the winter when very low temperatures may start the process of thermohaline convection.

*Late Winter, 1996*

In March, 1996 most locations exhibited well mixed profiles with minimal ranges in temperature and salinity as expected for this time of year in PWS (Meunch and Schmidt 1975). However, a minor amount of cold runoff from early snow melt appeared to have begun to enter into two fjords: Eaglek Bay and Whale Bay (Fig. 9a and d). Eaglek Bay has a number of tributaries, such as Cascade Falls, that were observed to provide early input of freshwater, and although this was not observed directly for tributaries into Whale Bay the air temperatures were quite warmer during early spring in comparison to previous years indicating that an early snow melt was occurring at lower elevations (Fig. 2). It is possible that the main basin of Whale Bay was also affected by glacial water from Icy Bay at this time, where the T/S profiles also indicated some early input of meltwater (Fig. 9b). However, the profiles of water beyond the shallow sill were well mixed and this can be seen in the differences in T/S signatures between the inner basin and Knight Island Pass in Figures 9b and c.

The combined effects of thermohaline convection and wind induced circulation was likely to have created the more uniform conditions observed within the other fjords (Drier Bay, Jack Bay, and Galena Bay) and most shallow bays (Fig. 9). A southeast gale prevented immediate sampling of stations in Drier Bay and winds were observed to be channeled and accelerated into this bay by the topography of Knight Island. This storm was evident in the weather records for the central sound in the later part of March, followed by a second storm event in early April immediately following the March 1996 cruise (Fig. 3). The mixed T/S conditions within Jack and Galena Bay were not related to this storm activity, however, and were probably caused by local katabatic winds similar to those observed during the fall. This weather pattern was reported to occur frequently within Port Valdez during the winter (Meunch and Nebert 1973), and was also observed within PWS in March 1996 (personal observation).

The two glacial fjords surveyed in late winter, Icy Bay and Unakwik Inlet, exhibited very uniform conditions below 10 m depth, and with the exceptions of whale Bay and Eaglek Bay the surface layers tended to be colder and fresher than all other locations (Fig. 9b). The water below the sills at these fjords tended to be warmer at the surface, but more saline in general indicating a marked difference in density between the basins. The thoroughly mixed profiles within the upper basins were most likely related to strong thermohaline convection, as evident from sea-ice covering their entire basins over the winter (personal observation). Although air temperatures well below 0° C typically occur during the winter along the coastal regions of the Chugach Mountains, and were observed at Main Bay in January, 1996 (Fig. 2), the extent of annual sea-ice formation is apparently quite variable. For example, conditions occurring during the winter of 1972 described by Meunch and Heggie included slush ice and growler ice bergs, however, no mention was made of extensive sea-ice formation. The T/S conditions within these fjords were

found to be similar to those measured 24 years prior by the Institute of Marine Science, UAF, and the density variation of water located above and below the shallow sill was conducive to deep water exchange (Gay,1996).

*Summer, 1996*

In June, 1996 the two bays and one fjord that were surveyed varied considerably in ranges of temperature and salinity, with Zaikof Bay still exhibiting very mixed conditions (Fig. 10a). By July, however, all locations showed marked increases in heat and fresh water within the surface layer, with varying degrees of stratification (Fig. 10b to i). The fjords tended to exhibit more shallow vertical temperature and salinity gradients (i.e. thermoclines and haloclines) and rather isothermal and isohaline deep layers in comparison to the bays and two larger basins located in the eastern sound: Port Gravina and Port Fidalgo (Fig. 10h). Both Elrington Pass (southwest: region 5) and the nearshore location at Green Island remained more mixed, and exhibited deep temperature gradients. The T/S signature at Green Island appeared much colder than North Elrington Pass partly because ctd casts were made to greater depths at Green Island (~ 120 m. vs 60 m.). However, Elrington Pass has strong tidal currents (observed in 1995) which apparently account for the consistently more uniform conditions observed there since the summer of 1994.

The other basins which had exceptional T/S conditions during the summer included the two glacial fjords, Icy Bay and Unakwik Inlet, and Whale Bay (Fig. 10b,c and d). The cold brackish layer in the upper 10 to 15 m. within the glacial locations reflects the substantial cooling caused by the melting of ice calved from Chenega Glacier in Nassau Fjord and the Meares Glacier in Unakwik Inlet. These same conditions were described by Walters et.al. (1988) for Columbia Bay, in which the heat sink created by the latent heat of fusion required to melt the glacial ice overcomes solar heating, thus creating the excessive cold, fresh conditions in the surface layer. The substantially colder surface conditions within Whale Bay appeared to reflect the exchange of this glacial water during summer from Knight Island Pass. The T/S depth profiles within this bay showed both a shallow minimum and subsurface maximum unlike any other nonglacial fjord, but similar to temperature anomalies that occurred in water below the sills at Icy Bay and Unakwik Inlet (Fig. 10c). The surface currents in Whale Bay flow into the mouth during both the ebb and the flood tides and the effect of this circulation on the upper layer hydrography is discussed in the sections below regarding tidal currents.

**Seasonal Hydrography of Selected Bays and Fjords**

In the following section the seasonal patterns in water mass physical properties are presented for two bays, Simpson Bay and Zaikof Bay, and two fjords, Whale Bay and Eaglek Bay. The data cover the period beginning in August, 1996 and ending in March, 1998, with winter ctd measurements occurring in 1996-97 only.

*Late Summer and Fall, 1996*

The physical conditions within the bays and fjords in August, 1996 showed varying degrees of vertical stratification, with well developed thermoclines and haloclines occurring in all fjords and in Simpson Bay (Fig. 11). Zaikof Bay exhibited a limited amount of stratification, but the

vertical gradients in temperature and salinity penetrate almost to the bottom (60 to 100 m.). This bay exhibits only a very short duration in summer stratification and by fall both bays have become much more isothermal and isohaline in comparison with the fjords which, remained stratified (Fig. 11d and e).

The surface temperatures in Whale Bay continued to remain much cooler than Eaglek Bay, with the same minima and maxima within the surface layer as in July. This pattern occcurs within the deep, main basin only, and the shallow southern arm exhibits thermoclines without minima and maxima. The fall conditions for these two fjords were quite interesting in that the seasonal cooling of the average surface layer to 20 m. was much greater in Eaglek Bay than the cooling observed at Whale Bay ($\Delta$Tbar ~ -5.5°C vs. -1.5°C). Again, the effect of glacial water in moderating the heat gain and loss at Whale Bay may have caused the disparity between these fjords, however, this remains to be investigated further.

The glacial fjord, Unakwik Inlet was also resurveyed in August, and the T/S signatures of water masses above and below the shallow sill revealed that separate conditions persist between these two basins between winter and summer (Fig. 11 b).

By late fall the two bays exhibited partially mixed T/S profiles with minor temperature and salinity gradients in the surface layers , whereas the one fjord, Whale Bay still showed some vertical stratification (Fig. 12 a). All locations exhibited continued cooling at the surface in November, and by December both bays were well mixed with minimal vertical T/S gradients (Fig. 12 b). The physical conditions in Whale Bay in November showed a significant erosion of both the fall temperature maximum and the seasonal thermocline that developed during the previous summer. Because of the sheltered nature of this fjord, it is presumed that most vertical mixing occurs there due to thermohaline convection caused by strong surface cooling from late fall through early spring.

*Winter, 1997*

T/S conditions within Simpson Bay during winter showed a gradual trend towards very isothermal conditions in January and February, 1997 with gradual cooling of the water column during this period by almost 1°C on average (Fig. 13a and b). Zaikof Bay also was very isothermal within the deeper layers, however, there was a marked reduction in the surface salinity within this bay in February, that corresponded with a period of warmer temperatures and slight runoff from low elevation snow-pack (personal observation). This moderation of the winter climate appears to have affected watersheds of Zaikof much more than those of Simpson Bay, in that the reduction in surface salinity was very minor in the latter. This was not unexpected since the bulk of the watershed for Simpson Bay is comprised of high elevation snow-fields and alpine glaciers and it was not affected by the milder air temperatures as much as the lower elevations of Zaikof Bay's watershed. By late winter (March 1997) both bays were well mixed with only very minor T/S gradients within the surface layers (Fig. 13c).

Whale Bay also exhibited moderate vertical temperature and salinity gradients in February, 1997(Fig. 13b) , and although the temperatures continued to cool within the water column in March, the salinity gradient appeared to continue to degrade further, indicating that mixing did not stabilize until late winter (Fig. 13c). It appears that this fjord remains partly stratified during all seasons, however, a more thorough time series during the winter would help to confirm this. At this time it is unknown if the reduction in salinity relative to bays observed during February resulted from early snow-melt or was a remnant of the fall halocline.

*Spring and Summer, 1997*

The spring pattern in hydrography among the bays and fjords reflected the relative amounts of initial heating and freshwater runoff that occurred at the various locations (Fig. 13d and e). With the exception of Zaikof Bay all locations exhibited early thermal stratification, but both fjords appeared to receive greater amounts of runoff relative to the bays. Zaikof remained fairly well mixed despite the warming and surface freshening typical at this time of year. This may be partly due to the early runoff that occurred within this bay in February which precluded the contribution of low elevation snow-pack from runoff later in spring. However, the action of wind and tides within this bay appeared to also cause the water column to remain relatively well mixed until late summer, at which time heating and freshwater runoff created enough vertical stability to allow a minimal amount of stratification, albeit the vertical gradients extend through the entire water column (Figs. 14b and d). Note that in Figure 14b and d, a cluster of points can be seen at the top of the T/S plot. These reflect a shallow wind mixed layer that occurred in both July and August to depths of about 8 m. This bay is prone to the effects of wind mixing during any season.

Simpson Bay showed a T/S signature similar to the Whale Bay in late summer, 1997 (Fig. 14d). This resulted from a significant release of glacial water from its watershed sometime between the July and August survey. This bays watershed area is approximately 6 times the area of the bay (Table 2), and any large discharge of freshwater would be expected to concentrate within the upper arm of this bay. Such was the case as salinity at 1 m. depth ranged from 13 psu in the upper arm to 21psu at the mouth.

The two fjords exhibited differing T/S signatures throughout the spring and summer (Figs.13d, 14a and c). Whale was consistently cooler than Eaglek within the upper layer (40 to 50 m.). This fjord also showed a substantially different pattern in surface layer temperatures in 1997 than in either 1996 or 1994. The surface temperatures were higher in 1997 by almost 3.5°C, but decreased rapidly within the subsurface layers to a value close to 6°C by 50 m. depth, which is similar to prior years. The T/S signature for this bay exhibited the subsurface temperature maximum in 1997, indicating that input of glacial water had still affected the hydrography of this bay. However, this effect may have been moderated by warming of the glacially derived water prior to its entering Whale Bay, caused by atypically high summer air temperatures in 1997. Eaglek Bay also showed significant differences in the surface layer hydrography between 1996 and 1997, in which the highest temperatures occurred as a subsurface maximum in July at 10 m. depth. This maximum had eroded by August and a temperature minimum occurred instead at 5 m. depth. These features were probably also a response to much warmer air temperatures that occurred during the summer of 1997, and the minimum temperatures which occurred at 3 m. during both months may reflect greater releases of stored glacial water from Cascade Bay, which drains a high elevation alpine region.

*Fall, 1997 and Late Winter, 1998*

T/S conditions during the fall of 1997 were similar to 1996 with certain exceptions (Fig. 15). Eaglek Bay exhibited a higher surface salinity and warmer upper layer temperatures in 1997 than in 1996, and although Whale Bay exhibited similar salinities to 1996, increased cooling occurred within the upper 20 m. in 1997. Zaikof Bay exhibited a substantially greater deep vertical salinity gradient in 1997 in comparison to the previous fall. This may have been a remnant of the

deep stratification in August, 1997 which was greater on average throughout the water column that year (Δ Sbar ~ -5.3 psu over 100 m. in 1997 vs. -3.2 psu over 80 m. in 1996). However, this may also have been moderated by the milder climatic conditions that occured during October, 1997, which would have possibly prolonged more thorough mixing until later in the season. Simpson Bay exhibited opposite trends between years with a vertical salinity gradient being higher in the fall of 1996 than in 1997, despite the substantial surface freshening that occurred in August, 1997.

These trends again indicate that fall is a period of high variability in terms of climatic effects across the sound, and bays and fjords exhibit trends in hydrography that are inconsistent with general weather patterns, and reflect the effects of local factors which moderate or intensify the climatic influences during this season.

Over three separate winters between 1996 and 1998, some long-term trends in average temperature were evident among the four locations. With only one exception in 1997, all bays and fjords exhibited a consistent warming throughout the deeper water column from 1996 to 1997, indicating that deep temperatures track the changes in annual atmospheric temperatures over time. The surface layers were more variable, but if averaged vertically they appeared to also exhibit a gradual increase over time as well. The one exception occurred at Whale Bay in the winter of 1997 in which the upper 3 m. layer average decreased by almost 1°C and the deep layer decreased by 0.7 °C (Figs. 9,13, and 15). The most striking increases occurred over the winter in 1998 and temperatures are summarized over all years in the following table. Values are degrees C and the depth is the level at which the deep average basin temperature was taken.

| | *1996* | | *1997* | | *1998* | | |
|---|---|---|---|---|---|---|---|
| | *deep* | *surface* | *deep* | *surface* | *deep* | *surface* | *depth* |
| Whale Bay | 5.5 | 3.2 | 5.2 | 2.5 | 6.5 | 4.5 | 160 m. |
| Eaglek Bay | 4.7 | 3.0 | 5.2 | 3.2 | 6.5 | 5.0 | 140 m. |
| Simpson Bay | ~4.3 | ~4.3 | 5.0 | 4.5 | 6.2 | 5.7 | 80 m. |
| Zaikof Bay | 4.0 | 3.7 | 4.7 | 4.2 | 5.9 | 5.8 | 80 m. |

These values are approximate and were taken from the T/S profiles. Further analysis needs to be done to determine more accurate long-term trends, however, these values serve as examples of the of the general trends of increasing mean annual air temperatures within the PWS region.

Long-term changes in average salinity did not follow a particular trend, and varied in the pattern between years at the two fjords. The long-term salinity of the two bays, however, appeared to remain consistent between years. The trend in more highly mixed profiles within the bays in comparison to the fjords over winter remained consistent (Fig.15).

Stations located within Nassau Fjord and Icy Bay were also resurveyed during late winter, 1997. The results indicated that the deeper layers of both fjords were warmer on average in 1998 in comparison to measurements taken in 1996. The increase was most evident in Icy Bay which went from about 4.6 C in 1996 to almost 6.0 C in 1998. The surface temperatures in Nassau Fjord were similar (~ 1.0 C) due to the melting of ice in both years, however, the profiles in 1998 appeared to be slightly colder down to 5 m. Below this layer the temperatures became warmer in 1998. Although the salinity of the water just below the sill at Icy Bay appeared to be higher than the water inside the sill, the density difference is less than that observed in 1996, and further analysis will be needed to determine if deep water exchange had occurred in 1998.

## Seasonal Tidal Currents

In this section of the report, examples of seasonal variability in tidal currents is presented for selected locations, and discussed in relation to general patterns observed between ebb and flood tide stages and features of circulation such as fronts and eddies. References to bathymetric effects will be limited, as these are beyond the scope of this initial report and will be reserved for future analysis.

### *Zaikof Bay*

Tidal circulation for Zaikof Bay is presented in Figures 16 to 19 for all months that adcp data were collected. One consistent feature in the currents was the strong flow at the mouth of the bay and across the shallow shelf that extends north and eastward from Montague Island. The adcp transects followed this shelf almost to its edge, where the depths drop from less than 100 m. to over 300 m. within Hinchinbrook Entrance. Variability in the direction and strength of this flow occurred both seasonally and also between successive flood or ebb tide stages within a given semidiurnal period. For example, the general direction of the flood currents across this shelf was from the east in all months except August, in which the direction is out of the north and west. The motion of the ebb tide, however, seemed to consistently occur from the north and west during all months, and with the exception of March, 1996 there appeared to be an acceleration in this flow to the southeast across the east peninsula at Schooner Rocks.

The relative strength and direction of the shelf flow appeared to influence the circulation within the lower reaches inside the mouth of Zaikof Bay. Inflows at the surface during both ebb and flood tides created areas of velocity sheer and convergence of the tidal currents, which may enhance turbulent mixing and the development of frontal zones respectively. The latter were a consistent feature observed at the mouth of this bay during all cruises, and were evident in the form of flotsam lines with varying surface water properties appearing on either side (i.e. slicks vs. ripples). Currents located along certain areas of the shoreline in this part of the bay also exhibited a consistent direction regardless of the tide stage. One such area is located along the eastern side where currents appear to be either forced back out of the bay (eastward) during strong flood tides (Figs. 16a, 17b, and 19b), or deflected eastward during the ebb tide (Figs. 17a, 17c, 18a, 18c, and 19a, 19c). Another area is located along the northwest shoreline where the direction of currents is to the north or northeast during both ebb and flood tides. This flow may be either forced out of the bay during the flood tide or drawn into the cross shelf flow during the ebb tide (Fig. 17 and 18). The strength and direction of the inflow during the ebb tide appears to be important in the formation of an anticyclonic eddy which was observed during October, 1996. This appeared to be more prominent during the first ebb tide, but it may have also remained in a reduced form during the second ebb tide (Fig. 18a and c).

The horizontal vectors of the deeper currents are shown for the 22 to 30 m. depth layer in Figures 16 and 19. In general, the high velocity flow at the mouth tended to be barotrophic, and the $u$ and $v$ components were observed to be consistently high throughout the water column during data acquisition in all months. The currents within the remainder of Zaikof Bay, however, tended to be of low magnitude and generally more variable in direction. August, 1996 was somewhat exceptional in that stronger surface currents occurred farther into the bay on both flood tide 1 and ebb tide 2 (Fig 17b and c). These two stages may have had the highest tidal prisms of

the semidiurnal tidal period, however, this was also the only season in which Zaikof Bay became partially stratified in density due to freshwater input, and this may affect the baroclinic tidal flow creating greater vertical sheer in the current.

*Simpson Bay*

The tidal currents at Simpson Bay were highly variable and did not exhibit the consistent velocities at the mouth, as were observed for Zaikof Bay (Figs. 20 to 23). For this reason, separating seasonal and declinational effects on flow patterns will be difficult. Like Zaikof, Simpson Bay is also shallow and certain features of the morphometry (topography and bathymetry) may influence the circulation. The basin of this bay is formed by a shallow shelf, which rises from depths of over 200 m. in Orca Bay (to the south) to depths ranging from 40 to 50 m. inside the mouth. A shallow reef separates the upper arm from the main basin, and depths drop to 70 m. just north of this reef. Although the highest velocities tended to occur at the mouth of the bay during most months, this pattern was not observed for all months or tide stages.

In March, 1996, the tidal currents across the shelf from Hanks Island (west) to the mouth of Simpson Bay were very low in magnitude (Fig. 20). Surface flows during flood tides appeared to accelerate slightly into the mouth, but this diminished with depth. The opposite situation occurred within the upper arm, however, in which subsurface flows at 25 m. were stronger than the surface flows (Fig. 20a and c). The highest velocities during this month occurred during the ebb tide within the upper northern arm. Here there appeared to be an acceleration in outflow caused by the narrows and shallow reef (Fig 20b).

Surface tidal currents in August, 1996 exhibited marked differences between the two successive flood tides and the two ebb tides (Fig. 21). The currents in the first flood stage indicated an outflow at the mouth and east arm, cross channel flow in the main basin, and inflow within the northern arm (Fig. 21a). The deeper currents, however, showed the inflow expected during the flood tide, resulting in a two layer flow. This type of circulation was most likely related to the strong estaurine conditions that prevailed within the surface layer to about 20 m. depth (Fig. 11c). At all other times of the year the density of the water column was not stratified. The only case during August in which surface and subsurface flows were strongly unidirectional was during flood tide 2 within the main basin (Fig. 21c). Here there is evidence of formation of an anticyclonic eddy resulting when the outflow from the east arm converges with the stronger inflow to the west. Although currents at 25 m. are not shown for this bay, replay of the data revealed that a two layer pattern in the circulation occurred within the east arm and northern arm. A similar situation existed during the ebb tides as well, however, during ebb tide 2 the outflows along the west side near the mouth extended into the subsurface circulation.

In both October, 1996 and 1997 the tidal currents were more similar in pattern than during the other months (Figs. 22 and 23). Surface flows tended to conform with outflow during the ebb tides and inflow during the flood stages, particularly at the mouth of the bay. Although reversals in the direction of the currents are evident, the differences between the surface and subsurface velocities appeared to be caused more by changes in magnitude and some change in direction. However, the strong two layer flow observed in August, 1996 was not evident. Again, this change in pattern was probably a partial response to the return to lower gradients in density that typically occurred during the fall (see Figs. 8f, 11e, and 15c).

*Whale Bay*

The magnitude of the tidal currents at Whale Bay were generally low (<25 cm/sec) during all months this location was surveyed (Figs. 24 to 27). Whale Bay is a deep fjord with depths exceeding 300 m. within the main basin (Table 1). The two arms are much shallower and silled at about 60 m. depth. however. the main basin has no sill. Depths within the southern arm are over 100 m. inside the sill. but shoal rapidly in the lower portion of the basin. This fjord remains stratified in density through most of the year and currents exhibited varied velocities at depths below the surface layer.

During late winter (March. 1996) the water column was the most uniform in density (Fig. 9a) and the surface currents. though very limited in magnitude. tend to exhibit inflow and outflow with the respective ebb and flood tide stages (Fig. 24). The subsurface flow at 25 m. is primarily into the bay at the mouth. but is highly variable elsewhere over the basin. These data appear to need more processing as well to determine if some vectors are actually bad. In August. 1996 and October of both 1996 and 1997. however. the patterns in the currents are much different. and a moderately strong surface inflow occurred during the ebb tide. This appeared to be the strongest in August. and may be correlated with the period of maximum discharge of glacial water from Icy Bay. The spacial variability in the hydrography within the surface layer was affected by these patterns in tide flow and is discussed below in the final section of this paper.

Surface inflows occurred at the mouth of the bay during the flood tides as well during all three months (Aug.96-Oct.97), but the flow was much reduced in comparison to the inflows of the ebb tide (Figs. 25. 26. and 27). The deeper flows at 25 m. at the mouth showed either outflow or deflection of the stronger ebb currents moving down Knight Island Pass (Figs. 25e. 26e. and 27c). The convergence of currents that occurred at the mouth during both tides apparently was responsible for the formation of ephemeral tidal fronts which were observed to trap flotsam and ice bergs along the convergence lines. Another interesting feature of the circulation on the ebb tide was the tendency for the surface inflow to turn to the right as it enters the lower portion of the main basin. This westward flow was evident at 25 m. depth during the ebb tides for August and October. 1996 (Figs. 25e. 26e. and 27c). but appeared mostly in the surface flow in October. 1997 (Fig. 27c). From the T/S profiles this water appeared to be glacial in origin and tended to be much cooler and slightly lower in salinity. Since its density was less than the surface water outflowing from the southern arm. it probably sinks beneath the outflowing water. forming a frontal zone. Evidence of a convergence zone was observed along the lower portion of the main basin during the cruises and was also evident in the spacial distribution of the hydrography. Individual cast profiles indicated that the cold. fresher layer existed within the main basin only. and this formed a prominent temperature maximum in the profiles where it overlaid the seasonal thermocline.

During the flood tides in August. 1996 and Ocober. 1997. the circulation appeared to reverse between the western and eastern sides of the bay. in which surface currents were outflowing from the western arm and inflowing into the southern arm (Figs. 25b and d. 27b). There was a tendency for this same pattern in October. 1996. however. it was not a very prominent flow (Fig. 26a and d).

*Eaglek Bay*

The most variable tidal currents from among all four locations occurred within Eaglek Bay (Figs. 28, 29 and 30). During all months and between successive tide stages the currents exhibited strong directional changes which initially raised questions regarding data quality. However, the adcp measured substantially different patterns in the flow field and most of the anomalous vectors are not isolated but occurred in groups, therefore, suggesting that localized characteristics unique to this bay were responsible for what at first appeared to be random motion over many locations of the basin.

In general, the magnitude of the currents was fairly low (10-15 cm/sec), with the exceptions occurring at locations where acceleration of the currents to velocities exceeding 50 cm/sec was evident. These anomalies were possibly caused by both local factors in the bathymetry and differential effects of winds within this bay. The winds were observed to be channeled by the surrounding topography and thus affecting certain regions of the bay strongly and leaving other areas such as the head becalmed. For example, wind directions from the north or northwest typically caused wind to flow only out from the two western arms, creating strong plumes across the bay. Southeasterly winds, however, were observed to be channeled across and down the bay.

The direction of the currents during the ebb and the flood tides tended to vary in both March and October, 1996 (Fig. 28 and 29), with some general inflow for flood tide 3 in March and ebb tide 2 in October. In certain areas of the bay the general direction appeared to change and may correspond with zone s of convergence and possibly divergence. This was observed in ebb tide 1 in March, 1996 (Fig. 28b) and also in both the ebb and flood tides in October, 1997 (Fig. 30). Examples of the spacial variability in the surface layer hydrography are presented below, and these provide evidence of horizontal gradients possibly reflecting the downwelling and upwelling associated with the changes in direction in the currents. This bay also exhibited the strongest vertical velocity components as well, and these were mostly negative and associated with downwelling.

## Spacial Gradients in the Hydrography Associated with Tidal Currents

This section of the paper involves recent analysis of hydrography data sets collected with the Aquashuttle and Biosonics tow-sled described above in the methods. These instruments were deployed continuously while the vessel was underway conducting surveys of tidal currents, and the resulting continuous profiles were geo-referenced by synchronizing sample time and gps time, then layer averaged for each cast. The midpoint gps coordinates of each depth layer average were used as the latitude and longitude of each cast. Temperature, salinity, fluorescence, and density were averaged over 5 to 10 m. and 20 to 30 m. in depth. Examples of these data will be presented for the surface layer from selected locations to illustrate the effect of the tidal currents in enhancing spacial variability in the surface layer hydrography and the formation of fronts within various regions of the bays.

### *Late Winter-Early Spring, 1996*

In March, 1996 the horizontal gradients of average temperature within the upper 5 to 10 m. were limited due to the highly mixed T/S conditions that typically occur by late winter. However, the ranges in both temperature and salinity varied between most locations, reflecting

the differences in local conditions during winter (Figs. 31 to 34). Eaglek Bay exhibited the lowest temperature and salinity, and also the widest range (2.6 to 3.8 C and 30.7 to 31.7 psu). Simpson Bay had the highest values, but the lowest variance (4 to 4.4 C and 31.5 to 31.8 psu). Whale and Zaikof Bay were similar in temperature range (3.3 to 4.3 C), but Whale was similar to Eaglek in terms of salinity (30.8 to 31.5 psu) which reflects the differences in general between fjords and bays. With the exception of Zaikof Bay, all locations had moderately high fluorescence indicating that the spring phytoplankton bloom had started within most of the nearshore regions.

The spacial distributions in the horizontal T/S gradients within bays and fjords varied substantially, and apparently reflected the unique patterns of the tidal currents within each location. These distributions also changed temporally at Zaikof and Eaglek Bays from a generally less complex gradient from the head to the mouth during ebb tide, to a more complicated distribution on the flood tide (Fig. 31 and 34). This apparently occurs whenever there is inflow of water from outside the basins, which can take place on either tide stage (see previous section on tidal currents). Both of these bays exhibited some evidence of pooling of water with differing T/S properties that may be associated with frontal formation (i.e. divergence and convergence). The marked regions of high to low fluorescence within Eaglek Bay reflected the significant changes in water mass property distribution between tides.

*Summer, 1996*

The effects of seasonal increases in heat and freshwater were observed in the horizontal T/S gradients of all locations in August, 1996 (Figs. 32,33, and 35), however, there was also a wide range in these values among locations. The fjord, Whale Bay, exhibited the widest range in average temperature, but also the lowest values in both variables in comparison to the bays (7.5 to 11.0 C, and 25.5 to 27.5 psu). Simpson Bay, as in March, had the lowest overall range in horizontal T/S gradient (12.6 to 13.6 C, and 27.5 to 27.8 psu), however, Zaikof Bay exhibited relatively high values for both variables (12.5 to 14.8 C and 28 to 30 psu). Although Zaikof had a relatively well developed vertical temperature gradient in August, haline stratification was much more limited in comparison to Simpson Bay (Fig. 11c). The well developed halocline in Simpson indicated that vertical stability was higher within this Bay than in Zaikof Bay, which may have contributed to the low range in horizontal gradients observed there. Zaikof Bay, however, tended to remain more mixed seasonally, and the lower stability which results from this fact probably acts to promote more vertical motion within the water column due to the greater amount of current shear that occurs there. Higher vertical velocities were observed within this bay in comparison to either Whale or Simpson Bays.

The spacial distribution of the T/S properties in Whale Bay showed that gradients in both temperature and salinity occurred within the lower portion of the main basin (Fig. 33d and e). This was apparently the edge of a frontal region that results from the surface inflow of cold, lower salinity water from Knight Island Pass (Fig. 25a). The data do not cover the entire transects within the lower reaches of this fjord, and therefor, this phenomenon will be discussed in later months when the data are more complete. Pooling of water with varying T/S properties was evident within Zaikof Bay (Fig. 35). Two adjacent regions appear in which water with opposite properties occurs; one with warmer, less saline conditions indicative of surface water, and one with cooler, more saline conditions indicative of deeper water. These zones possibly

correspond with convergence and divergence of tidal flow respectively, in which deeper water would be upwelled and surface water would be pooled. The higher values of fluorescence are also correlated with the area of potential upwelling (Fig. 35c).

*Fall, 1996*

In the fall of 1996, the fjord, Whale Bay, exhibited a higher range in horizontal temperature than the two bays (Figs. 35,36 and 37), but of lower values (8.8 to 10 C vs 9.6 to 10 C for Zaikof, and 9.8 to 10.3 C for Simpson). The horizontal salinity values were also lower than those within the bays (25.2 to 25.8 psu), and the highest range occurred within Zaikof Bay (29.2 to 30.2 psu). Simpson Bay was intermediate in terms of horizontal salinity range (28.8 to 29.5 psu), and was the only location to exhibit high values of fluorescence, indicating a fall phytoplankton bloom was occurring there (Fig. 36c).

The data for Zaikof Bay were not complete beyond the mouth of the bay, however, the spacial distribution shows some cross-channel gradients on the ebb tide as were observed in March. The areas of higher salinity evident along the northern side of this bay (Fig. 35e) were also observed in October, 1997, but the pattern was somewhat different (Fig. 38). These may be associated with diverging currents and this possibility will be discussed for October, 1997, when the data were completed for both ebb and flood tides.

Simpson Bay exhibited a change in T/S gradients between the tide stages in which a cross-channel gradient in salinity occurred on the ebb, but became a longitudinal gradient during the flood tide (Fig. 36b and e). The currents associated with these tides are shown in Figure 22a and b. From the vectors there appeared to be some horizontal shear on the west side during both tides, and this seemed to create a consistent cross-channel gradient in temperature, but not salinity. Why this occurred is uncertain, however, the gradient that forms on the ebb tide must be related to water mass properties within the main basin, as this is where the strongest flow occurred.

At Whale Bay the temperature gradient showed a gradual increase in temperature from the mouth inward, however, the gradient in salinity was concentrated along the northeast shore (Fig. 37a and b). These gradients appeared to be related to the inflow at the mouth of the bay, which occurred during both tide stages.

*Fall, 1997*

In October , 1997 the ranges of the horizontal T/S gradients were greater at all locations than those occurring in the fall, 1996 (Figs. 37,38,39 and 40). The fjords exhibited the highest values of temperature (8.3 to 10.1 C for Whale and 9.0 to 11.0 C for Eaglek). Temperatures were lower in range at the two bays, but tended to be warmer at Simpson than at Zaikof (9.3 to 10 C at Simpson, vs. 8.7 to 9.5 C at Zaikof). The salinity range at Simpson Bay was narrower and the values higher than at Zaikof Bay (29.2 to 29.6 psu vs. 27.4 to 28.6 psu). The two fjords exhibited relatively wider ranges in salinity (25.2 to 26.4 psu for Whale and 27.6 to 29.4 psu for Eaglek). These differences reflect the various conditions occurring locally within the fjords and bays. For example, the wider range in the horizontal salinity gradient at Zaikof Bay in comparison to that of Simpson Bay agrees with the differences in average vertical salinity gradients over the respective basins. The vertical salinity gradient at Simpson Bay was much more uniform (i.e.

more mixed) than that of Zaikof Bay, and thus the higher values and narrower range would be expected there (Fig. 15b). In this same regard, the differences in horizontal T/S gradient values observed between Whale Bay and Eaglek Bay were also apparent from the variance in the hydrography (Fig. 15a). Whale Bay was much cooler and less saline on average within the surface layer than was Eaglek Bay.

The spacial distribution of the horizontal T/S gradients exhibited substantial differences between the ebb and flood tide stages at both Zaikof Bay and Whale Bay (Figs. 38 and 39). In Zaikof Bay the higher salinity water located at mid basin along the north side of the bay during the ebb tide is also slightly warmer, indicating that it is of deeper origin. This would occur over an area of diverging flow, and the currents in this region of the bay show directional changes giving some evidence that this was the case (Fig. 19a). However, the low magnitude does not give a clear indication of flow separation, therefor, the inference was drawn more from the pattern in hydrography. A region of pooled water with lower average temperature and salinity occurred within an area where surface convergence should occur according to the pattern in the currents. Here the stronger inflow into the mouth appeared to converge with outflowing currents and an area of low flow results, which turns to the west (Fig. 19a). Evidence of a tidal front was typically observed within this area of the bay during most cruises.

The changes in spacial distribution of T/S conditions within Whale Bay also appeared related to the tidal currents. The inflow into the mouth of this bay during the ebb tide appeared to move glacially derived water, with much lower average temperature, into the main basin (Figs. 27a and 39a).

The average salinity of this water is slightly lower as well and the tidal currents apparently direct this water westward into the mouth of the west arm, however, the direction of the flow under this layer at 25 m. depth was outward (Fig. 27c). This water mass formed a frontal region located along the southern portion of the main basin, which appeared as both a temperature and salinity horizontal gradient in relation to the more uniform water mass properties occurring within the main basin. The changes occurring during the flood tide were less clear, however, the cross-channel gradients in both temperature and salinity (i.e. density) that occurred within the main basin appeared correlated with an outflow from the west arm and west basin to the mouth and a reciprocal inflow along the eastern basin (Fig. 27b). The inflow continued southward into the lower arm of the bay.

The horizontal T/S gradients for Simpson Bay are shown for the flood tide only (Fig. 37). The tidal flow within this bay appeared to have a considerable eastward tendency within the lower and upper regions of the bay. This pattern was even more evident in the deeper layer (Fig. 23b and d). These currents apparently affected the salinity, producing a cross-channel gradient, but the temperature gradient remained longitudinal (gradually increasing up the bay). A density front resulted from this gradient, particularly at the mouth of the east arm.

Tidal currents within Eaglek bay were very low in magnitude, however, they did exhibit directional changes that indicated possible convergence within the main basin (Fig. 30.). The changes in horizontal distribution of temperature and salinity between the tide stages did not show the marked variability that was observed in late winter, possibly because of the vertical stratification that existed in conjunction with the very small tidal flows (Fig. 15a and 30). There was some evidence at mid basin of a front developing during both tide stages, in which there is a slight gradient in salinity (i.e. density). This is a region of the bay where an inflow appeared to converge with outflow during both the ebb and the flood tides.

## Summary and Conclusions

Bays and fjords within Prince William Sound exhibited marked seasonal changes in heat and freshwater content that generally reflected the extremes of the Subarctic climate between summer and winter. Inter-annual variability in the seasonal extremes of the physical water mass properties occurred between 1994 and 1998 at all locations surveyed, and this tended to reflect the general climatic trends towards warmer, drier summers and milder winters, particularly from the summer of 1996 to the spring of 1998. The temperatures of the deep water of both bays and fjords increased over the above time period in response to the increased average air temperatures. However, the most striking changes occurred seasonally in the surface layer temperatures of fjords, which developed much greater vertical temperature gradients than bays during the warmest period in summer of 1997.

General trends in hydrography observed among most locations during the spring and summer of 1994 showed initial surface heating as average air temperatures increased during April and May, however, this was moderated by substantial variance in cold, freshwater input from melting of the lower elevation snowpack along with higher precipitation rates. These factors contributed to the observations of strong sub-regional patterns in freshwater input, especially evident within fjords with high watershed to bay surface area ratios. During the summer of 1994 certain fjords continued to show high rates of surface freshening relative to other regions despite a general drop in the precipitation rate. These increases were presumably from continued melting of higher elevation snow fields, and therefor, watershed characteristics played a large part in influencing seasonal differences in physical properties.

Other factors affecting the hydrography sub-regionally included general differences in basin morphometry and proximity to sources of water derived from fjords with tidewater glaciers. For example, many of the locations within the extreme southwestern part of the sound are narrow, shallow passes which tend to have higher tidal current velocities than most bays and fjords. These areas exhibited much lower vertical T/S gradients during the summer presumably as a result of increased mixing, and this appeared to affect the hydrography within the bays of this sub-region as well which have connections with these passes. Fjords located near the glacial region of Icy Bay exhibited unique temperature characteristics in the T/S signatures which indicated advection of glacially derived water into their main basins.

In the fall and winter the general loss of heat through surface cooling was evident in all bays and fjords, however, the process of vertical mixing occurred much earlier within the bays. Fjords tended to remain stratified well into the late fall, but by late winter the water column of all locations typically became nearly vertically homogeneous.

The tidal current velocities varied substantially among the two bays and two fjords surveyed in 1996 and 1997. The only location which exhibited consistently higher velocities of over 50 cm/sec was Zaikof Bay. Inflows observed during the ebb tides were barotrophic, but also exhibited horizontal shear. The portions of the mouth where these flows occurred showed the presence of frontal zones due to convergence with outflows from the bay. Tidal front were also observed during the flood tide where strong inflows tended to create reversals in currents out of the basin along the shoreline. Patterns in the horizontal T/S gradients also indicated formation of zones of convergence and possibly divergence in which water with surface and deeper T/S properties tended to form sequential gradients. The patterns at Simpson and Eaglek Bays were much more variable, however, horizontal T/S gradients occurred on various tides seasonally and indicated the formation of fronts episodically. The patterns in the currents and hydrography at

Whale Bay exhibited surface inflows during both the ebb and flood during all seasons except late winter. However, these flows were baroclinic and varied with depth, showing outflow in the deeper layers during the ebb tide and weak subsurface inflow during the flood tide. Reverse flow was also observed occasionally at 25 m, under the surface flows at ebb tide within both the main basin and the lower arm. The horizontal T/S gradients exhibited evidence of tidal fronts forming at the mouth and lower portions of the deep main basin during the ebb tide and a cross-channel gradient forming during the flood tide; these forming in response to changes in the surface flow beteen tides.

***Conclusions.*** From this research we can conclude that estuarine conditions within bays and fjords of Prince William Sound generally follow the annual cycles of air temperature and precipitation and as such, would be expected to vary considerably from year to year, similar to annual variation in hydrography within PWS and the North Gulf Coast. However, smaller scale local factors also appear to play a prominent role in determining the relative extent and timing of both surface heating and estuarine conditions. These local factors include the following: 1) relative sizes of bays and fjords and their respective watersheds, 2) topography and aspect, 3) sub-regional variation in precipitation and winds, and 4) proximity to glacial regions.

The sub-regional variability in T/S conditions and circulation patterns of the bays, fjords and smaller passes within PWS may have important implications in the distribution of larval fish species. These areas serve as nursery habitats for salmonid smolts and larval Pacific herring during spring and summer, and as over-wintering areas for juvenile herring. Circulation patterns and their affect on seasonal hydrography and formation of tidal fronts may have influence the biological productivity among these bays and fjords, and serve as mechanisms in either the retention of locally produced larval fish or advection of larval fish into nursery areas. Comparisons of larval and juvenile fish distribution with the physical characteristics of these habitats is the focus of future research on Pacific herring.

*Acknowledgments.* Weather data from the C-Lab Buoy were provided by Dr. Dave Eslinger with IMS/UAF and data from the PWSAC hatcheries were provided by both Dr. Ted Cooney with IMS/UAF and Mark Summerville with PWSAC. Also I would like to especially thank Dave Janka, Captain of the M/V Auklet, his wife Annette and the crew of the F/V Miss Kayley for their generous assistance and support during the field portions of this project. Funding support for this study was provided by the EVOS Trustee Council as part of the Sound Ecosystem Assessment Project No. 97320M .

## REFERENCES


Colonell, J. M. 1981. Deep Water Renewal in a Subarctic Fjord. Journal of the Waterway, Port, Coastal and Ocean Division, Proceedings of the Society of Civil Engineers, Vol. 107, No.WW4, pp. 223 - 231.

Gay, S.M. III (In review). Seasonal changes in hydrography of embayments and fjords of Prince William Sound, Alaska during spring and summer 1994, fall 1995, and late winter 1996. Submitted in 1996 to Journal of Marine Systems.

Meunch, R. D. and Nebert, D. L., 1973. Physical Oceanography, *Environmental Studies of Port Valdez*, D. W. Hood, W. E. Shiels, and E. J. Kelly, eds., University of Alaska, Fairbanks, Alaska, pp. 103-149.

Meunch, R. D. and and G. M. Schmidt. 1975. Variations in the hydrographic structure of Prince Sound. *Sea Grant Report R75-1.* Institute of Marine Science Report, R75-1, University of Alaska, Fairbanks, 135 pp.

Meunch, R. D. and D.T. Heggie. 1978. Deep Water Exchange in Alaskan Subarctic Fjords. In *Estuarine Transport Processes.* (Kjerfve, B., ed.) The Belle W. Baruch Library in Marine Science, No. 7, pp. 239-267.

Niebauer, H. J., T. C. Royer, and T. J. Weingartner 1994. Circulation of Prince William Sound, Alaska. Journal of Geophysical Research, Vol. 99, No. C7, pp. 14,113-14,126.

Pickard, G. L. 1961. Oceanographic Features of Inlets in the British Columbia Mainland Coast.. J. Fish. Res. Bd. Canada, 18(6), pp 907- 999.

Pickard, G. L. 1967. Some oceanographic characteristics of the larger inlets of Southeast Alaska. J. Fish. Res. Bd. Canada, 24, pp 1475-1505.

Pritchard, D. W. 1967. What is an estuary: physical viewpoint. In *Estuaries:* 3-5. G. H. Lauff (editor). American Association for the Advancement of Science Publication No. 83.

Rattray, M. Jr. 1967. Some aspects of the dynamics of circulations in fjords. In *Estuaries* (ed. G. H. Lauff), American Association for the Advancement of Science pp. 53-62.

Royer, T. C. 1979. On the effect of precipitation and runoff on coastal circulation in the Gulf of Alaska, Journal of Physical Oceanography, 9, 555-563.

Royer, T. C. 1982. Coastal fresh water discharge in the northeast Pacific. Journal of Geophysical Research 87: 2017-2021.

Walters, R.A.,E.G. Josberger and C.L. Driedger. 1988. Columbia Bay, Alaska: an 'Upside Down' Estuary. Estuarine, Coastal and Shelf Science 26: 607-617.

LIST OF TABLES AND FIGURES

Figure 33. Horizontal contours of temperature, salinity and fluorescence averaged over 5 to 10 m. depth for Whale Bay, March, 1996 (top) and August, 1996 (bottom).

Figure 34. Horizontal contours of temperature, salinity and fluorescence averaged over 5 to 10 m. depth for Eaglek Bay, March, 1996.

Figure 35. Horizontal contours of temperature, salinity and fluorescence averaged over 5 to 10 m. depth for Zaikof Bay, August 1996 (top), and October, 1996 (bottom).

Figure 36. Horizontal contours of temperature, salinity and fluorescence averaged over 5 to 10 m. depth for Simpson Bay, October, 1996.

Figure 37. Horizontal contours of temperature, salinity, fluorescence, and density averaged over 5 to 10 m. depth for Whale Bay, October 1996 (top), and Simpson Bay, October, 1997 (bottom)

Figure 38. Horizontal contours of temperature, salinity and density averaged over 5 to 10 m. depth for Zaikof Bay, October, 1997.

Figure 39. Horizontal contours of temperature, salinity and density averaged over 5 to 10 m. depth for Whale Bay, October, 1997.

Figure 40. Horizontal contours of temperature, salinity and density averaged over 5 to 10 m. depth for Eaglek Bay, October, 1997.

Table 1. General physiography and observation dates of fjords, bays and passes within Prince William Sound, Alaska sampled from May 1994 through March, 1998.

| Location | Median Width (km) | Maximum Length (km) | Basin Depth (m) | Sill Depth (m) | Observation Period (month/year) | No. of Ctd Stations |
|---|---|---|---|---|---|---|
| ***Western and Northwestern PWS:*** | | | | | | |
| *Region 1.* | | | | | | |
| Herring Bay | 3.70 | 9.3 | 230 | unsilled | May, June, July 94; Oct. 95 | 22 |
| Drier Bay | 2.80 | 11.1 | 180 | 40 - 60 | June, July 94; Mar., July 96 | 16 |
| Long Channel | 0.75 | 7.5 | 50-200 | unsilled | June, July 94 | 8 |
| Mummy Bay | 1.30 | 7.5 | 100 | unsilled | July 94 | 9 |
| Little Bay | 0.90 | 1.8 | 50 | unsilled | July 94 | 3 |
| *Region 2.* | | | | | | |
| South Bay | 1.85 | 3.2 | 160 | unsilled | May, June 94 | 9 |
| Culross Bay | 0.65 | 3.0 | 170 | unsilled | May 94 | 8 |
| N. Applegate I. | --- | --- | --- | nearshore | May 94 | 5 |
| W. Twin Bay | 0.90 | 5.0 | 80 | unsilled | May 94 | 6 |
| Quillion Bay | 0.37 | 2.8 | 60 | unsilled | May 94 | 5 |
| *Region 3.* | | | | | | |
| Main Bay | 1.40 | 5.2 | 160 | 50 | May, June 94 | 8 |
| Eshamy Bay | 1.85 | 3.2 | 200 | 50 - 60 | May, June 94 | 14 |
| W. Crafton I. | --- | --- | --- | nearshore | May, June 94 | 4 |
| Ewan Bay | 1.00 | 5.6 | 100 | unsilled | Mar., July 96 | 3 |
| Paddy Bay | 0.74 | 4.1 | 100 | unsilled | Mar., July 96 | 5 |
| ***Southwestern PWS:*** | | | | | | |
| *Region 4.* | | | | | June, July 94; Oct. 95 | 17 |
| Whale Bay | 2.80[1] | 4.2[1] | 280 | unsilled | Mar., July, Aug.,Oct., Nov. 96 Feb., Mar.,May, Jul.,Aug.,Oct. 97; Mar. 98 | |
| Bainbridge Pass | 2.00[2] | 6.3[2] | 340 | unsilled | June, July 94 | 14 |
| Shelter Bay | 0.70 | 3.7 | 100 | unsilled | June 94 | 12 |
| Flemming I. | --- | --- | 120 | nearshore | June, July 94 | 6 |
| N. Prince of Wales P. | --- | --- | 130 | pass | June, July 94 | 14 |
| *Region 5.* | | | | | | |
| Sawmill Bay | 0.70 | 4.8 | 160 | 60 | Nov. 95 | 6 |
| N. Elrington Pass | --- | --- | 70 | pass | July 94; Nov 95; July96 | 9 |
| Hogg Bay | 8.33 | 1.8 | 120 | unsilled | Nov 95 | 8 |
| L. Bainbridge Pass | --- | --- | 90 | unsilled | Nov 95 | 3 |

Table 1. (Continued)

| | | | | | | |
|---|---|---|---|---|---|---|
| ***Northern PWS:*** | | | | | | |
| Jack Bay | 0.93 | 10.2 | 200 | 30 | Nov 95: Mar.. Jul. 96 | 12 |
| Galena Bay | 1.50 | 8.3 | 200 | 25 | Mar.. Jul. 96 | 6 |
| Eaglek Bay | 3.70 | 14.4 | 200 | unsilled | Nov 95: Mar..Jun..Jul..Aug..Oct. 96 Mar.. May. Jul..Aug..Oct. 97: Mar.98 | 16 |
| ***Eastern PWS:*** | | | | | | |
| Sheep Bay | 3.50 | 13.8 | 80 | unsilled | Mar. 96:Jul 96 | 5 |
| Port Gravina | --- | --- | 80 | | Mar.. Jul. 96 | 8 |
| Port Fidalgo | --- | --- | 100 | | Jul. 96 | 2 |
| Knowles Head | --- | --- | 60 | | Nov. 95 | 12 |
| Snug Corner Cove | --- | --- | 120 | | Nov. 95 | 11 |
| Simpson Bay | 1.70 | 9.5 | 90 | unsilled | Oct 95: Mar..Jun..Jul..Aug..Oct..Nov.. Dec. 96: Jan..Feb..Mar.. May. Jul.. Aug.. Oct. 97: Mar. 98 | 9 |
| ***South Central PWS:*** | | | | | | |
| Green Island | --- | --- | 120 | | Oct. 95: Mar.. Jul. 96 | 14 |
| Zaikof Bay | 3.00 | 12.9 | 100 | unsilled | Oct 95; Mar.,Jun..Aug.,Oct..Nov.,Dec. 96 Feb..Mar..May, Jul.,Aug.,Oct. 97; Mar. 98 | |
| ***Glacial Fjords:*** | | | | | | |
| Unakwik Inlet | 2.50 | 30.5 | 270 | 4 | Mar.. Jul..Aug. 96 | 6 |
| Icy Bay | 1.80 | 18.5 | 168 | 30 | Mar.. Jul. 96; Mar. 98 | 3 |
| Nassau Fjord | 1.90 | 5.4 | 350 | 20 - 30 | Mar. 96; Mar. 98 | 2 |

1 Data for main basin only; widths of S arm and narrows at SW inlet are 1.5 and 0.7 km respectively, and lengths are 4.1 and 11 km.

2 Data for main basin only; widths of NW and S arms of the fjord are 1.3 and 1.5 km respectively, and lengths are 5.9 and 7.4 km.

Table 2. Watershed and fjord/bay surface areas, area ratios, and mean salinities at 1.0 m depth for 1994, 1995 and 1996.

| *Location* | *Watershed Area (ha)* | *Fjord or Bay Surface Area (ha)* | *Ratio* | *May 94* | *June 94* | *July 94* | *Oct/Nov 95* | *March 96* |
|---|---|---|---|---|---|---|---|---|
| Herring Bay | 2,541 | 2,088 | 1.2 | 27.89 | 27.49 | 27.03 | 25.08 | --- |
| Lower Herring | 1,639 | 708 | 2.3 | 28.20 | 26.75 | 26.13 | --- | --- |
| Drier Bay | 5,091 | 1,906 | 2.7 | --- | 26.25 | 25.04 | --- | 31.50 |
| South Bay | 656 | 526 | 1.3 | 29.57 | 25.65 | --- | --- | --- |
| Culross Bay | 3,497 | 538 | 6.5 | 23.37 | --- | --- | --- | --- |
| Main Bay | 2,732 | 664 | 4.1 | 24.77 | 22.28 | --- | --- | --- |
| Eshamy Bay | 5,637 | 1,109 | 5.1 | 27.38 | 21.12 | --- | --- | --- |
| Whale Bay | 5,411 | 2,566 | 2.1 | --- | 23.44 | 24.16 | 19.64 | 30.32 |
| Sawmill Bay | 1,092 | 572 | 1.9 | --- | --- | 26.14 | 27.22 | --- |
| Twin Bays | 489 | 635 | 0.8 | --- | --- | 29.03 | --- | --- |
| Simpson Bay | 16,980 | 2,792 | 6.1 | --- | --- | --- | 27.50 | 31.20 |
| Jack Bay | 13,853 | 1,429 | 9.7 | --- | --- | --- | 27.54 | 31.84 |
| Zaikof Bay | 5,488 | 2,614 | 2.1 | --- | --- | --- | 29.41 | 31.38 |
| Ewan Bay | 2,590 | 676 | 3.8 | --- | --- | --- | --- | 31.09 |
| Paddy Bay | 1,295 | 457 | 2.8 | --- | --- | --- | --- | 31.15 |

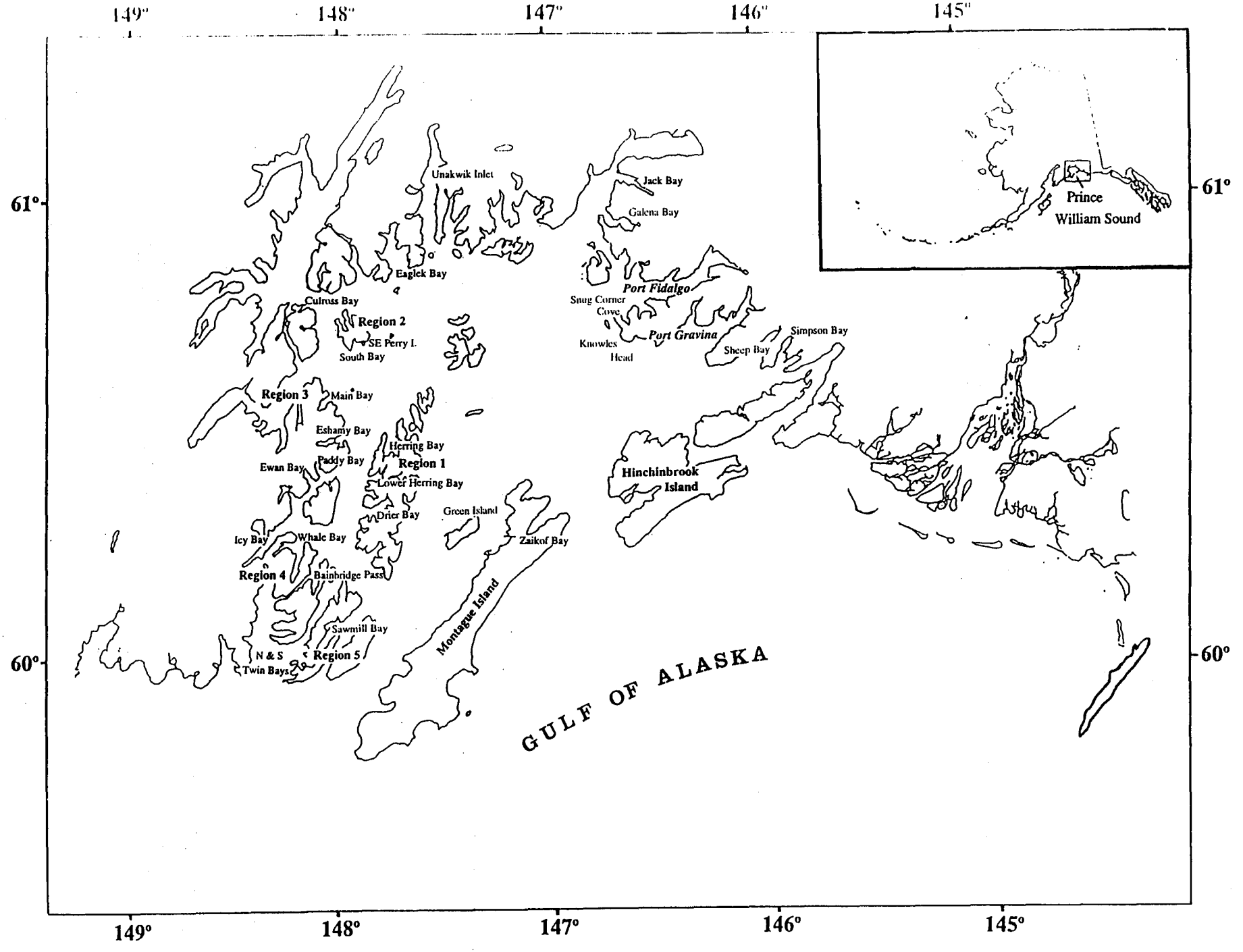


8-124

**Figure 1a.**

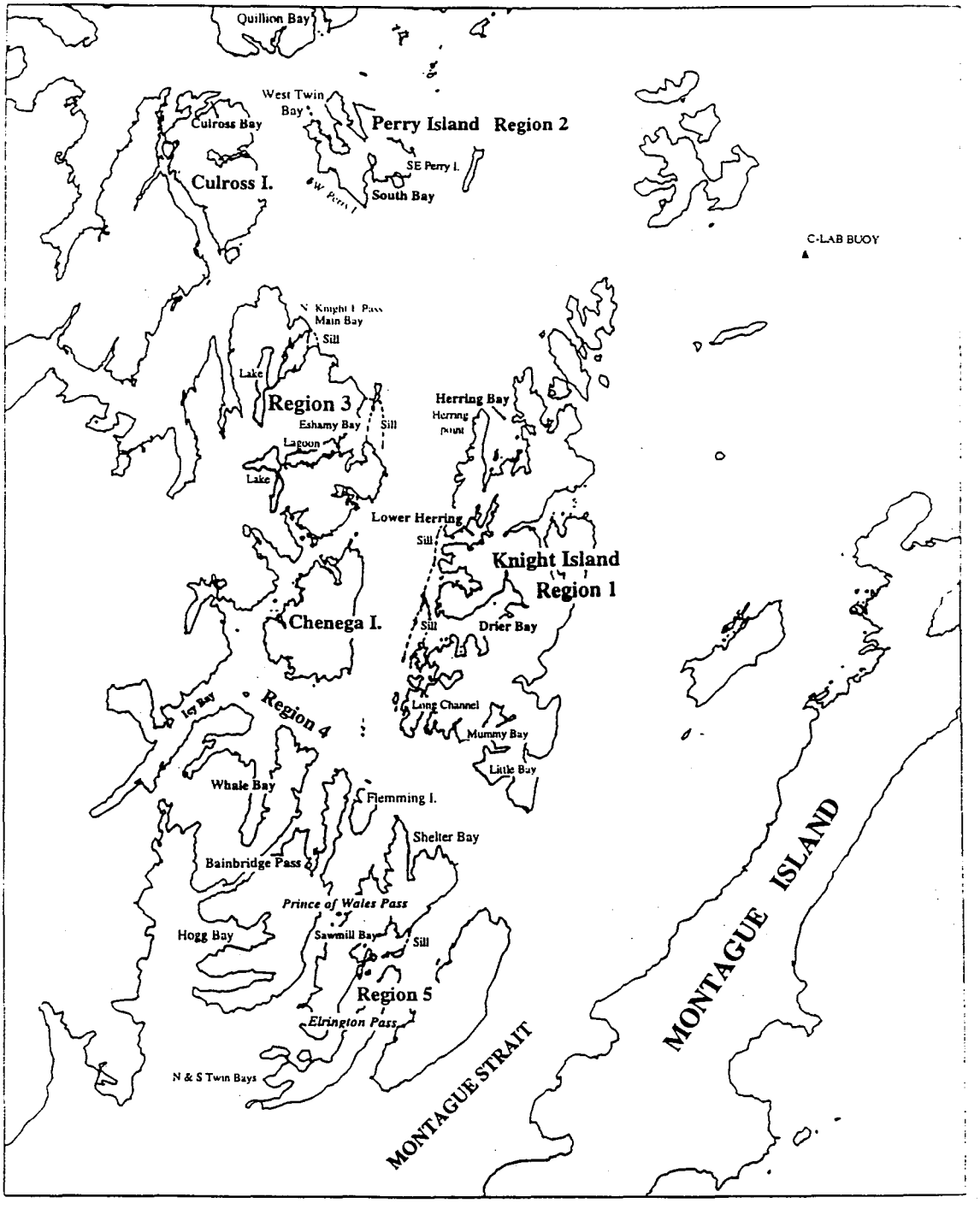
Quillion Bay
West Twin Bay
Culross Bay
Perry Island Region 2
SE Perry I.
Culross I.
W. Perry I.
South Bay
C-LAB BUOY
N. Knight I. Pass
Main Bay
Sill
Lake
Region 3
Herring Bay
Herring Point
Eshamy Bay
Sill
Lagoon
Lake
Lower Herring
Sill
Knight Island Region 1
Chenega I.
Sill
Drier Bay
Long Channel
Ivy Bay
Region 4
Mummy Bay
Little Bay
Whale Bay
Flemming I.
Shelter Bay
Bainbridge Pass
Prince of Wales Pass
Hogg Bay
Sawmill Bay
Sill
Region 5
Elrington Pass
N & S Twin Bays
MONTAGUE STRAIT
MONTAGUE ISLAND

**Figure 1b.**

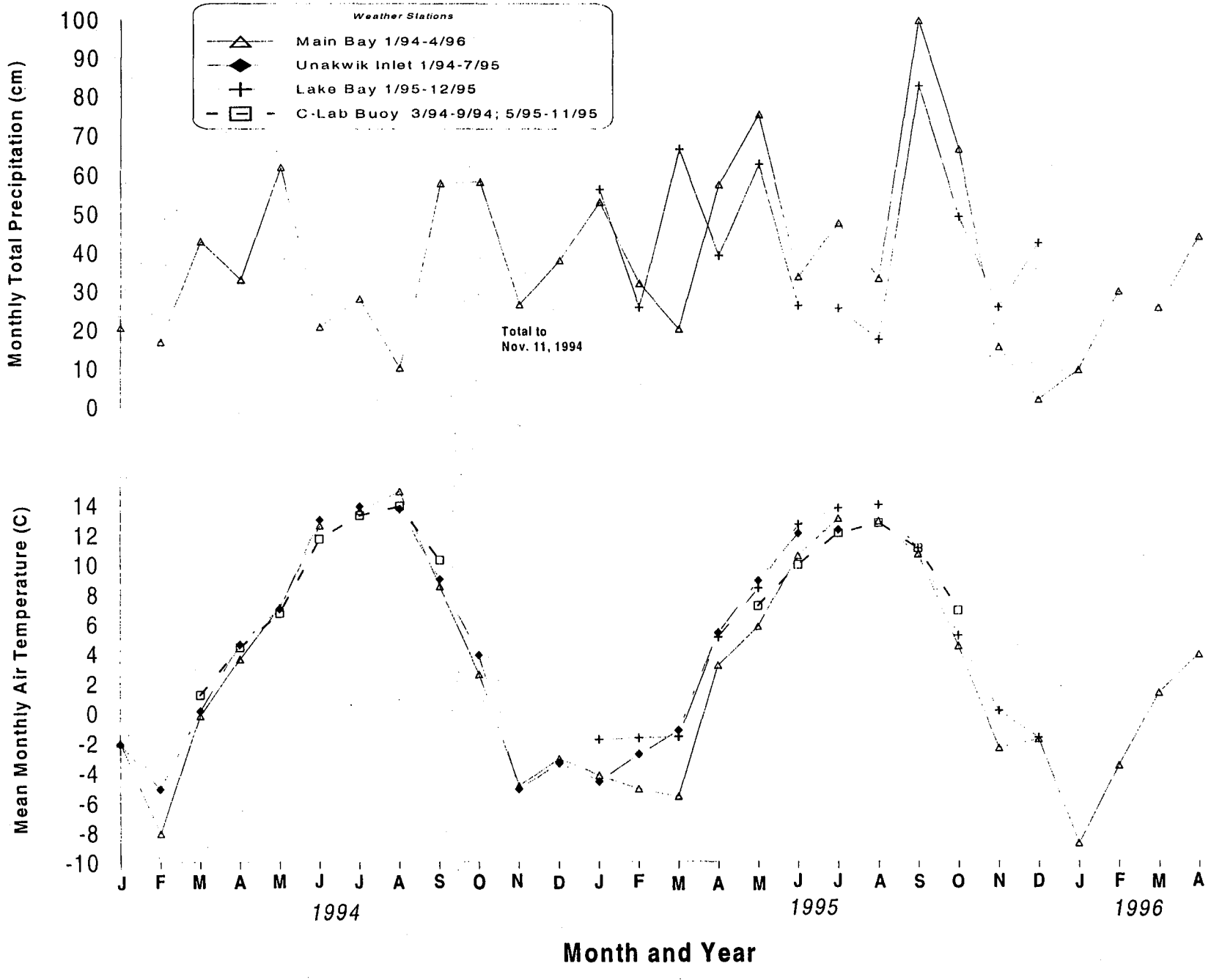


Fig. 2. Annual air temperature and precipitation cycles for stations within PWS. 1994-1996

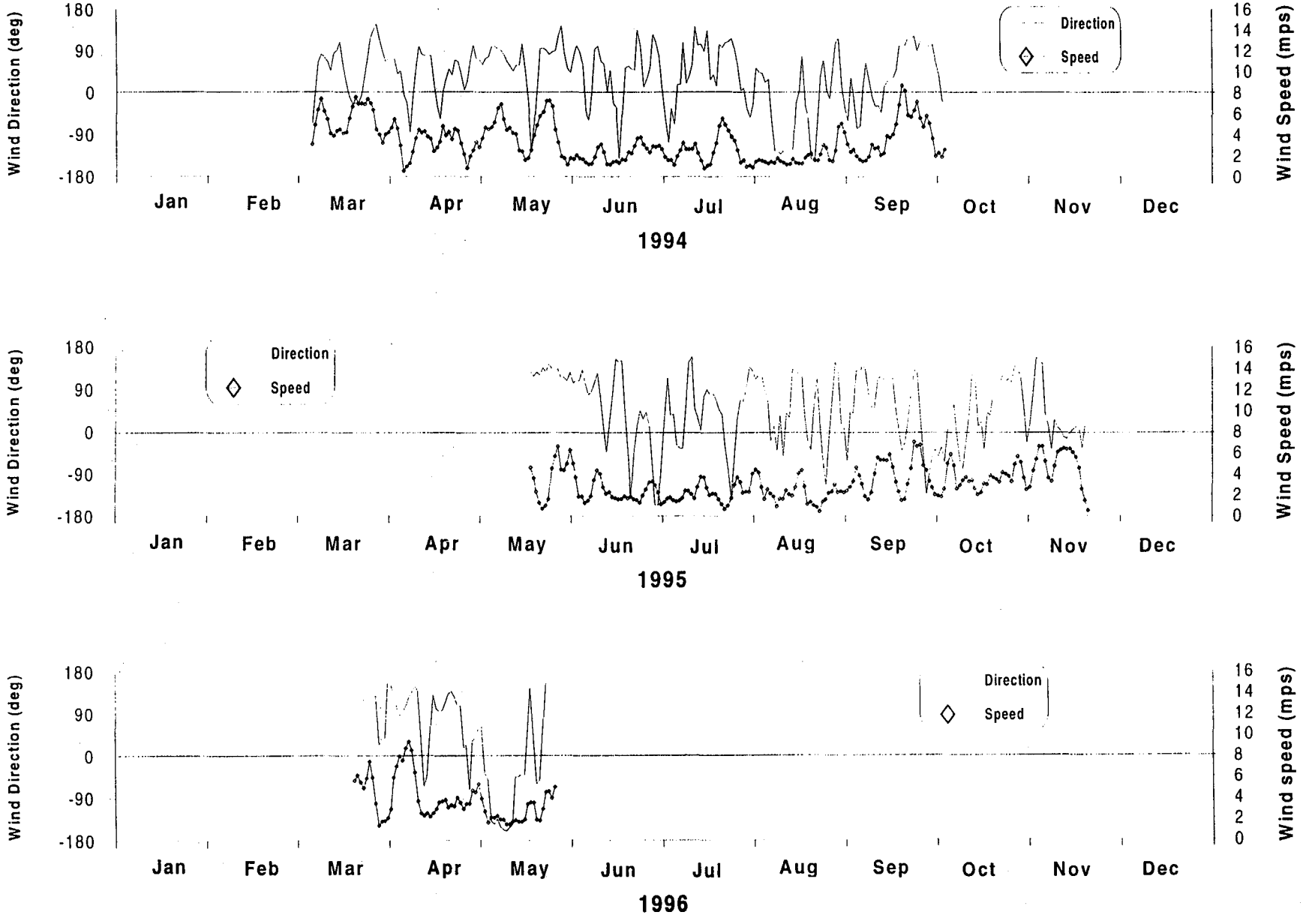


Figure 3. Wind directions and speeds measured at the C-Lab Buoy, 1994 to 1996. Directions and speeds are daily vector averages, low pass filtered by a running average using a 3 day window. Easterly directions are +90 and westerly directions are -90.

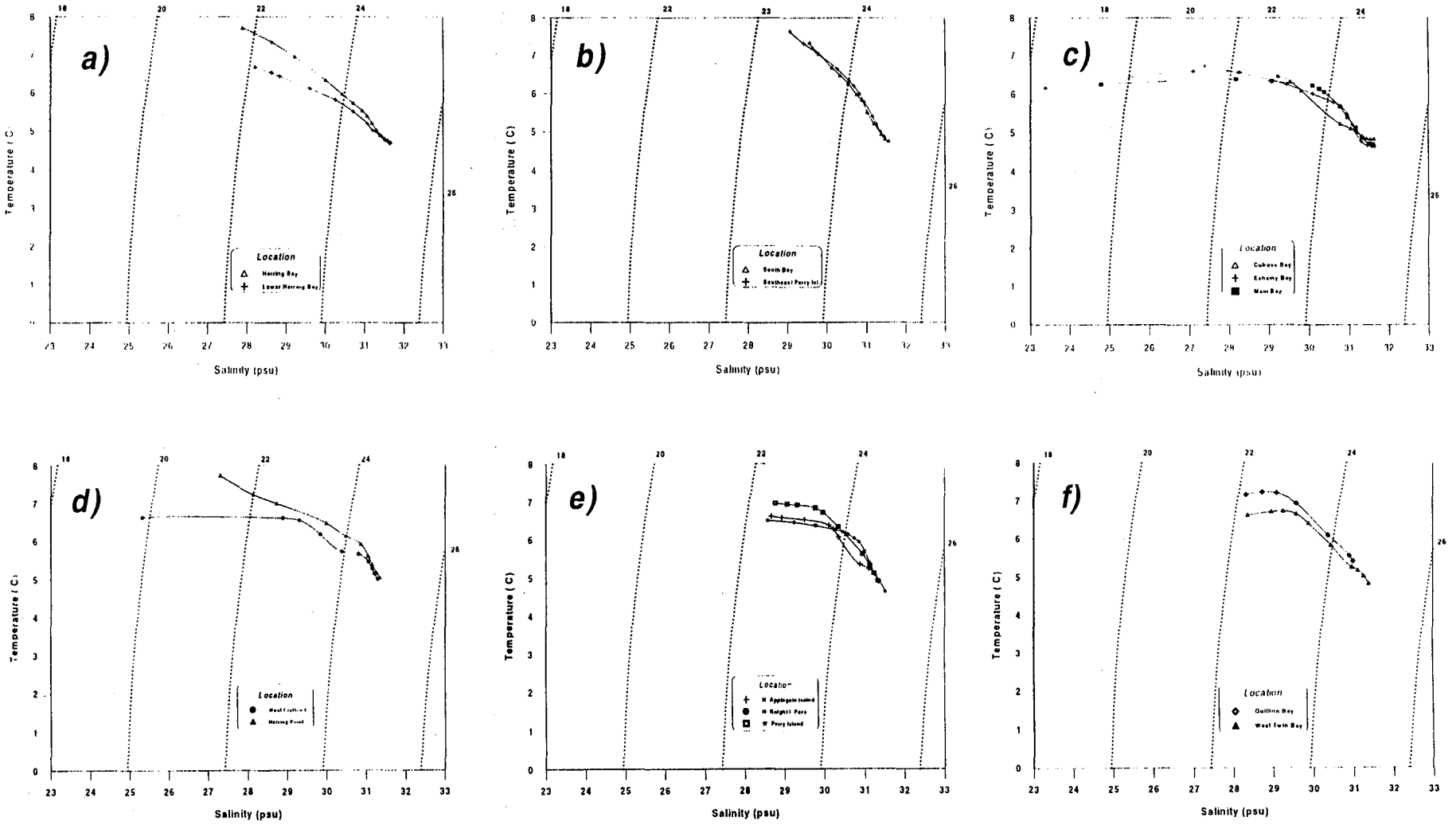


Figure 4

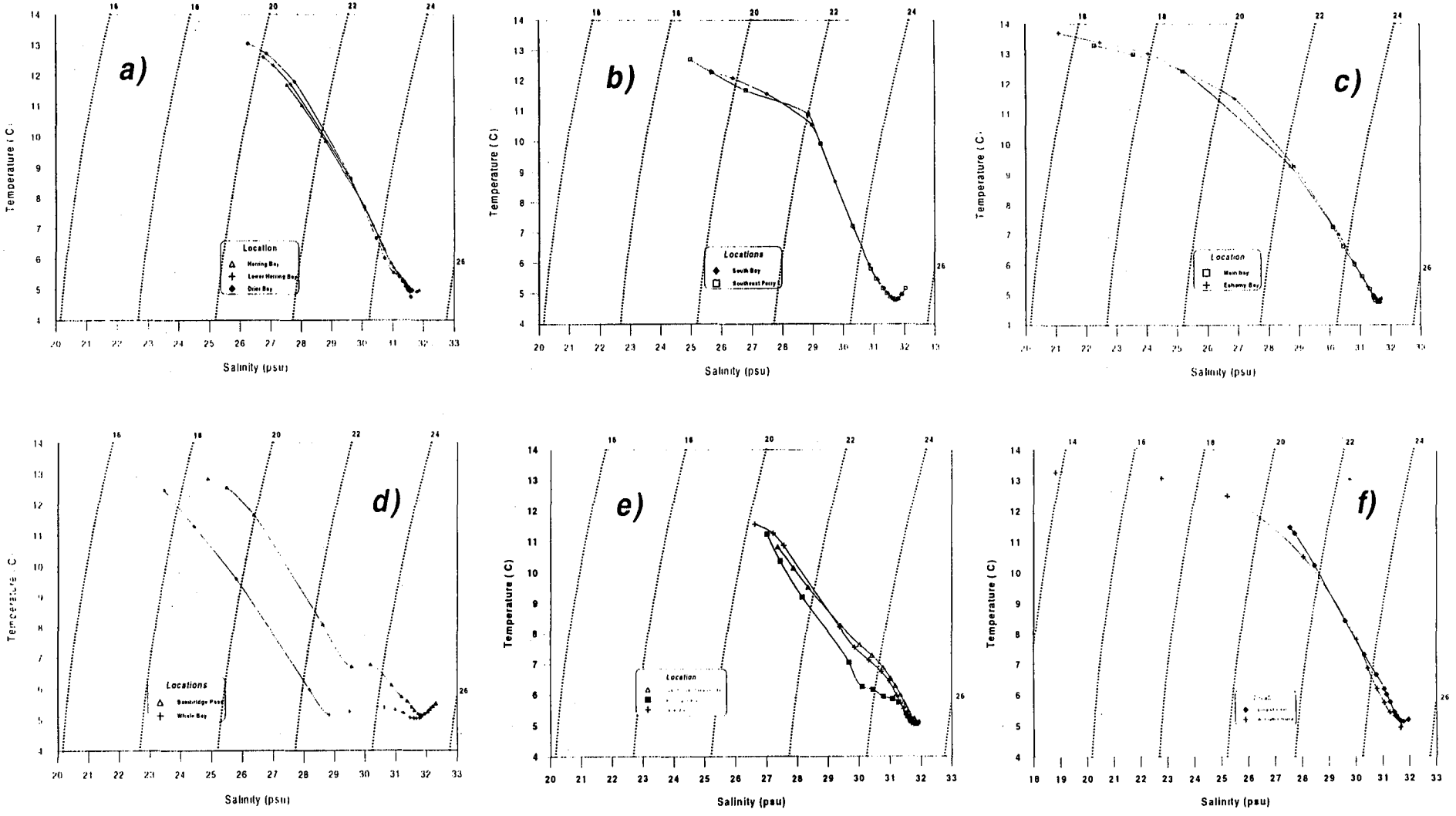


**Figure 5.**

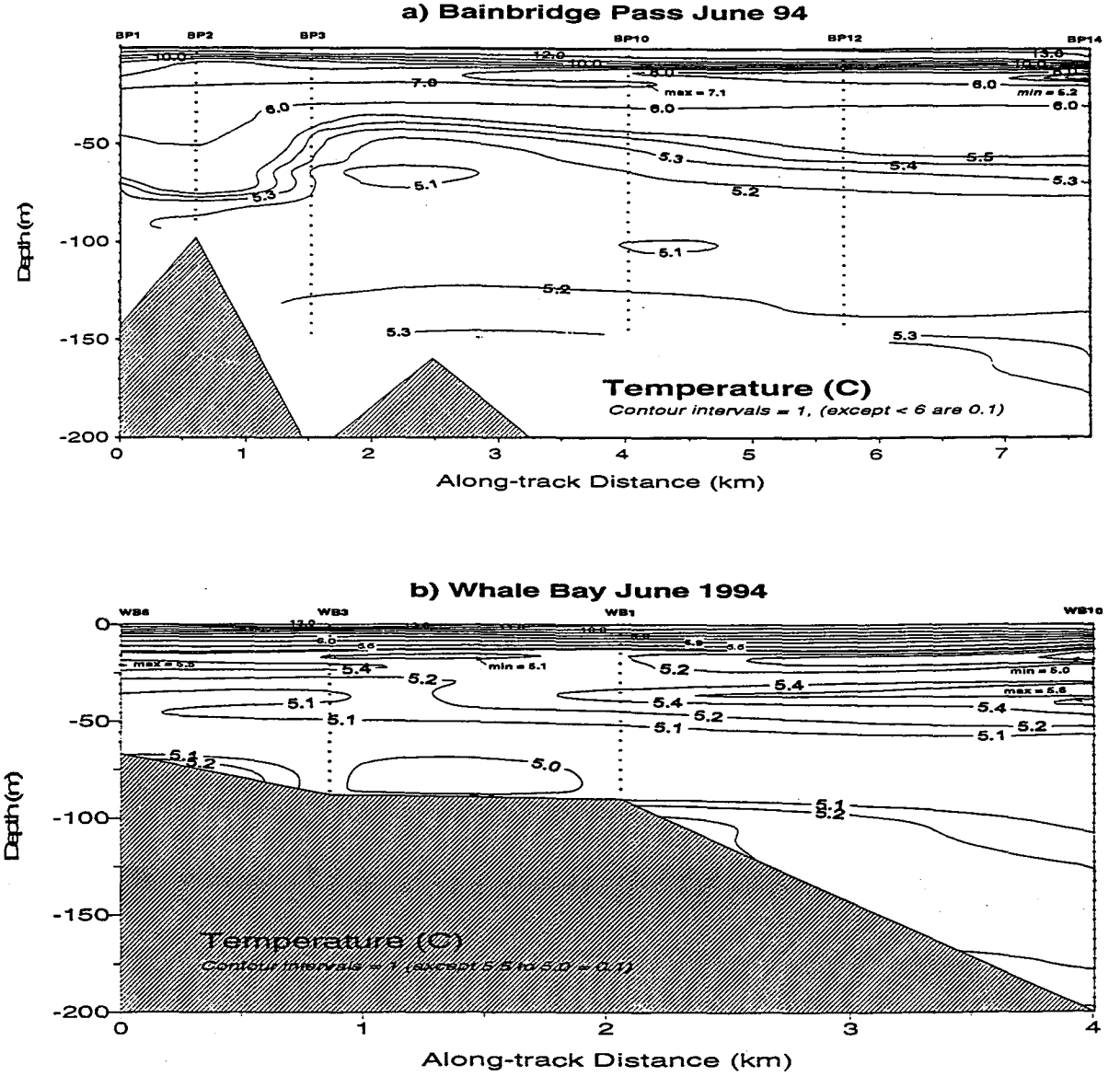


Figure 6. Temperature contours for Whale Bay and Bainbridge Pass, June 1994 showing fine scale subthermocline maxima and minima. Also shown is the deep temperature minmum below 70 m depth.

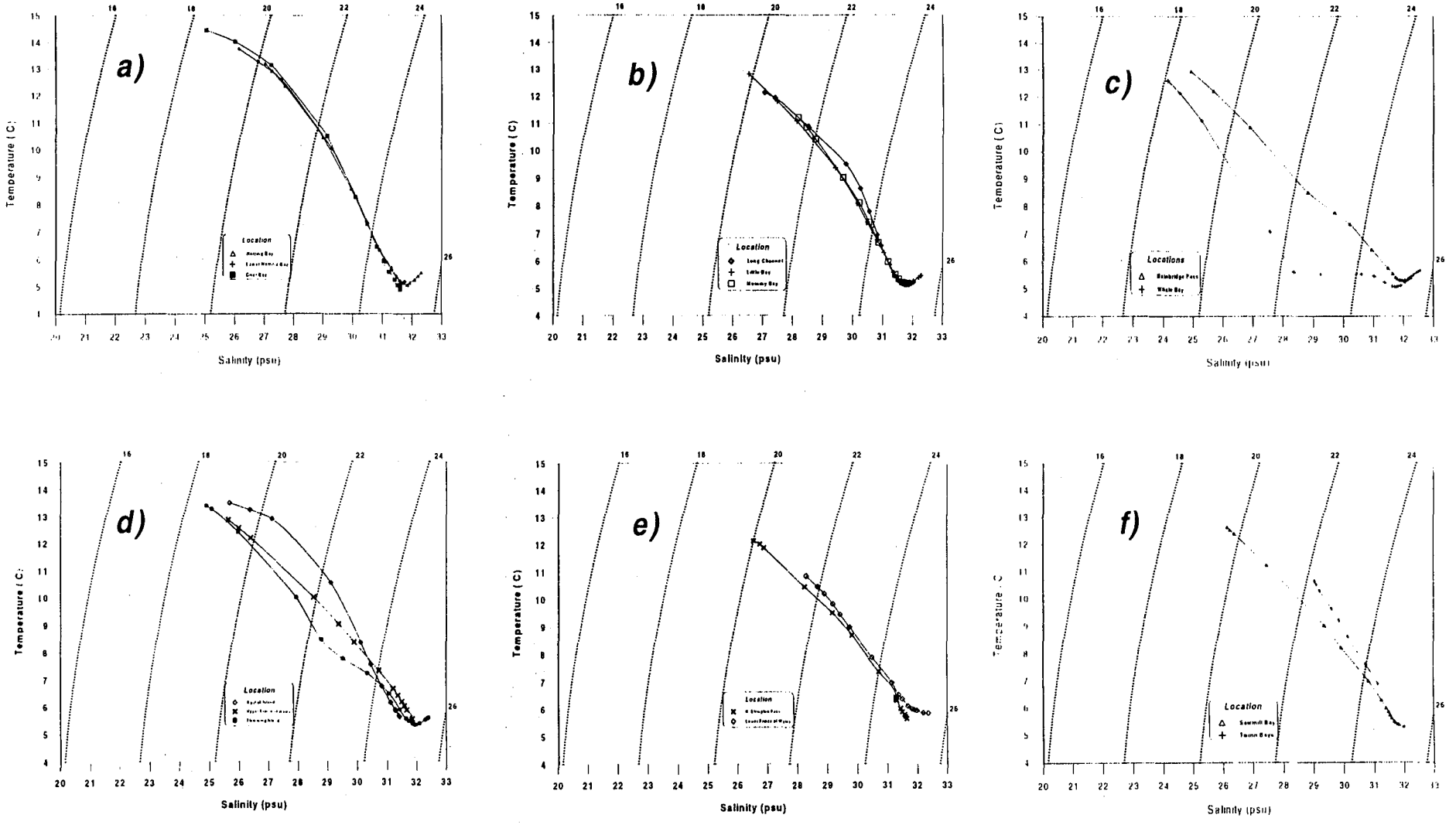


**Figure 7.**

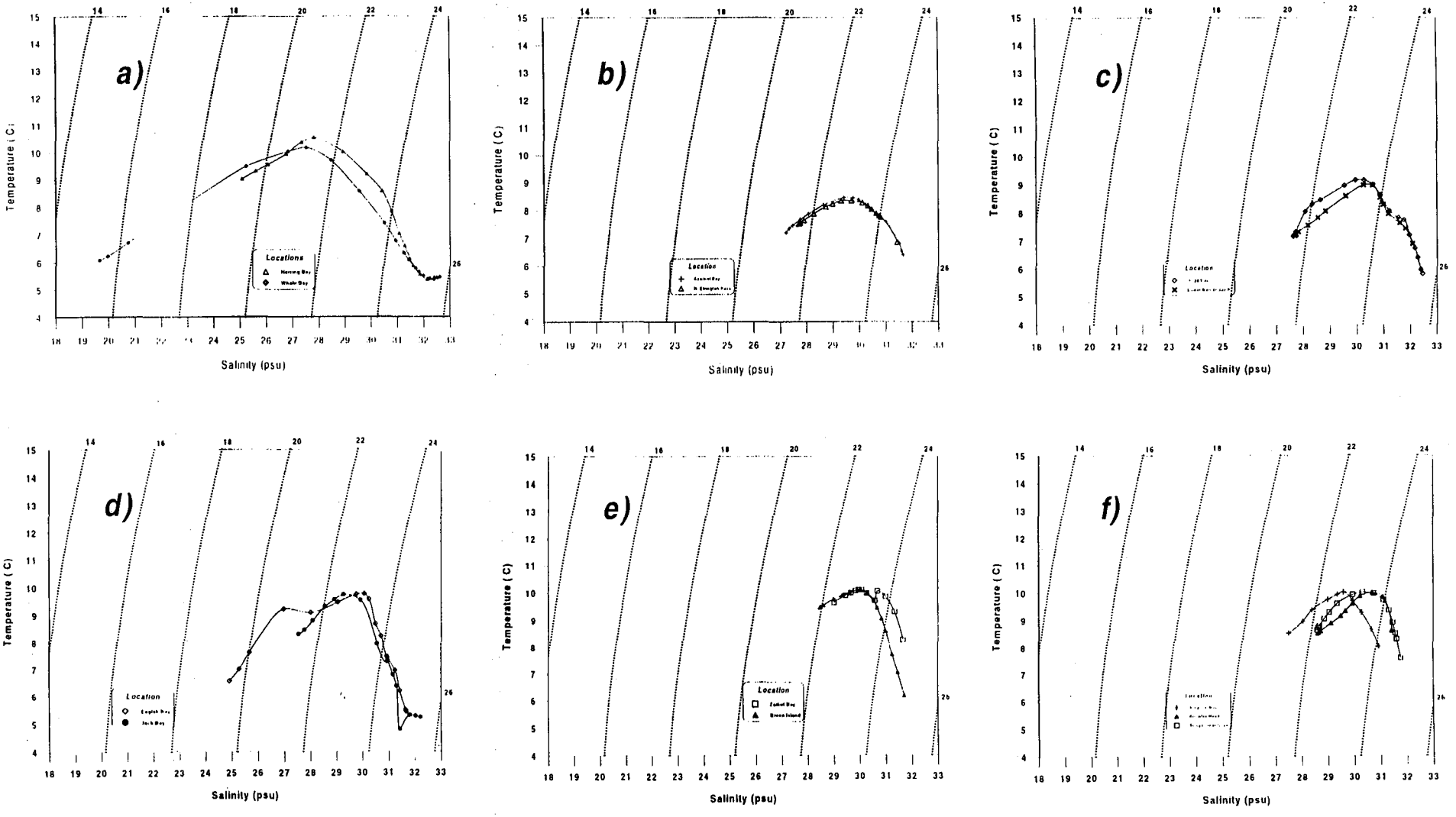


**Figure 8.**

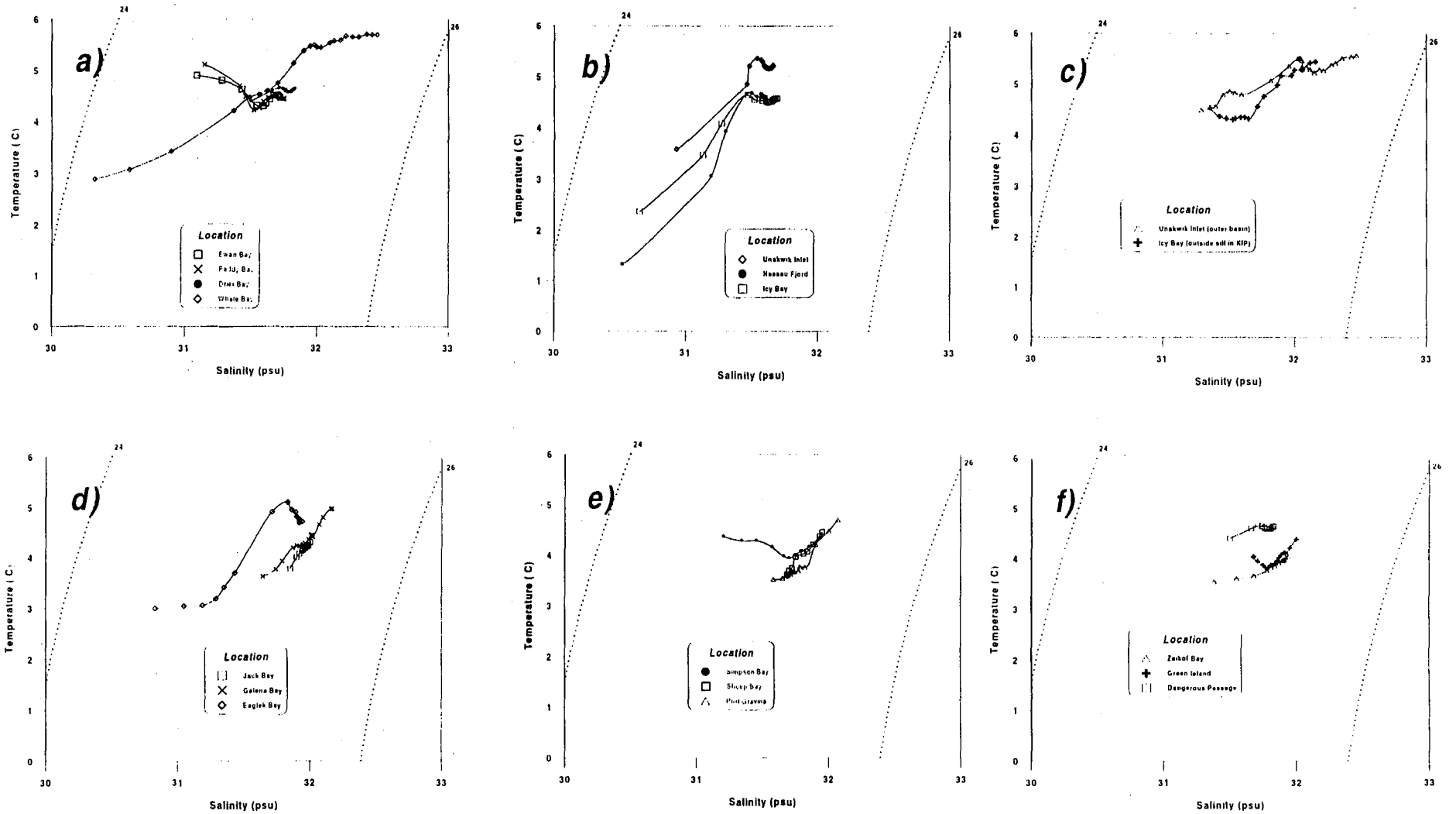
a)
b)
c)
d)
e)
f)
Temperature ( C)
Salinity (psu)
Location
Unakwik Inlet
Nassau Fjord
Icy Bay
Jack Bay
Galena Bay
Eagle Bay
Zaikof Bay
Green Island
Dangerous Passage

**Figure 9.**

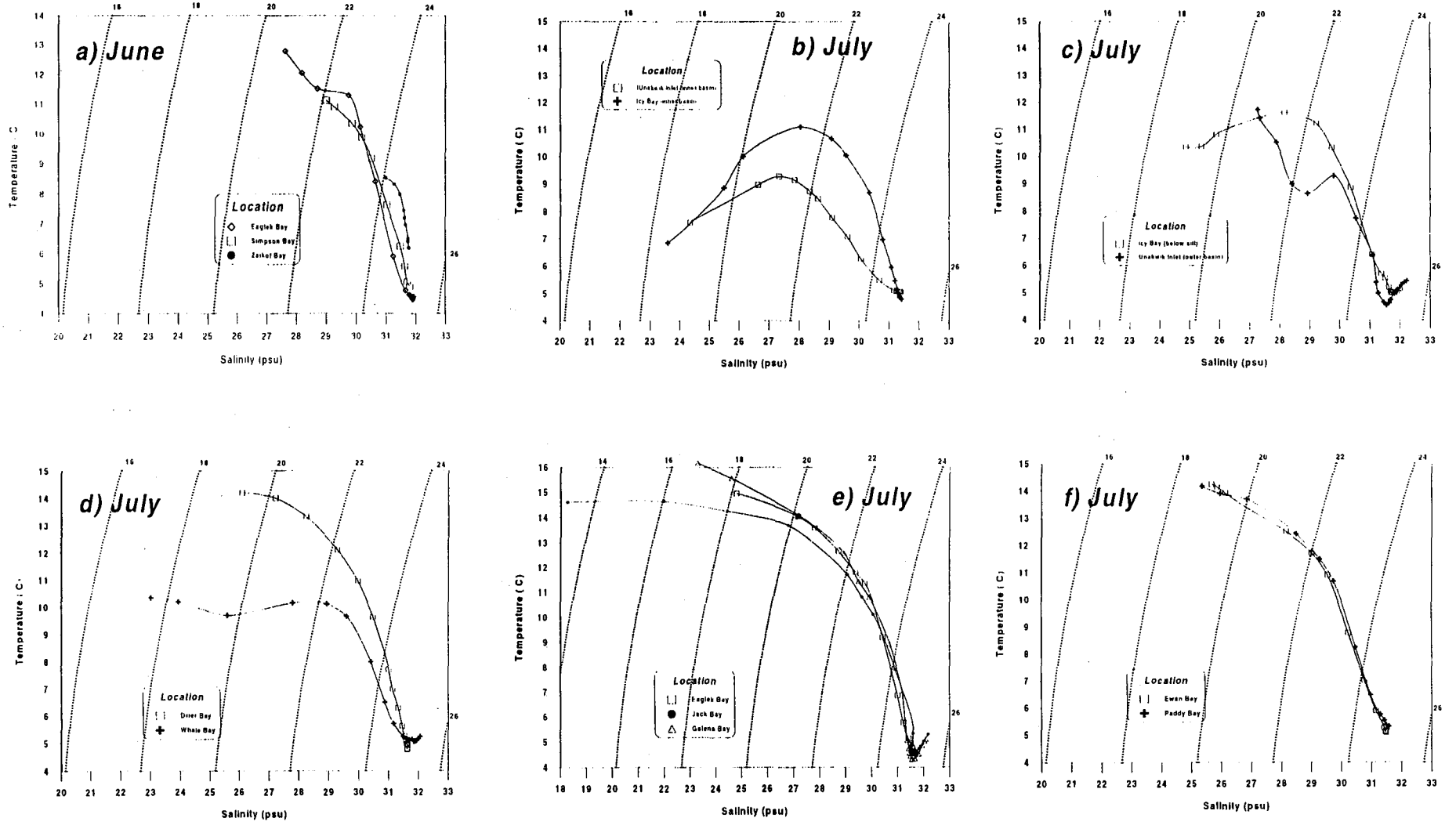
a) June
Location
Eagle Bay
Simpson Bay
Zaikof Bay
Temperature ( C)
Salinity (psu)
b) July
Location
Temperature ( C)
Salinity (psu)
c) July
Location
Icy Bay (below sill)
Temperature ( C)
Salinity (psu)
d) July
Location
Diner Bay
Whale Bay
Temperature ( C)
Salinity (psu)
e) July
Location
Eagle Bay
Jack Bay
Galena Bay
Temperature ( C)
Salinity (psu)
f) July
Location
Ewan Bay
Paddy Bay
Temperature ( C)
Salinity (psu)

**Figure 10.**

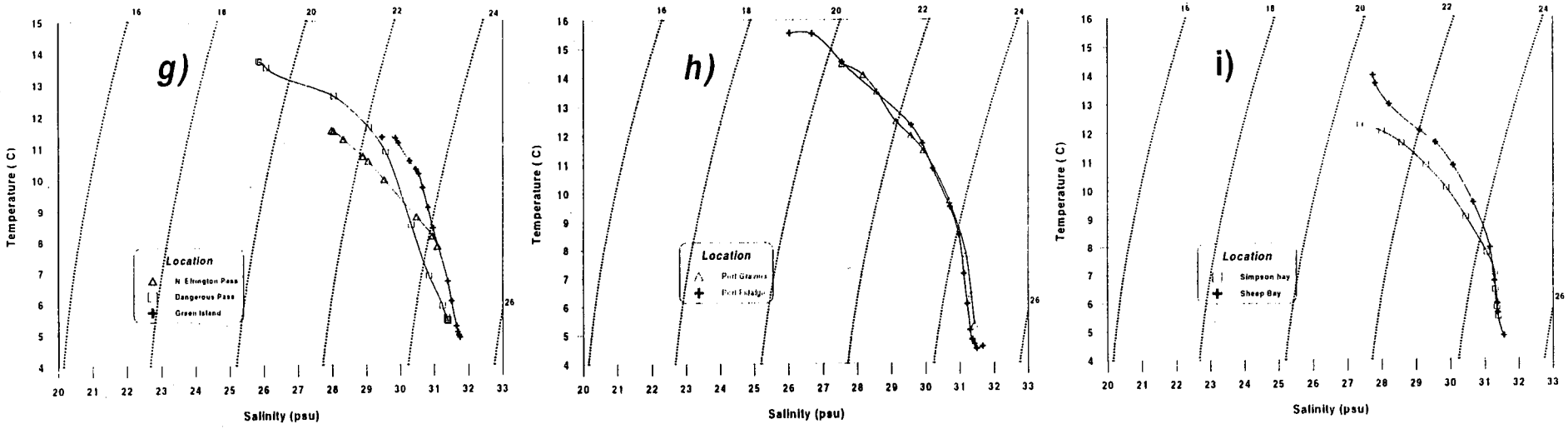


**Figure 10 (Continued).**

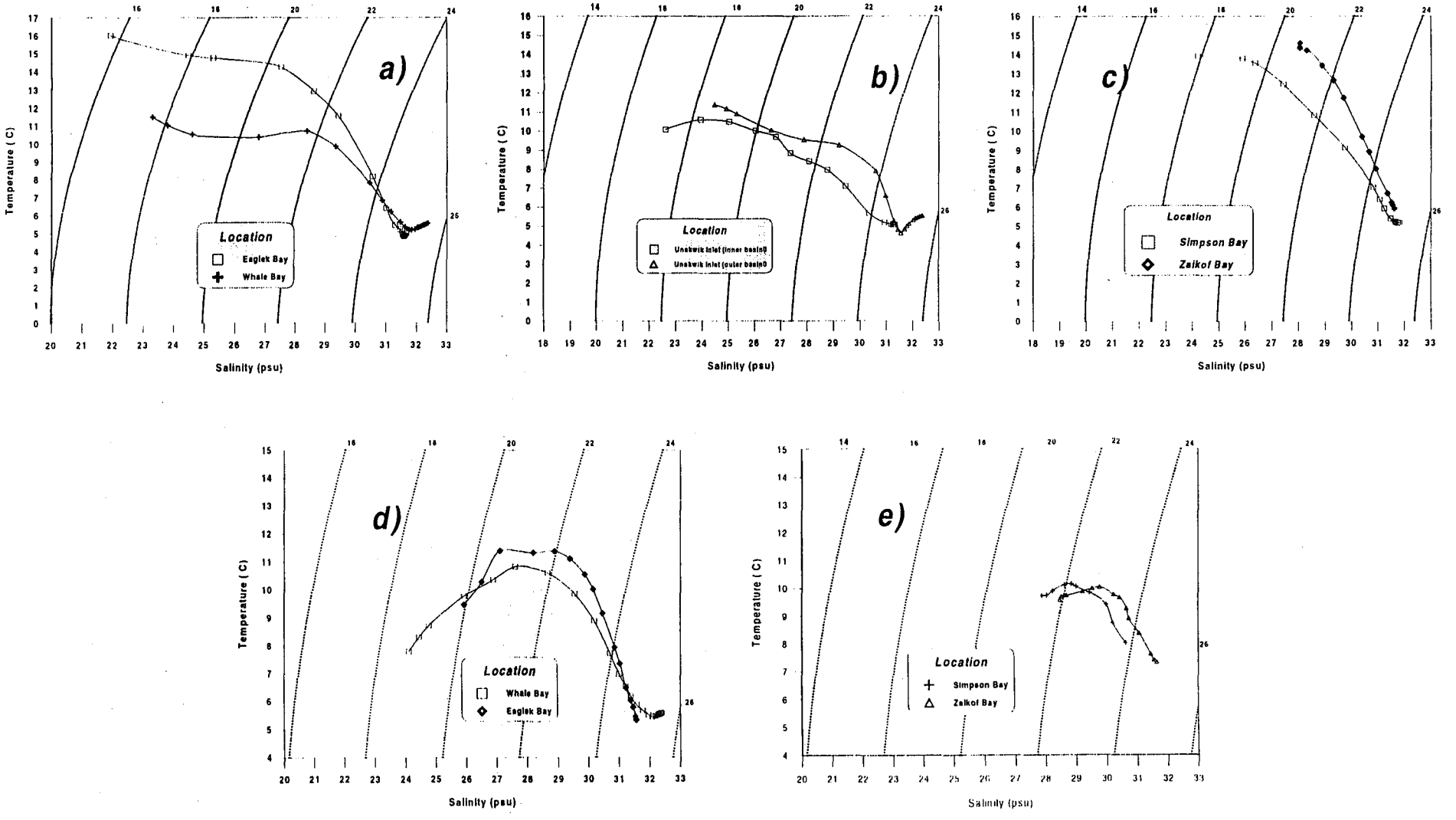
a)
Temperature ( C)
Salinity (psu)
Location
Eaglek Bay
Whale Bay
b)
Temperature ( C)
Salinity (psu)
Location
Unakwik Inlet (inner basin)
Unakwik Inlet (outer basin)
c)
Temperature ( C)
Salinity (psu)
Location
Simpson Bay
Zaikof Bay
d)
Temperature ( C)
Salinity (psu)
Location
Whale Bay
Eaglek Bay
e)
Temperature ( C)
Salinity (psu)
Location
Simpson Bay
Zaikof Bay

**Figure 11.**

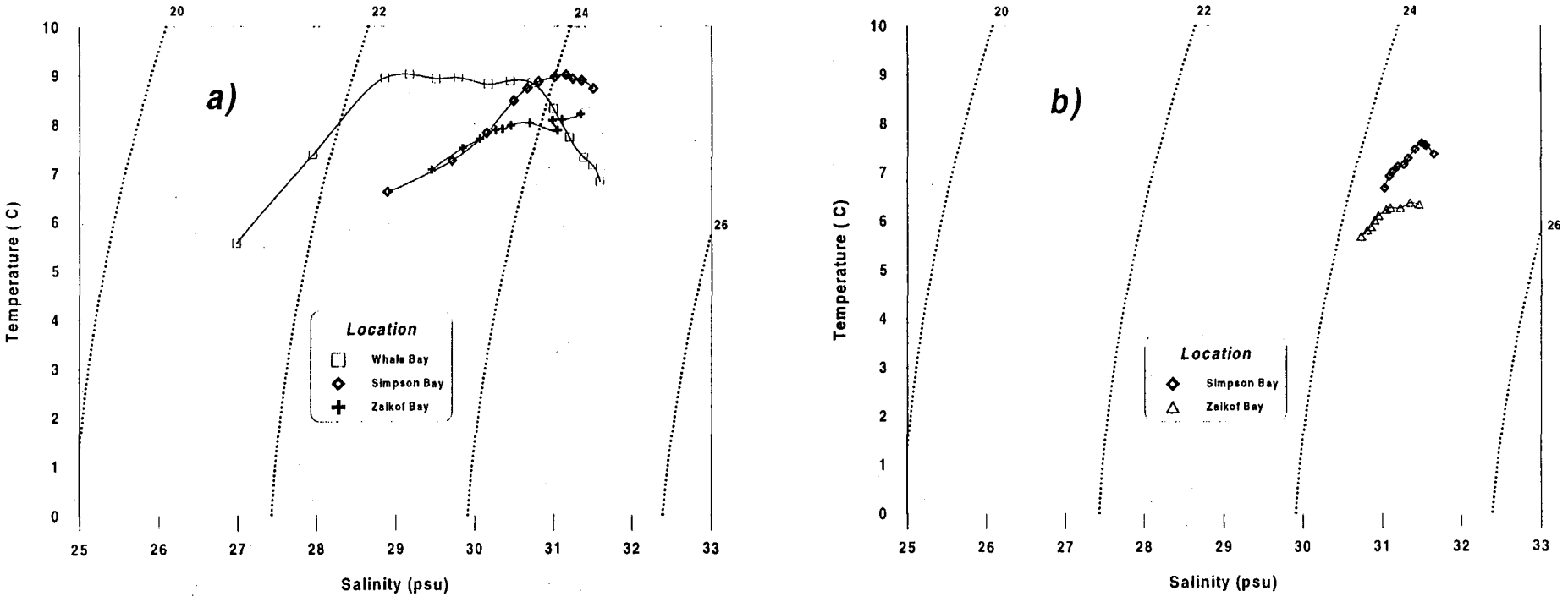
a)
b)
Temperature ( C)
Salinity (psu)
Location
Whale Bay
Simpson Bay
Zaikof Bay
20
22
24
26

**Figure 12.**

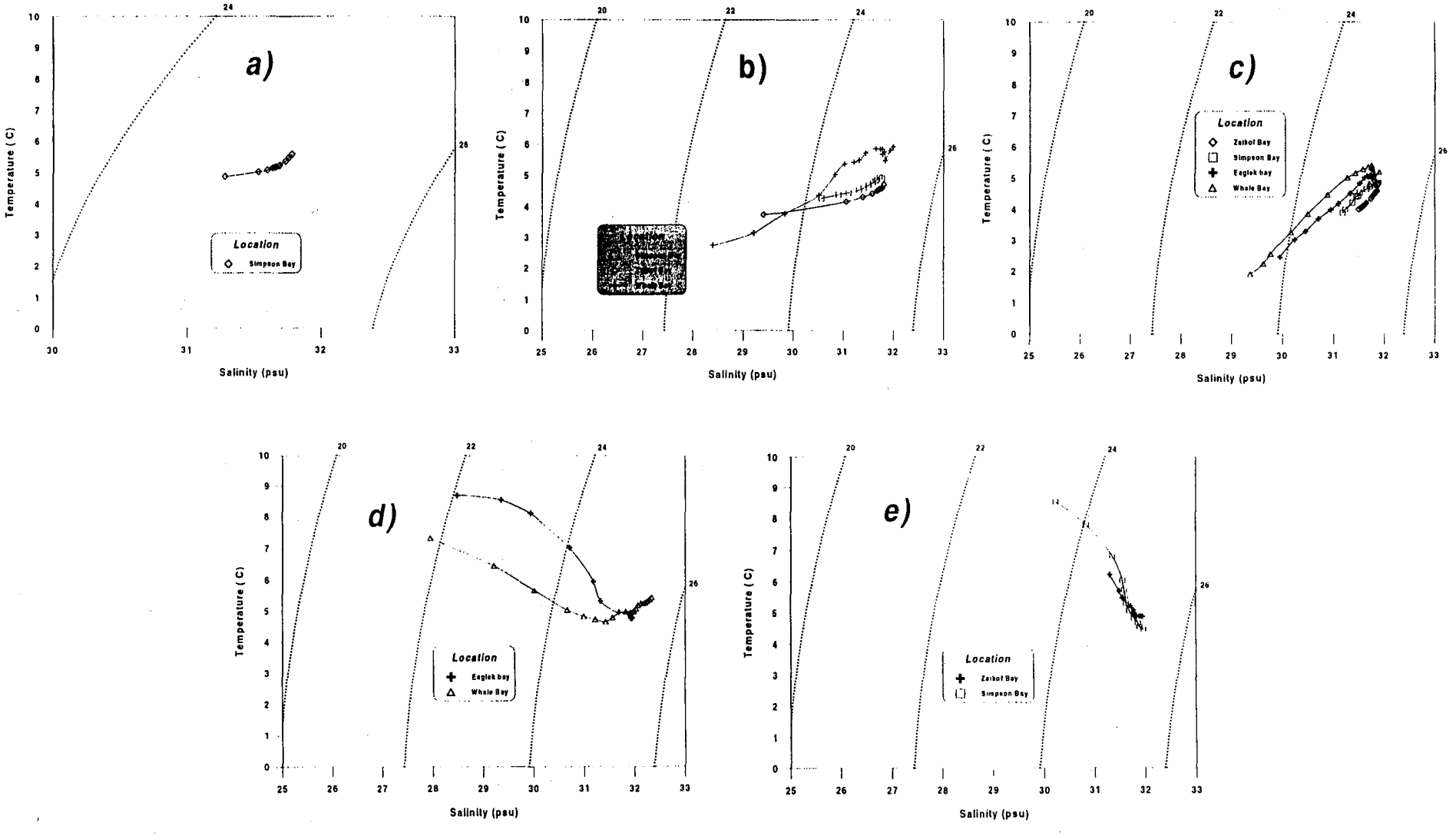
a)
b)
c)
d)
e)
Temperature ( C)
Salinity (psu)
Location
Simpson Bay
Zelkof Bay
Eaglek bay
Whale Bay

**Figure 13.**

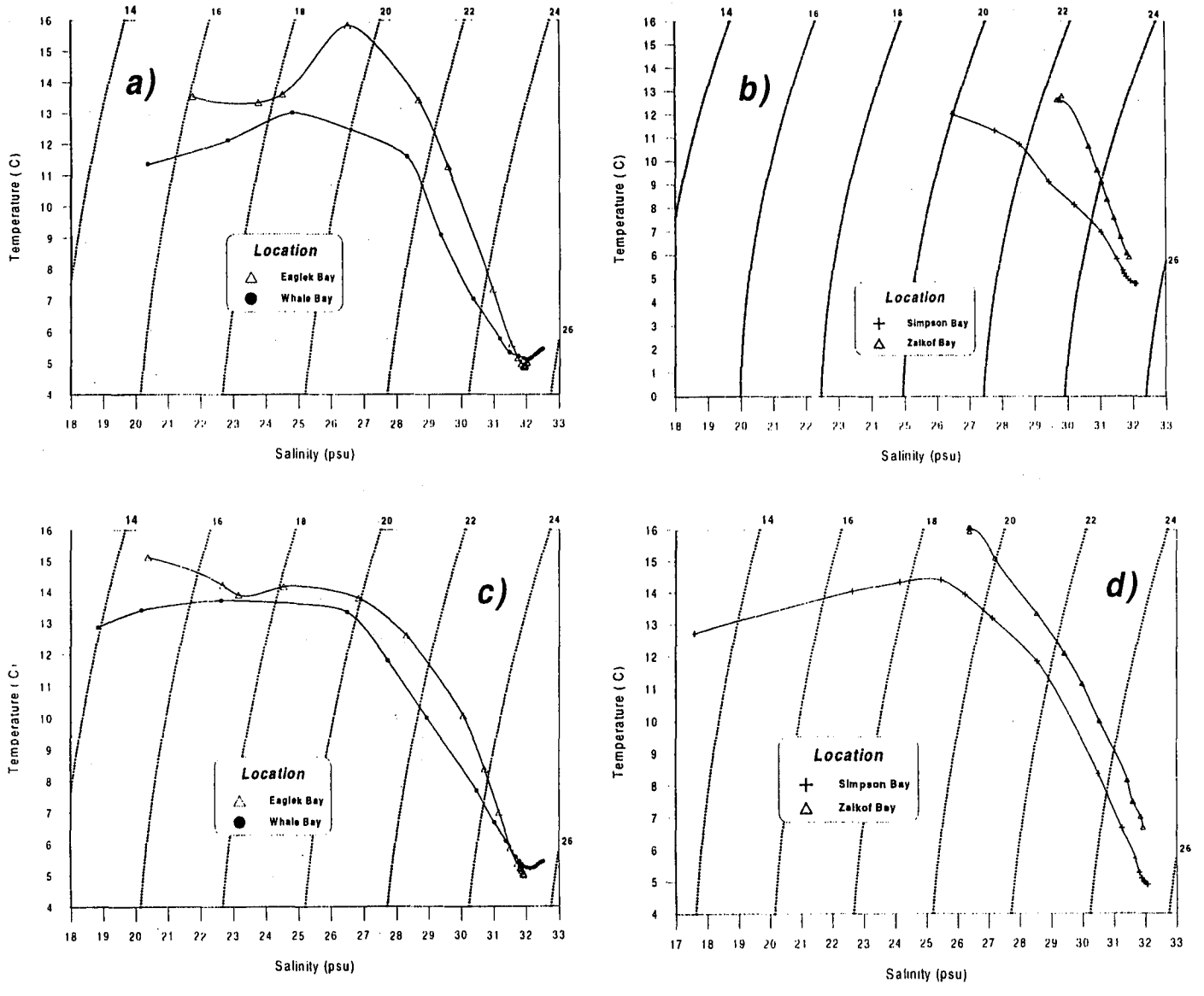
a)
b)
c)
d)
Temperature ( C)
Salinity (psu)
Location
Eaglek Bay
Whale Bay
Simpson Bay
Zaikof Bay
14
16
18
20
22
24
26

***Figure 14.***

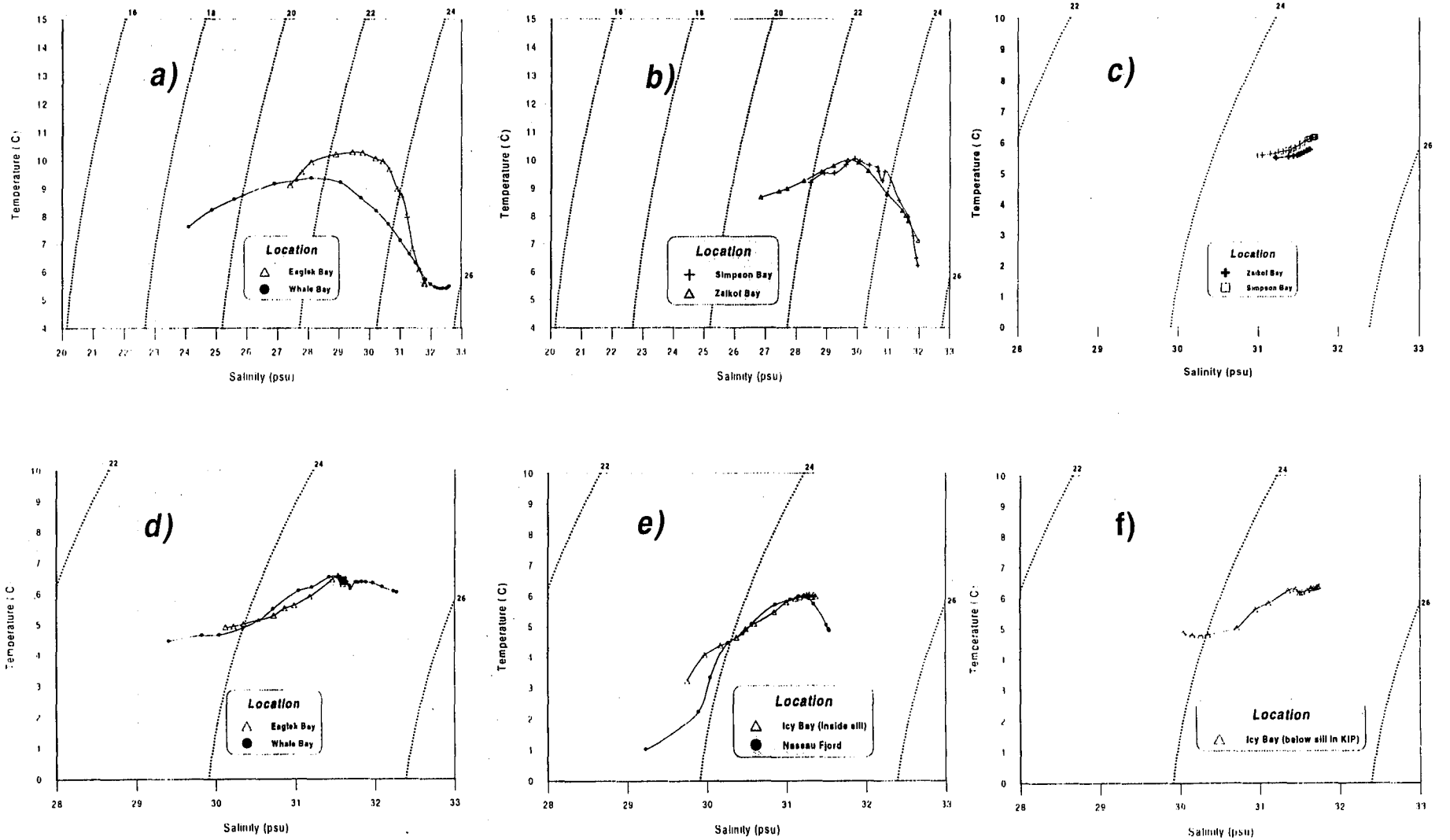
a)
Location
Eaglek Bay
Whale Bay
Temperature ( C)
Salinity (psu)
b)
Location
Simpson Bay
Zaikof Bay
Temperature ( C)
Salinity (psu)
c)
Location
Zaikof Bay
Simpson Bay
Temperature ( C)
Salinity (psu)
d)
Location
Eaglek Bay
Whale Bay
Temperature ( C)
Salinity (psu)
e)
Location
Icy Bay (inside sill)
Naseau Fjord
Temperature ( C)
Salinity (psu)
f)
Location
Icy Bay (below sill in KIP)
Temperature ( C)
Salinity (psu)

**Figure 15.**

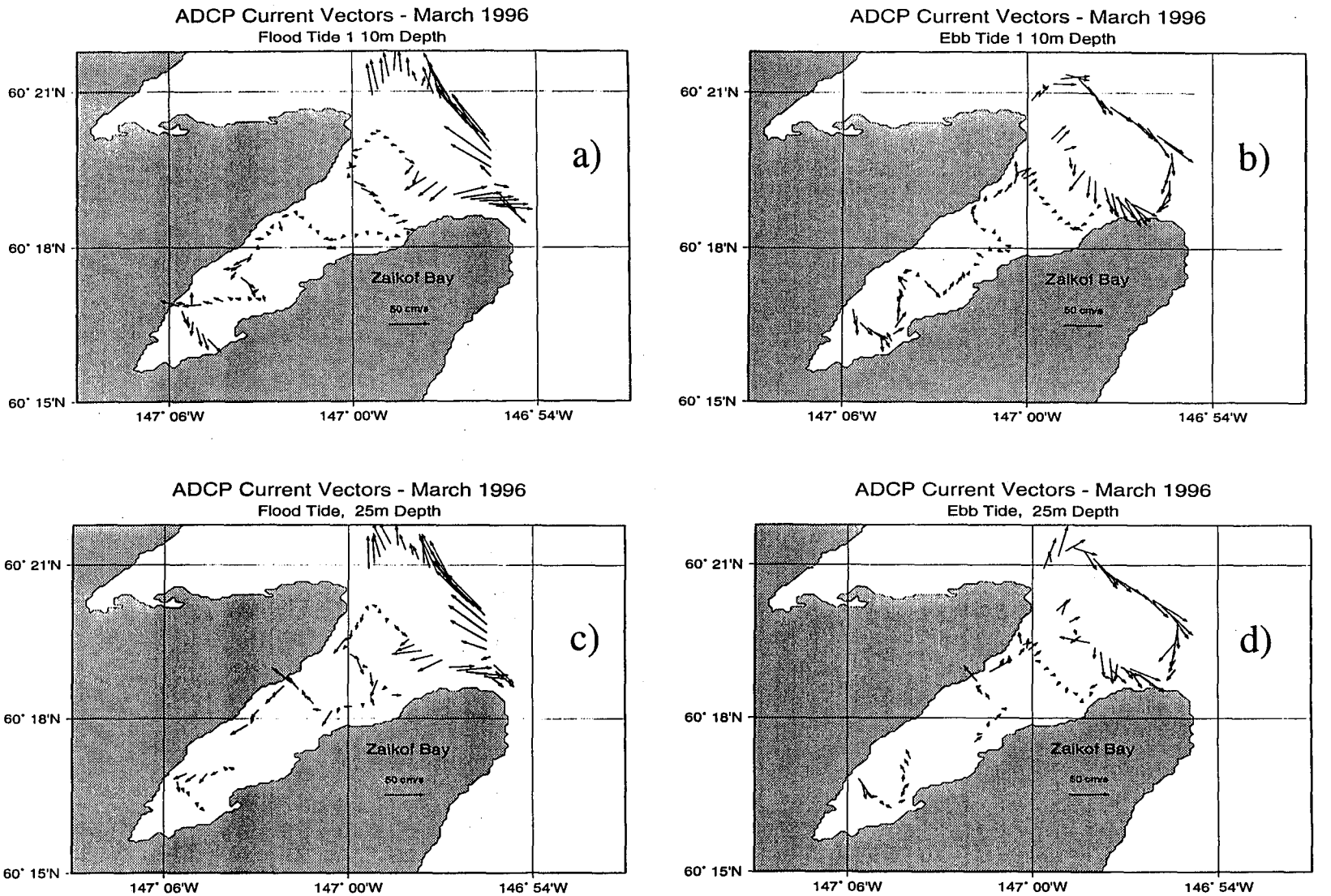


Figure 16. Tidal currents for Zaikof Bay, March 1996 averaged over 8 m. depth bins centered at 10 and 25 m. a) Flood tide, 10 m., b) ebb tide, 10 m., c) flood tide, 25 m., and d) ebb tide, 25 m.

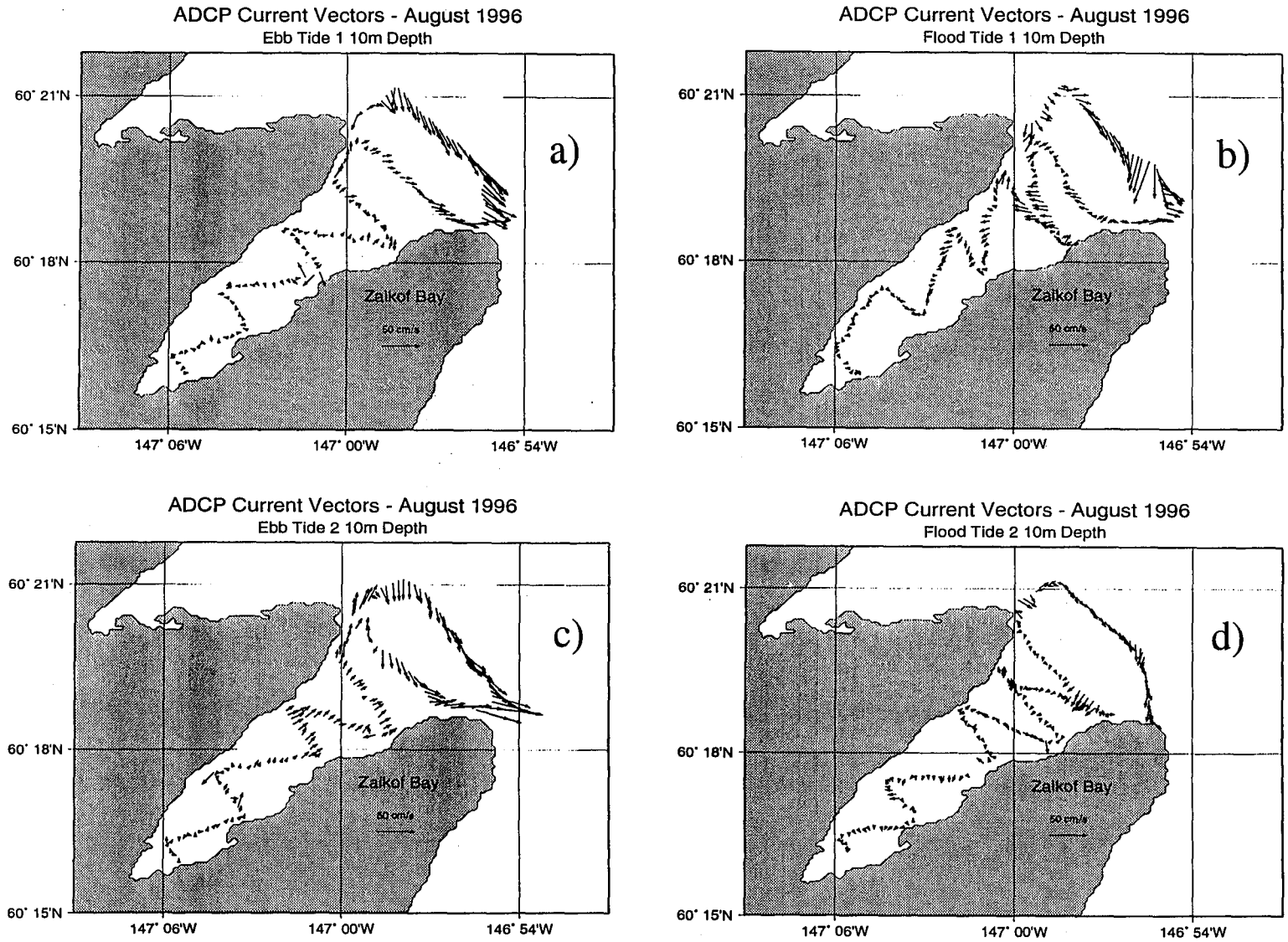


Figure 17. Tidal currents for Zaikof Bay, August 1996 averaged over 8 m. depth bins centered at 10 m. Complete semidiurnal cycle shown for first ebb and flood tides (a and b), and the second ebb and flood tides (c and d).

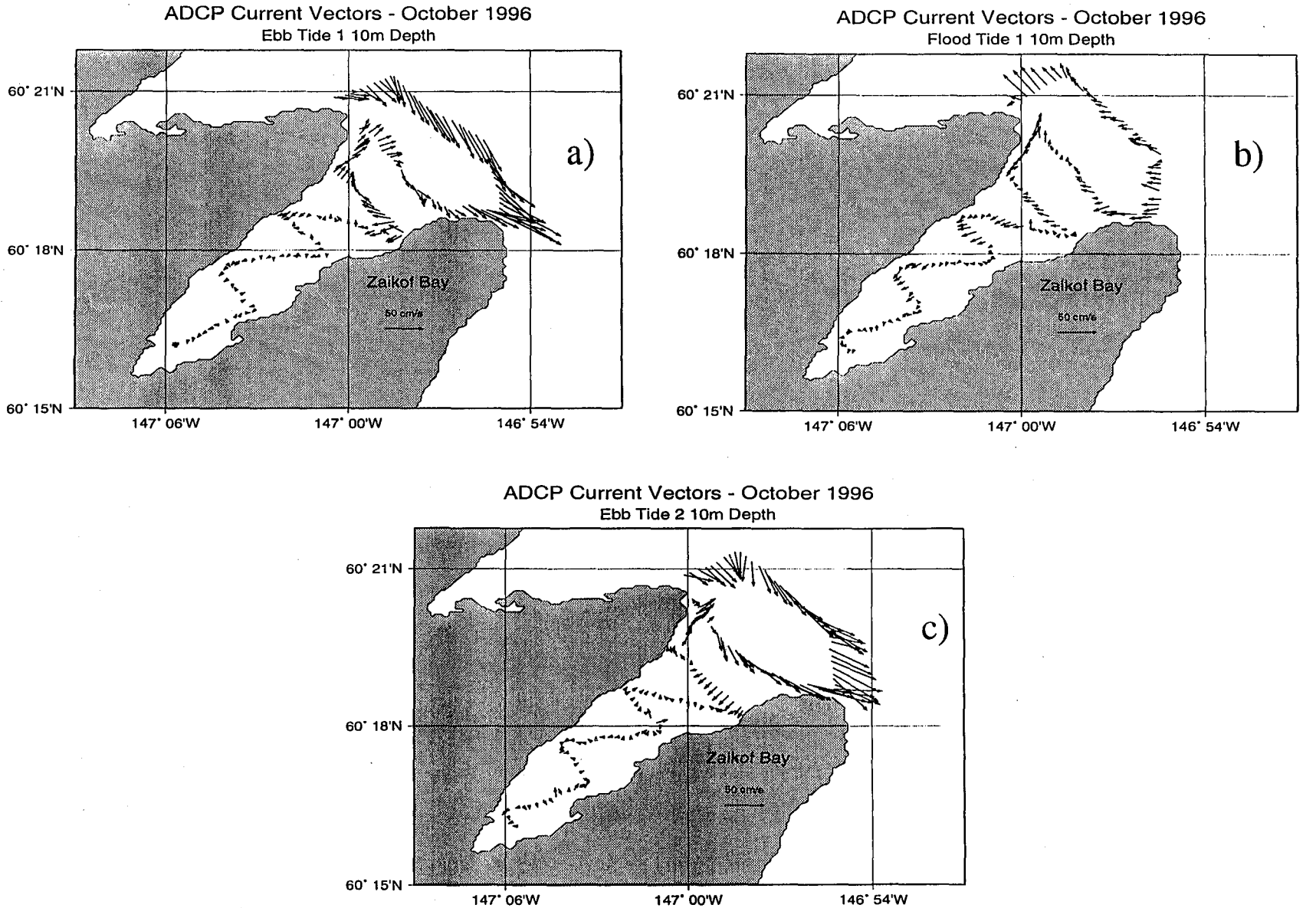


Figure 18. Tidal currents for Zaikof Bay, October 1996 averaged over 8 m. depth bins centered at 10 m. First part of the semidurnal cycle shown for ebb and flood (a and b), and second ebb tide (c).

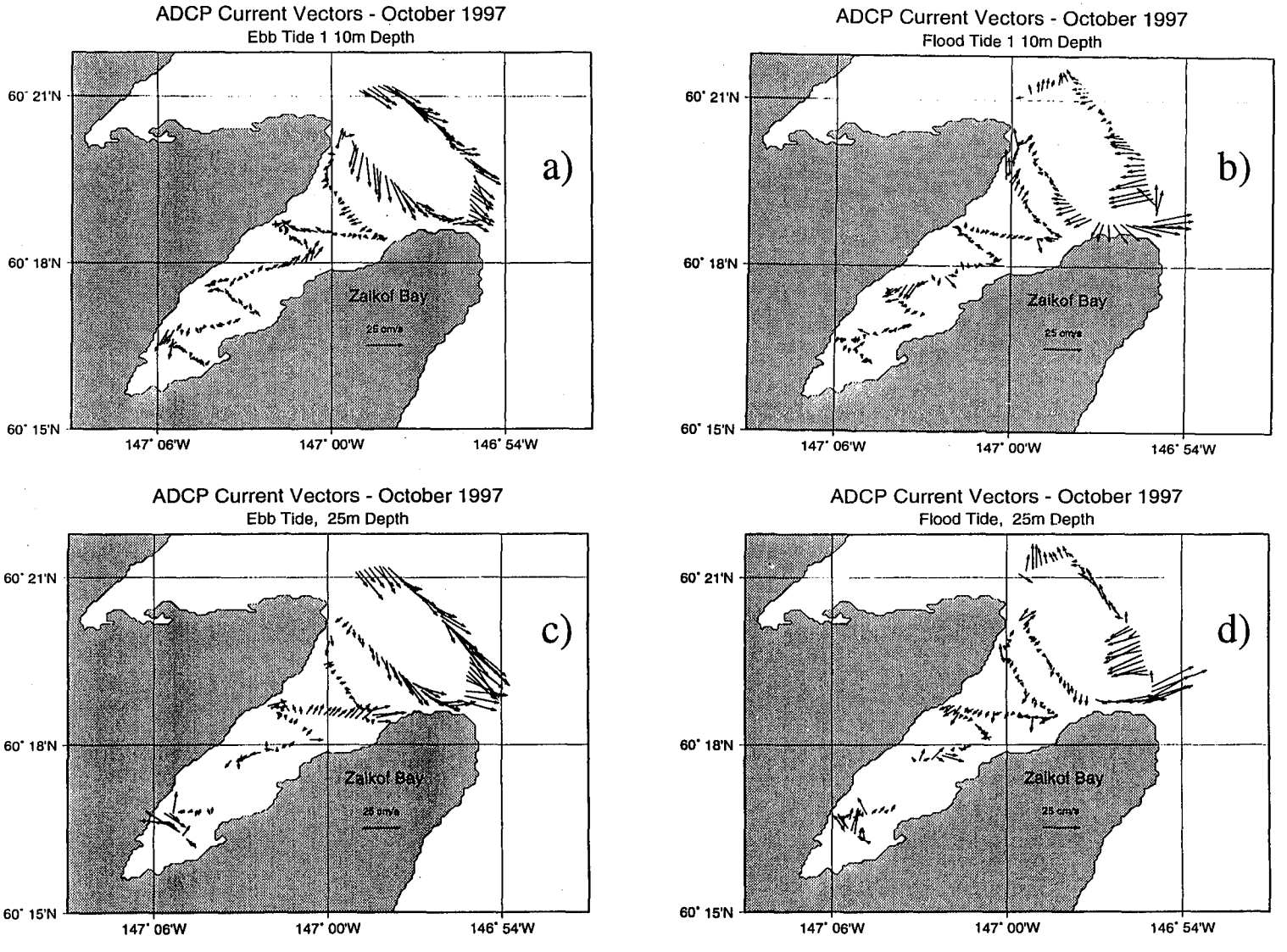


Figure 19. Tidal currents for Zaikof Bay, October 1997 averaged over 8 m. depth bins centered at 10 m. Second portion of the semidurnal cycle shown for ebb and flood currents, at 10 m. (a and b), and at 25 m. (c and d).

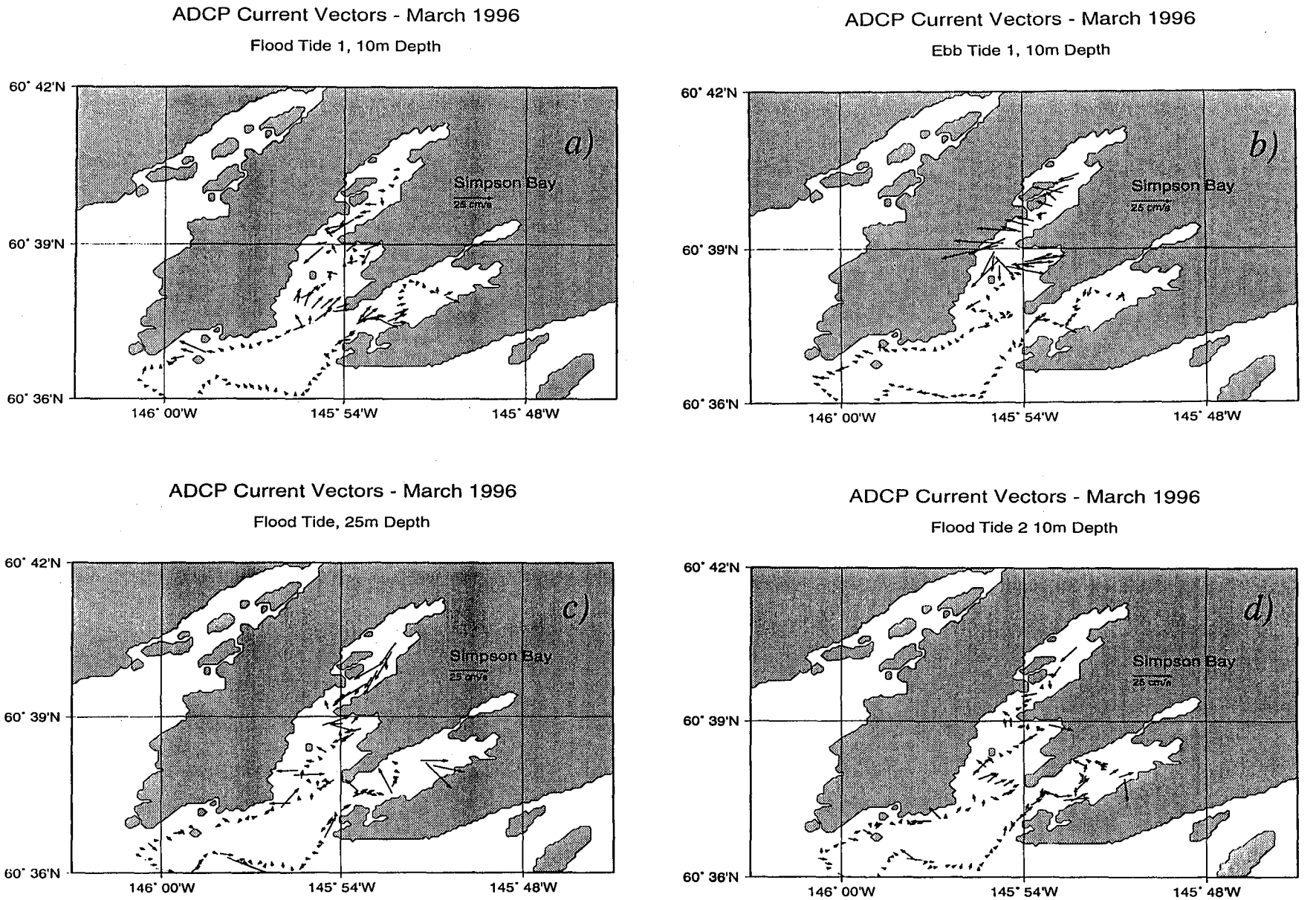


Figure 20. Tidal currents for Simpson Bay, March 1996 averaged over 8 m. depth bins centered at 10 and 25 m. First cycle of the semidiurnal period shown for 10 m curents in (a) and (b), first cycle, flood currents at 25 m. in (c), and second cycle flood curents shown in (d).

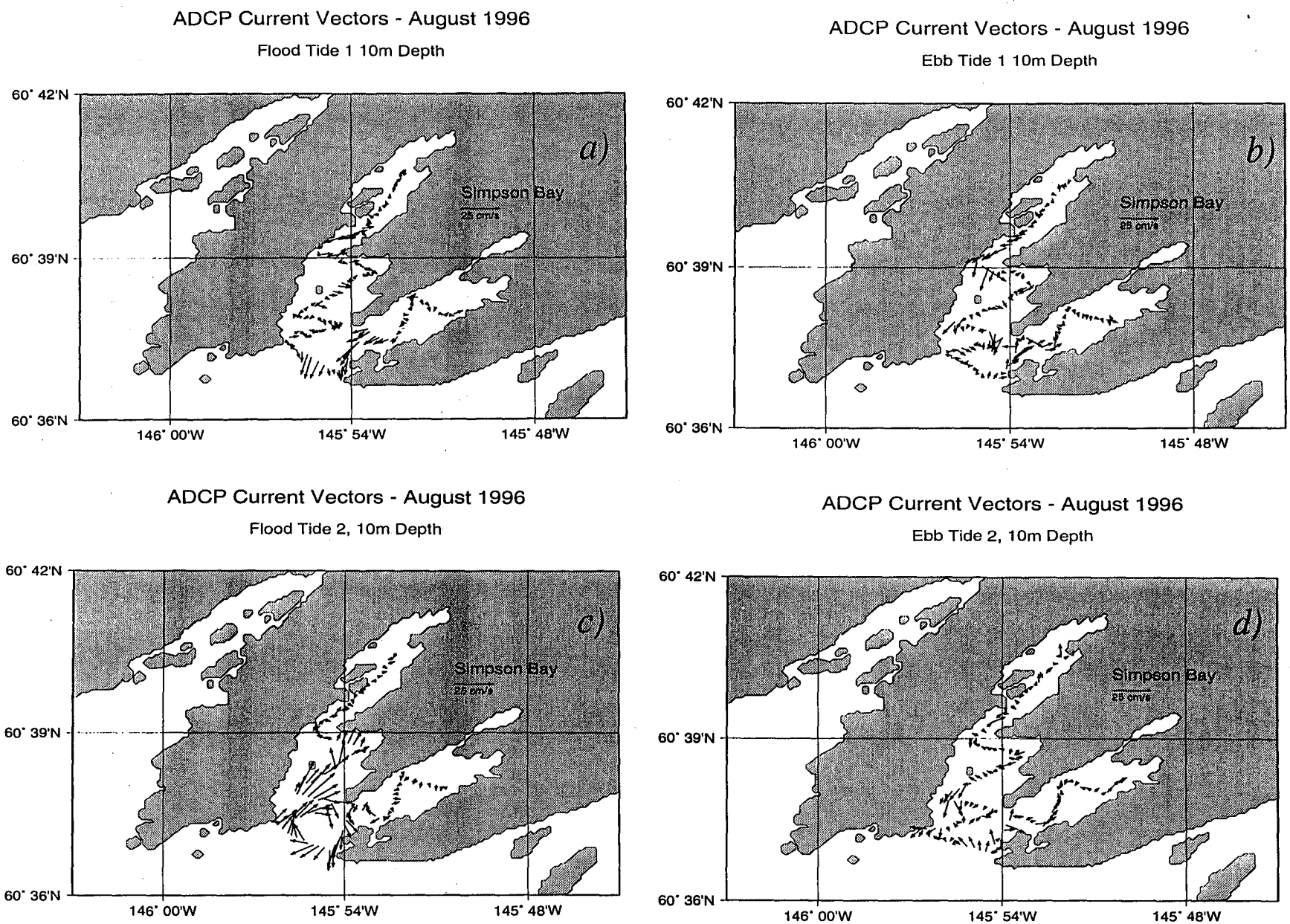


Figure 21. Tidal currents for Simpson Bay, August 1996 averaged over 8 m. depth bins centered at 10 m. Full semidiurnal period shown with first cycle flood and ebb in (a) and (b), and second cycle flood and ebb in (c) and (d) respectively.

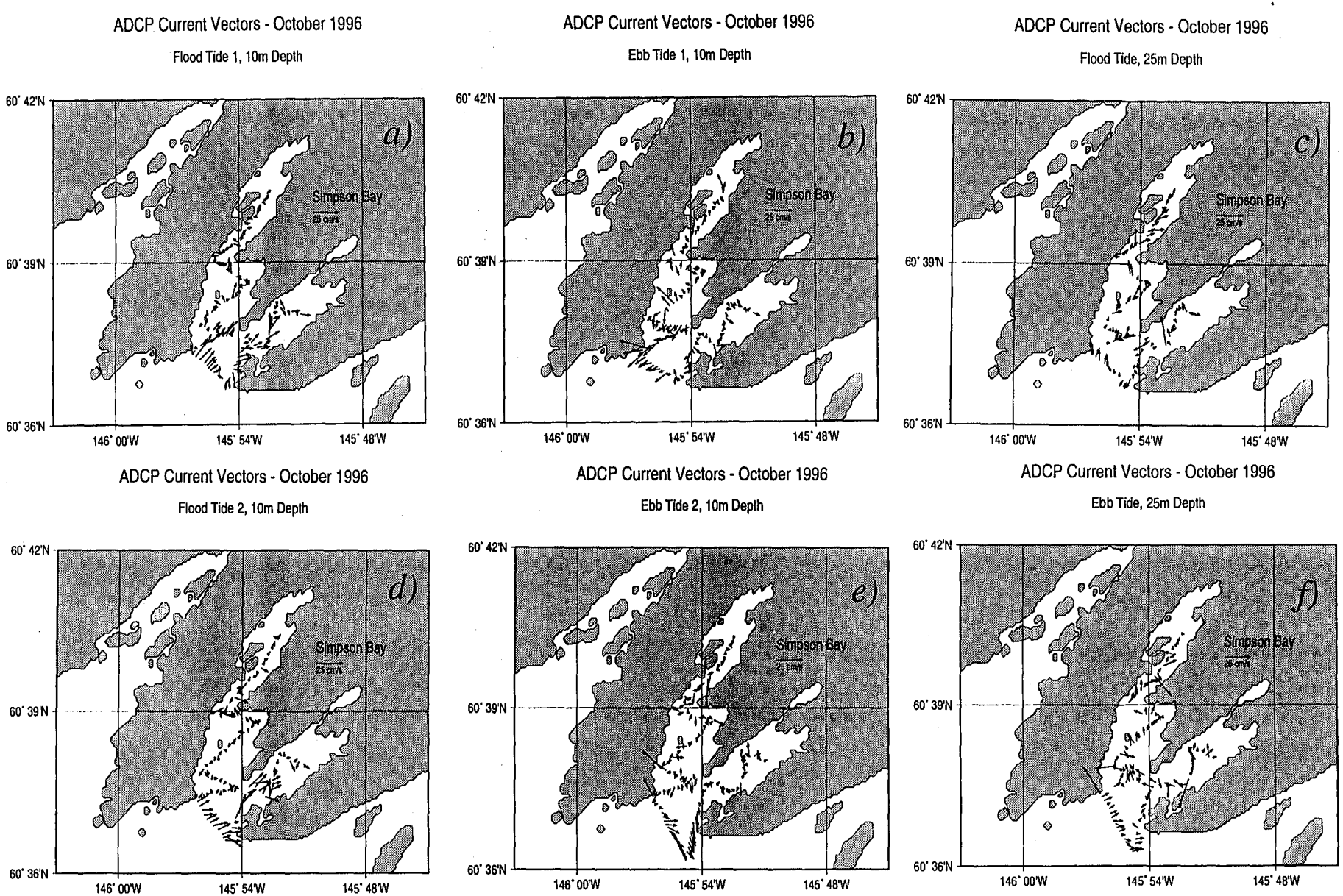


Figure 22. Tidal curents for Simpson Bsy, October 1996 averaged over 8 m. depth bins centered at 10 and 25 m. Full semidiurnal period shown with first cycle flood and ebb currents in (a) and (b), 25 m. currents for flood tide 1 in (c), second cycle in (d) and (e), and 25 m. currents for ebb tide 2 in (f).

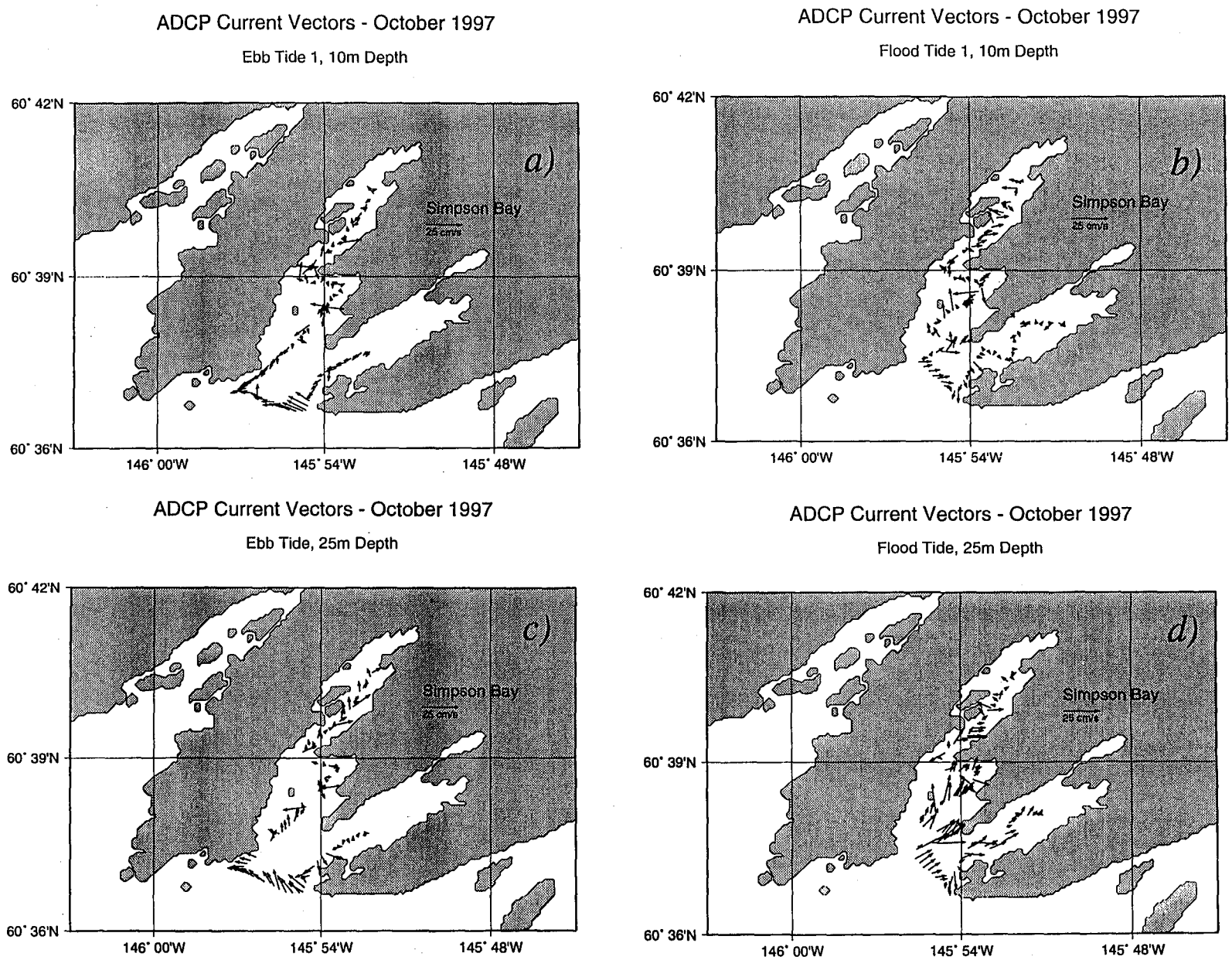


Figure 23. Tidal currents for Simpson Bay, October 1997 averaged over 8 m. depth bins centered at 10 and 25 m. Second cycle of the semidiurnal period is shown with ebb and flood currents at 10 m. in (a) and (b),and 25 m. currents in (c) and (d).

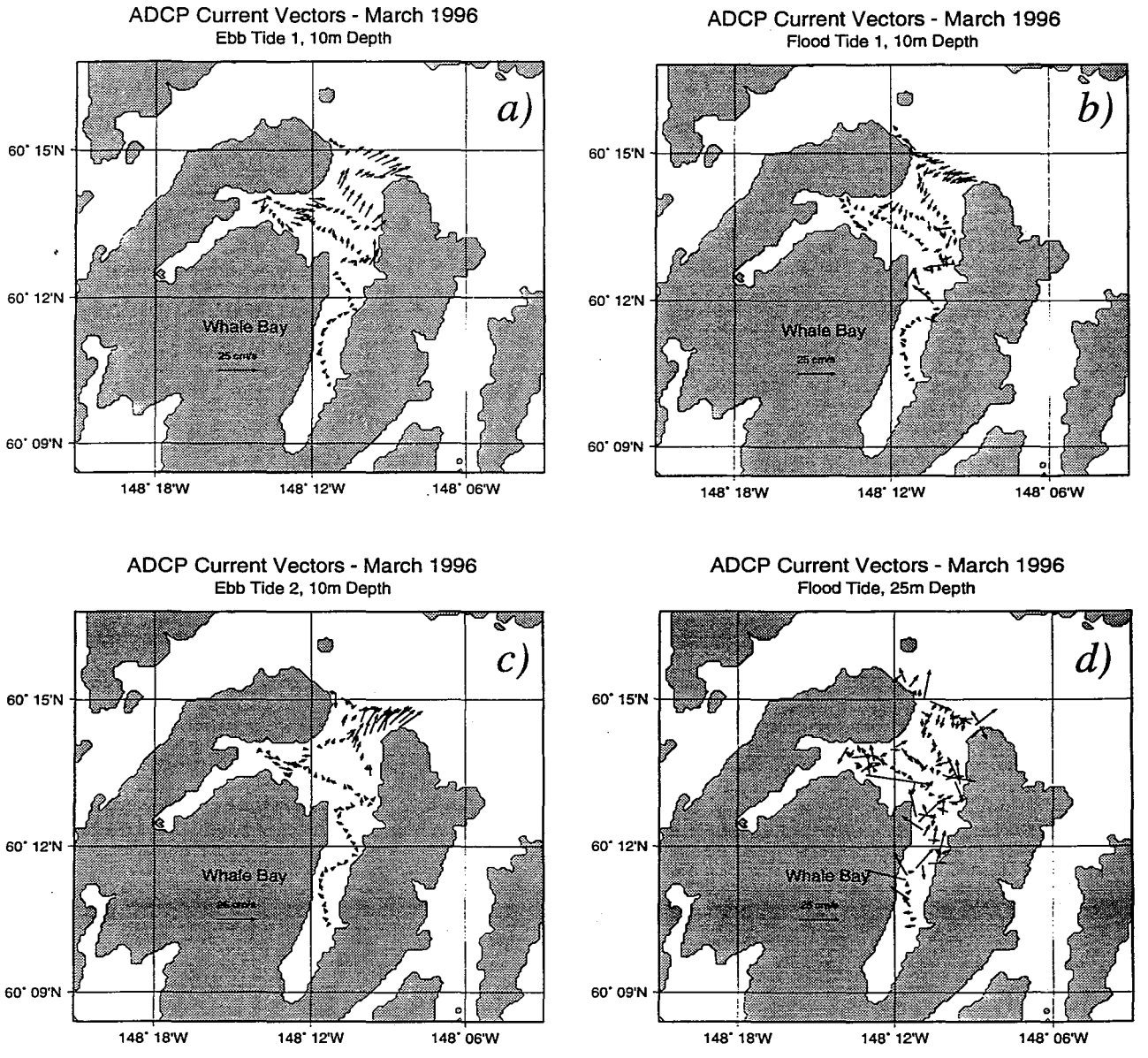


Figure 24. Tidal currents for Whale Bay, March 1996 averaged over 8 m. depth bins centered at 10 m. Currents for the first cycle of the semidiurnal period is shown for the ebb and flood tides (a and b), second ebb tide (c), and first flood at 25 m. depth (d).

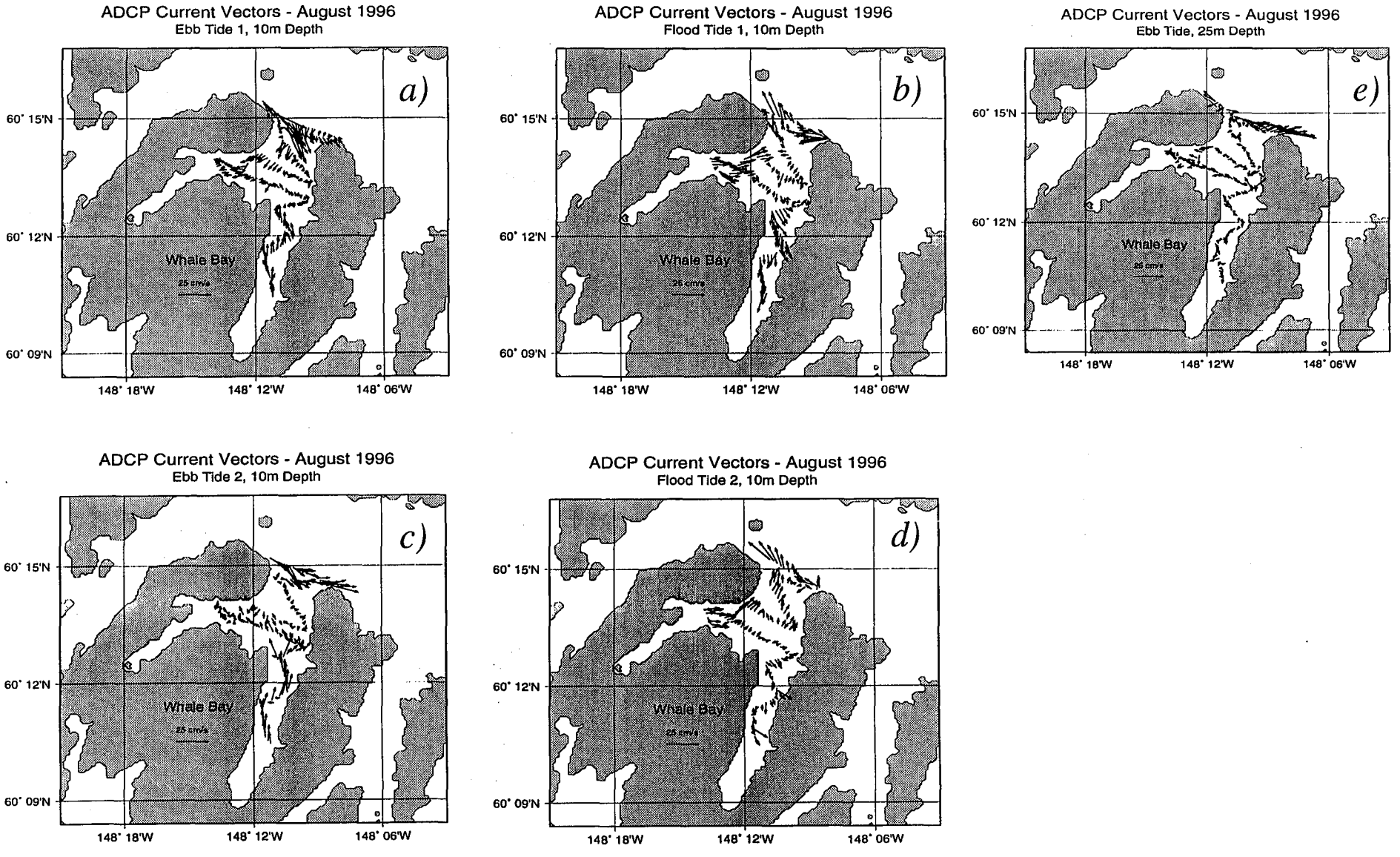


Figure 25. Tidal currents for Whale Bay, August 1996 averaged over 8 m. depth bins centered at 10 m. and 25 m. depth. First cycle of the semidiurnal period is shown for ebb and flood tides in (a) and (b); second cycle shown in (c) and (d); and 25 m. currents for the first ebb tide shown in (e).

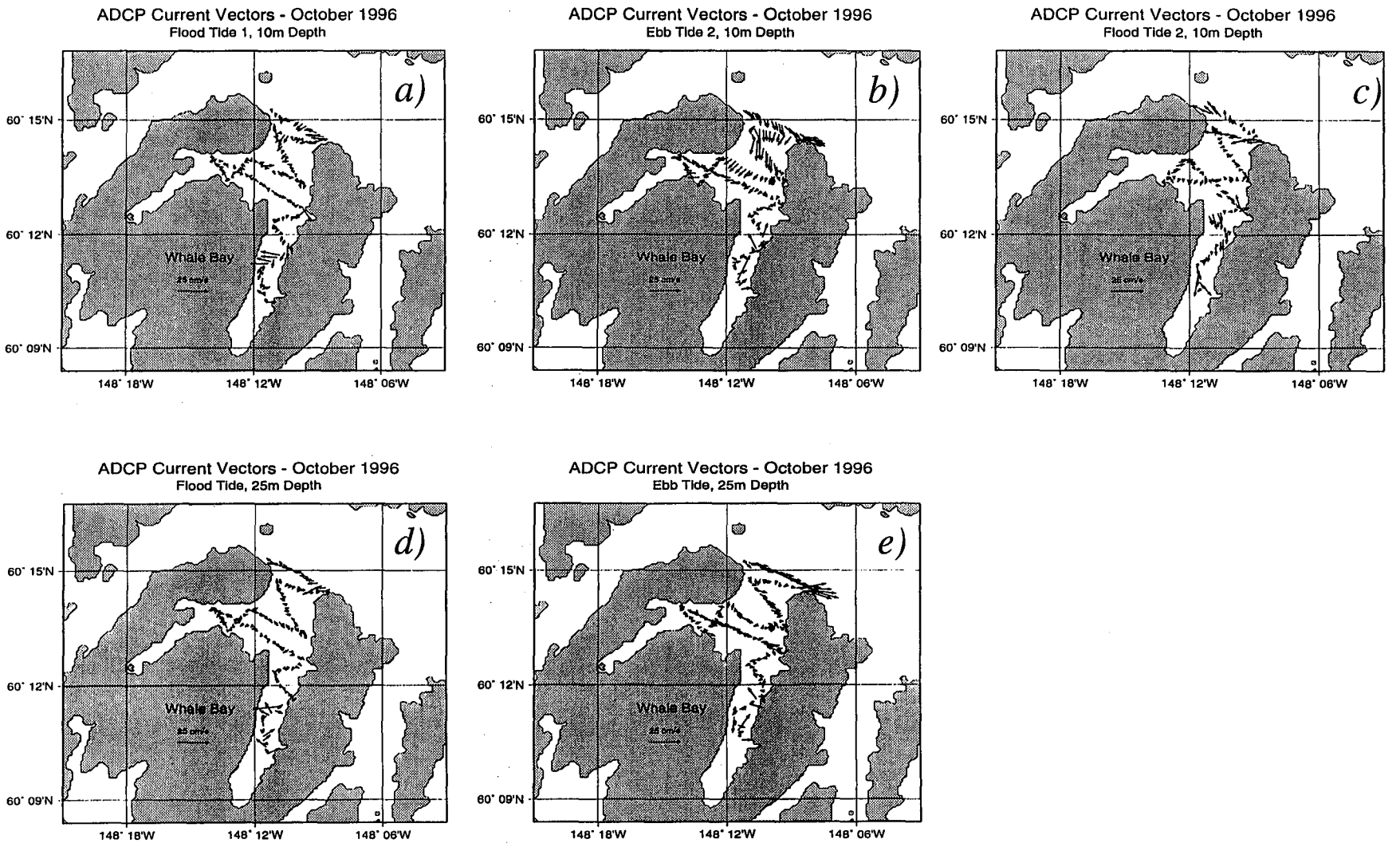


Figure 26. Tidal curents for Whale Bay, October 1996 averaged over 8 m. depth bins centered at 10 and 25 m. First cycle flood tide of the semidiurnal period is shown in (a), second cycle for ebb and flood phases in (b) and (c), and currents centered at 25 m. depth are shown for first cycle flood tide in (d) and second cycle ebb tide in (e).

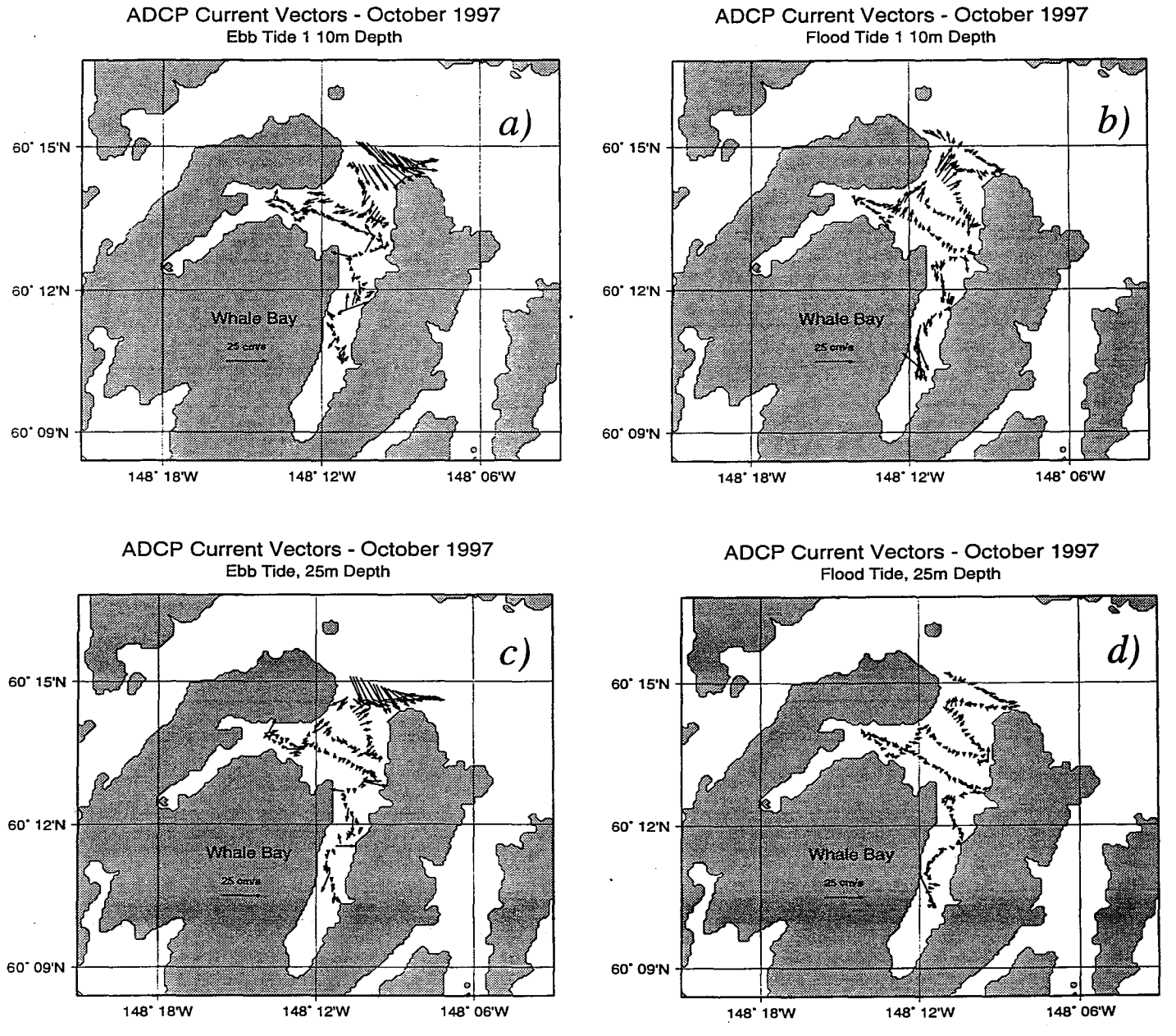


Figure 27. Tidal currents for Whale Bay, October 1997 averaged over 8 m. depth bins centered at 10 and 25 m. Second cycle of the semidiurnal period is shown for the ebb (a) and flood (b) currents at 10 m. and ebb (c) and flood (d) currents at 25 m.

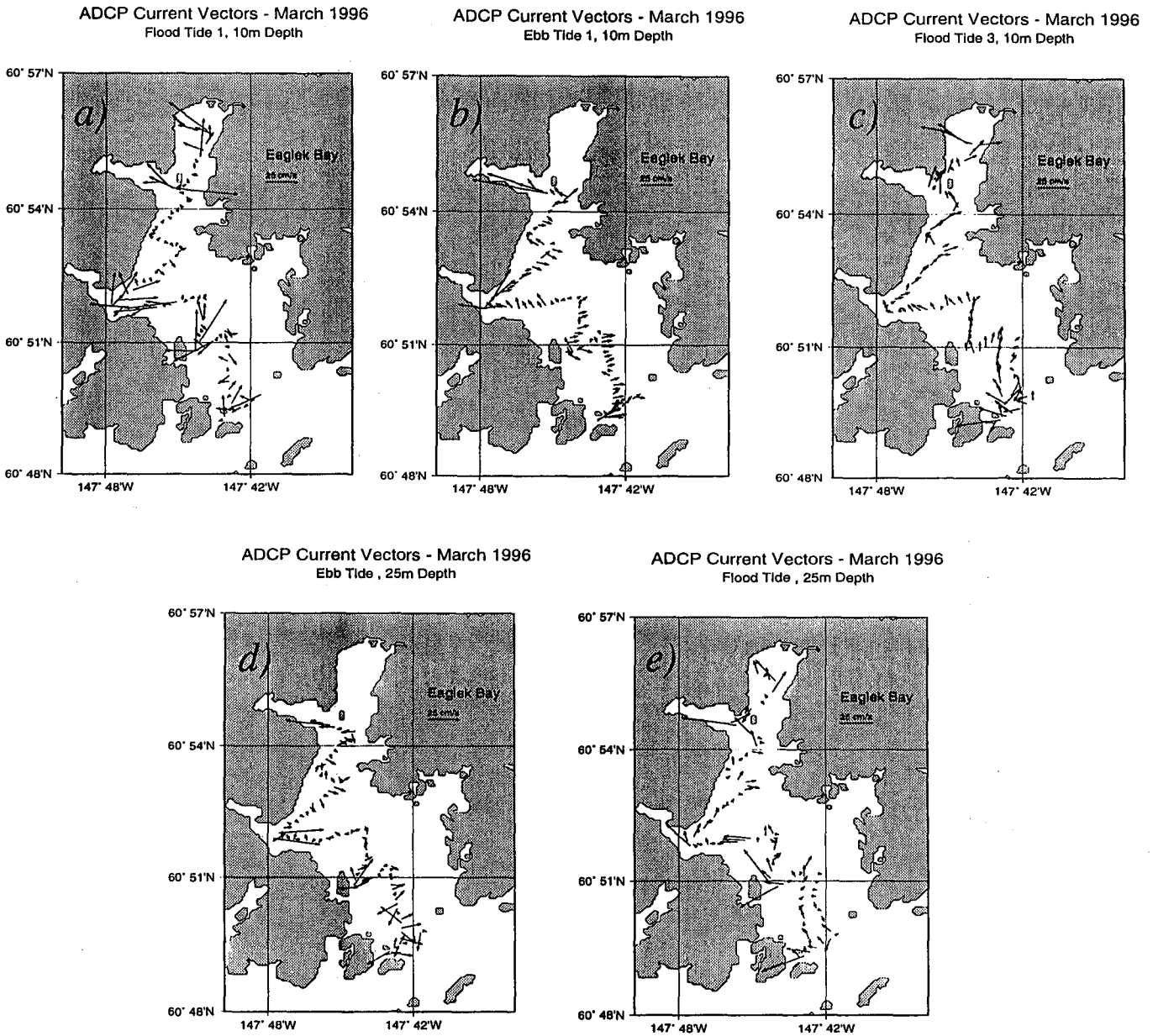


Figure 28. Tidal currents for Eaglek Bay, March 1996 averaged over 8 m. depth bins centered at 10 and 25 m. First cycle of the semi diurnal period shown in (a) and (b), first flood tide of the second semidiurnal period in (c), and currents at 25 m. for first ebb tide(d) and third flood tide (e).

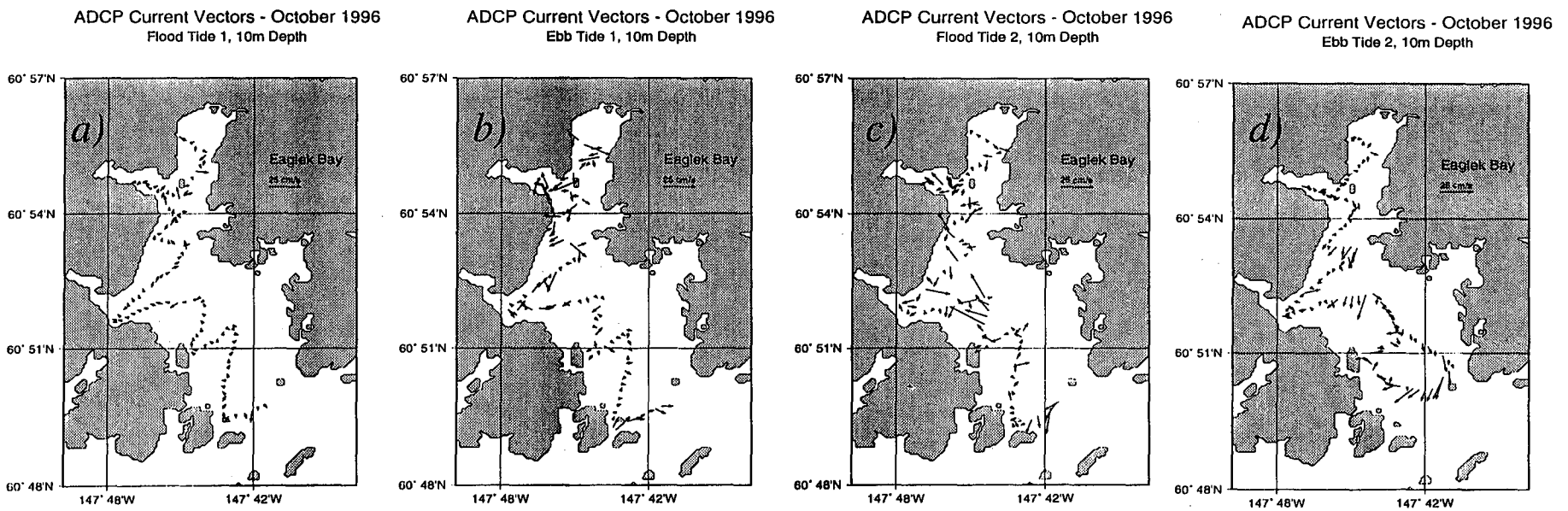


Figure 29. Tidal currents for Eaglek Bay, October 1996 averaged over 8 m. depth bins centered at 10 m. Full semidiurnal tidal period shown; first flood and ebb tides in (a) and (b), and second flood and ebb tides in (c) and (d).

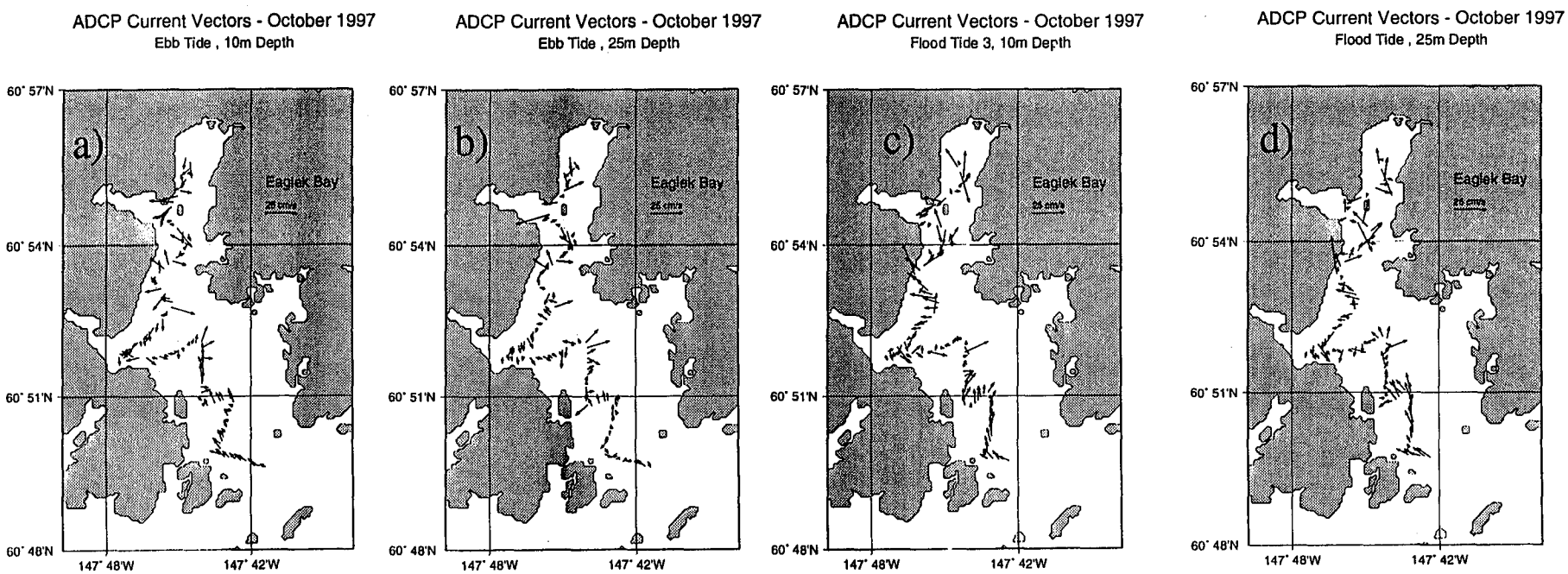


Figure 30 Tidal currents for Eaglek Bay, October 1997 averaged over 8 m. depth bins, centered at 10 and 25 m. Second cycle of the semidiurnal tidal period shown for ebb tide at 10 m, (a) and 25 m. (b), and flood tide at 10 m.. (c) and 25 m. (d).

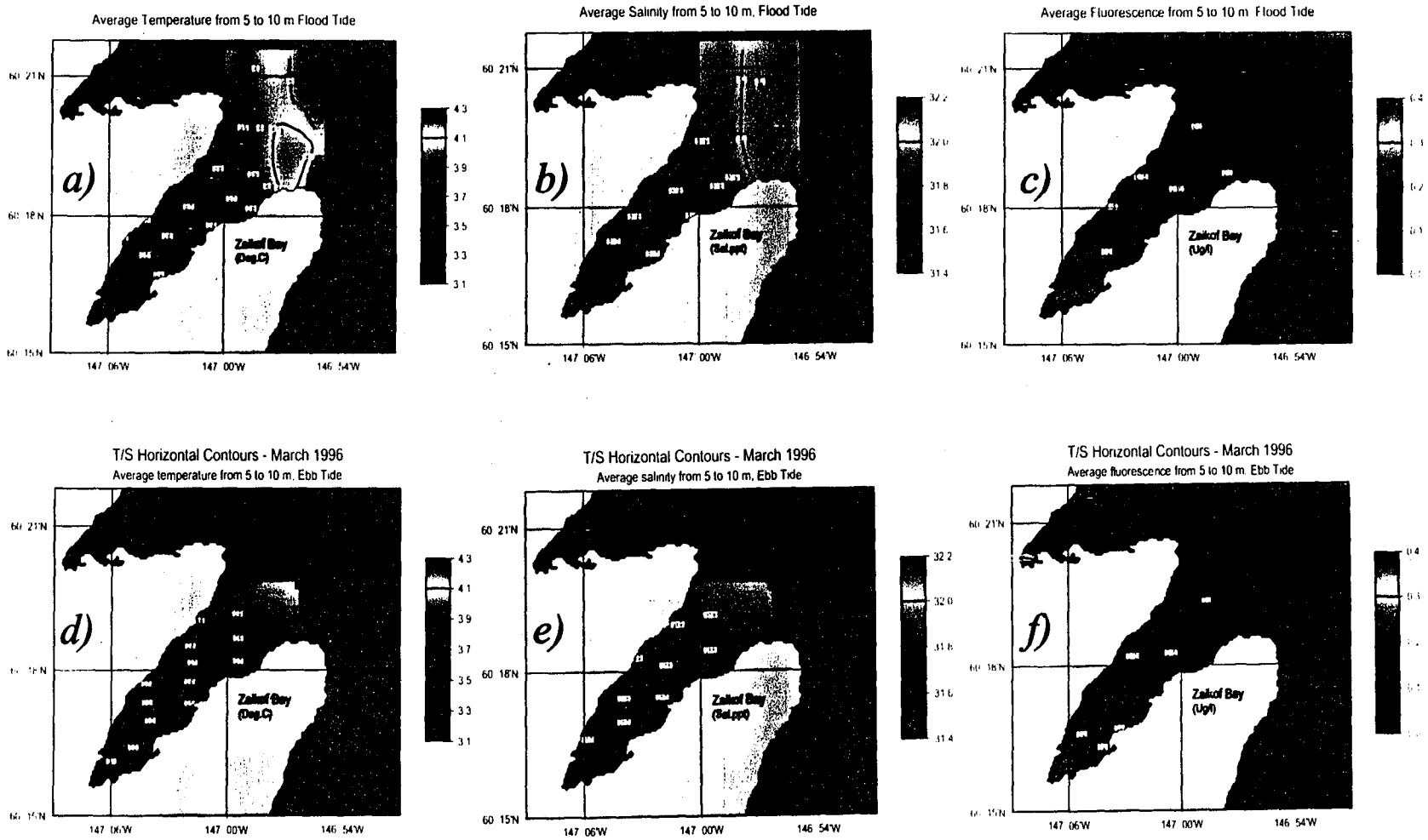
Average Temperature from 5 to 10 m Flood Tide
Average Salinity from 5 to 10 m, Flood Tide
Average Fluorescence from 5 to 10 m Flood Tide
a)
b)
c)
Zaikof Bay
(Deg.C)
(Sal,ppt)
(Ug/l)
60 21'N
60 18'N
60 15'N
147 06'W
147 00'W
146 54'W
4.3
4.1
3.9
3.7
3.5
3.3
3.1
32.2
32.0
31.8
31.6
31.4
T/S Horizontal Contours - March 1996
Average temperature from 5 to 10 m, Ebb Tide
Average salinity from 5 to 10 m, Ebb Tide
Average fluorescence from 5 to 10 m, Ebb Tide
d)
e)
f)

Figure 31.

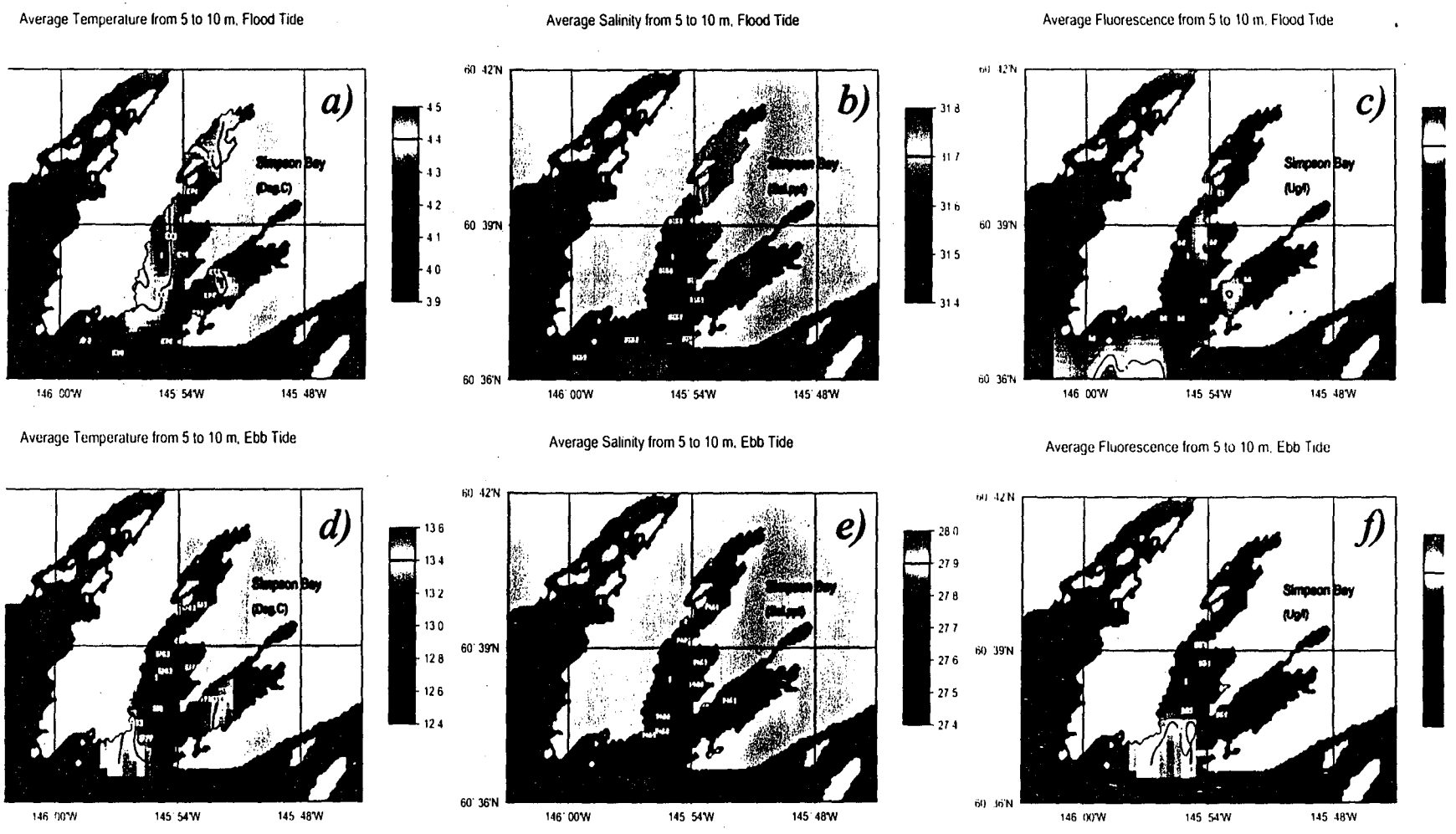
Average Temperature from 5 to 10 m, Flood Tide
Average Salinity from 5 to 10 m, Flood Tide
Average Fluorescence from 5 to 10 m, Flood Tide
a)
b)
c)
Simpson Bay
(Deg.C)
(Upl)
4.5
4.4
4.3
4.2
4.1
4.0
3.9
31.8
31.7
31.6
31.5
31.4
60 42'N
60 39'N
60 36'N
146 00'W
145 54'W
145 48'W
Average Temperature from 5 to 10 m, Ebb Tide
Average Salinity from 5 to 10 m, Ebb Tide
Average Fluorescence from 5 to 10 m, Ebb Tide
d)
e)
f)
13.6
13.4
13.2
13.0
12.8
12.6
12.4
28.0
27.9
27.8
27.7
27.6
27.5
27.4

Figure 32.

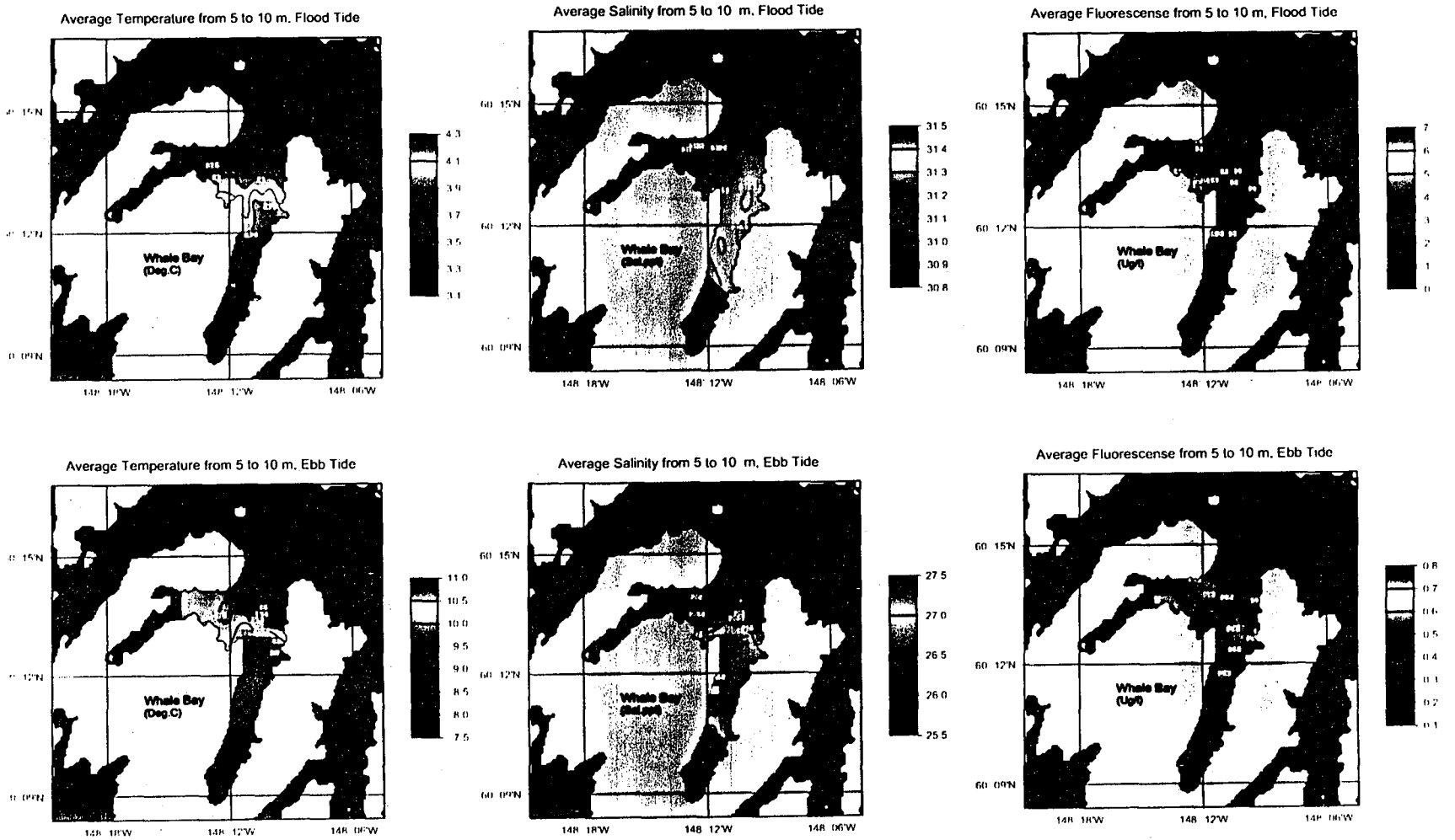
Average Temperature from 5 to 10 m, Flood Tide
Average Salinity from 5 to 10 m, Flood Tide
Average Fluorescense from 5 to 10 m, Flood Tide
Average Temperature from 5 to 10 m, Ebb Tide
Average Salinity from 5 to 10 m, Ebb Tide
Average Fluorescense from 5 to 10 m, Ebb Tide
Whale Bay
(Deg.C)
(Ug/l)
60 15'N
60 12'N
60 09'N
148 18'W
148 12'W
148 06'W
4.3
4.1
3.9
3.7
3.5
3.3
3.1
31.5
31.4
31.3
31.2
31.1
31.0
30.9
30.8
7
6
5
4
3
2
1
0
11.0
10.5
10.0
9.5
9.0
8.5
8.0
7.5
27.5
27.0
26.5
26.0
25.5
0.8
0.7
0.6
0.5
0.4
0.3
0.2
0.1

Figure 33.

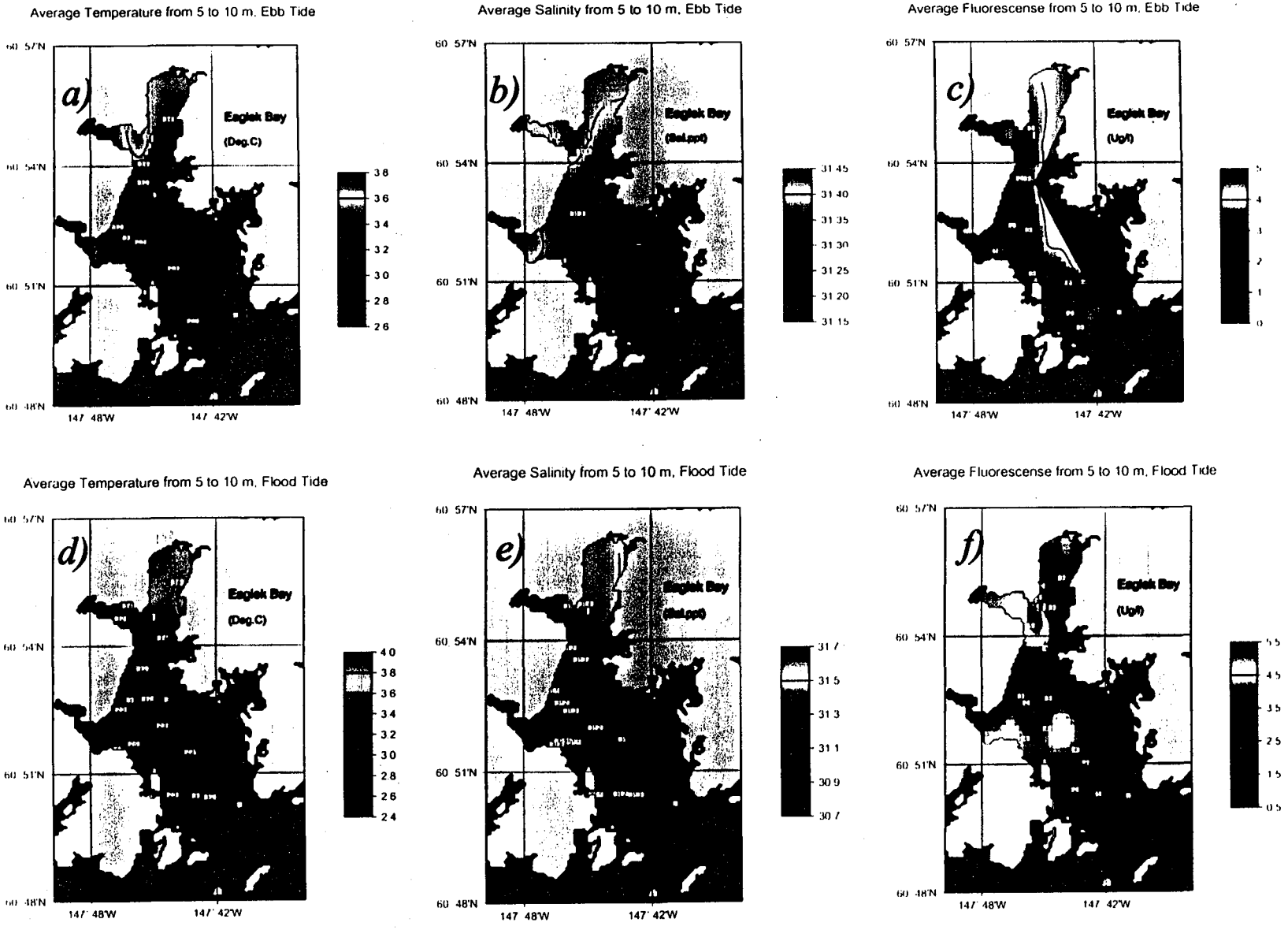
Average Temperature from 5 to 10 m, Ebb Tide
Average Salinity from 5 to 10 m, Ebb Tide
Average Fluorescense from 5 to 10 m, Ebb Tide
Average Temperature from 5 to 10 m, Flood Tide
Average Salinity from 5 to 10 m, Flood Tide
Average Fluorescense from 5 to 10 m, Flood Tide
a)
b)
c)
d)
e)
f)
Eaglek Bay
(Deg.C)
(Ug/l)
60 57'N
60 54'N
60 51'N
60 48'N
147 48'W
147 42'W

Figure 34.

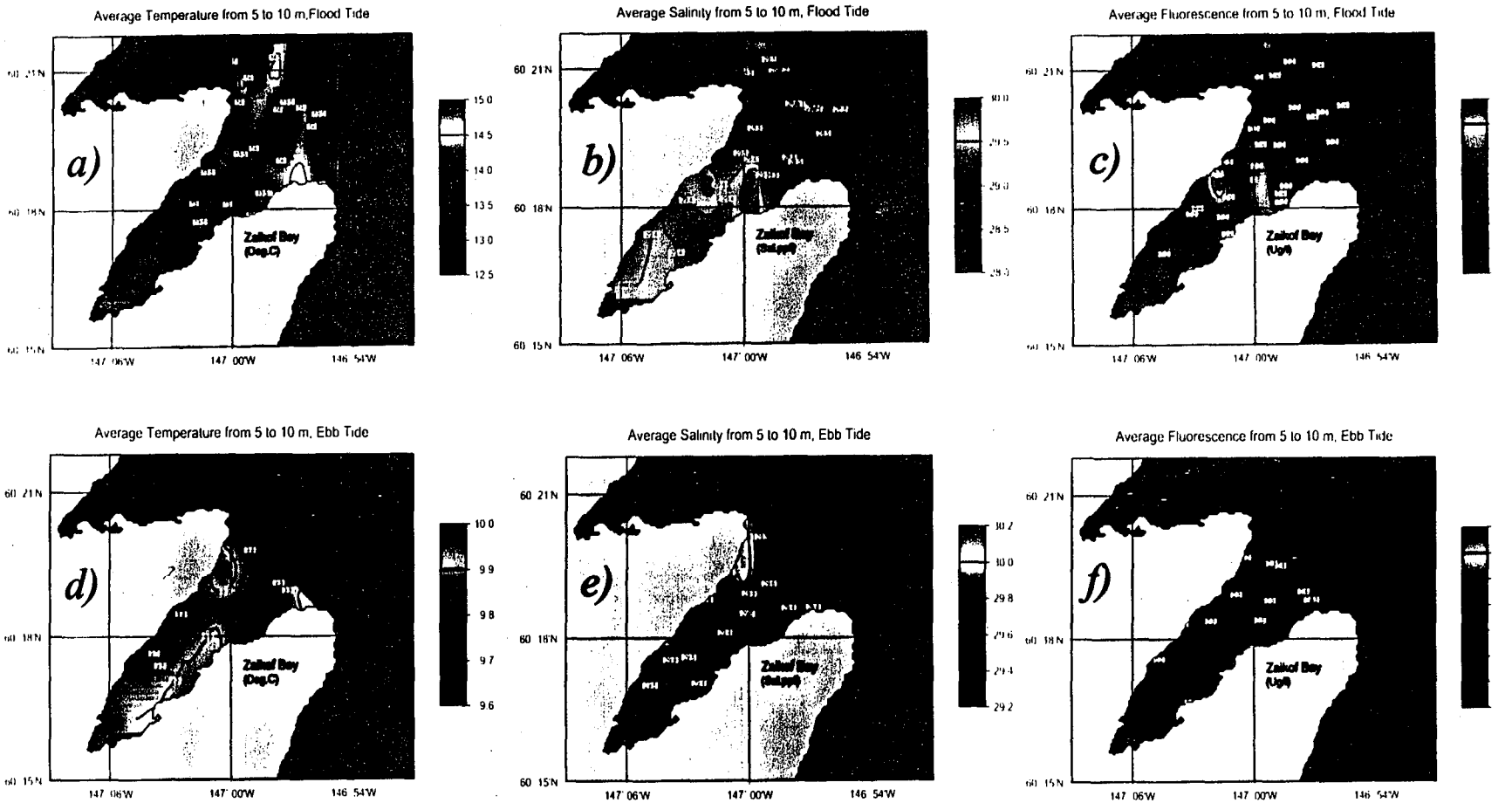
Average Temperature from 5 to 10 m,Flood Tide
Average Salinity from 5 to 10 m, Flood Tide
Average Fluorescence from 5 to 10 m, Flood Tide
Average Temperature from 5 to 10 m, Ebb Tide
Average Salinity from 5 to 10 m, Ebb Tide
Average Fluorescence from 5 to 10 m, Ebb Tide
a)
b)
c)
d)
e)
f)
Zaikof Bay
(Deg.C)
(Ug/l)
60 21N
60 18N
60 15N
147 06W
147 00W
146 54W
15.0
14.5
14.0
13.5
13.0
12.5
10.0
9.9
9.8
9.7
9.6
30.2
30.0
29.8
29.6
29.4
29.2

Figure 35.

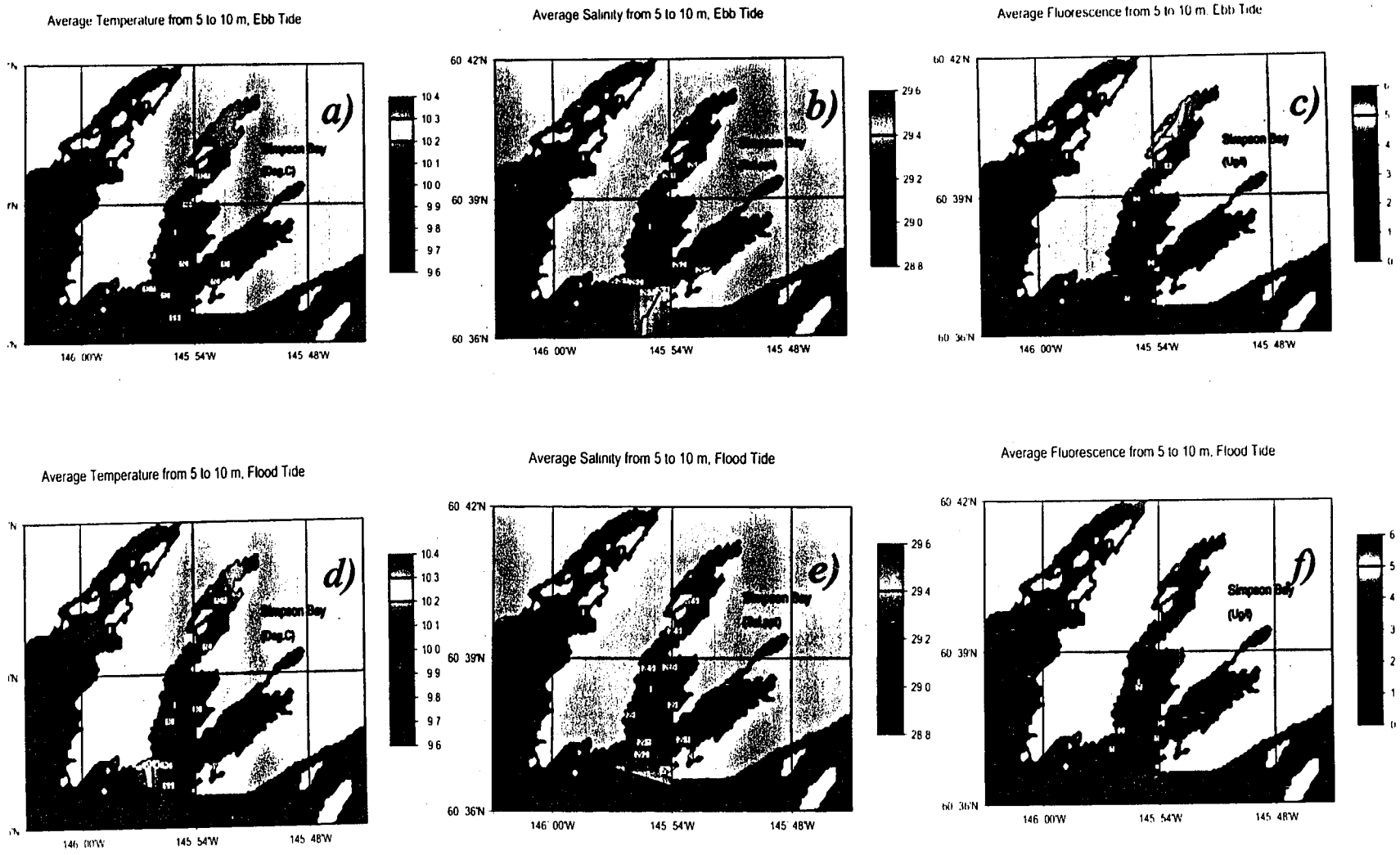
Average Temperature from 5 to 10 m, Ebb Tide
a)
Average Salinity from 5 to 10 m, Ebb Tide
b)
Average Fluorescence from 5 to 10 m, Ebb Tide
c)
Average Temperature from 5 to 10 m, Flood Tide
d)
Average Salinity from 5 to 10 m, Flood Tide
e)
Average Fluorescence from 5 to 10 m, Flood Tide
f)
Simpson Bay
(Up)
60 42'N
60 39'N
60 36'N
146 00'W
145 54'W
145 48'W

Figure 36.

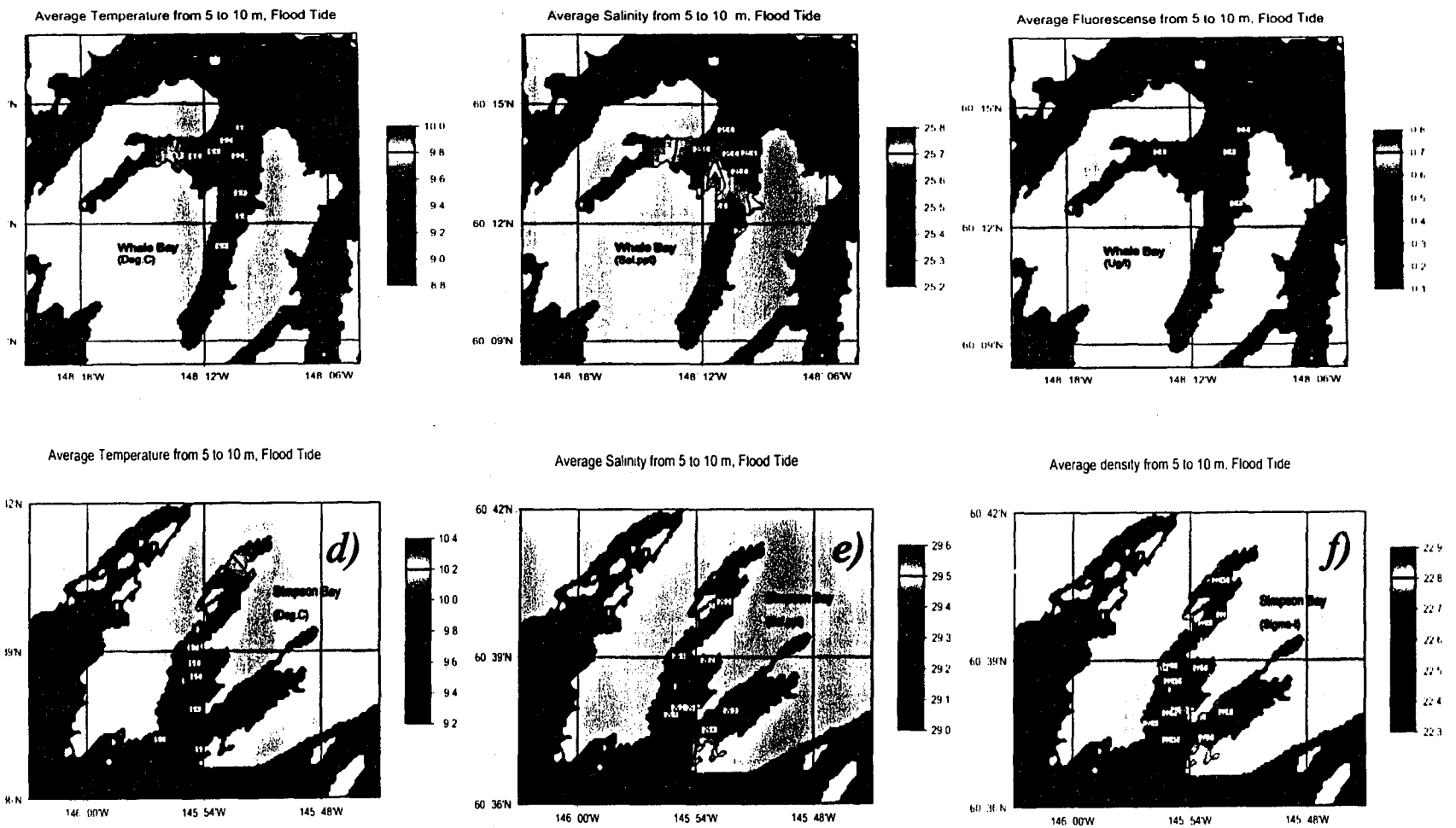
Average Temperature from 5 to 10 m, Flood Tide
Average Salinity from 5 to 10 m, Flood Tide
Average Fluorescense from 5 to 10 m, Flood Tide
Whale Bay
(Deg.C)
(Sal.ppt)
(Ug/l)
148 18'W
148 12'W
148 06'W
60 15'N
60 12'N
60 09'N
Average Temperature from 5 to 10 m, Flood Tide
Average Salinity from 5 to 10 m, Flood Tide
Average density from 5 to 10 m, Flood Tide
d)
e)
f)
Simpson Bay
(Deg.C)
(Sigma-t)
146 00'W
145 54'W
145 48'W
60 42'N
60 39'N
60 36'N

Figure 37.

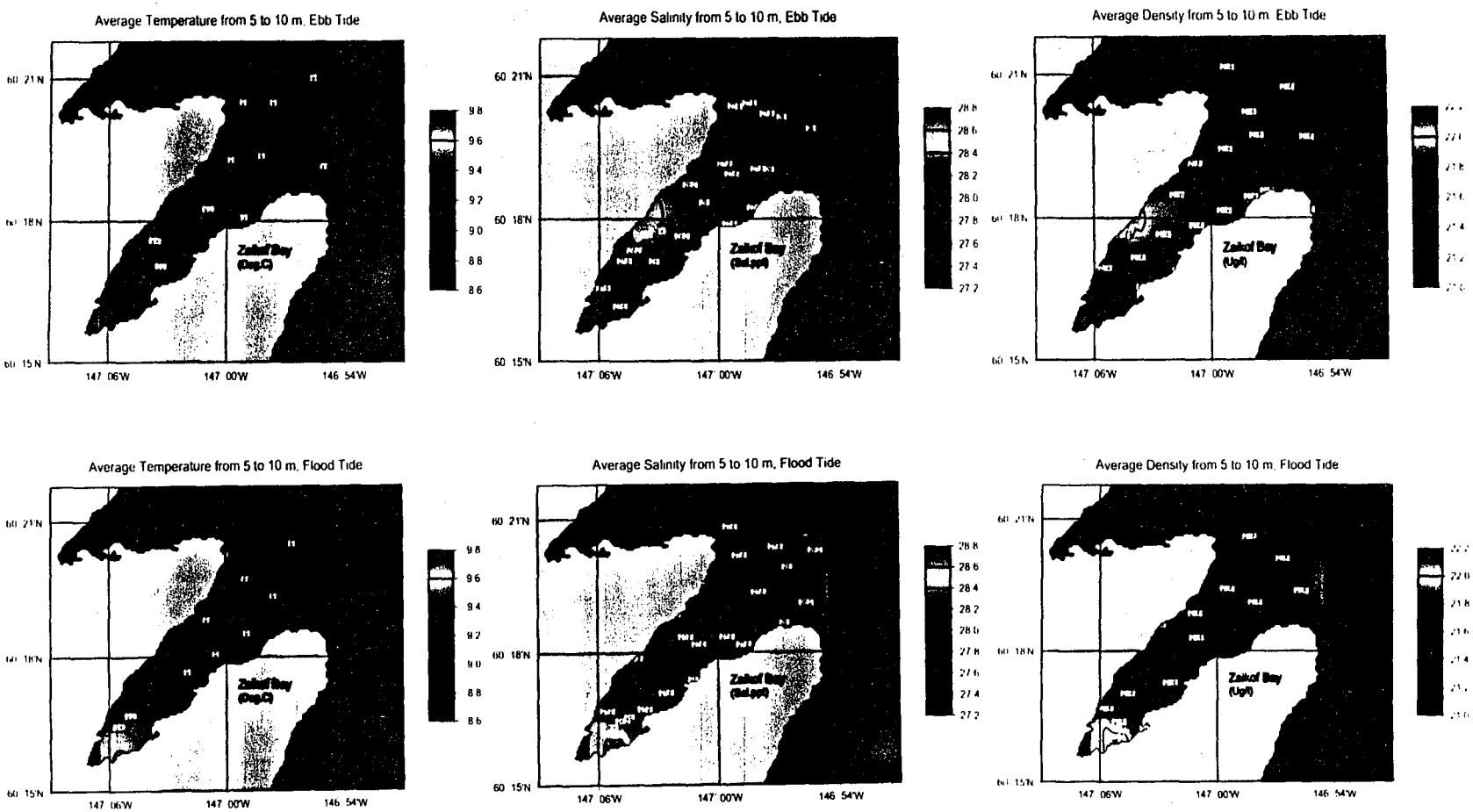
Average Temperature from 5 to 10 m, Ebb Tide
Average Salinity from 5 to 10 m, Ebb Tide
Average Density from 5 to 10 m, Ebb Tide
Average Temperature from 5 to 10 m, Flood Tide
Average Salinity from 5 to 10 m, Flood Tide
Average Density from 5 to 10 m, Flood Tide
60 21'N
60 18'N
60 15'N
147 06'W
147 00'W
146 54'W
Zaikof Bay

Figure 38.

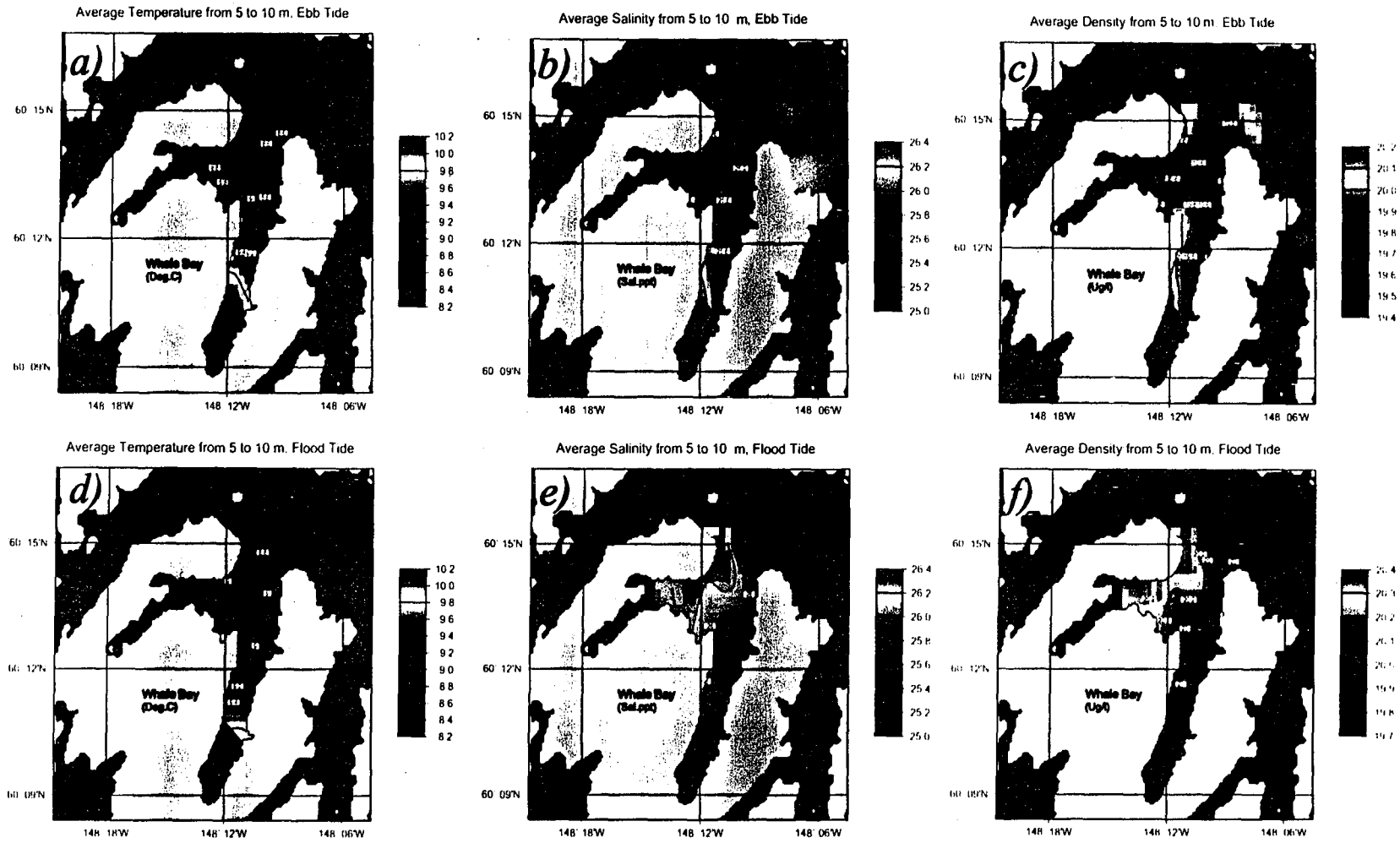
Average Temperature from 5 to 10 m, Ebb Tide
a)
Whale Bay
(Deg.C)
10.2
10.0
9.8
9.6
9.4
9.2
9.0
8.8
8.6
8.4
8.2
Average Salinity from 5 to 10 m, Ebb Tide
b)
Whale Bay
(Sal.ppt)
26.4
26.2
26.0
25.8
25.6
25.4
25.2
25.0
Average Density from 5 to 10 m, Ebb Tide
c)
Whale Bay
(Ug/l)
Average Temperature from 5 to 10 m, Flood Tide
d)
Whale Bay
(Deg.C)
10.2
10.0
9.8
9.6
9.4
9.2
9.0
8.8
8.6
8.4
8.2
Average Salinity from 5 to 10 m, Flood Tide
e)
Whale Bay
(Sal.ppt)
26.4
26.2
26.0
25.8
25.6
25.4
25.2
25.0
Average Density from 5 to 10 m, Flood Tide
f)
Whale Bay
(Ug/l)
60 15'N
60 12'N
60 09'N
148 18'W
148 12'W
148 06'W

Figure 39.

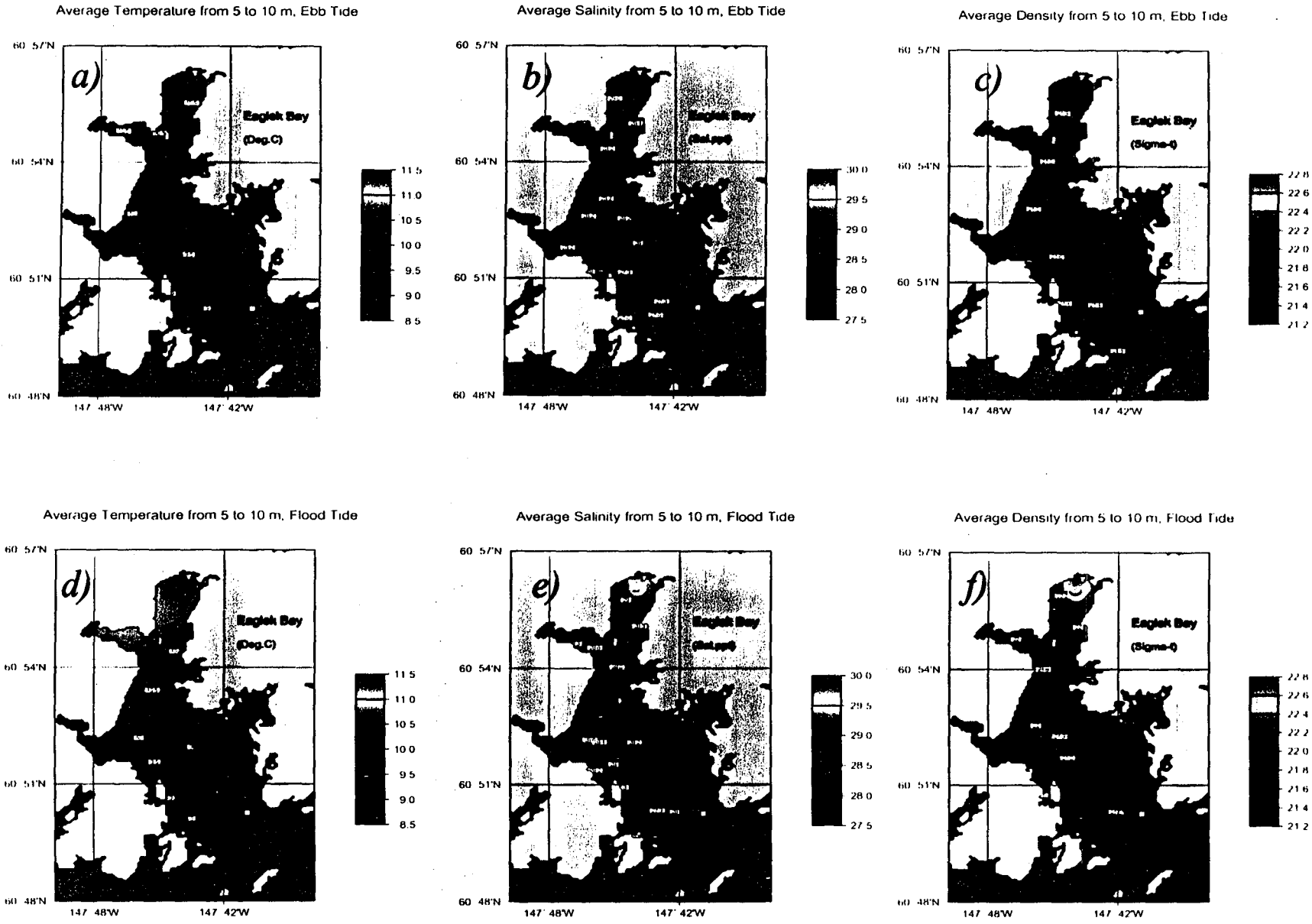
Average Temperature from 5 to 10 m, Ebb Tide
Average Salinity from 5 to 10 m, Ebb Tide
Average Density from 5 to 10 m, Ebb Tide
a)
b)
c)
Eaglek Bay
(Deg.C)
(Sigma-t)
60 57'N
60 54'N
60 51'N
60 48'N
147 48'W
147 42'W
11.5
11.0
10.5
10.0
9.5
9.0
8.5
30.0
29.5
29.0
28.5
28.0
27.5
22.8
22.6
22.4
22.2
22.0
21.8
21.6
21.4
21.2
Average Temperature from 5 to 10 m, Flood Tide
Average Salinity from 5 to 10 m, Flood Tide
Average Density from 5 to 10 m, Flood Tide
d)
e)
f)

Figure 40.